WEAK GALERKIN FINITE ELEMENT METHODs FOR TIME DEPENDENT PROBLEMS ON POLYGONAL MESHES

by

NARESH KUMAR

DEPARTMENT OF MATHEMATICS
INDIAN INSTITUTE OF TECHNOLOGY GUWAHATI
GUWAHATI-781039, INDIA

February, 2022

WEAK GALERKIN FINITE ELEMENT METHODs FOR TIME DEPENDENT PROBLEMS ON POLYGONAL MESHES

A thesis submitted

in partial fulfillment of the requirements

for the degree of

DOCTOR OF PHILOSOPHY

by

NARESH KUMAR

(Roll No. 176123101)

Under the supervision of

Prof. Bhupen Deka

Department of Mathematics

INDIAN INSTITUTE OF TECHNOLOGY GUWAHATI

February, 2022

This thesis

is

dedicated

to the memory of

my Grandmother
Late. Smt. Nikko Devi

CERTIFICATE

It is certified that the work contained in this thesis entitled **"WEAK GALERKIN FINITE ELEMENT METHODs FOR TIME DEPENDENT PROBLEMS ON POLYGONAL MESHES"** by **Naresh Kumar,** a student of Department of Mathematics, Indian Institute of Technology Guwahati, for the award of the degree of Doctor of Philosophy has been carried out under my supervision and that this work has not been submitted elsewhere for a degree.

February, 2022

Prof. Bhupen Deka
Professor
Department of Mathematics
Indian Institute of Technology Guwahati

ACKNOWLEDGEMENT

This thesis represents not only the work I did in the lab but also my journey from being a layman to growing as a researcher. My experience at IIT Guwahati has been nothing short of amazing, since my first day. Throughout these years, I have learned many aspects of research and techniques. Today, along with my thesis, I wish to acknowledge dozens of remarkable individuals who have directly or indirectly contributed to the accomplishment of this dream.

First and foremost, I wholeheartedly thank my Ph.D. research supervisor, Prof. Bhupen Deka, Department of Mathematics for providing me an excellent platform to follow my passion. I am grateful for getting an opportunity to work under his expert guidance. His constant efforts oblige me from the beginning to the completion of my research work. His supervision has improved my research and teaching aptitude and, his Never Give Up approach has always kept me motivated. I would like to express sincere gratitude to my doctoral committee: Prof. R. K. Sinha, Prof. D.C. Dalal and Prof. S.N. Bora, Department of Mathematics, for their constructive evaluation of the research work. Further, I would like to heartily thank Prof. R. K. Sinha for his insightful comments which led to improvement in the quality of my research work.

This work would not have been possible without the infrastructural and administrative support from the department, for which I thank Prof. K. Kapoor, Head of the Department and Prof. M. G. P. Prasad, Prof. N. Selvaraju, Prof. S. N. Bora, former Heads of the Department for their timely guidance and support regarding the academic formalities throughout the thesis work.

I sincerely acknowledge IIT Guwahati for providing me various facilities necessary to carry out my research. I am most grateful to Ministry of Human and Resource Development, Government of India, for providing me financial assistance for the completion of my thesis work. I would also like to thank all the faculty members and research scholars, Department of Mathematics, for extending their help and support during my research and teaching practices. I am also grateful to all the technical and nontechnical staff members of the department for their help and cooperation throughout the period of my research.

I will forever cherish the warmth shown by my friends and lab members, Dr. Jogen Dutta, Uttam dada, Ram manohar, Kuldeep, Raman, Deepak, Monu, Gouranga, and Navneet Redhu. I thank you all for the cooperation and assistance given during the tenure.

I owe my deepest gratitude to my family for their constant support and understanding of my goals and aspirations. The unfailing love and blessings of my parents Mrs. Kamla Devi and Mr. Bhajan Lal Jhorar, have always been my strength; their patience and efforts will keep me inspiring throughout life. I am eternally grateful to my brother Mr. Raam Murti Jhorar and his wife Veetu (sister-in-law), who not only supported me throughout my journey but also made me realize my potential. Heartfelt thanks to my wife Leena, for always being so compassionate. I express my indebtedness to her for always being there for me. I will never forget her constructive and fun-filled advices which always kept me motivated while completing this journey.

February, 2022

(Naresh Kumar)

Department of Mathematics

Indian Institute of Technology Guwahati

ABSTRACT

In this thesis an attempt has been made to study higher order of convergence for time dependent problems. A diverse collection of finite element algorithms for time dependent problems have gained importance in the literature because of its high applicability. However, there still lies a challenge to design higher order accurate and computationally efficient methods for PDEs posed in the complicated geometries, especially for time dependent problems with general polygonal meshes. In practice, allowing arbitrary shape in a finite element partition provides a convenient flexibility in both numerical approximation and general mesh generation such as hybrid meshes, polygonal and polyhedral meshes and meshes with hanging nodes. More recently, the weak Galerkin finite element methods (WG-FEMs) has attracted much attention in the field of numerical PDEs. The objective of this thesis is to design and analyze higher order convergence of weak Galerkin finite element approximations to the true solutions for time dependent problems on polygonal meshes. The mathematical analysis of higher order convergence for time dependent problems with polygonal meshes adds more challenge than one could imagine. At first, we describe a systematic numerical study on WG-FEMs for second order linear parabolic problems by allowing polynomial approximations with various degrees for each local element. Convergence of both semidiscrete and fully discrete WG solutions are established in $L^\infty(L^2)$ and $L^\infty(H^1)$ norms for a general WG element $(\mathcal{P}_k(K),\ \mathcal{P}_j(\partial K),\ \left[\mathcal{P}_l(K)\right]^2)$, where $k \geq 1$, $j \geq 0$ and $l \geq 0$ are arbitrary integers. Fully discrete schemes are based on backward Euler and Crank-Nicolson time discretizations. Here, we assume that the true solution u satisfies full regularity assumptions i.e. $u \in H^1(0,T;H^{k+1}(\Omega))$. Next, we proceed to discuss the WG algorithm to the parabolic problems, when the solution $u \in L^2(0,T;H^{k+1}(\Omega)) \cap H^1(0,T;H^{k-1}(\Omega))$. Such regularity holds where forcing function $f \in L^2(0,T;H^{k-1}(\Omega))$ and initial function $u^0 \in H^k(\Omega)$ for some $k \geq 1$. Optimal order error estimates in $L^2(L^2)$ and $L^2(H^1)$ norms are shown to hold for both the spatially discrete continuous time and the discrete time weak Galerkin finite element schemes. This allows using the discontinuous piecewise polynomials on finite element partitions with the arbitrary shape of polygons having certain shape regularity. Further, we explore the L^2 error convergence of weak Galerkin finite element

approximations for homogeneous parabolic equation with non-smooth initial data using polygonal meshes. We analyze the weak Galerkin finite element methods for second order linear parabolic problems with L^2 initial data, both in a spatially semidiscrete case and in a completely discrete case based on the backward Euler method. We establish optimal L^2 error estimates of order $\mathrm{O}(h^2/t)$ for semisdiscrete scheme. Subsequently, the results are extended for fully discrete scheme.

Our next focuss is to describe WG-FEMs for solving wave equation using the WG finite element space $(\mathcal{P}_k(K), \mathcal{P}_k(\partial K), [\mathcal{P}_{k-1}(K)]^2),\ k \geq 1$. We propose both semidiscrete and fully discrete schemes to numerically solve the second-order linear wave equation. For sufficiently smooth solutions, optimal order error estimate in the $L^\infty(L^2)$ norm is shown to hold as $\mathrm{O}(h^{k+1} + \tau^2)$, where h is the mesh size and τ the time step. In our last problem, we design and analyze the WG-FEMs to approximate a general linear second order hyperbolic equation with variable coefficients on polygonal meshes. The convergence analysis is carried out for the semidiscrete and fully discrete weak Galerkin approximations. The fully discrete scheme can be reinterpreted as an implicit second-order accurate Newmark scheme that is unconditionally stable. Optimal order error estimates in $L^\infty(L^2)$ and $L^\infty(H^1)$ norms are shown to hold for both the schemes.

Finally, we describe and analyze several numerical experiments to establish the efficiency of WG-FEMs in scientific computing. Our numerical results broadly cover the scope of various applied problems under one umbrella, including discontinuous coefficients, variable coefficients and meshes with hanging nodes, aiming to fill the gap in existing literature.

Contents

List of Figures

List of Tables

1 Introduction

The objective of this thesis is to design and analyze higher order WG-FEMs for time dependent problems on polygonal meshes. Numerical solutions of time-dependent problems draw significant attention in various fields of applied sciences, engineering and medicines like acoustics, fluid mechanics, astrophysics, aerodynamics, and high intensity focused ultrasound etc. This chapter is introductory and includes a description of the problems, some notations, and preliminary material. It also includes a brief survey of the relevant literature and motivation behind the current study. The chapter-wise description of the thesis is reported in the last section of this chapter.

1.1 Problem Description

In this section, we introduce time dependent problems which are to be studied in this thesis. It also contains a brief overview on the occurrence of these problems and their applications in the fields of science and engineering.

Linear Parabolic IBVP: We consider linear parabolic equation of the form

$$u_t - \nabla \cdot (\alpha(x)\nabla u) = f \ \text{ in } \Omega \times (0,T], \tag{1.1.1}$$

with initial and boundary conditions

$$u(x,0) = u^0 \ \text{ in } \Omega; \quad u = 0 \quad \text{on } \partial\Omega \times (0,T], \tag{1.1.2}$$

where $\Omega \subset \mathbb{R}^2$ is a convex polygonal domain with boundary $\partial\Omega$. We assume that the coefficient matrix $\alpha = (\alpha_{ij}(x))_{2\times 2} \in [L^\infty(\Omega)]^{2^2}$ is symmetric and uniformly positive definite in Ω. The initial function $u^0 : \Omega \to \mathbb{R}$ and the forcing function $f : \Omega \times [0,T] \to \mathbb{R}$ are assumed to be smooth functions in their respective domains of definition, and T is the finite terminal observation time.

Numerous physical problems of significant interest are modeled by the parabolic problems in science and engineering such as modeling of heat conduction in composite

materials [84], thermodynamics and elasticity [46], moisture transport problems in soil [109], heat conduction problems in different mediums [112], homogeneous fluid flow in fissile materials such as soil and rock [11], Penne's bio-heat model [98] etc.

Second Order Linear Wave Equation: Let $\Omega \subset \mathbb{R}^2$ be a convex polygonal domain with boundary $\partial\Omega$. In Ω, we consider following wave equation

$$u_{tt}(x,t) - \nabla \cdot (\alpha(x)\nabla u(x,t)) = f(x,t) \text{ in } \Omega \times (0,T], \tag{1.1.3}$$

with initial and boundary conditions

$$u(x,0) = u^0(x),\ u_t(x,0) = v^0(x) \text{ in } \Omega;\ \text{ and } \ u(x,t) = 0 \text{ on } \partial\Omega \times (0,T]. \tag{1.1.4}$$

We assume that the coefficient matrix $\alpha = (\alpha_{ij}(x))_{2\times 2} \in [L^\infty(\Omega)]^{2^2}$ is symmetric and uniformly positive definite in Ω. The initial functions $\{u^0, v^0\}$ and the load term f are assumed to be smooth functions in their respective domains of definition, and T is the finite terminal observation time.

The wave equation is a primary archetype of a hyperbolic partial differential equations, and models propagation of various types of waves like elastic waves [50], sound waves in a gas or fluid [51], wave equation in cosmology [87], or electromagnetic waves [55]. In addition to the above applications, modeling of wave equations is also important in acoustics and hydrodynamics. Applications are readily found in geophysics [66], the prediction of earthquakes and other seismic activity often relies on numerical simulations of wave equations [83].

General Linear Second Order Hyperbolic Equation: Let Ω be a convex polygonal domain in $\mathbb{R}^2$ with boundary $\partial\Omega$. In Ω, we consider following general linear second order hyperbolic equation

$$\gamma u_{tt} - \nabla \cdot (\alpha \nabla u) - \nabla \cdot (\beta \nabla u_t) + \sigma u_t = f(x,t) \text{ in } \Omega \times (0,T], \tag{1.1.5}$$

with initial and boundary conditions;

$$u(x,0) = u^0,\ u_t(x,0) = v^0 \text{ in } \Omega;\ u(x,t) = 0 \text{ on } \partial\Omega \times (0,T]. \tag{1.1.6}$$

We assume that the coefficient matrices $\alpha = (\alpha_{ij}(x))_{2\times 2}$ and $\beta = (\beta_{ij}(x))_{2\times 2}$ are in $[L^\infty(\Omega)]^{2\times 2}$, which are symmetric and uniformly positive definite in Ω. The damping coefficients $\gamma = \gamma(x)$ and $\sigma = \sigma(x)$ are non-negative real valued functions defined on Ω. The initial data $\{u^0, v^0\}$ and the forcing term f are assumed to be smooth functions in their respective domains of definition, and T is the finite terminal observation time.

Equation (1.1.5)-(1.1.6) represents a type of hyperbolic equation which is widely applicable in fields like acoustics, fluid mechanics, astrophysics, aerodynamics such as

airplanes, helicopters, and high intensity focused ultrasound by appropriate selection of the coefficients [56, 74]. Upon changing $\sigma := \sigma(x,t)$ and $\gamma := \gamma(x,t)$ in equation (1.1.5), it represents a linearized Westervelt's equation, which has several applications including treatment of kidney and bladder stones via thermal therapy [63], ultrasound cleaning and sonochemistry [24]. When $\sigma = 0$, the equation (1.1.5) describes the wave propagation phenomena of actual vibration through a viscoelastic medium representing a viscoelastic wave equation [81]. For instance, during the heat conduction in memory materials [53], and propagation of sound through viscous media [103]. Equation (1.1.5) is also known as dual-phase-lag (DPL) bio heat model problem. Although Maxwell-Cattaneo law (cf. [116]) has taken care of thermal relaxation time, the validity of the thermal wave model becomes debatable in view of the fast-transient response with micro-structural interaction effects [113]. In order to consider the effect of micro-structural interaction in the fast transient process of heat transport, a phase lag for temperature gradient, τ_T, which is absent in the Maxwell-Cattaneo model, has been introduced in [113, 128, 129]. The corresponding model is called the dual-phase-lag (DPL) model. Mathematically, DPL model is described by a time-dependent equation [128, 129]

$$\begin{aligned}\tau_q \rho c \frac{\partial^2 T}{\partial t^2} &= k\nabla^2 T + \tau_T k \nabla^2 \frac{\partial T}{\partial t} - \omega_b \rho_b c_b T - (\tau_q \omega_b \rho_b c_b + \rho c)\frac{\partial T}{\partial t} \\ &\quad + \big(\omega_b \rho_b c_b T_a + q_{\text{met}} + q_{\text{ext}} + \tau_q \frac{\partial q_{\text{met}}}{\partial t} + \tau_q \frac{\partial q_{\text{ext}}}{\partial t}\big),\end{aligned}$$

where ρ, c, k are the density, specific heat and thermal conductivity of skin tissue, respectively; ρ_b, c_b are the density and specific heat of blood, ω_b is the blood perfusion rate; T_a and T are the temperatures of arterial blood and skin tissue respectively; q_{met} is the metabolic heat generation in the skin tissue and q_{ext} is the heat source due to external heating, and τ_q is defined as the thermal relaxation time.

1.2 Preliminaries

1.2.1 Basic notation

In this section, we shall introduce some basic notations, function spaces and preliminary materials to be used in this thesis. All functions considered here are real valued. For the purpose of introducing notations, we assume Ω to be a convex polygonal domain in $\mathbb{R}^d$ (d-dimensional Euclidean space) and $\partial\Omega$ denote the boundary of Ω. For $x = (x_1, x_2, \ldots, x_d) \in \Omega$, set $dx = dx_1 \ldots dx_d$. Further, let $\alpha = (\alpha_1, \ldots, \alpha_d)$ be an d-tuple with non-negative integer component and denote the order of α as $|\alpha| = \alpha_1 + \alpha_2 + \ldots + \alpha_d$.

Then, by $D^\alpha\phi$, we shall mean the αth derivative of ϕ defined by

$$D^\alpha\phi = \frac{\partial^{|\alpha|}\phi}{\partial {x_1}^{\alpha_1}\dots\partial {x_n}^{\alpha_d}}.$$

By support of a function ϕ, denoted by supp(ϕ), we mean the closure of all points x with $\phi(x) \neq 0$, i.e.,

$$\text{supp}(\phi) = \overline{\{x \in \Omega : \phi(x) \neq 0\}}.$$

For any nonnegative integer m, $C^m(\overline{\Omega})$ denotes the space of functions with continuous derivatives upto and including order m in $\overline{\Omega}$. $C_0^m(\Omega)$ is the space of all $C^m(\Omega)$ functions with compact support in Ω and $C_0^\infty(\Omega)$ is the space of all infinitely differentiable functions with compact support in Ω.

Now we introduce the following function spaces which we shall refer frequently. For any domain $\mathcal{M} \subseteq \Omega \subset \mathbb{R}^d$, $d = 2,\ 3$, with $1 \leq p \leq \infty$, $L^p(\mathcal{M})$ denotes the linear space of equivalence classes of measurable functions ϕ on Ω such that $\|\phi\|_{L^p(\mathcal{M})} < \infty$, where

$$\begin{aligned} \|\phi\|_{L^p(\mathcal{M})} &:= \left(\int_{\mathcal{M}} |\phi(x)|^p dx\right)^{\frac{1}{p}}, \quad 1 \leq p < \infty, \\ \|\phi\|_{L^\infty(\mathcal{M})} &:= \operatorname*{ess\,sup}_{x\in\mathcal{M}} |\phi(x)| < \infty. \end{aligned}$$

When $p = 2$, $L^2(\mathcal{M})$ is a Hilbert space with respect to the inner product

$$(\phi, \psi)_{\mathcal{M}} = \int_{\mathcal{M}} \phi(x)\psi(x)dx.$$

For simplicity of notation, we write the norm $\|\cdot\|_{L^2(\mathcal{M})}$ of $L^2(\mathcal{M})$ by $\|\cdot\|_{\mathcal{M}}$ and remove the subscript $\mathcal{M}$ whenever $\mathcal{M} = \Omega$.

We now introduce the notion of Sobolev spaces. For each integer $k \geq 0$ and real number p with $1 \leq p \leq \infty$, $W^{k,p}(\mathcal{M})$ denotes the standard Sobolev space of functions with their distributional derivatives of order up to k in the Lebesgue space $L^p(\mathcal{M})$, i.e.

$$W^{k,p}(\mathcal{M}) = \{\phi \in L^p(\mathcal{M}) :\ D^\alpha\phi \in L^p(\mathcal{M}) \text{ for } 0 \leq |\alpha| \leq k\}.$$

The spaces $W^{k,p}(\mathcal{M})$ are Banach spaces endowed with the norm

$$\begin{aligned} \|\phi\|_{k,p,\mathcal{M}} &:= \left(\sum_{0\leq|\alpha|\leq k} \|D^\alpha\phi\|^p_{L^p(\mathcal{M})}\right)^{\frac{1}{p}}, \quad 1 \leq p < \infty, \\ \|\phi\|_{k,\infty,\mathcal{M}} &:= \max_{0\leq|\alpha|\leq k} \|D^\alpha\phi(x)\|_{L^\infty(\mathcal{M})}, \quad p = \infty, \end{aligned}$$

also, the semi-norm on $W^{k,p}(\mathcal{M})$ is defined as

$$|\phi|_{k,p,\mathcal{M}} := \sum_{|\alpha|=k} \|D^\alpha\phi\|_{L^p(\mathcal{M})}.$$

When $p = 2$, we write $H^k(\mathcal{M})$ for $W^{k,2}(\mathcal{M})$ with the norm $\|\cdot\|_{k,2,\mathcal{M}} = \|\cdot\|_{k,\mathcal{M}}$ and the semi-norm $|\cdot|_{k,2,\mathcal{M}} = |\cdot|_{k,\mathcal{M}}$. For simplicity of notation, we skip the subscript $\mathcal{M}$ in the norm and inner product notation when $\mathcal{M} = \Omega$.

The space $H^k(\mathcal{M})$ is a Hilbert space with natural inner product defined by

$$(\phi, \psi)_{k,\mathcal{M}} = \sum_{0 \le |\alpha| \le k} \int_{\mathcal{M}} D^\alpha \phi D^\alpha \psi dx, \quad \phi, \psi \in H^k(\mathcal{M}).$$

The Sobolev space $H_0^k(\Omega)$ is defined as the closure of $C_0^\infty(\Omega)$ with respect to the norm $\|\phi\|_k = \|\phi\|_{k,2}$. This result is true under some smoothness assumption on the boundary $\partial\Omega$. For a complete discussion on Sobolev spaces, (see Adams and Fournier [1]).

We shall also use the following space-time function spaces in our error analysis. For $1 \le p \le \infty$, we also define the standard Bôchner spaces $L^p(J; \mathcal{B})$, where $\mathcal{B}$ is a real Banach space with norm $\|\cdot\|_{\mathcal{B}}$ and $J = [0, T]$, consisting of all measurable functions $\phi : J \to \mathcal{B}$ for which

$$\begin{aligned} \|\phi\|_{L^p(0,T;\mathcal{B})} &= \Big(\int_0^T \|\phi(t)\|_{\mathcal{B}}^p dt \Big)^{\frac{1}{p}} < \infty \quad \text{for } 1 \le p < \infty, \\ \|\phi\|_{L^\infty(0,T;\mathcal{B})} &= \operatorname*{ess\,sup}_{t \in [0,T]} \|\phi(t)\|_{\mathcal{B}} < \infty \quad \text{for } p = \infty. \end{aligned}$$

We denote by $H^m(0, T; \mathcal{B})$, $1 \le m < \infty$, the space of all measurable functions $\phi : J \to \mathcal{B}$ for which

$$\|\phi\|_{H^m(0,T;\mathcal{B})} = \left(\sum_{j=0}^{m} \int_0^T \left\| \frac{\partial^j \phi(t)}{\partial t^j} \right\|_{\mathcal{B}}^2 dt \right)^{\frac{1}{2}} < \infty.$$

When no risk of confusion exists, we shall write $L^2(\mathcal{B})$ for $L^2(J; \mathcal{B})$, $L^\infty(\mathcal{B})$ for $L^\infty(J; \mathcal{B})$ and $H^m(\mathcal{B})$ for $H^m(J; \mathcal{B})$. Furthermore, $C(0, T; \mathcal{B})$ is defined as the space of continuous functions $\phi : [0, T] \to \mathcal{B}$ with norm $\|\phi\|_{C(0,T;B)} := \max_{t \in [0,T]} |\phi(t)| < \infty$. For a complete discussion on Sobolev Spaces, one may refer to Adams and Fourier [1], Dautray and Lions [33] and Evans [45].

Further, $H^{-m}(\Omega)$ denotes the space of all bounded linear functionals on $H_0^m(\Omega)$. For a functional $f \in H^{-m}(\Omega)$, its action on a function $\phi \in H_0^m(\Omega)$ is denoted by (f, ϕ), which represents the duality pairing between $H^{-m}(\Omega)$ and $H_0^m(\Omega)$. The negative Sobolev norm is defined as

$$\|f\|_{-m} = \sup_{0 \ne \phi \in H_0^m(\Omega)} \frac{(f, \phi)}{\|\phi\|_m}. \tag{1.2.1}$$

Now we shall recall some important inequalities for our subsequent use [54].

Young's inequality: For $a, b \geq 0$ and $\mu > 0$, the following inequality holds

$$ab \leq \frac{a^2}{2\mu} + \frac{\mu b^2}{2}.$$

An important consequence of the Young's inequality is the Hölder's inequality. The discrete version of Hölder's inequality is stated below.

Hölder's inequality: Let $p > 1$ and q be such that $\frac{1}{p} + \frac{1}{q} = 1$. Then, for any real numbers $a_i, b_i \in \mathbb{R}, i = 1, 2, \cdots, d$,

$$\sum_{i=1}^{d} |a_i b_i| \leq \left(\sum_{i=1}^{d} |a_i|^p \right)^{\frac{1}{p}} \left(\sum_{i=1}^{d} |b_i|^q \right)^{\frac{1}{q}}.$$

In particular, for $p = q = 2$, the above inequality is known as the *Cauchy-Schwarz inequality* in $\mathbb{R}^d$.

The integral analogue of Hölder's inequality is as follows: Let $p > 1$ and q be such that $\frac{1}{p} + \frac{1}{q} = 1$. Then, for any measurable functions $\phi, \psi : \Omega \to \mathbb{R}$

$$\|\phi\psi\|_{L^1(\Omega)} \leq \|\phi\|_{L^p(\Omega)} \|\psi\|_{L^q(\Omega)}.$$

For $p = q = 2$, the above inequality is known as the *Cauchy-Schwarz inequality.*

Poincaré inequality: Let Ω be a bounded open domain in $\mathbb{R}^d$. Then there exists a positive constant $C = C(\Omega)$ such that

$$\|\phi\| \leq C \|\nabla \phi\| \quad \forall \phi \in H_0^1(\Omega).$$

In view of the Poincaré inequality, $\|\nabla(\cdot)\|$ defines a norm on $H_0^1(\Omega)$.

Next we state without proof, the following continuous version of Grownwall's lemma [101].

Lemma 1.2.1 (Gronwall's lemma)**.** *Let $G(t)$ be a continuous function and $H(t)$ a non-negative continuous function on its interval $t_0 \leq t \leq t_0 + a$. If a continuous function $F(t)$ has the property*

$$F(t) \leq G(t) + \int_{t_0}^{t} F(s)H(s)ds \quad \textit{for } t \in [t_0, t_0 + a],$$

then

$$F(t) \leq G(t) + \int_{t_0}^{t} G(s)H(s) exp\left[\int_{s}^{t} H(\tau)d\tau \right] ds \quad \textit{for } t \in [t_0, t_0 + a].$$

In particular, when $G(t) = C$ a non-negative constant, we have

$$F(t) \leq C exp\left[\int_{t_0}^{t} H(s)ds \right] \quad \textit{for } t \in [t_0, t_0 + a].$$

For our notational convenience, we will be using $\frac{\partial u}{\partial t}$ or u_t or u' interchangeably to denote the first order time derivative of u with respect to t. Similar notions are used for higher order time derivatives.

1.3 Background and Motivation

This section briefly explains the existing relevant literature including our contributions with the rationale behind present study.

The modeling of partial differential equations (PDEs) has become a prime topic in science and engineering. Its application ranges from simulating the aerodynamics of large aircraft to modeling of atoms on a quantum mechanic level. For example, quantum physics problems are described by the Schrödinger equation, electromagnetic fields involve the Maxwell equations, incompressible gases and fluids are given by the Navier-Stokes equations, and stresses and deformations in a structure are discussed by the Cauchy-Navier equations, to name a few. The analytic solution to these PDEs is often difficult to derive, rather, numerical methods are applied to capture the solution behavior. In this thesis, we emphasize on the fundamental time-dependent problems like heat equation, wave equation and extending it to second order general hyperbolic equations.

Various numerical methods exist in literature which are designed for numerical approximation of such kind of problems. In practice, a discretization procedure such as finite difference methods (FDMs) and finite element methods (FEMs) are adapted. For many years, Finite difference methods (FDMs) has been known as the most practical and dominant numerical algorithm for solving PDEs appeared in various scientific fields, which approximates the PDEs on a uniform grid and its implementation is very efficient on simple geometries. The alignment of the grid points with sharp material interfaces and boundaries of the domain decides the precision of this method. There are wide range of articles available to solve parabolic problems using FDMs [40, 97, 107]. The hyperbolic equations, particularly for nonlinear conservation laws the finite difference methods has been continuously playing a significant role till now, initiated with work by, e.g., Friedrichs, Lax, and Wendroff. There exists an ample amount of work for the same, see [75], and references therein.

However, unstructured meshes offer more flexibility as it shows alignment with many complex geometries and thus, can be used with finite element methods. In the last few decades, tremendous progress has been made in the development of improved finite element methods for different class of problems and has become an active research area for applied mathematicians. The ability of this method to solve a wide class of problems with complicated structures in a simple and systematic way facilitates its use over other numerical procedures in different fields of science and engineering. In this thesis, we have described efficient and accurate finite element methods for time dependent prob-

lems. A diverse collection of finite element algorithms have been stated in the literature for time dependent problems. Numerical methods applied for parabolic equations based on finite element framework can be mainly grouped into standard conforming FEMs, mixed FEMs and discontinuous Galerkin (DG) methods. The finite element approximations of linear parabolic equations using these methods have been extensively studied, references [18, 21, 22, 23, 39, 95, 104, 106, 111] includes the list of citations. It is challenging to obtain a higher order of convergence for parabolic problems under the low regularity of the exact solution. In classical finite element methods, the error analysis for parabolic equations under low regularity of solution have been investigated and can be traced back in [21, 110]. The standard finite element methods for parabolic problems with non-smooth initial data have been studied broadly so far, an extensive literature for the same can be obtained from [85, 111]. Numerical methods to accurately simulate hyperbolic problems are constantly being developed and applied with increasing levels of sophistication. Nevertheless, the accuracy and consistency of these methods are often poorly understood. Dupont [41] initiated the derivation of a priori error estimates for continuous Galerkin approximations and discrete time schemes of the wave equation which was further explored by Baker [7]. Multi-step methods for the time discretization of second-order hyperbolic equations was analyzed by [49]. A two-step high-order accurate approximations for second-order hyperbolic equations were developed in [9]. A priori error estimates for the classical finite element approximation of Westervelt's quasi-linear strongly damped wave equation with linear elements have been discussed in [94]. Also, a high order discontinuous Galerkin (DG) method for the Westervelt's equation has been carried out in [4]. It is worthwhile to note that only the semi-discrete scheme has been discussed in [4, 94]. The fully discrete scheme error analysis is still unexplored. A substantial amount of research on a priori and a posteriori error estimates in the design of standard conforming finite element methods for the hyperbolic equations is available in literature (e.g., [8, 48, 73] and references therein). Standard continuous (conforming) Galerkin methods show restrictions on mesh and discretization as it does not easily assist hanging nodes for local mesh refinement. Also, if explicit time stepping is subsequently employed, the mass matrix must be inverted at each time step which arises from the spatial discretization, contributing towards a major drawback in terms of efficiency. The standard Galerkin approximation of the second-order wave equation can also be interpreted as mixed discretization of the first order system. We refer to [29, 59] and references therein for broad analysis of mixed finite element methods for wave propagation problems. Pani et al. [96] discussed a mixed finite element formulation for the strongly damped wave equation. However, there still lies a challenge

to design higher order accurate and computationally efficient methods for PDEs posed in complicated geometries, especially for time-dependent problems with general polygonal meshes. Discontinuous Galerkin (DG) methods can be used for different types and shapes of irregular non-matching grids, and for locally varying polynomial order. Since their inception DG-FEMs have become popular in solving hyperbolic equations among the research community. In the last few decades several discontinuous finite element methods for solving the wave equation have been discussed in the literature, e.g. the penalty DG method (PDG) (cf. [52]), the local DG (LDG) (cf. [28]), the hybrid DG (HDG) (cf. [27]), hybrid high-order (HHO) method (cf. [17]). It is worthwhile to note that rigorous error analysis for the discontinuous Galerkin fully discrete scheme (space-time discretization) to general hyperbolic equation is still open.

More recently, the weak Galerkin finite element methods (WG-FEMs) has gained attention in the field of numerical partial differential equations. The WG-FEMs refers to the numerical algorithms for differential equations which are derived from weak formulations of the problems by replacing the involved differential operators by its weak forms and adding parameter free stabilizers [122]. The WG method in [122] has many new features including symmetric positive definite formulation, fewer unknowns and, more importantly, allowing the use of general meshes such as hybrid meshes, polygonal and polyhedral meshes and meshes with hanging nodes. In practice, allowing arbitrary shape in a finite element partition provides a convenient flexibility in both numerical approximation and mesh generation. Especially, we have fewer elements, and we could evaluate integrals and solve the resulting linear systems in more expedited manner [64]. However, one disadvantage is that instead of integrals of polynomials on the reference element, we may have to evaluate integrals of rational functions [133]. Unlike classical finite element method, the WG-FEM is applicable for unstructured polygonal meshes making it more suitable for complex geometry usually appeared in real life problems. In fact, WG formulation is a natural extension of conforming finite element formulation when nonconforming elements are used. In [122], a weak Galerkin method was introduced and analyzed for second order elliptic equations based on a *discrete weak gradient* arising from local RT ([102]) or BDM ([16]) elements. Due to the use of the RT and BDM elements, the weak Galerkin finite element formulation of [122] was limited to classical finite element partitions of triangles ($d = 2$) and tetrahedral ($d = 3$). A computational study of the weak Galerkin method for second-order elliptic equations has been carried out in [89]. In [123], a WG-FEM was developed for the second order elliptic equation in mixed form. The use of stabilization for the flux variable in the mixed formulation is the key to the WG mixed finite element method of [123]. The resulting

WG mixed finite element schemes turned out to be applicable for general finite element partitions consisting of shape regular polytopes, and the stabilization idea opened a new door for weak Galerkin method. Considering the application of WG method, various PDEs arising from the mathematical modeling of practical problems in sciences uses the concept of weak derivatives. There exists vast literature on such PDEs; for e.g., elliptic equation [76, 80, 91, 120, 121, 123], parabolic equation [34, 35, 77, 132, 135], hyperbolic equation [2, 58, 88, 125, 131]. Hybrid high-order (HHO) method is closely related to WG finite element method as the reconstruction operator in the HHO method corresponds to the weak gradient in WG methods [17, 38]. The only difference between HHO and WG methods lies in the choice of the discrete unknowns and in the pattern of stabilization. However, the links between HHO and WG methods are not fully explored yet, nevertheless they share something in their roots (cf. [12, 25]). It is noteworthy that WG, HHO and HDG are based on different devising viewpoints, and also use somewhat different analysis techniques.

For understanding the dynamics of nature the time evolution equations (which often leads to parabolic PDEs) are considered. In this thesis, our aim is to analyze the parabolic problems (1.1.1)-(1.1.2) in a different way. At first, we analyze a systematic numerical study on weak Galerkin finite element method for second order linear parabolic problem with variable coefficient by allowing polynomial approximations with various degrees for each local element. The goal of this study is to explore all possible combinations of polynomial functions in the reconstruction of the underlying differential operators. The preciseness and computational complexity of the corresponding WG scheme is influenced by the selection of such polynomials. Convergence of both semidiscrete and fully discrete WG solutions are established in $L^\infty(L^2)$ and $L^\infty(H^1)$ norms for a general WG element $(\mathcal{P}_k(K),\ \mathcal{P}_j(\partial K),\ \left[\mathcal{P}_l(K)\right]^2)$, where $k \geq 1$, $j \geq 0$ and $l \geq 0$ are arbitrary integers. The fully discrete space-time discretization is based on a first order in time Euler scheme and second order in time Crank-Nicolson scheme. The results for parabolic equation with variable coefficient are particularly useful because it demonstrates the robustness of the WG-FEMs with various combinations of polynomials in the numerical scheme and it fills a gap in existing literature. Here, we have assumed the regularity of the solution is very smooth, but we are well aware of the fact that the rate of convergence of the finite element approximation depends on the smoothness of a solution. Under the low regularity solution of parabolic problems, the higher order convergence analysis has remained a major part of the mathematical study up to the present day. Our second problem is devoted to study the weak Galerkin finite element approximations of second order linear parabolic equation under the low regularities of

the solution. Optimal order error estimates in $L^2(L^2)$ and $L^2(H^1)$ norms are shown to hold for both the spatially discrete continuous time and the discrete time weak Galerkin finite element schemes, which allow using the discontinuous piecewise polynomials on finite element partitions with the arbitrary shape of polygons with certain shape regularity. The fully discrete scheme is based on first order in time Euler method. We have derived $\mathrm{O}(h^{k+1})$ in $L^2(L^2)$ norm and $\mathrm{O}(h^k)$ in $L^2(H^1)$ norm when the exact solution $u \in L^2(0,T;H^{k+1}(\Omega)) \cap H^1(0,T;H^{k-1}(\Omega))$, for some $k \geq 1$. Notably, the solutions of parabolic problems have the smoothing property that is for positive time t, the solution is sufficiently smooth even when the initial data are not H^1 regular. Useful numerical schemes are also expected to have an analogous smoothing property, which results in obtaining the optimal order convergence for positive time under data of low regularity. An attempt has been made in this thesis to study the convergence analysis with lesser regularity assumption on the initial data. Our concerned is to study the convergence of weak Galerkin finite element approximations for homogeneous parabolic equation with L^2 initial data using polygonal meshes, both in a spatially semidiscrete case and in a completely discrete case based on the backward Euler method. In this work, assuming initial data in L^2, we have shown the convergence of WG finite element solution to the true solution at an optimal rate in L^2 norm on WG finite element space $(\mathcal{P}_1,\ \mathcal{P}_1,\ \mathcal{P}_0^2)$. Subsequently, the results are extended for fully discrete scheme. Finally, the numerical experimentation confirms our theoretical convergence results and efficiency of the scheme for above described problems.

The higher order methods have become popular in recent years for investigating the wave propagation phenomena and is acting as an effective approach for solving a wide range of hyperbolic problems. We describe the WG-FEMs for second-order linear wave equation (1.1.3)-(1.1.4), where we have reported both semidiscrete and fully discrete schemes. The fully discrete space-time finite element discretizations can be revised as the Crank-Nicolson discretization of the reformulation of the governing equation in the first-order system. For sufficiently smooth solutions, optimal order error estimate in the $L^\infty(L^2)$ norm is shown to hold as $\mathrm{O}(h^{k+1} + \tau^2)$, where h is the mesh size and τ the time step. Our last problem is provoked by numerous applications of nonlinear hyperbolic problems in medicine and industry. A general linear second-order hyperbolic equation was introduced in [119] which includes different types of damping. Lim et al. [78] concerned an accurate and efficient numerical algorithm for solving viscous and nonviscous wave equations. To investigate the solvability of these problems wtih high order of convergence in general mesh, we design and analyze the WG-FEMs to approximate a second order general linear hyperbolic equation (1.1.5)-(1.1.6) with variable

coefficients on polygonal meshes. The convergence analysis is carried out for the semi-discrete and fully discrete weak Galerkin approximations. The fully discrete scheme can be reinterpreted as an implicit second-order accurate Newmark scheme. Optimal order error estimates in $L^\infty(L^2)$ and $L^\infty(H^1)$ norms are shown to hold for both the schemes. The main aspect of our proof is the use of a non-standard projection operator instead of the usual elliptic projection. Several numerical experiments are performed in a two-dimensional setting that illustrates our theoretical convergence findings. These experiments confirms the robustness, reliability and accuracy of the proposed method. Thus, this thesis intends to enhance the numerical analysis of time dependent problems with polygonal meshes.

1.4 WG Discretization for Elliptic Problems

In this section, we shall briefly introduce WG-FEMs for the elliptic problem and review the definition of the weak gradient operator and its discrete analog to better understand the weak Galerkin algorithm for time-dependent problems.

Let $\Omega \subset \mathbb{R}^2$ be a convex polygonal domain with boundary $\partial\Omega$. In Ω, we consider the following linear elliptic problem

$$-\nabla \cdot (\alpha \nabla u) = f \ \text{ in } \Omega, \tag{1.4.1}$$

with Dirichlet boundary conditions

$$u = 0 \quad \text{on } \partial\Omega. \tag{1.4.2}$$

We assume that the coefficient matrix $\alpha = (\alpha_{ij}(x))_{2\times 2} \in [L^\infty(\Omega)]^{2^2}$ is symmetric and uniformly positive definite in Ω. The load term f is assumed to be smooth functions in their respective domains of definition.

For some $h_0 > 0$ and $h \in (0, h_0]$, let $\mathcal{T}_h$ be a partition of the domain Ω consisting of polygons in two dimension satisfying a set of conditions specified in [123]. Denote by $\mathcal{F}_h$ the set of all edges in $\mathcal{T}_h$ and let $\mathcal{F}_h^0 = \mathcal{F}_h \backslash \partial\Omega$ be the set of all interior edges. For every element $K \in \mathcal{T}_h$, we denote by $|K|$ the measure of K and by h_K its diameter and mesh size $h = \max_{K\in\mathcal{T}_h} h_K$ for $\mathcal{T}_h$.

The key in weak Galerkin methods is the use of weak derivatives in the place of strong derivatives in the variational form for the underlying partial differential equations. Thus, it is essential to introduce a weak version for the gradient operator. Weak gradient operators and its discrete version were introduced in [123]. Let K be any polygonal domain with interior K^0 and boundary ∂K. A weak function on the region K refers to a pair of scalar valued functions $v = \{v_0, v_b\}$ such that $v_0 \in L^2(K)$ and $v_b \in L^2(\partial K)$.

Note that v_b may not be necessarily related to the trace of v_0 on ∂K. Denote by $\mathcal{V}(K)$ the space of weak scalar valued functions on K; i.e.,

$$\mathcal{V}(K) = \{v = \{v_0, v_b\} : v_0 \in L^2(K), v_b \in L^2(\partial K)\}. \tag{1.4.3}$$

Define a space

$$H(\text{div}, K) = \{\mathbf{q} : \mathbf{q} \in [L^2(K)]^2, \ \ \nabla \cdot \mathbf{q} \in L^2(K)\}.$$

For any weak function $v = \{v_0, v_b\}$, its weak gradient $\nabla_w v$ is defined (interpreted) as a linear functional on $H(\text{div}, K)$ whose action on each $\mathbf{q} \in H(\text{div}, K)$ is given by

$$(\nabla_w v, \mathbf{q})_K = -\int_K v_0 \nabla \cdot \mathbf{q} dK + \int_{\partial K} v_b \mathbf{q} \cdot \mathbf{n} ds, \tag{1.4.4}$$

where $\mathbf{n}$ is the unit outward normal to ∂K.

For any given integer $k \geq 0$, denote $\mathcal{P}_k(K)$ the space of polynomials of total degree k or less on the element $K \in \mathcal{T}_h$. Analogously, for any given integer $j \geq 0$, $\mathcal{P}_j(e)$ denotes the space of polynomials of total degree j or less on the edge $e \in \mathcal{F}_h$. On each element $K \in \mathcal{T}_h$, define the following local weak finite element space

$$\mathcal{V}(k, j, K) = \{v_h = \{v_0, v_b\} : \ v_0 \in \mathcal{P}_k(K), \ v_b \in \mathcal{P}_j(\partial K)\}. \tag{1.4.5}$$

A global weak finite element space $\mathcal{V}_h$ is constructed by patching local space $\mathcal{V}(k, j, K)$ through a common value of v_b on all interior edges

$$\mathcal{V}_h = \{v_h = \{v_0, v_b\} : \ v_h|_K \in \mathcal{V}(k, j, K), \ [v_h]_e = 0, \ \forall e \in \mathcal{F}_h^0\}. \tag{1.4.6}$$

Here, $[v_h]_e = [v_b]$ denotes the jump of $v_h \in \mathcal{V} = \prod_{K \in \mathcal{T}_h} \mathcal{V}(k, j, K)$ across an interior edge $e \in \mathcal{F}_h^0$. Denote by $\mathcal{V}_h^0$ the subspace of $\mathcal{V}_h$ consisting of all finite element functions with vanishing boundary value

$$\mathcal{V}_h^0 = \{v_h \in \mathcal{V}_h : v_b|_{\partial\Omega} = 0\}. \tag{1.4.7}$$

Next, we introduce a discrete weak gradient operator, denoted by ∇_w, is defined as the unique polynomial $(\nabla_w v_h) \in [\mathcal{P}_l(K)]^2$ that satisfies the following equation

$$(\nabla_w v_h, \mathbf{q})_K = -\int_K v_0 (\nabla \cdot \mathbf{q}) dK + \int_{\partial K} v_b (\mathbf{q} \cdot \mathbf{n}) ds \ \ \forall \mathbf{q} \in [\mathcal{P}_l(K)]^2, \tag{1.4.8}$$

where $\mathbf{n}$ is the unit outward normal to ∂K and $l \geq 0$ is prescribed non-negative integer. By applying the divergence theorem to the first term on the right-hand side of (1.4.8), we arrive at

$$(\nabla_w v_h, \mathbf{q})_K = (\nabla v_0, \mathbf{q})_K + \langle v_b - v_0, \mathbf{q} \cdot \mathbf{n} \rangle_{\partial K} \ \ \forall \mathbf{q} \in [P_l(K)]^2. \tag{1.4.9}$$

Using the discrete weak gradient operator ∇_w, we define the bilinear map $\mathcal{A}_w : \mathcal{V}_h \times \mathcal{V}_h \to \mathbb{R}$ by

$$\mathcal{A}_w(u_h, v_h) = \sum_{K\in\mathcal{T}_h} \big(\alpha\nabla_w u_h, \nabla_w v_h\big)_K + \mathcal{S}(u_h, v_h) \;\; \forall u_h, v_h \in \mathcal{V}_h. \tag{1.4.10}$$

Here, $\mathcal{S}(\cdot,\cdot)$ is known as stabilizer, which is a semi-positive definite bilinear form defined on $\mathcal{V}_h \times \mathcal{V}_h$. Stabilizer $\mathcal{S}(\cdot,\cdot)$ is often chosen in such a way that it fits well into the theory and implementation of the WG numerical scheme. For examples (cf. [121]):

Example 1.4.1. *(Projected Element-Boundary Discrepancy) For $v_h = \{v_0, v_b\} \in \mathcal{V}_h$, the continuity of v_h can be measured by the quantity $v_b - v_0|_{\partial K}$ for each element $K \in \mathcal{T}_h$. The projected element-boundary-discrepancy method is based on the following stabilizer*

$$\mathcal{S}(u_h, v_h) = \sum_{K\in\mathcal{T}_h} h_K^{-1}\langle \mathcal{Q}_m(u_b - u_0|_{\partial K}), \mathcal{Q}_m(v_b - v_0|_{\partial K})\rangle_{\partial K}, \tag{1.4.11}$$

where $\mathcal{Q}_m : L^2(\partial K) \to \mathcal{P}_m(\partial K)$ is the usual L^2- projection operator and $m = \max\{j, l\}$.

Example 1.4.2. *(Element-Boundary Discrepancy) The element-boundary-discrepancy method is based on the following stabilizer*

$$\mathcal{S}(u_h, v_h) = \sum_{K\in\mathcal{T}_h} h_K^{-1}\langle u_b - u_0|_{\partial K}, v_b - v_0|_{\partial K}\rangle_{\partial K}. \tag{1.4.12}$$

Notation $\langle\cdot,\cdot\rangle_{\partial K}$ denotes the L^2 inner product on ∂K and accordingly, we write

$$\langle\cdot,\cdot\rangle_{\partial K} = \sum_{e\in\partial K} \langle\cdot,\cdot\rangle_e, \tag{1.4.13}$$

where $\langle\cdot,\cdot\rangle_e$ denotes the L^2 inner product on $e \in \mathcal{F}_h$.

In the WG methods, the polynomial degree and the stabilizer must be chosen so that the bilinear form $\mathcal{A}_w(\cdot,\cdot)$ is coercive with respect to the semi-norm $\|\cdot\|_{1,h}$ (cf. [121]) defined by

$$\|v_h\|_{1,h} = \Big(\sum_{K\in\mathcal{T}_h} (\|\nabla v_0\|_K^2 + h_K^{-1}\|v_0 - v_b\|_{\partial K}^2)\Big)^{\frac{1}{2}}, \;\; v_h = \{v_0, v_b\} \in \mathcal{V}_h. \tag{1.4.14}$$

More precisely, there exist constants $C_1 > 0$ & $C_2 > 0$ such that for any $v_h \in \mathcal{V}_h$, the following inequality holds true

$$C_1\|v_h\|_{1,h}^2 \le \mathcal{A}_w(v_h, v_h) \le C_2\|v_h\|_{1,h}^2. \tag{1.4.15}$$

The coercivity inequality (1.4.15), for both the stabilizers on weak Galerkin space $(\mathcal{P}_k(K),\ \mathcal{P}_j(\partial K),\ \big[\mathcal{P}_l(K)\big]^2)$, is stated below (cf. [121]).

Lemma 1.4.1. *Assume that $l \geq k-1$ and $m = \max\{j, l\}$. Then the coercivity inequality (1.4.15) holds true.*

In fact, $\mathcal{V}_h^0$ is a normed linear space with respect to discrete H^1 norm $\|\cdot\|_{1,h}$. For simplicity, we shall only verify the positive length property for $\|\cdot\|_{1,h}$. Assume that $\|w_h\|_{1,h} = 0$ for some $w_h = \{w_0, w_b\} \in \mathcal{V}_h^0$. It follows that $\nabla w_0 = 0$ on each element $K \in \mathcal{T}_h$ and $w_b = w_0$ on ∂K. It follows that $w_0 =$ constant on every $K \in \mathcal{T}_h$. This, together with the fact that $w_b = w_0$ on ∂K and $w_b = 0$ on $\partial\Omega$, implies that $w_0 = 0$ and $w_b = 0$.

The weak Galerkin finite element approximation for (1.4.1)-(1.4.2) is to find $u_h = \{u_0, u_b\} \in \mathcal{V}_h^0$ such that

$$\mathcal{A}_w(u_h, v_h) = (f, v_0) \quad \forall v_h = \{v_0, v_b\} \in \mathcal{V}_h^0, \tag{1.4.16}$$

where the bilinear map $\mathcal{A}_w(\cdot,\cdot)$ is as defined in (1.4.10).

The following result deals with the existence and uniqueness of the WG solution u_h.

Theorem 1.4.1. *For each $h \in (0, h_0]$, there exists a function $u_h \in \mathcal{V}_h^0$ satisfying (1.4.16).*

Proof. For a given element $K \in \{\mathcal{T}_h\}_{0<h\leq h_0}$, let $\{\phi_{0,i} : \ i = 1, 2, \ldots, N_0\}$ be a set of basis functions for $\mathcal{P}_k(K)$ and $\{\phi_{b,i} : \ i = 1, 2, \ldots, N_b\}$ be a set of basis function for $\mathcal{P}_k(e)$. Then every $v_h = \{v_0, v_b\} \in \{\mathcal{V}_h^0\}_{0<h\leq h_0}$ can be written as

$$v_h|_K = \left\{ \sum_{i=1}^{N_0} d_{0,i}\phi_{0,i}, \sum_{j=1}^{N_b} d_{b,j}\phi_{b,j} \right\},$$

where $d_{0,i}, d_{b,j}$ are the coefficient functions for $1 \leq i \leq N_0$ and $1 \leq j \leq N_b$. For $1 \leq i \leq N_0 + N_b$, we write $\hat{\phi}_{i,h} = \{\hat{\phi}_{0,i}, \hat{\phi}_{b,i}\}$ with

$$\begin{aligned} \hat{\phi}_{0,i} = \phi_{0,i} \ \text{ for } 1 \leq i \leq N_0 \quad \& \quad \hat{\phi}_{0,i} = 0 \ \text{ for } \ N_0 + 1 \leq i \leq N_0 + N_b, \\ \hat{\phi}_{b,i} = 0 \ \text{ for } \ 1 \leq i \leq N_0 \quad \& \quad \hat{\phi}_{b,i} = \phi_{b,i-N_0} \ \text{ for } \ N_0 + 1 \leq i \leq N_0 + N_b, \end{aligned}$$

and similarly to capture the unknown coefficient functions, we define

$$\hat{d}_{i,h} = d_{0,i} \ \text{ for } 1 \leq i \leq N_0 \ \ \& \ \ \hat{d}_{i,h} = d_{b,i-N_0} \ \text{ for } N_0 + 1 \leq i \leq N_0 + N_b.$$

Then, we seek our WG solution $u_h = \{u_0, u_b\} \in \mathcal{V}_h^0$ such that

$$u_h|_K = \sum_{i=1}^{N_0+N_b} \hat{d}_{i,h}\hat{\phi}_{i,h} = \left\{ \sum_{i=1}^{N_0+N_b} \hat{d}_{i,h}\hat{\phi}_{0,i}, \sum_{j=1}^{N_0+N_b} \hat{d}_{j,h}\hat{\phi}_{b,j} \right\}, \quad K \in \mathcal{T}_h.$$

Now, set $v_h = \hat{\phi}_{j,h},\ j = 1, 2, \ldots, N_0 + N_b$ in (1.4.16) to obtain

$$\mathcal{A}_w\left(\sum_{i=1}^{N_0+N_b} \hat{d}_{i,h}\hat{\phi}_{i,h}, \hat{\phi}_{j,h}\right) = (f, \hat{\phi}_{0,j}),\quad j = 1, \ldots, N_0 + N_b.$$

We can rearrange the above equations as

$$\sum_{i=1}^{N_0+N_b} \hat{d}_{i,h}\mathcal{A}_w\big(\hat{\phi}_{i,h}, \hat{\phi}_{j,h}\big) = (f, \hat{\phi}_{0,j}),\ j = 1, \ldots, N_0 + N_b.$$

On each element K, the local stiffness matrix $\mathcal{A}_K$ associated with the bilinear map $\mathcal{A}_w(\cdot,\cdot)$ defined by (1.4.10) can thus be written as a block matrix

$$\mathcal{A}_K = \begin{bmatrix} \mathcal{A}_{0,0} & \mathcal{A}_{0,b} \\ \mathcal{A}_{b,0} & \mathcal{A}_{b,b} \end{bmatrix}, \tag{1.4.17}$$

where $\mathcal{A}_{0,0}$ is a $N_0 \times N_0$, $\mathcal{A}_{0,b}$ is a $N_0 \times N_b$, $\mathcal{A}_{b,0}$ is a $N_b \times N_0$, and $\mathcal{A}_{b,b}$ is a $N_b \times N_b$ matrices. More precisely, these matrices are given by

$$\mathcal{A}_{0,0} = [\mathcal{A}_w(\phi_{0,j}, \phi_{0,i})_K]_{i,j},\quad \mathcal{A}_{0,b} = [\mathcal{A}_w(\phi_{0,j}, \phi_{b,i})_K]_{i,j}$$

$$\mathcal{A}_{b,0} = [\mathcal{A}_w(\phi_{b,j}, \phi_{0,i})_K]_{i,j},\quad \mathcal{A}_{b,b} = [\mathcal{A}_w(\phi_{b,j}, \phi_{b,i})_K]_{i,j},$$

where i, j are the row and column indices, respectively.

Then, for our WG solution, we need to find unknown vector $\hat{d}_h = [\hat{d}_{1,h}, \ldots, \hat{d}_{N_0+N_b,h}]^T$ such that

$$\mathcal{A}_K\hat{d}_h = F_K, \tag{1.4.18}$$

where the source vector is given by

$$F_K = [F_1, \ldots, F_{N_0+N_b}],\quad F_j = (f, \hat{\phi}_{j,h})_K,\quad 1 \le i, j \le N_0 + N_b.$$

It is easy note that

$$|(f, \hat{\phi}_{j,h})| \le \|f\|\|\hat{\phi}_{j,h}\| \ \ \& \ \ |\mathcal{A}_w(\hat{\phi}_{i,h}, \hat{\phi}_{j,h})| \le C\|\hat{\phi}_{i,h}\|_{1,h}\|\hat{\phi}_{j,h}\|_{1,h}.$$

Now, the existence of the solution $u_h \in \mathcal{V}_h^0$ follows from the coercive property of the bilinear map $\mathcal{A}_w(\cdot,\cdot)$. This completes the rest of the proof. □

Let K be an element with e as an edge. For any function $\varphi \in H^1(K)$, the following trace inequality holds true [123]

$$\|\varphi\|_e^2 \le C(h_K^{-1}\|\varphi\|_K^2 + h_K\|\nabla\varphi\|_K^2). \tag{1.4.19}$$

The usual L^2-inner product can be written locally on each element as follows

$$(\nabla_w v_h, \nabla_w w_h) \ = \ \sum_{K\in\mathcal{T}_h} (\nabla_w v_h, \nabla_w w_h)_K,\quad w_h, v_h \in \mathcal{V}_h. \tag{1.4.20}$$

1.5 Organization of the Thesis

The proposed contents of the thesis are as follows:

Chapter 1 contains the description of the problems, notations and preliminary materials to be used in the thesis. It also provides a brief survey on the relevant literature concerning the problems and their numerical solutions. Further, motivations for the present study is also discussed.

In **Chapter 2**, we describe a systematic numerical study on weak Galerkin finite element method for second order linear parabolic problem with variable coefficient by allowing polynomial approximations with various degrees for each local element. Convergence of both semidiscrete and fully discrete WG solutions are established in $L^\infty(L^2)$ and $L^\infty(H^1)$ norms. The fully discrete space-time discretizations are based on backward Euler and Crank-Nicolson schemes. Numerical experiments are reported to justify the robustness, reliability and accuracy of the WG finite element method. Results and findings of this Chapter are communicated in [35, 69].

Chapter 3 is devoted to study the weak Galerkin finite element approximations of second order linear parabolic problems in two-dimensional convex polygonal domains under the low regularities of the solutions. Optimal order error estimates in $L^2(L^2)$ and $L^2(H^1)$ norms are shown to hold for both the spatially discrete continuous time and the discrete time weak Galerkin finite element schemes, which allow using the discontinuous piecewise polynomials on finite element partitions. The fully discrete scheme is based on first order in time Euler method. Results and findings of this Chapter are published in [34].

In **Chapter 4**, we analyze the weak Galerkin finite element methods for second order linear parabolic problems with L^2 initial data, both in a spatially semidiscrete case and in a completely discrete case based on the backward Euler method. We have established optimal L^2 error estimates of order $\mathrm{O}(h^2/t)$ for semisdiscrete scheme. Subsequently, the results are extended for fully discrete scheme. The error analysis has been carried out on polygonal meshes for discontinuous piecewise polynomials in finite element partitions. Results and findings of this Chapter are communicated in [71].

In **Chapter 5**, we describe WG-FEMs for solving hyperbolic problems using the WG finite element space $(\mathcal{P}_k(K), \mathcal{P}_k(\partial K), [\mathcal{P}_{k-1}(K)]^2)$, $k \geq 1$. We propose both semidiscrete and fully discrete schemes to numerically solve the second-order linear wave equation. For the time discretization, we have used implicit second order Newmark scheme. For sufficiently smooth solutions, optimal order error estimate in the $L^\infty(L^2)$ norm is shown to hold as $\mathrm{O}(h^{k+1} + \tau^2)$, where h is the mesh size and τ the time step. Results and findings of this Chapter are communicated in [43].

In **Chapter 6**, we design and analyze the WG-FEMs to approximate a second order general linear hyperbolic equation with variable coefficients on polygonal meshes. The proposed method has numerous assets, including the support for higher order of accuracy and general polygonal meshes. The convergence analysis is carried out for the semidiscrete and fully discrete weak Galerkin approximations. The fully discrete scheme can be reinterpreted as an implicit second-order accurate Newmark scheme that is unconditionally stable. Optimal order error estimates in $L^\infty(L^2)$ and $L^\infty(H^1)$ norms are shown to hold for both the schemes. Results and findings of this Chapter are communicated in [70].

Finally, in **Chapter 7**, we discuss the critical evaluation of the results reported in above. This chapter concludes with a brief discussion on the possible extensions and future scopes of the research work done in this thesis.

2

A Systematic Study of Weak Galerkin Finite Element Methods for Second Order Parabolic Problems

This chapter provides a systematic study for the weak Galerkin (WG) finite element method for second order parabolic problems (1.1.1)-(1.1.2) by exploring polynomial approximations with various degrees for each local element. Convergence of both semidiscrete and fully discrete WG solutions are established in L^2 and H^1 norms assuming full regularity of the true solution for a general WG element $(\mathcal{P}_k(K),\ \mathcal{P}_j(\partial K),\ \left[\mathcal{P}_l(K)\right]^2)$, where $k \geq 1$, $j \geq 0$ and $l \geq 0$ are arbitrary integers. The fully discrete space-time discretizatios are based on backward Euler and Crank-Nicolson schemes. Our results extend the numerical analysis of WG methods for elliptic problems [J. Sci. Comput., 74 (2018), 1369-1396] to parabolic problems with variable coefficients. Numerical experiments are reported to justify the robustness, reliability and accuracy of the WG finite element method.

2.1 Introduction

To begin with, let us first recall the second order linear parabolic problem of the form

$$u_t - \nabla \cdot (\alpha \nabla u) = f \quad \text{in } \Omega \times (0, T], \tag{2.1.1}$$

with initial and Dirichlet boundary condition

$$u(x, 0) = u^0(x) \ \text{ in } \Omega; \ \ u = 0 \quad \text{on } \partial\Omega \times (0, T], \tag{2.1.2}$$

where $\Omega \subset \mathbb{R}^2$ is a convex polygonal domain with boundary $\partial\Omega$. We assume that the coefficient matrix $\alpha = (\alpha_{ij}(x))_{2\times 2} \in [L^\infty(\Omega)]^{2^2}$ is symmetric and uniformly positive

Some parts of this chapter are under review in *Numer. Methods Partial Differential Equations* and *Examples and Counterexamples.*

definite in Ω. The initial function $u^0 : \Omega \to \mathbb{R}$ and the forcing function $f : \Omega \times [0, T] \to \mathbb{R}$ are assumed to be smooth functions in their respective domains of definition, and T is the finite terminal observation time. For the higher regularity of the solution to the parabolic problem (2.1.1)-(2.1.2), we refer [45, 72, 86].

The objective of the present work is to propose a systematic framework of WG-FEMs for second order linear parabolic equations by using polynomials of various degrees in the weak finite element space. Finite element approximations of linear parabolic equations have been studied extensively, [111] contains a comprehensive list of references. The classical finite element methods based on conforming finite element discretization have limitations in practical computation. The conforming finite element space is restricted to piecewise polynomials with prescribed continuity that ensures conformity and stability of the corresponding weak formulation, which is often very difficult to implement, particularly for problems in high dimensions and/or on general polytopal partitions. In scientific computing, higher order of convergence is always one of the major research goals, because high order methods are more accurate. Although conforming finite element methods have simple formulations with many fewer unknowns, however, construction of conforming finite element spaces of any orders would be either challenging or impossible. Keeping in mind the applicability of numerical methods of higher order with polygonal meshes, recent attempts have been made to develop certain technologies which make the use of polygonal meshes, for instance, see [14, 30, 117] for virtual element methods, [5, 18, 19, 25, 26] for discontinuous Galerkin methods. Due to the use of discontinuous approximation functions, WG-FEMs are highly flexible in construction of finite element spaces of any orders with the price of more degrees of freedom and more complex formulations. Unlike classical finite element method, the WG-FEMs is applicable for unstructured polygonal meshes making it more suitable for complex geometry usually appearing in real life problem. A typical local WG element is of the form $(\mathcal{P}_k(K),\ \mathcal{P}_j(\partial K),\ \left[\mathcal{P}_l(K)\right]^2)$, where $k \geq 1$ is the degree of polynomials in the interior of the element K, $j \geq 0$ is the degree of polynomials on the boundary of K, and $l \geq 0$ is the degree of polynomials employed in the computation of weak gradients or weak first order partial derivatives. The accuracy and the computational complexity of the corresponding WG scheme is significantly impacted by the selection of such polynomials. The goal of this study is to explore all possible combinations of polynomial functions in the reconstruction of the underlying differential operators. Our results are intended to extend the weak Galerkin analysis in [121] for elliptic problems to linear parabolic equations with polygonal meshes and variable coefficients. It is worth to note that only discrete H^1 norm error estimates are established in [121]. The error analysis

reported in this chapter shows that the WG finite element solutions approximate the true solutions with an optimal order in $L^\infty(L^2)$ and $L^\infty(H^1)$ norms. The results for parabolic equation are particularly useful because it demonstrates the robustness of the WG-FEMs with various combinations of polynomials in the numerical scheme and it fills a gap in existing literature. Finally, theoretical convergence results are validated for several combination of the polynomial spaces.

The rest of the chapter is organized as follows. In Section 2.2, we recall the definitions of weak gradient with its discrete analogs in suitable polynomial spaces and derive an error equation. Section 2.3 is devoted to the optimal order error estimates of semidiscrete WG-FEMs algorithm. In Section 2.4, a backward Euler and Crank-Nicolson schemes are described along with a priori error bounds in $L^\infty(H^1)$ and $L^\infty(L^2)$ norms. Section 2.5 focuses on some numerical results that confirm the convergence theory developed in earlier section with concluding remarks.

2.2 Semidiscrete Approximation

This section deals with spatially discrete scheme for the parabolic problem (2.1.1)-(2.1.2).

Let $\mathcal{T}_h$ be the finite element discretization of Ω as described in Chapter 1. Based on the discretization $\mathcal{T}_h$, for $k \geq 1$, we recall following weak Galerkin finite element space

$$\mathcal{V}_h = \{v = \{v_0, v_b\} : \ v|_K \in \mathcal{V}(k, j, K), \ [v]_e = 0, \ \forall e \in \mathcal{F}_h^0\}. \tag{2.2.1}$$

Here, $[v_h]_e = [v_b]$ denotes the jump of $v_h \in \prod_{K\in\mathcal{T}_h} \mathcal{V}(k, j, K)$ across an interior edge $e \in \mathcal{F}_h^0$ and $\mathcal{V}(k, j, K)$ is the local weak Galerkin space as defined in (1.4.5).

Denote by $\mathcal{V}_h^0$ the subspace of $\mathcal{V}_h$ consisting of all finite element functions with vanishing boundary value

$$\mathcal{V}_h^0 = \{v \in \mathcal{V}_h : v_b|_{\partial\Omega} = 0\}. \tag{2.2.2}$$

Next, we recall a discrete weak gradient operator, denoted by ∇_w, is defined as the unique polynomial $(\nabla_w v) \in [\mathcal{P}_l(K)]^2$ that satisfies the following equation

$$(\nabla_w v, \mathbf{q})_K = -\int_K v_0(\nabla \cdot \mathbf{q})dK + \int_{\partial K} v_b(\mathbf{q} \cdot \mathbf{n})ds \ \ \forall \mathbf{q} \in [\mathcal{P}_l(K)]^2, \tag{2.2.3}$$

where $\mathbf{n}$ is the unit outward normal to ∂K

For each element $K \in \mathcal{T}_h$ and edge $e \in \mathcal{F}_h$, operators $\mathcal{Q}_k^0 : L^2(K) \to \mathcal{P}_k(K)$ and $\mathcal{Q}_j^b : L^2(e) \to \mathcal{P}_j(e)$ are the usual L^2 projections. Denote by $\mathcal{Q}_h$ the L^2 projection onto the weak finite element space $\mathcal{V}_h$ such that $\mathcal{Q}_h|_K = \{\mathcal{Q}_k^0, \mathcal{Q}_j^b\}$. In addition to $\mathcal{Q}_h$, let $\mathbb{Q}_l : [L^2(K)]^2 \to [\mathcal{P}_l(K)]^2$ be an another local L^2 projection.

A time-dependent weak function $v_h : [0,T] \to \mathcal{V}_h$ is written as $v_h(t) := \{v_0(t), v_b(t)\}$ and subsequently we define $v_{ht}(t) := \{v_0'(t), v_b'(t)\}$, where '$\prime$' denotes the time derivatives. For simplicity, we use $v_h = \{v_0, v_b\}$ for $v_h(t)$ and $v_{ht} = \{v_0', v_b'\}$ for $v_{ht}(t)$.

The continuous-time weak Galerkin finite element approximation to (2.1.1)-(2.1.2) can be obtained by seeking $u_h = \{u_0, u_b\} : [0,T] \to \mathcal{V}_h^0$ satisfying following equation

$$(u_{ht}, v_0) + \mathcal{A}_w(u_h, v_h) = (f, v_0) \ \ \forall v_h \in \mathcal{V}_h^0, \tag{2.2.4}$$

where $u_h(0) \in \mathcal{V}_h^0$ is a suitable approximation of the initial function u^0. The bilinear map $\mathcal{A}_w(\cdot,\cdot)$ is as that defined in (1.4.10). Well-posedness of the scheme (2.2.4) can be verified from the fact that weak finite element space $\mathcal{V}_h^0$ is a normed linear space with respect to the triple norm $|||\cdot|||$ defined as (see, Lemma 1.4.1)

$$|||v_h||| = \sqrt{\mathcal{A}_w(v_h, v_h)}, \ v_h \in \mathcal{V}_h^0.$$

As a standard procedure in finite element method, we split our error into two components using an intermediate operator. We write

$$u - u_h = (u - \mathcal{Q}_h u) + (\mathcal{Q}_h u - u_h).$$

For simplicity, we introduce the following notation

$$e_h(t) := \{e_0(t), e_b(t)\} = u_h(t) - \mathcal{Q}_h u(t), \ \ t \in [0,T]. \tag{2.2.5}$$

Then e_h satisfies following error equation which is crucial for our later analysis.

Lemma 2.2.1. *Let e_h be the error as defined in (2.2.5). Then, for all $v_h = \{v_0, v_b\} \in \mathcal{V}_h^0$, we have*

$$(e_{ht}, v_0) + \mathcal{A}_w(e_h, v_h) = l_1(u, v_h) + l_2(u, v_h) + l_3(u, v_h) + \mathcal{S}(\mathcal{Q}_h u, v_h), \tag{2.2.6}$$

where bilinear forms $l_1(\cdot,\cdot)$, $l_2(\cdot,\cdot)$ and $l_3(\cdot,\cdot)$ are given by

$$\begin{aligned}
l_1(u, v_h) &= \sum_{K \in \mathcal{T}_h} \Big(\mathbb{Q}_l(\alpha \mathbb{Q}_l \nabla \mathcal{Q}_k^0 u) - \alpha \nabla u, \nabla v_0 \Big)_K, \\
l_2(u, v_h) &= \sum_{K \in \mathcal{T}_h} \langle (\mathbb{Q}_l(\alpha \mathbb{Q}_l \nabla \mathcal{Q}_k^0 u) - \alpha \nabla u) \cdot \mathbf{n}, v_b - v_0 \rangle_{\partial K}, \\
l_3(u, v_h) &= \sum_{K \in \mathcal{T}_h} \langle \mathcal{Q}_j^b u - \mathcal{Q}_k^0 u, \mathbb{Q}_l(\alpha \nabla_w v) \cdot \mathbf{n} \rangle_{\partial K}.
\end{aligned}$$

Proof. For any $v_h = \{v_0, v_b\} \in \mathcal{V}_h^0$, we test equation (2.1.1) against v_0 on each element $K \in \mathcal{T}_h$ to obtain

$$\begin{aligned}(f, v_0) &= (u_t, v_0) - \sum_{K\in\mathcal{T}_h} (\nabla\cdot(\alpha\nabla u), v_0)_K \\ &= (\mathcal{Q}_h u_t, v_0) + \sum_{K\in\mathcal{T}_h} (\alpha\nabla u, \nabla v_0)_K - \sum_{K\in\mathcal{T}_h} \langle \alpha\nabla u\cdot\mathbf{n}, v_0\rangle_{\partial K} \\ &= ((\mathcal{Q}_h u)_t, v_0) + \sum_{K\in\mathcal{T}_h} (\alpha\nabla u, \nabla v_0)_K - \sum_{K\in\mathcal{T}_h} \langle \alpha\nabla u\cdot\mathbf{n}, v_0 - v_b\rangle_{\partial K}, \qquad (2.2.7)\end{aligned}$$

where we have used the divergence theorem and the fact that

$$\sum_{K\in\mathcal{T}_h} \langle \alpha\nabla u\cdot\mathbf{n}, v_b\rangle_{\partial K} = 0.$$

Combining (2.2.4) and (2.2.7), we have

$$\begin{aligned}(u_{ht}, v_0) + \mathcal{A}_w(u_h, v_h) &= ((\mathcal{Q}_h u)_t, v_0) + \sum_{K\in\mathcal{T}_h} (\alpha\nabla u, \nabla v_0)_K \\ &\quad - \sum_{K\in\mathcal{T}_h} \langle \alpha\nabla u\cdot\mathbf{n}, v_0 - v_b\rangle_{\partial K}. \qquad (2.2.8)\end{aligned}$$

Then integration by parts together with the identity (1.4.9) and the definition of $\mathbb{Q}_l$ operator yields

$$\begin{aligned}&(\alpha\nabla_w \mathcal{Q}_h u, \nabla_w v)_K \\ &= (\nabla_w \mathcal{Q}_h u, \mathbb{Q}_l(\alpha\nabla_w v))_K \\ &= \Big(\nabla\mathcal{Q}_k^0 u, \mathbb{Q}_l(\alpha\nabla_w v)\Big)_K + \langle \mathcal{Q}_j^b u - \mathcal{Q}_k^0 u, \mathbb{Q}_l(\alpha\nabla_w v)\cdot\mathbf{n}\rangle_{\partial K} \\ &= \Big(\mathbb{Q}_l(\alpha\mathbb{Q}_l(\nabla\mathcal{Q}_k^0 u)), \nabla_w v)\Big)_K + \langle \mathcal{Q}_j^b u - \mathcal{Q}_k^0 u, \mathbb{Q}_l(\alpha\nabla_w v)\cdot\mathbf{n}\rangle_{\partial K} \\ &= \Big(\mathbb{Q}_l(\alpha\mathbb{Q}_l(\nabla Q_k^0 u)), \nabla v_0)\Big)_K + \langle Q_j^b u - Q_k^0 u, \mathbb{Q}_l(\alpha\nabla_w v)\cdot\mathbf{n}\rangle_{\partial K} \\ &\quad + \langle v_b - v_0, \mathbb{Q}_l(\alpha\mathbb{Q}_l(\nabla Q_k^0 u))\cdot\mathbf{n}\rangle_{\partial K},\end{aligned}$$

so that

$$\begin{aligned}\mathcal{A}_w(\mathcal{Q}_h u, v_h) &= \sum_{K\in\mathcal{T}_h} \big(\alpha\nabla_w \mathcal{Q}_h u, \nabla_w v_h\big)_K + \mathcal{S}(\mathcal{Q}_h u, v_h) \\ &= \sum_{K\in\mathcal{T}_h} \Big(\mathbb{Q}_l(\alpha\mathbb{Q}_l(\nabla Q_k^0 u)), \nabla v_0)\Big)_K + \sum_{K\in\mathcal{T}_h} \langle Q_j^b u - Q_k^0 u, \mathbb{Q}_l(\alpha\nabla_w v)\cdot\mathbf{n}\rangle_{\partial K} \\ &\quad + \sum_{K\in\mathcal{T}_h} \langle v_b - v_0, \mathbb{Q}_l(\alpha\mathbb{Q}_l(\nabla Q_k^0 u))\cdot\mathbf{n}\rangle_{\partial K} + \mathcal{S}(\mathcal{Q}_h u, v_h),\end{aligned}$$

and hence,

$$\begin{aligned}
&((\mathcal{Q}_h u)_t, v_0) + \mathcal{A}_w(\mathcal{Q}_h u, v_h) \\
&= ((\mathcal{Q}_h u)_t, v_0) + \sum_{K\in\mathcal{T}_h} \Big(\mathbb{Q}_l(\alpha \mathbb{Q}_l(\nabla Q_k^0 u)), \nabla v_0)\Big)_K \\
&\quad + \sum_{K\in\mathcal{T}_h} \langle Q_j^b u - Q_k^0 u, \mathbb{Q}_l(\alpha \nabla_w v)\cdot \mathbf{n}\rangle_{\partial K} \\
&\quad + \sum_{K\in\mathcal{T}_h} \langle v_b - v_0, \mathbb{Q}_l(\alpha \mathbb{Q}_l(\nabla Q_k^0 u))\cdot \mathbf{n}\rangle_{\partial K} + \mathcal{S}(\mathcal{Q}_h u, v_h). \qquad (2.2.9)
\end{aligned}$$

Subtracting (2.2.8) from (2.2.9) leads to desire result. □

Next, for a shape regular weak Galerkin discretization $\mathcal{T}_h$, we recall following crucial estimates for the bilinear maps l_1, l_2 and l_3 from literature [121].

Lemma 2.2.2. *Let $\sigma = min\{l+1, k\}$. Assume that $u \in H^{\sigma+1}(\Omega) \cap H_0^1(\Omega)$ then the following estimate holds true*

$$|l_1(u, v_h)| \le Ch^{\sigma}\|u\|_{\sigma+1}\|v_h\|_{1,h} \quad \forall v_h \in \mathcal{V}_h^0,$$

where C is a positive constant depending on $\|\alpha\|_{l+1,\infty}$-the element wise $W^{l+1,\infty}$ norm of the coefficient matrix α.

Lemma 2.2.3. *Under the assumptions of Lemma 2.2.2, for all $v_h \in \mathcal{V}_h^0$, we have*

$$|l_2(u, v_h)| \le Ch^{\sigma}\|u\|_{\sigma+1}\|v_h\|_{1,h}.$$

Lemma 2.2.4. *Let k, j, l be the non-negative integers that define the weak finite element space $\mathcal{V}_h$. Set $s = min\{k, j\}$ and assume that $s \ge 1$. In addition, assume that $u \in H^{s+1}(\Omega) \cap H_0^1(\Omega)$ then the following estimate holds true*

$$|l_3(u, v_h)| \le Ch^{s}\|u\|_{s+1}\|v_h\|_{1,h} \quad \forall v_h \in \mathcal{V}_h^0.$$

In the case $j \ge l$, we have

$$|l_3(u, v_h)| \le Ch^{k}\|u\|_{k+1}\|v_h\|_{1,h} \quad \forall v_h \in \mathcal{V}_h^0. \qquad (2.2.10)$$

2.3 Error Analysis for the Semidiscrete Scheme

This section deals with the error analysis for the spatially discrete scheme (2.2.4). Optimal order of convergence in both $L^\infty(L^2)$ and $L^\infty(H^1)$ norms are established.

2.3.1 Error estimates with projected element-boundary-discrepancy

Here, convergence results for the semidiscrete weak Galerkin approximation based on projected element-boundary-discrepancy are presented.

For our convenience, following result is borrowed from [121].

Lemma 2.3.1. *Assume that*

$$\mathcal{S}(u_h, v_h) = \sum_{K\in\mathcal{T}_h} h_K^{-1}\langle \mathcal{Q}_m(u_b - u_0|_{\partial K}), \mathcal{Q}_m(v_b - v_0|_{\partial K})\rangle_{\partial K},$$

where $\mathcal{Q}_m : L^2(\partial K) \to \mathcal{P}_m(\partial K)$ is the usual L^2- projection operator and $m = \max\{j, l\}$. The following results hold true:

(a) *Assume that the solution of (2.1.1)-(2.1.2) is so regular that $u \in H^{k+1}(\Omega) \cap H_0^1(\Omega)$ and $j \geq l$, then*

$$|\mathcal{S}(\mathcal{Q}_h u, \mathcal{Q}_h u)| \leq Ch^{2k}\|u\|_{k+1}^2.$$

(b) *Assume that the solution of (2.1.1)-(2.1.2) is so regular that $u \in H^{s+1}(\Omega) \cap H_0^1(\Omega)$ and $j < l$, then*

$$|\mathcal{S}(\mathcal{Q}_h u, \mathcal{Q}_h u)| \leq Ch^{2s}\|u\|_{s+1}^2,$$

where $s = \min\{k, j\}$.

The convergence results for the stabilizer with projected element-boundary-discrepancy can be summarized as follows.

Theorem 2.3.1. *Let k, j, and l be the non-negative integers with $l \geq k - 1$ that define the weak finite element space $\mathcal{V}_h$. Assume that*

$$\mathcal{S}(u_h, v_h) = \sum_{K\in\mathcal{T}_h} h_K^{-1}\langle \mathcal{Q}_m(u_b - u_0|_{\partial K}), \mathcal{Q}_m(v_b - v_0|_{\partial K})\rangle_{\partial K},$$

where $\mathcal{Q}_m : L^2(\partial K) \to \mathcal{P}_m(\partial K)$ is the usual L^2 projection operator and $m = \max\{j, l\}$. Then the following error estimates hold true:

(a) *For $j < l$, set $s = \min\{k, j\}$ and assume $s \geq 1$. Assume that the solution of (2.1.1)-(2.1.2) is so regular that $u \in H^{s+1}(\Omega) \cap H_0^1(\Omega)$. Then*

$$\|e_h(t)\|^2 + \int_0^t \|e_h\|_{1,h}^2 ds \leq C\Big(\|e_h(0)\|^2 + h^{2s}\int_0^t \|u\|_{s+1}^2 ds\Big), \tag{2.3.1}$$

$$\int_0^t \|e_{ht}(t)\|^2 ds + \|e_h(t)\|_{1,h}^2$$
$$\leq C\Big(|||e_h(0)|||^2 + \|e_{ht}(0)\|^2 + h^{2s}\int_0^t \|u\|_{s+1}^2 ds\Big). \tag{2.3.2}$$

(b) *For $j \geq l$, assume that the solution of (2.1.1)-(2.1.2) is so regular that $u \in H^{k+1}(\Omega) \cap H_0^1(\Omega)$. Then*

$$\|e_h(t)\|^2 + \int_0^t \|e_h\|_{1,h}^2 ds \leq C\Big(\|e_h(0)\|^2 + h^{2k}\int_0^t \|u\|_{k+1}^2 ds\Big), \tag{2.3.3}$$

$$\int_0^t \|e_{ht}(t)\|^2 ds + \|e_h(t)\|_{1,h}^2$$
$$\leq C\Big(|||e_h(0)|||^2 + \|e_{ht}(0)\|^2 + h^{2k}\int_0^t \|u\|_{k+1}^2 ds\Big). \tag{2.3.4}$$

Proof. Set $v_h = e_h$ in the error equation (2.2.6) to obtain

$$\frac{1}{2}\frac{d}{dt}\|e_h(t)\|^2 + \mathcal{A}_w(e_h, e_h) \leq |l_1(u, e_h)| + |l_2(u, e_h)| + |l_3(u, e_h)| + |\mathcal{S}(\mathcal{Q}_h u, e_h)|.$$

Then by integrating from 0 to t and using the coercive inequality (1.4.15), we have

$$\begin{aligned}\frac{1}{2}\|e_h(t)\|^2 + C_1\int_0^t \|e_h\|_{1,h}^2 ds &\leq \int_0^t |l_1(u, e_h)| ds + \int_0^t |l_2(u, e_h)| ds \\ &\quad + \int_0^t |l_3(u, e_h)| ds + \int_0^t |\mathcal{S}(\mathcal{Q}_h u, e_h)| ds \\ &:= I_1 + I_2 + I_3 + I_4. \end{aligned} \tag{2.3.5}$$

For the terms I_1 and I_2, we first observe that $\sigma = \min\{l+1, k\} = k$. Then, we apply Lemma 2.2.2 and Lemma 2.2.3 to have

$$I_1,\ I_2 \leq Ch^k \int_0^t \|u\|_{k+1}\|e_h\|_{1,h} ds. \tag{2.3.6}$$

Assume that $j < l$ and $s = \min\{k, j\}$, so that Lemma 2.2.4 and Lemma 2.3.1 yields

$$I_3,\ I_4 \leq Ch^s \int_0^t \|u\|_{s+1}\|e_h\|_{1,h} ds. \tag{2.3.7}$$

Combining (2.3.5)-(2.3.7), we have following $L^\infty(L^2)$ norm and $L^2(|||\cdot|||)$ norm error estimates

$$\|e_h(t)\|^2 + \int_0^t \|e_h\|_{1,h}^2 ds \leq C\Big\{\|e_h(0)\|^2 + h^{2s}\int_0^t \|u\|_{s+1}^2 ds\Big\}. \tag{2.3.8}$$

In the last inequality, we have used the standard Young's inequality.

Next, we differentiate (2.2.6) with respect to t and then set $v_h = e_{ht}$ in the resulting equation to have

$$\frac{1}{2}\frac{d}{dt}\|e_{ht}(t)\|^2 + \mathcal{A}_w(e_{ht}, e_{ht}) \leq |l_1(u, e_{ht})| + |l_2(u, e_{ht})| + |l_3(u, e_{ht})| + |\mathcal{S}(\mathcal{Q}_h u, e_{ht})|.$$

Arguing as in (2.3.8), we note that

$$\|e_{ht}(t)\|^2 + \int_0^t \|e_{ht}\|_{1,h}^2 ds \leq C\Big(\|e_{ht}(0)\|^2 + h^{2s}\int_0^t \|u\|_{s+1}^2 ds\Big). \tag{2.3.9}$$

Next, we set $v_h = e_{ht}$ in the error equation (2.2.6) and arguing as in (2.3.8), we obtain following error estimate

$$\int_0^t \|e_{ht}(t)\|^2 ds + \|e_h(t)\|_{1,h}^2 \leq C\Big(|||e_h(0)|||^2 + \|e_{ht}(0)\|^2 + h^{2s}\int_0^t \|u\|_{s+1}^2 ds\Big).$$

Here, we have used the estimate (2.3.9).

Part (b) can be realized in a similar manner. We omit the details. This completes the rest of the proof. □

Next, we derive an optimal order of estimate for e_h in L^2 norm, the basic idea applied is to use elliptic projection. For $v \in H^2(\Omega) \cap H_0^1(\Omega)\}$, we define

$$f_v = -\nabla\cdot(\alpha\nabla v) \text{ in } \Omega.$$

Clearly, $f_v \in L^2(\Omega)$. Define $\mathcal{R}_h : H^2(\Omega)\cap H_0^1(\Omega) \to \mathcal{V}_h^0$ by

$$\mathcal{A}_w(\mathcal{R}_h v, v_h) = (f_v, v_h) \ \ \forall v_h = \{v_0, v_b\} \in \mathcal{V}_h^0, \ v \in H^2(\Omega)\cap H_0^1(\Omega). \tag{2.3.10}$$

It is easy to observe from the definition of elliptic projection and equation (2.2.4) that

$$(u_{ht}, v_h) + \mathcal{A}_w(u_h - \mathcal{R}_h u, v_h) = (f, v_h) + (\nabla\cdot(\alpha\nabla u), v_h) = (u_t, v_h), \tag{2.3.11}$$

for all $v_h = \{v_0, v_b\} \in \mathcal{V}_h^0$. Here, we have used equation (2.1.1).

Remark 2.3.1. *From the identity (2.3.11), for $u_h(0) = \mathcal{R}_h u^0$, it is easy to see that*

$$\begin{aligned}(e_{ht}(0), v_h) &= (u_{ht}(0) - \mathcal{Q}_h u_t(0), v_h)\\ &= (u_t(0) - \mathcal{Q}_h u_t(0), v_h) \ \ \forall v_h = \{v_0, v_b\} \in \mathcal{V}_h^0,\end{aligned}$$

which implies

$$\|e_{ht}(0)\| \leq \|u_t(0) - \mathcal{Q}_h u_t(0)\| \leq Ch^\lambda \|u_t(0)\|_\lambda, \ \ 0 \leq \lambda \leq k. \tag{2.3.12}$$

Here, we have used standard approximation properties for L^2 projection (see, Lemma 4.1 in [123]). Again, from the equation (2.1.1) it follows that

$$\|u_t(0)\|_\lambda \leq C\big(\|u^0\|_{\lambda+2} + \|f\|_{H^1(J;H^\lambda)}\big). \tag{2.3.13}$$

Combining estimates (2.3.12) and (2.3.13), we obtain

$$\|e_{ht}(0)\| \leq Ch^\lambda\big(\|u^0\|_{\lambda+2} + \|f\|_{H^1(J;H^\lambda)}\big), \ \ 0 \leq \lambda \leq k. \tag{2.3.14}$$

In view of (2.3.10), we observe that $\mathcal{R}_h v$ is the WG finite element approximation of the elliptic problem with exact solution $v \in H^2(\Omega) \cap H_0^1(\Omega)$ satisfying following equation

$$-\nabla \cdot (\alpha \nabla v) = f_v \quad \text{in } \Omega. \tag{2.3.15}$$

Then the error $\rho_v := \mathcal{Q}_h v - \mathcal{R}_h v$ satisfies following error equation (see, Lemma 4.1 in [121])

$$\mathcal{A}_w(\rho_v, w_h) = l_1(v, w_h) + l_2(v, w_h) + l_3(v, w_h) + \mathcal{S}(\mathcal{Q}_h v, w_h), \tag{2.3.16}$$

for all $w_h \in \mathcal{V}_h^0$.

Further, following discrete H^1 norm error estimates for R_h hold true [121].

Lemma 2.3.2. *Let k, j, and l be the non-negative integers with $l \geq k-1$ that define the weak finite element space $\mathcal{V}_h$. Assume that*

$$\mathcal{S}(u_h, v_h) = \sum_{K \in \mathcal{T}_h} h_K^{-1} \langle \mathcal{Q}_m(u_b - u_0|_{\partial K}), \mathcal{Q}_m(v_b - v_0|_{\partial K}) \rangle_{\partial K},$$

where $\mathcal{Q}_m : L^2(\partial K) \to \mathcal{P}_m(\partial K)$ is the usual L^2 projection operator and $m = \max\{j, l\}$. Then the following error estimates hold true:

(a) *For $j < l$, set $s = \min\{k, j\}$ and assume $s \geq 1$. For $v \in H^{s+1}(\Omega) \cap H_0^1(\Omega)$, we have*

$$\|\mathcal{Q}_h v - \mathcal{R}_h v\|_{1,h} \leq C h^s \|v\|_{s+1}. \tag{2.3.17}$$

(b) *For $j \geq l$ and $v \in H^{k+1}(\Omega) \cap H_0^1(\Omega)$. Then*

$$\|\mathcal{Q}_h v - \mathcal{R}_h v\|_{1,h} \leq C h^k \|v\|_{k+1}. \tag{2.3.18}$$

Next, the error $e_h = u_h - \mathcal{Q}_h u$ is expressed in terms of standard ρ and θ as

$$e_h(t) = u_h(t) - \mathcal{Q}_h u(t) = \theta(t) - \rho(t), \tag{2.3.19}$$

where $\rho := \mathcal{Q}_h u - \mathcal{R}_h u$ and $\theta := u_h - \mathcal{R}_h u$.

For $\theta \in \mathcal{V}_h^0$, we note that (cf. [36])

$$(\theta_t, v_h) + \mathcal{A}_w(\theta, v_h) = (\rho_t, v_h) \ \ \forall v_h \in \mathcal{V}_h^0. \tag{2.3.20}$$

For $v_h = \theta$ in (2.3.20), we have

$$(\theta_t, \theta) + |||\theta|||^2 \leq \|\rho_t\| |||\theta|||,$$

which leads to

$$\|\theta\|^2 + \int_0^t |||\theta|||^2 ds \leq \|\theta(0)\|^2 + C\int_0^t \|\rho_t\|^2 ds + C\int_0^t \|\theta\|^2 ds.$$

A simple application of Grownwall's inequality yields

$$\|\theta\|^2 \leq C\Big(\|\theta(0)\|^2 + \int_0^t \|\rho_t\|^2 ds\Big) = C\int_0^t \|\rho_t\|^2 ds, \tag{2.3.21}$$

where we have used the fact that $\theta(0) = u_h(0) - \mathcal{R}_h u(0) = 0$.

Remark 2.3.2. *To best of our knowledge, optimal error estimates in L^2 norm for elliptic problems on general WG finite element space*

$$(\mathcal{P}_k(K),\ \mathcal{P}_j(\partial K),\ \big[\mathcal{P}_l(K)\big]^2)$$

with arbitrary non-negative integers $\{k,\ j,\ l\}$ have not been established earlier. Article [121] is only concerned about the discrete H^1 norm convergence. Therefore, we can not use optimal convergence results directly for the term ρ_t in the L^2 norm.

Next, for the L^2 norm error estimate, we now consider the following auxiliary problem: For every $t \in [0, T]$, find $z(t) \in H_0^1(\Omega) \cap H^2(\Omega)$ such that

$$-\nabla \cdot (\alpha \nabla z(t)) = \rho_t(t). \tag{2.3.22}$$

Then, we may define $z_h(t) := \{z_0(t), z_b(t)\} \in \mathcal{V}_h^0$ as the solution to following discrete elliptic problem

$$\mathcal{A}_w(z_h(t), v_h) = (\rho_t(t), v_h)\ \ \forall v_h \in V_h^0,\ \ t \in [0, T]. \tag{2.3.23}$$

Clearly, z_h is the weak Galerkin finite element approximation to z and satisfies following estimates (cf. [121])

$$\|z - z_h\|_{1,h} \leq Ch\|z\|_2 \leq Ch\|\rho_t\|. \tag{2.3.24}$$

Here, we have used the standard a priori estimate for elliptic problem and the WG space $(\mathcal{P}_k(K),\ \mathcal{P}_j(\partial K),\ \big[\mathcal{P}_l(K)\big]^2)$ with k, j and $l \geq k-1$ are non-negative integers.

Setting $v_h = \rho_t$ in (2.3.23) and further using identity (2.3.16), we have

$$\begin{aligned} \|\rho_t\|^2 &= \mathcal{A}_w(z_h, \rho_t) \\ &= l_1(u_t, z_h) + l_2(u_t, z_h) + l_3(u_t, z_h) + \mathcal{S}(Q_h u_t, z_h). \end{aligned} \tag{2.3.25}$$

Hence, integrating (2.3.25) from 0 to T, we arrive at following estimate

$$\begin{aligned}\int_0^T \|\rho_t\|^2 ds &\leq \int_0^T l_1(u_t, z_h)ds + \int_0^T l_2(u_t, z_h)ds \\ &\quad + \int_0^T l_3(u_t, z_h)ds + \int_0^T \mathcal{S}(\mathcal{Q}_h u_t, z_h)ds \\ &:= I_1 + I_2 + I_3 + I_4. \end{aligned} \tag{2.3.26}$$

We now estimate each term separately. For the term I_1, we use the definition of L^2 projection and the fact that $\nabla z_0 \in [\mathcal{P}_{k-1}(K)]^2 \subseteq [\mathcal{P}_l(K)]^2$ to have

$$\begin{aligned}|l_1(u_t, z_h)| &= \left| \sum_{K\in\mathcal{T}_h} \Big(\mathbb{Q}_l(\alpha \mathbb{Q}_l \nabla \mathcal{Q}_k^0 u_t) - \alpha \nabla u_t, \nabla z_0\Big)_K \right| \\ &\leq \sum_{K\in\mathcal{T}_h} \left| \Big(\alpha \mathbb{Q}_l \nabla \mathcal{Q}_k^0 u_t - \alpha \nabla u_t, \nabla z_0\Big)_K \right| \\ &\leq \sum_{K\in\mathcal{T}_h} \left| \Big(\alpha \mathbb{Q}_l \nabla \mathcal{Q}_k^0 u_t - \alpha \nabla \mathcal{Q}_k^0 u_t, \nabla z_0\Big)_K \right| \\ &\quad + \sum_{K\in\mathcal{T}_h} \left| \Big(\alpha \nabla \mathcal{Q}_k^0 u_t - \alpha \nabla u_t, \nabla z_0\Big)_K \right| \\ &:= I_{11} + I_{12}. \end{aligned} \tag{2.3.27}$$

Now, we use approximation properties for L^2 projections to have

$$\begin{aligned} I_{11} &= \sum_{K\in\mathcal{T}_h} \left| \Big(\mathbb{Q}_l \nabla \mathcal{Q}_k^0 u_t - \nabla \mathcal{Q}_k^0 u_t, (\alpha - \bar{\alpha}) \nabla z_0\Big)_K \right| \\ &\leq Ch\|\alpha\|_{1,\infty} \sum_{K\in\mathcal{T}_h} \left| \Big(\mathbb{Q}_l \nabla \mathcal{Q}_k^0 u_t - \nabla \mathcal{Q}_k^0 u_t, \nabla z_0\Big)_K \right| \\ &\leq Ch\|\alpha\|_{1,\infty} \sum_{K\in\mathcal{T}_h} Ch^{\lambda_1+1} \|\nabla \mathcal{Q}_k^0 u_t\|_{\lambda_1+1,K} \|\nabla z_0\|_K \\ &\leq Ch^{\lambda_1+2} \|\alpha\|_{1,\infty} \|u_t\|_{\lambda_1+2} \|z_h\|_{1,h}. \end{aligned} \tag{2.3.28}$$

for some non-negative integer $\lambda_1 \leq l$. Here, $\bar{\alpha}$ is the average of α on each element $K \in \mathcal{T}_h$.

Next, for the term I_{12}, we have following estimate. For the proof, we refer to Appendix.

$$I_{12} \leq Ch^{\lambda_2+1} \|\alpha\|_{2,\infty} \|u_t\|_{\lambda_2+1} \|\rho_t\|, \tag{2.3.29}$$

for some non-negative integer $\lambda_2 \leq k$. Set $\lambda = \min\{\lambda_1 + 1, \lambda_2\}$ and combine above estimates (2.3.27)-(2.3.29) to obtain

$$I_1 \leq C\|\alpha\|_{2,\infty} h^{\lambda+1} \int_0^T \|u_t\|_{\lambda+1}\|\rho_t\| ds, \quad 0 \leq \lambda \leq k. \tag{2.3.30}$$

Then, following the lines of proof for the Lemma 4.3 in [121], we obtain

$$\begin{aligned} I_2 &\leq C\|\alpha\|_{l+1,\infty} h^{\lambda} \int_0^T \|u_t\|_{\lambda+1}\|z - z_h\|_{1,h} ds \\ &\leq C\|\alpha\|_{l+1,\infty} h^{\lambda+1} \int_0^T \|u_t\|_{\lambda+1}\|\rho_t\| ds, \quad 0 \leq \lambda \leq k. \end{aligned} \tag{2.3.31}$$

In the last inequality, we have used (2.3.24).

For $j < l$ and $s = \min\{k, j\}$, Lemma 4.4 in [121] yields

$$\begin{aligned} l_3(u_t, z_h) &\leq Ch^s \|u_t\|_{s+1} \left(\sum_{K \in \mathcal{T}_h} \|\alpha \nabla_w z_h\|_K^2 \right)^{\frac{1}{2}} \\ &\leq Ch^s \|u_t\|_{s+1} \left(\sum_{K \in \mathcal{T}_h} \|\alpha\|_{L^\infty(K)}^2 \|\nabla_w z_h\|_K^2 \right)^{\frac{1}{2}} \\ &\leq Ch^s \|u_t\|_{s+1} Ch \|\alpha\|_{2,\infty} \|z_h\|_{1,h} \\ &\leq Ch^{s+1} \|\alpha\|_{2,\infty} \|u_t\|_{s+1} \|\rho_t\|. \end{aligned} \tag{2.3.32}$$

Similarly, for $j \geq l$, we obtain

$$l_3(u_t, z_h) \leq Ch^{k+1} \|\alpha\|_{2,\infty} \|u_t\|_{k+1} \|\rho_t\|. \tag{2.3.33}$$

Combining estimates (2.3.32)-(2.3.33), we have

$$I_3 \leq \begin{cases} Ch^{s+1} \|\alpha\|_{2,\infty} \int_0^T \|u_t\|_{s+1} \|\rho_t\| ds & \text{for } j < l, \\ \\ Ch^{k+1} \|\alpha\|_{2,\infty} \int_0^T \|u_t\|_{k+1} \|\rho_t\| ds, & \text{for } j \geq l. \end{cases} \tag{2.3.34}$$

Here, $s = \min\{k, j\}$.

Again, for the term I_4, we apply Lemma 4.5 and Lemma 4.7 in [121] to have

$$\begin{aligned} \mathcal{S}(\mathcal{Q}_h u_t, z_h) &= \mathcal{S}(\mathcal{Q}_h u_t, z_h - \mathcal{Q}_h z) + \mathcal{S}(\mathcal{Q}_h u_t, \mathcal{Q}_h z) \\ &\leq Ch^s \|u_t\|_{s+1} \|z_h - \mathcal{Q}_h z\|_{1,h} \\ &\quad + \sum_{K \in \mathcal{T}_h} h_K^{-1} \langle \mathcal{Q}_m(\mathcal{Q}_k^0 u_t - \mathcal{Q}_j^b u_t), \mathcal{Q}_m(\mathcal{Q}_k^0 z - \mathcal{Q}_j^b z) \rangle_{\partial K} \\ &\leq Ch^{s+1} \|u_t\|_{s+1} \|z\|_2 + Ch^s \|u_t\|_2 Ch \|z\|_2 \\ &\leq Ch^{s+1} \|u_t\|_{s+1} \|\rho_t\|, \end{aligned} \tag{2.3.35}$$

with $j < l$ and $s = \{k, j\}$. Proceeding similarly, for $j \geq l$, we obtain

$$\mathcal{S}(\mathcal{Q}_h u_t, z_h) \leq Ch^{k+1}\|u_t\|_{k+1}\|\rho_t\|. \tag{2.3.36}$$

Combining estimates (2.3.35)-(2.3.36), we have

$$I_4 \leq \begin{cases} Ch^{s+1}\int_0^T \|u_t\|_{s+1}\|\rho_t\|ds & \text{for } j < l, \\ \\ Ch^{k+1}\int_0^T \|u_t\|_{k+1}\|\rho_t\|ds & \text{for } j \geq l, \end{cases} \tag{2.3.37}$$

with $s = \min\{k, j\}$.

Substituting estimates for I_i $(1 \leq i \leq 4)$ in (2.3.26), we obtain

$$\|\rho(t)\|^2 \leq \int_0^T \|\rho_t\|^2 ds \leq \begin{cases} Ch^{2(s+1)}\int_0^T \|u_t\|_{s+1}^2 ds & \text{for } j < l, \\ \\ Ch^{2(k+1)}\int_0^T \|u_t\|_{k+1}^2 & \text{for } j \geq l. \end{cases} \tag{2.3.38}$$

Remark 2.3.3. *In the previous estimate (2.3.39) for $\|\rho\|$, we have assumed that $u \in H^1(H^{s+1})$ or $u \in H^1(H^{k+1})$. In fact, following estimates can be derived in a similar fashion*

$$\|\rho(t)\|^2 \leq \begin{cases} Ch^{2(s+1)}\|u\|_{s+1}^2 & \text{for } j < l, \\ \\ Ch^{2(k+1)}\|u\|_{k+1}^2 & \text{for } j \geq l. \end{cases} \tag{2.3.39}$$

We omit the details.

Finally, use estimate (2.3.39) in (2.3.21) to obtain following $L^\infty(L^2)$ norm error estimate.

Theorem 2.3.2. *Let k, j, and l be the non-negative integers with $l \geq k-1$ that define the weak finite element space $\mathcal{V}_h$. Assume that*

$$\mathcal{S}(u_h, v_h) = \sum_{K \in \mathcal{T}_h} h_K^{-1}\langle \mathcal{Q}_m(u_b - u_0|_{\partial K}), \mathcal{Q}_m(v_b - v_0|_{\partial K})\rangle_{\partial K},$$

where $\mathcal{Q}_m : L^2(\partial K) \to \mathcal{P}_m(\partial K)$ is the usual L^2 projection operator and $m = \max\{j, l\}$. Then the following error estimates hold ture:

(a) *For $j < l$, set $s = \min\{k, j\}$ and assume $s \geq 1$. Assume that the solution of (2.1.1)-(2.1.2) is so regular that $u_t \in H^{s+1}(\Omega) \cap H_0^1(\Omega)$. Then*

$$\|e_h(t)\|^2 \leq Ch^{2(s+1)}\int_0^t \|u_t\|_{s+1}^2 dt. \tag{2.3.40}$$

(b) *For $j \geq l$, assume that the solution of (2.1.1)-(2.1.2) is so regular that $u_t \in H^{k+1}(\Omega) \cap H_0^1(\Omega)$. Then*

$$\|e_h(t)\|^2 \leq Ch^{2(k+1)} \int_0^t \|u_t\|_{k+1}^2 dt. \tag{2.3.41}$$

We assume following convergence results for the semidiscrete weak Galerkin approximation with the stabilizer based on element-boundary-discrepancy.

Theorem 2.3.3. *Let k, j, and l be the non-negative integers with $l \geq k-1$ that define the weak finite element space $\mathcal{V}_h$. Assume that*

$$\mathcal{S}(u_h, v_h) = \sum_{K \in \mathcal{T}_h} h_K^{-1} \langle u_b - u_0|_{\partial K}, v_b - v_0|_{\partial K} \rangle_{\partial K}.$$

Then, we have following error estimates

$$\|e_h(t)\| + h\|e_h(t)\|_{1,h} \leq Ch^{s+1} \left(\int_0^T \|u_t\|_{s+1}^2 dt \right)^{\frac{1}{2}}, \tag{2.3.42}$$

where $s = \min\{k, j\}$.

2.4 Error Analysis for the Fully Discrete Scheme

This section is devoted to the extension of spatially semidiscrete a priori error analysis to the fully discrete approximations. First order backward Euler and second order Crank-Nicolson schemes are applied for the temporal discretization.

We, now, turn our attention to some discrete time weak Galerkin procedures. First, we divide the time interval $J = [0, T]$ into M equally spaced subintervals $I_n = (t_{n-1}, t_n]$, $n = 1, 2, \ldots, M$ with $t_0 = 0$, and $t_M = T$ and $\tau = t_n - t_{n-1}$, the time step. For a sequence $\{\omega^n\}_{n=0}^M \subset L^2(\Omega)$, we define

$$\partial_\tau \omega^n = \frac{\omega^n - \omega^{n-1}}{\tau}, \quad \omega^{n-\frac{1}{2}} = \frac{\omega^n + \omega^{n-1}}{2}, \quad n = 1, 2, \ldots, M.$$

Also, for a continuous mapping $\phi : [0, T] \to L^2(\Omega)$, we define $\phi^n = \phi(., t_n)$, $0 \leq n \leq M$.

The fully discrete weak Galerkin finite element approximation to the problem (2.1.1)-(2.1.2) for backward Euler scheme is defined as: Let $U_h^0 = \mathcal{R}_h u^0$ and $U_h^n = \{U_0^n, U_b^n\} \in \mathcal{V}_h^0$ be the fully discrete solution of u at $t = t_n$ which we shall define through the following scheme

$$(\partial_\tau U_h^n, v_h) + \mathcal{A}_w(U_h^n, v_h) = (f^n, v_h) \ \ \forall v_h \in \mathcal{V}_h^0, \ \ n = 1, 2, \ldots, M. \tag{2.4.1}$$

The Crank-Nicolson scheme can be defined through the following scheme: Let $U_h^0 = \mathcal{R}_h u^0$ and $U_h^n = \{U_0^n, U_b^n\} \in \mathcal{V}_h^0$ be the fully discrete solution of u at $t = t_n$. Then, seek a solution $U_h^n \in \mathcal{V}_h^0$ such that

$$(\partial_\tau U_h^n, v_h) + \mathcal{A}_w(U_h^{n-\frac{1}{2}}, v_h) = (f^{n-\frac{1}{2}}, v_h) \ \ \forall v_h \in \mathcal{V}_h^0, \ \ n = 1, 2, \ldots, M. \tag{2.4.2}$$

2.4.1 Error analysis for backward Euler scheme

This section is devoted to optimal pointwise-in-time error estimate in L^2 norm and discrete H^1 norm for the fully discrete approximation given by backward Euler scheme (2.4.1). Convergence results for the fully discrete weak Galerkin approximation with the stabilizer based on projected element-boundary-discrepancy are reported.

For fully discrete error estimates, we now split the errors at $t = t_n$ as follows

$$u^n - U_h^n = u^n - \mathcal{Q}_h u^n + \mathcal{Q}_h u^n - U_h^n.$$

We denote our error as

$$e^n = U_h^n - \mathcal{Q}_h u^n = \{e_0^n, e_b^n\}.$$

Further, using standard ρ and θ, error e^n can be separated as

$$e^n = \theta^n + \rho^n, \tag{2.4.3}$$

where $\theta^n = U_h^n - \mathcal{R}_h u^n$ and $\rho^n = \mathcal{R}_h u^n - \mathcal{Q}_h u^n$.

For θ^n, we have the following error equation

$$\begin{aligned} (\partial_\tau \theta^n, v_0) + \mathcal{A}_w(\theta^n, v) &= -(\partial_\tau \mathcal{R}_h u^n - u_t^n, v_0) \\ &:= -(w^n, v_0) \ \forall v = \{v_0, v_b\} \in V_h^0, \end{aligned} \tag{2.4.4}$$

where $w^n = \partial_\tau \mathcal{R}_h u^n - u_t^n$. For simplicity of the exposition, we write $w^n = \mathcal{R}_1^n + \mathcal{R}_2^n$, where $\mathcal{R}_1^n = \partial_\tau \mathcal{R}_h u^n - \partial_\tau u^n$ and $\mathcal{R}_2^n = \partial_\tau u^n - u_t^n$.

Set $v = \theta^n$ in (2.4.4), we have

$$(\partial_\tau \theta^n, \theta^n) + \mathcal{A}_w(\theta^n, \theta^n) \le \|w^n\| \|\theta^n\|.$$

Then using the positivity of $\mathcal{A}_w(\cdot, \cdot)$, we obtain

$$\|\theta^n\| \le \|\theta^{n-1}\| + \tau \|w^n\|,$$

where we have used the fact that $\theta^0 = U_h^0 - \mathcal{R}_h u^0 = 0$. Hence, we have

$$\|\theta^n\| \le \tau \sum_{j=1}^{n} \|w^j\| \le \tau \sum_{j=1}^{n} \|\mathcal{R}_1^j\| + \tau \sum_{j=1}^{n} \|\mathcal{R}_2^j\|. \tag{2.4.5}$$

For the term $\mathcal{R}_1^j$, it is easy to verify that

$$\tau\mathcal{R}_1^j = \int_{t_{j-1}}^{t_j} (\mathcal{R}_h u_t - u_t)ds,$$

which together with estimates (2.3.39) leads to the following

$$\tau\sum_{j=1}^{n}\|\mathcal{R}_1^j\| \leq \begin{cases} Ch^{(s+1)}\Big(\int_0^T \|u_t\|_{s+1}^2 ds\Big)^{\frac{1}{2}} & \text{for } j < l, \\ Ch^{k+1}\Big(\int_0^T \|u_t\|_{k+1}^2 ds\Big)^{\frac{1}{2}} & \text{for } j \geq l. \end{cases} \tag{2.4.6}$$

Now, for the term $\mathcal{R}_2$, we use Taylor's series expansion to have

$$\tau\sum_{j=1}^{n}\|\mathcal{R}_2^j\| \leq C\tau\int_0^T \|u_{tt}\|ds. \tag{2.4.7}$$

Finally, estimates (2.4.5)-(2.4.7) together with (2.3.39) leads to following L^2 norm error estimates.

Theorem 2.4.1. *Let k, j, and l be the non-negative integers with $l \geq k-1$ that define the weak finite element space $\mathcal{V}_h$. Assume that*

$$\mathcal{S}(u_h, v_h) = \sum_{K\in\mathcal{T}_h} h_K^{-1}\langle \mathcal{Q}_m(u_b - u_0|_{\partial K}), \mathcal{Q}_m(v_b - v_0|_{\partial K})\rangle_{\partial K},$$

where $\mathcal{Q}_m : L^2(\partial K) \to \mathcal{P}_m(\partial K)$ is the usual L^2 projection operator and $m = \max\{j, l\}$. Then the following error estimates hold true:

(a) *For $j < l$, set $s = \min\{k, j\}$ and assume $s \geq 1$. Assume that the solution of (2.1.1)-(2.1.2) is so regular that $u_t \in H^{s+1}(\Omega) \cap H_0^1(\Omega)$. Then*

$$\|e^n\|^2 \leq C\Big(h^{2(s+1)} + \tau^2\Big)\int_0^T \Big(\|u_t\|_{s+1}^2 + \|u_{tt}\|^2\Big)dt. \tag{2.4.8}$$

(b) *For $j \geq l$, assume that the solution of (2.1.1)-(2.1.2) is so regular that $u_t \in H^{k+1}(\Omega) \cap H_0^1(\Omega)$. Then*

$$\|e^n\|^2 \leq C\Big(h^{2(k+1)} + \tau^2\Big)\int_0^T \Big(\|u_t\|_{k+1}^2 + \|u_{tt}\|^2\Big)dt. \tag{2.4.9}$$

Next, setting $v_h = -\tau\partial_\tau\theta^n$ in (2.4.4), we have

$$\tau\|\partial_\tau\theta^n\|^2 + \mathcal{A}_w(\theta^n, \theta^n - \theta^{n-1}) \leq \tau\|w^n\|\|\partial_\tau\theta^n\|, \tag{2.4.10}$$

which yields

$$\begin{aligned}\tau\|\partial_\tau\theta^n\|^2+|||\theta^n|||^2-|||\theta^{n-1}|||^2 &\leq C\tau\|w^n\|^2\\ &\leq C\tau(\|\mathcal{R}_1^n\|^2+\|\mathcal{R}_2^n\|^2). \qquad (2.4.11)\end{aligned}$$

From (2.4.6), we note that

$$\tau\mathcal{R}_1^j\leq\tau^{\frac{1}{2}}\left(\int_{t_{j-1}}^{t_j}(\mathcal{R}_hu_t-u_t)^2dt\right)^{\frac{1}{2}}$$

so that following estimates hold true

$$\tau\sum_{j=1}^{n}\|\mathcal{R}_1^j\|^2\leq\begin{cases}Ch^{2(s+1)}\int_0^T\|u_t\|_{s+1}^2ds & \text{for } j<l,\\ Ch^{2(k+1)}\int_0^T\|u_t\|_{k+1}^2ds & \text{for } j\geq l.\end{cases} \qquad (2.4.12)$$

Again, we know that

$$\mathcal{R}_2^j=\frac{u^j-u^{j-1}}{\tau}-u_t^j=-\frac{1}{\tau}\int_{t_{j-1}}^{t_j}(s-t_{j-1})u_{tt}ds.$$

Hence, we have

$$\begin{aligned}|\mathcal{R}_2^j|^2 &\leq \frac{1}{\tau^2}\left(\int_{t_{j-1}}^{t_j}(s-t_{j-1})^2ds\right)\left(\int_{t_{j-1}}^{t_j}u_{tt}^2ds\right)\\ &\leq C\tau\int_{t_{j-1}}^{t_j}u_{tt}^2ds,\end{aligned}$$

which integration over Ω yields

$$\|\mathcal{R}_1^j\|^2\leq C\tau\int_{t_{j-1}}^{t_j}\|u_{tt}\|^2ds. \qquad (2.4.13)$$

Now, estimates (2.4.11)-(2.4.13) together with (2.3.39) leads to following discrete H^1 norm error estimates.

Theorem 2.4.2. *Let k, j, and l be the non-negative integers with $l\geq k-1$ that define the weak finite element space $\mathcal{V}_h$. Assume that*

$$\mathcal{S}(u_h,v_h)=\sum_{K\in\mathcal{T}_h}h_K^{-1}\langle\mathcal{Q}_m(u_b-u_0|_{\partial K}),\mathcal{Q}_m(v_b-v_0|_{\partial K})\rangle_{\partial K},$$

where $\mathcal{Q}_m:L^2(\partial K)\to\mathcal{P}_m(\partial K)$ is the usual L^2 projection operator and $m=\max\{j,l\}$. Then the following error estimates hold true:

(a) *For $j < l$, set $s = \min\{k, j\}$ and assume $s \geq 1$. Assume that the solution of (2.1.1)-(2.1.2) is so regular that $u_t \in H^{s+1}(\Omega) \cap H_0^1(\Omega)$. Then*

$$|||e^n|||^2 \leq C\Big(h^{2s} + \tau^2\Big) \int_0^T \Big(\|u_t\|_{s+1}^2 + \|u_{tt}\|^2\Big) dt. \tag{2.4.14}$$

(b) *For $j \geq l$, assume that the solution of (2.1.1)-(2.1.2) is so regular that $u_t \in H^{k+1}(\Omega) \cap H_0^1(\Omega)$. Then*

$$|||e^n|||^2 \leq C\Big(h^{2k} + \tau^2\Big) \int_0^T \Big(\|u_t\|_{k+1}^2 + \|u_{tt}\|^2\Big) dt. \tag{2.4.15}$$

We assume following convergence results for the fully discrete weak Galerkin approximation with the stabilizer is based on element-boundary-discrepancy.

Theorem 2.4.3. *Let k, j, and l be the non-negative integers with $l \geq k-1$ that define the weak finite element space $\mathcal{V}_h$. Assume that*

$$\mathcal{S}(u_h, v_h) = \sum_{K \in \mathcal{T}_h} h_K^{-1} \langle u_b - u_0|_{\partial K}, v_b - v_0|_{\partial K} \rangle_{\partial K}.$$

Then, we have following error estimates

$$\|e^n\|^2 \leq C\Big(h^{2(s+1)} + \tau^2\Big) \int_0^T \Big(\|u_t\|_{s+1}^2 + \|u_{tt}\|^2\Big) dt, \tag{2.4.16}$$

$$|||e^n|||^2 \leq C\Big(h^{2s} + \tau^2\Big) \int_0^T \Big(\|u_t\|_{s+1}^2 + \|u_{tt}\|^2\Big) dt, \tag{2.4.17}$$

where $s = \min\{k, j\}$.

2.4.2 Error analysis for Crank-Nicolson scheme

Here, we describe the optimal order of convergence in L^2 norm for the Crank-Nicolson scheme (2.4.2) with the stabilizer based on projected element-boundary-discrepancy.

At $t = t_n$, for the Crank-Nicolson scheme, we define the fully discrete error as $e_h^n := U_h^n - \mathcal{Q}_h u^n$, which can be further expressed in terms of standard ρ^n and θ^n as

$$e_h^n = U_h^n - \mathcal{Q}_h u^n := \theta^n + \rho^n, \tag{2.4.18}$$

where $\theta^n := U_h^n - \mathcal{R}_h u^n$ and $\rho^n := \mathcal{R}_h u^n - \mathcal{Q}_h u^n$.

For θ^n, we have the following error equation

$$\begin{aligned} (\partial_\tau \theta^n, v_0) + \mathcal{A}_w(\theta^{n-\frac{1}{2}}, v) &= -(\partial_\tau \mathcal{R}_h u^n - u_t^{n-\frac{1}{2}}, v_0) \\ &:= -(w^n, v_0) \ \ \forall v = \{v_0, v_b\} \in \mathcal{V}_h^0, \end{aligned} \tag{2.4.19}$$

where $w^n = \partial_\tau \mathcal{R}_h u^n - u_t^{n-\frac{1}{2}}$.

For the sake of brevity, we express $w^n := \mathcal{W}_1^n + \mathcal{W}_2^n$, where $\mathcal{W}_1^n = \partial_\tau \mathcal{R}_h u^n - \partial_\tau u^n$ and $\mathcal{W}_2^n = \partial_\tau u^n - u_t^{n-\frac{1}{2}}$.

Set $v = \theta^{n-\frac{1}{2}}$ in (2.4.19), we have

$$(\partial_\tau \theta^n, \theta^{n-\frac{1}{2}}) + \mathcal{A}_w(\theta^{n-\frac{1}{2}}, \theta^{n-\frac{1}{2}}) \leq \|w^n\| \|\theta^{n-\frac{1}{2}}\|.$$

Then using the positivity of $\mathcal{A}_w(\cdot,\cdot)$, we obtain

$$\frac{1}{2\tau}\Big(\|\theta^n\|^2 - \|\theta^{n-1}\|^2\Big) \leq \frac{1}{2}\Big(\|\theta^n\| + \|\theta^{n-1}\|\Big)\|w^n\|.$$

Which imply that

$$\|\theta^n\| \leq \|\theta^{n-1}\| + \tau\|w^n\|.$$

Now, summing over n with the fact that $\theta^0 = U_h^0 - \mathcal{R}_h u^0 = 0$, we have

$$\|\theta^n\| \leq \tau \sum_{j=1}^{n} \|w^j\| \leq \tau \sum_{j=1}^{n} \|\mathcal{W}_1^j\| + \tau \sum_{j=1}^{n} \|\mathcal{W}_2^j\|. \tag{2.4.20}$$

For the term $\mathcal{W}_1^j$, it is easy to verify that

$$\tau \mathcal{W}_1^j = \int_{t_{j-1}}^{t_j} (\mathcal{R}_h u_t - u_t) ds,$$

which together with estimate (2.3.39) leads to the following

$$\tau \sum_{j=1}^{n} \|\mathcal{W}_1^j\| \leq \begin{cases} Ch^{(s+1)}\Big(\int_0^T \|u_t\|_{s+1}^2 ds\Big)^{\frac{1}{2}} & \text{for } j < l, \\ \\ Ch^{k+1}\Big(\int_0^T \|u_t\|_{k+1}^2 ds\Big)^{\frac{1}{2}} & \text{for } j \geq l. \end{cases} \tag{2.4.21}$$

Now, for the term $\mathcal{W}_2$, we use Taylor's series expansion to have

$$\tau \sum_{j=1}^{n} \|\mathcal{W}_2^j\| \leq C\tau^2 \Big(\int_0^T \|u_{ttt}\|^2 ds\Big)^{\frac{1}{2}}. \tag{2.4.22}$$

Finally, estimates (2.4.20)-(2.4.22) together with (2.3.39) leads to following L^2 norm error estimates.

Theorem 2.4.4. *Let k, j, and l be the non-negative integers with $l \geq k-1$ that define the weak finite element space $\mathcal{V}_h$. Assume that*

$$\mathcal{S}(u_h, v_h) = \sum_{K \in \mathcal{T}_h} h_K^{-1} \langle \mathcal{Q}_m(u_b - u_0|_{\partial K}), \mathcal{Q}_m(v_b - v_0|_{\partial K}) \rangle_{\partial K},$$

where $\mathcal{Q}_m : L^2(\partial K) \to \mathcal{P}_m(\partial K)$ is the usual L^2 projection operator and $m = \max\{j, l\}$. Then the following error estimates hold true:

(a) *For $j < l$, set $s = \min\{k, j\}$ and assume $s \geq 1$. Assume that the solution of (2.1.1)-(2.1.2) is so regular that $u_t \in H^{s+1}(\Omega) \cap H_0^1(\Omega)$. Then*

$$\|e_h^n\| \leq C\Big(h^{s+1} + \tau^2\Big) \int_0^T \Big(\|u_t\|_{s+1} + \|u_{ttt}\|\Big) dt. \tag{2.4.23}$$

(b) *For $j \geq l$, assume that the solution of (2.1.1)-(2.1.2) is so regular that $u_t \in H^{k+1}(\Omega) \cap H_0^1(\Omega)$. Then*

$$\|e_h^n\| \leq C\Big(h^{k+1} + \tau^2\Big) \int_0^T \Big(\|u_t\|_{k+1} + \|u_{ttt}\|\Big) dt. \tag{2.4.24}$$

We assume following convergence results for the discrete time weak Galerkin approximation with the stabilizer which is based on element-boundary-discrepancy.

Theorem 2.4.5. *Let k, j, and l be the non-negative integers with $l \geq k-1$ that define the weak finite element space $\mathcal{V}_h$. Assume that*

$$\mathcal{S}(u_h, v_h) = \sum_{K \in \mathcal{T}_h} h_K^{-1} \langle u_b - u_0|_{\partial K}, v_b - v_0|_{\partial K} \rangle_{\partial K}.$$

Then, we have following error estimates

$$\|e_h^n\| \leq C\Big(h^{s+1} + \tau^2\Big) \int_0^T \Big(\|u_t\|_{s+1} + \|u_{ttt}\|\Big) dt, \tag{2.4.25}$$

where $s = \min\{k, j\}$.

2.5 Numerical Experiments

In this section, we will explore the results of computations for the parabolic problems (2.1.1)-(2.1.2) in $\Omega \times J$, where $\Omega = (0,1) \times (0,1)$ and $J = [0,1]$ with selected values on the degree of polynomials in the weak Galerkin finite element space. The coefficient matrix α is given by identity matrix I, the load function f, initial data u^0 and the Dirichlet boundary value are selected in such a way that exact solution is

$$u = \exp(-t)\sin(\pi x)\sin(\pi y).$$

Triangular meshes are used in these experiments. We have done uniform partitioning of the domain into $n \times n$ sub rectangles which is followed by dividing each rectangular element by the diagonal line with mesh size $h = 1/n$, where n is any non-negative integer. Further, we set $\tau = \mathrm{O}(h^{\gamma+1})$, where γ is selected according to Theorems 2.4.1 - 2.4.3 (for backward Eluer scheme), whereas, we set $\tau = \mathrm{O}(h^{\gamma})$, where γ is selected according to Theorems 2.4.4 - 2.4.5 (for Crank-Nicolson scheme) so that optimal order of convergence is maintained.

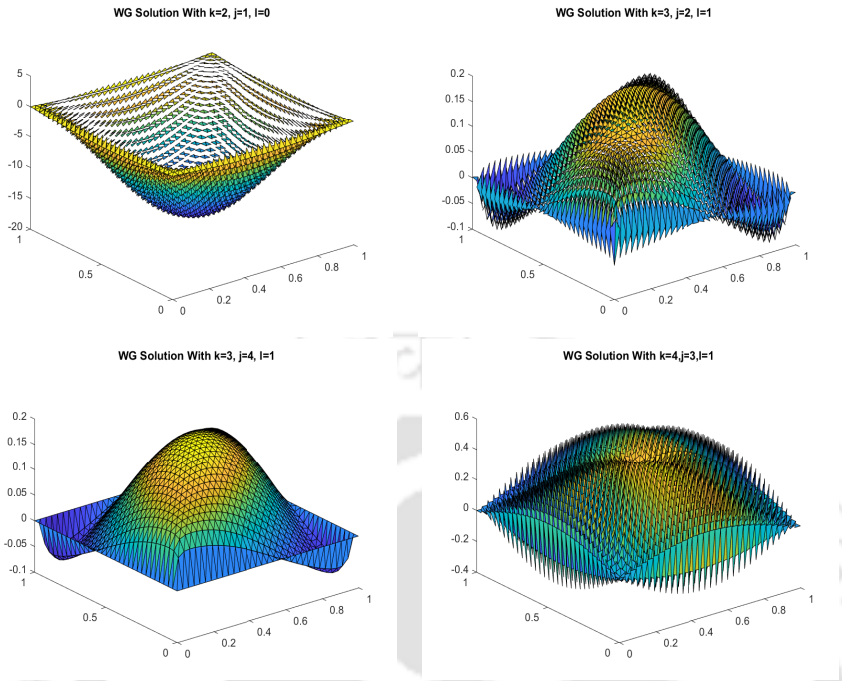

Figure 2.5.1: Plots of the WG approximations at time $t = 1$ for the method of projected element-boundary-discrepancy with $h = 1/32$.

Let U_h^n be the weak Galerkin solution defined by (2.4.1) or (2.4.2). Then, we have calculated the fully discrete error $U_h^n - \mathcal{Q}_h u^n$ with respect to triple bar norm and the L^2 norm at final time $T = 1$.

Recall that the stabilizer for the method of projected element-boundary-discrepancy is given by

$$\mathcal{S}(u_h, v_h) = \sum_{K \in \mathcal{T}_h} h_K^{-1} \langle \mathcal{Q}_m(u_b - u_0|_{\partial K}), \mathcal{Q}_m(v_b - v_0|_{\partial K}) \rangle_{\partial K},$$

where $m = \min\{j, l\}$. For different values of k $(1 \leq k \leq 4)$, j $(0 \leq j \leq 4)$ and l $(0 \leq l \leq 4)$, we have implemented the corresponding backward Euler WG scheme (2.4.1) and Crank-Nicolson scheme (2.4.2) for the problem (2.1.1)-(2.1.2). The rate of convergence for each combination is reported in Table 2.5.1, where NI means the corresponding WG scheme is unstable or not consistent. The convergence order for each particular combination is indicated in the form n/m, where n stand for the order of convergence in the triple bar norm and m for the order of convergence in the L^2 norm. For example, 2/3 would mean that the method is convergent at the rate of h^2 in the triple bar norm and h^3 in the L^2 norm. For $l < k - 1$, the method works poorly. This is an observation from the computation. For instance, we refer to Figure 2.5.1.

Table 2.5.1: Order of convergence with the stabilizer based on projection

$k=1$	$j=0$	$j=1$	$j=2$	$j=3$	$j=4$
$l=0$	1/2	1/2	1/2	1/2	1/2
$l=1$	0	1/2	1/2	1/2	1/2
$l=2$	0	1/2	1/2	1/2	1/2
$l=3$	0	1/2	1/2	1/2	1/2
$l=4$	0	1/2	1/2	1/2	1/2
$k=2$	$j=0$	$j=1$	$j=2$	$j=3$	$j=4$
$l=0$	NI	NI	NI	NI	NI
$l=1$	0	2/3	2/3	2/3	2/3
$l=2$	0	1/2	2/3	2/3	2/3
$l=3$	0	1/2	2/3	2/3	2/3
$l=4$	0	1/2	2/3	2/3	2/3
$k=3$	$j=0$	$j=1$	$j=2$	$j=3$	$j=4$
$l=0$	NI	NI	NI	NI	NI
$l=1$	NI	NI	NI	NI	NI
$l=2$	0	1/2	3/4	3/4	3/4
$l=3$	0	1/2	2/3	3/4	3/4
$l=4$	0	1/2	2/3	3/4	3/4
$k=4$	$j=0$	$j=1$	$j=2$	$j=3$	$j=4$
$l=0$	NI	NI	NI	NI	NI
$l=1$	NI	NI	NI	NI	NI
$l=2$	NI	NI	NI	NI	NI
$l=3$	0	1/2	2/3	4/5	4/5
$l=4$	0	1/2	2/3	3/4	4/5

The method of element-boundary-discrepancy is based on the selection of stabilizer $\mathcal{S}(u_h, v_h) = \sum_{K\in\mathcal{T}_h} h_K^{-1}\langle u_b - u_0|_{\partial K}, v_b - v_0|_{\partial K}\rangle_{\partial K}$. For all the values of $k = 1, 2\ldots, 4, j = 0, 1, \ldots, 4$, and $l = 0, 1, \ldots, 4$, we have implemented both fully discrete schemes. The order of convergence for each combination is listed in Table 2.5.2. Table 2.5.2 suggest that the WG algorithms corresponding to the case of $l = k - 2$ and $j < k$ are solvable. For $l = k - 2$ with $j \geq k$ and $l < k - 2$, the method is solvable but not consistent. At present, we do not have mathematical justification. This is an observation from the numerical experiments, which is illustrated in Figure 2.5.2.

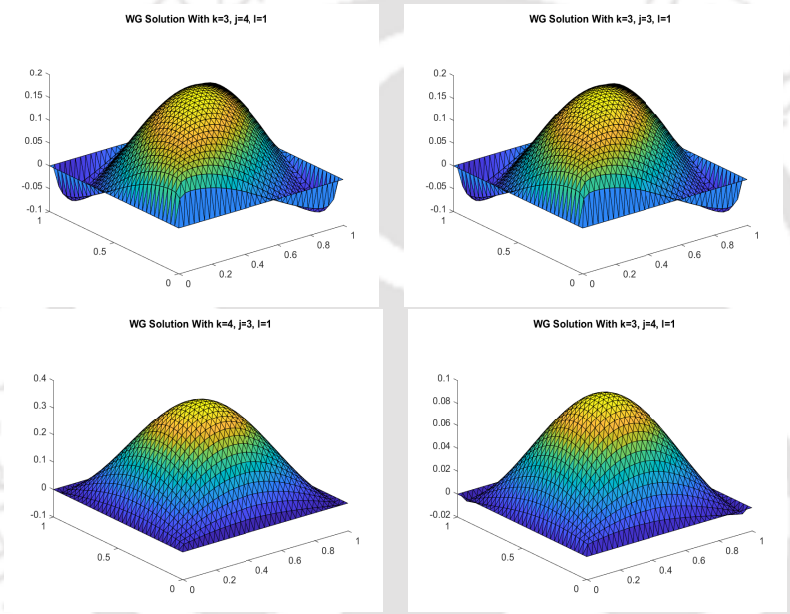

Figure 2.5.2: Plots of the WG approximations at time $t = 1$ for the method of element-boundary-discrepancy with $h = 1/32$.

Concluding Remarks

In this chapter we have conducted a systematic study for the WG-FEMs with local elements $(\mathcal{P}_k(K),\ \mathcal{P}_j(\partial K),\ \left[\mathcal{P}_l(K)\right]^2)$. For all values of k, j and l, we have established a theoretical framework for the convergence and error estimates in the triple bar norm and standard L^2 norm. The results are summarized as follows.

1. For the method of projected element-boundary-discrepancy, we have the following results:

   (a) For $l \geq k - 1$ and $j \geq l$, the corresponding WG scheme is stable and the convergence order of k in the triple bar norm and $k + 1$ in L^2 norm.

Table 2.5.2: Order of convergence with the stabilizer based on element-boundary

$k=1$	$j=0$	$j=1$	$j=2$	$j=3$	$j=4$
$l=0$	0	1/2	1/2	1/2	1/2
$l=1$	0	1/2	1/2	1/2	1/2
$l=2$	0	1/2	1/2	1/2	1/2
$l=3$	0	1/2	1/2	1/2	1/2
$l=4$	0	1/2	1/2	1/2	1/2
$k=2$	$j=0$	$j=1$	$j=2$	$j=3$	$j=4$
$l=0$	0	1/2	NI	NI	NI
$l=1$	0	1/2	2/3	2/3	2/3
$l=2$	0	1/2	2/3	2/3	2/3
$l=3$	0	1/2	2/3	2/3	2/3
$l=4$	0	1/2	2/3	2/3	2/3
$k=3$	$j=0$	$j=1$	$j=2$	$j=3$	$j=4$
$l=0$	NI	NI	NI	NI	NI
$l=1$	0	1/2	2/3	NI	NI
$l=2$	0	1/2	2/3	3/4	3/4
$l=3$	0	1/2	2/3	3/4	3/4
$l=4$	0	1/2	2/3	3/4	3/4
$k=4$	$j=0$	$j=1$	$j=2$	$j=3$	$j=4$
$l=0$	NI	NI	NI	NI	NI
$l=1$	NI	NI	NI	NI	NI
$l=2$	0	1/2	2/3	3/4	NI
$l=3$	0	1/2	2/3	3/4	4/5
$l=4$	0	1/2	2/3	3/4	4/5

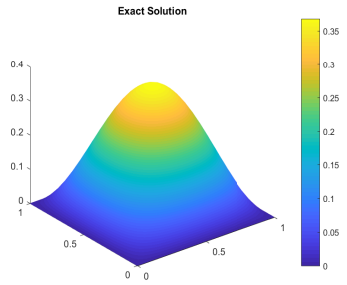

Figure 2.5.3: Exact solution at $t = 1$.

(b) For $l \geq k-1$ and $j < l$, the corresponding WG scheme is stable and has convergence order of $s = \min\{k, j\}$ in the triple bar norm and $s+1$ in L^2 norm.

(c) For $l < k-1$, the corresponding WG scheme is either unstable or not consistent.

2. For the stabilizer with element-boundary-discrepancy, the following results hold true:

(a) For $l \geq k-1$, the corresponding WG scheme is stable and the convergence order of $s = \min\{k, j\}$ in the triple bar norm and $s+1$ in L^2 norm.

(b) For $l = k-2$ and $j < k$, the corresponding WG scheme is stable and the convergence order of $s = \min\{k, j\}$ in the triple bar norm.

(c) For $l = k-2$ with $j \geq k$ and $l < k-2$ the corresponding WG scheme is solvable but not consistent.

Tables for Computational Results for Backward Euler Scheme

Here, we demonstrate some detailed numerical results for a set of selected values of k, j and l. These results will support the rate of convergence reported in Section 2.4. The numerical results are organized as follows. Tables 2.5.3-2.5.4 illustrate the table index numbers for the set value of (k, j, l), and the rest of the tables show the corresponding numerical results. For example, Table 2.5.3 points to the table index numbers when the stabilizer $\mathcal{S}(u_h, v_h) = \sum_{K\in\mathcal{T}_h} h_K^{-1}\langle \mathcal{Q}_m(u_b - u_0|_{\partial K}), \mathcal{Q}_m(v_b - v_0|_{\partial K})\rangle_{\partial K}$ was employed in the numerical scheme. This table has a fixed value of k while j and l are varying. The entry of the table at $(k, j, l) = (2, 1, 2)$ has value Table 2.5.7, which means the computational results for $(k, j, l) = (2, 1, 2)$ should be found in Table 2.5.7.

Table 2.5.3: Table of computations with projection based stabilizer

$k=2$	$j=0$	$j=1$	$j=2$	$j=3$	$j=4$
$l=1$	Table 2.5.5	Table 2.5.6			
$l=2$		Table 2.5.7	Table 2.5.8		
$l=3$				Table 2.5.9	
$l=4$					Table 2.5.10
$k=3$	$j=0$	$j=1$	$j=2$	$j=3$	$j=4$
$l=2$		Table 2.5.11	Table 2.5.12		
$l=3$			Table 2.5.13	Table 2.5.14	
$l=4$					Table 2.5.15
$k=4$	$j=0$	$j=1$	$j=2$	$j=3$	$j=4$
$l=3$			Table 2.5.16	Table 2.5.17	
$l=4$				Table 2.5.18	Table 2.5.19

Table 2.5.4: Table of computations with element boundary based stabilizer

$k=2$	$j=0$	$j=1$	$j=2$	$j=3$	$j=4$
$l=1$		Table 2.5.20			
$l=2$			Table 2.5.21		
$l=3$				Table 2.5.22	
$l=4$					Table 2.5.23
$k=3$	$j=0$	$j=1$	$j=2$	$j=3$	$j=4$
$l=1$		Table 2.5.24			
$l=2$			Table 2.5.25		
$l=3$				Table 2.5.26	
$l=4$					Table 2.5.27
$k=4$	$j=0$	$j=1$	$j=2$	$j=3$	$j=4$
$l=2$			Table 2.5.28	Table 2.5.29	
$l=3$				Table 2.5.30	
$l=4$					Table 2.5.31

Table 2.5.5: Orders of convergence for $k = 2, j = 0, l = 1$

h	$\|\|\|e^n\|\|\|$	*Order*	$\|e^n\|$	*Order*
1/4	8.122260e-01		9.918705e-02	
1/8	8.458429e-01	-5.850856e-02	1.024692e-01	-4.696613e-02
1/16	8.547738e-01	-1.515296e-02	1.030492e-01	-8.143834e-03
1/32	8.570361e-01	-3.813233e-03	1.031780e-01	-1.801845e-03

Table 2.5.6: Orders of convergence for $k = 2, j = 1, l = 1$

h	$\|\|\|e^n\|\|\|$	*Order*	$\|e^n\|$	*Order*
1/4	7.169166e-02		6.189540e-03	
1/8	1.805445e-02	1.989451e+00	7.725189e-04	3.002190e+00
1/16	4.522790e-03	1.997070e+00	9.652195e-05	3.000641e+00
1/32	1.131375e-03	1.999136e+00	1.208548e-05	2.997582e+00

Table 2.5.7: Orders of convergence for $k = 2, j = 1, l = 2$

h	$\|\|\|e^n\|\|\|$	*Order*	$\|e^n\|$	*Order*
1/4	1.652606e-01		1.071478e-02	
1/8	8.483399e-02	9.620281e-01	2.906554e-03	1.882220e+00
1/16	4.268569e-02	9.908899e-01	7.421362e-04	1.969554e+00
1/32	2.137580e-02	9.977740e-01	1.862606e-04	1.994361e+00

Table 2.5.8: Orders of convergence for $k = 2, j = 2, l = 2$

h	$\|\|\|e^n\|\|\|$	*Order*	$\|e^n\|$	*Order*
1/4	9.067179e-03		5.671533e-04	
1/8	1.342686e-03	2.755532e+00	3.809727e-05	3.895979e+00
1/16	2.412130e-04	2.476743e+00	2.851774e-06	3.739756e+00
1/32	5.269517e-05	2.194565e+00	2.672112e-07	3.415807e+00

Table 2.5.9: Orders of convergence for $k = 2, j = 3, l = 3$

h	$\|\|\|e^n\|\|\|$	*Order*	$\|e^n\|$	*Order*
1/4	5.196970e-03		1.247593e-04	
1/8	1.269027e-03	2.033948e+00	1.449317e-05	3.105703e+00
1/16	3.153325e-04	2.008777e+00	1.767677e-06	3.035446e+00
1/32	7.873437e-05	2.001809e+00	2.227589e-07	2.988299e+00

Table 2.5.10: Orders of convergence for $k = 2, j = 4, l = 4$

h	$\|\|\|e^n\|\|\|$	*Order*	$\|e^n\|$	*Order*
1/4	5.196970e-03		6.863976e-04	
1/8	1.269027e-03	1.974641e+00	8.241034e-05	3.046438e+00
1/16	3.153325e-04	1.993420e+00	1.012732e-05	3.024572e+00
1/32	7.873437e-05	1.998177e+00	1.328450e-06	2.930437e+00

Table 2.5.11: Orders of convergence for $k = 3, j = 1, l = 2$

h	$\|\|\|e^n\|\|\|$	*Order*	$\|e^n\|$	*Order*
1/4	1.670987e-01		1.040284e-02	
1/8	8.570960e-02	9.631714e-01	2.830643e-03	1.877776e+00
1/16	4.311791e-02	9.911696e-01	7.233917e-04	1.968281e+00
1/32	2.159118e-02	9.978453e-01	1.815894e-04	1.994097e+00

Table 2.5.12: Orders of convergence for $k = 3, j = 2, l = 2$

h	$\|\|\|e^n\|\|\|$	*Order*	$\|e^n\|$	*Order*
1/4	9.201438e-03		6.734277e-04	
1/8	1.164020e-03	2.982744e+00	4.245300e-05	3.98758e+00
1/16	1.459683e-04	2.995389e+00	2.659047e-06	3.986885e+00
1/32	1.8226353e-05	2.998617e+00	1.733472e-07	3.939173e+00

Table 2.5.13: Orders of convergence for $k = 3, j = 2, l = 3$

h	$\|\|\|e^n\|\|\|$	*Order*	$\|e^n\|$	*Order*
1/4	2.461944e-02		6.907415e-04	
1/8	6.266297e-03	1.974113e+00	8.841892e-05	2.965719e+00
1/16	1.572490e-03	1.994563e+00	1.106445e-05	2.998423e+00
1/32	3.935074e-04	1.998588e+00	1.452128e-06	2.929691e+00

Table 2.5.14: Orders of convergence for $k = 3, j = 3, l = 3$

h	$\|\|\|e^n\|\|\|$	*Order*	$\|e^n\|$	*Order*
1/4	8.712987e-04		4.796983e-05	
1/8	6.345320e-05	3.779402e+00	1.581963e-06	4.922340e+00
1/16	5.576660e-06	3.508220e+00	5.637939e-08	4.810404e+00
1/32	6.010600e-07	3.213821e+00	5.462454e-09	3.367547e+00

Table 2.5.15: Orders of convergence for $k = 3, j = 4, l = 4$

h	$\|\|\|e^n\|\|\|$	*Order*	$\|e^n\|$	*Order*
1/4	4.710535e-04		8.416242e-06	
1/8	5.781054e-05	3.026486e+00	4.870973e-07	4.110894e+00
1/16	7.207176e-06	3.003827e+00	2.990930e-08	4.025544e+00
1/32	9.014070e-07	2.999184e+00	5.234687e-09	2.514419e+00

Table 2.5.16: Orders of convergence for $k = 4, j = 2, l = 3$

h	$\|\|\|e^n\|\|\|$	*Order*	$\|e^n\|$	*Order*
1/4	2.476214e-02		6.646780e-04	
1/8	6.298864e-03	1.974973e+00	8.522381e-05	2.963327e+00
1/16	1.580428e-03	1.994777e+00	1.067046e-05	2.997635e+00
1/32	3.954779e-04	1.998646e+00	1.405669e-06	2.924293e+00

Table 2.5.17: Orders of convergence for $k = 4, j = 3, l = 3$

h	$\|\|\|e^n\|\|\|$	*Order*	$\|e^n\|$	*Order*
1/4	9.038281e-04		5.853914e-05	
1/8	5.715505e-05	3.983096e+00	1.849952e-06	4.983842e+00
1/16	3.583032e-06	3.995628e+00	5.818479e-08	4.990701e+00
1/32	2.251702e-07	3.992093e+00	5.232165e-09	3.475162e+00

Table 2.5.18: Orders of convergence for $k = 4, j = 3, l = 4$

h	$\|\|\|e^n\|\|\|$	*Order*	$\|e^n\|$	*Order*
1/4	2.705839e-03		6.050703e-05	
1/8	3.475762e-04	2.960675e+00	3.841695e-06	3.977288e+00
1/16	4.380892e-05	2.988033e+00	2.399965e-07	4.000658e+000
1/32	5.491110e-06	2.996055e+00	1.574981e-08	3.929607e+00

Table 2.5.19: Orders of convergence for $k = 4, j = 4, l = 4$

h	$\|\|\|e^n\|\|\|$	*Order*	$\|e^n\|$	*Order*
1/4	7.096378e-05		3.364898e-06	
1/8	2.503060e-06	4.825318e+00	7.897632e-08	5.412998e+00
1/16	1.067160e-07	4.551845e+00	2.586304e-09	4.932456e+00
1/32	2.247061e-08	2.247665e+00	1.980236e-10	3.707147e+00

Table 2.5.20: Orders of convergence for $k = 2, j = 1, l = 1$

h	$\|\|\|e^n\|\|\|$	*Order*	$\|e^n\|$	*Order*
1/4	2.476214e-02		6.436302e-03	
1/8	6.298864e-03	1.438592e+00	1.118485e-03	2.524686e+00
1/16	1.580428e-03	1.174826e+00	2.386911e-04	2.228330e+00
1/32	3.954779e-04	1.051661e+00	5.674560e-05	2.072564e+00

Table 2.5.21: Orders of convergence for $k = 2, j = 2, l = 2$

h	$\|\|\|e^n\|\|\|$	*Order*	$\|e^n\|$	*Order*
1/4	9.067179e-03		5.671533e-04	
1/8	1.342686e-03	2.755532e+00	3.809727e-05	3.895979e+00
1/16	2.412130e-04	2.476743e+00	2.851774e-06	3.739756e+00
1/32	5.269517e-05	2.194565e+00	2.672112e-07	3.415807e+00

Table 2.5.22: Orders of convergence for $k = 2, j = 3, l = 3$

h	$\|\|\|e^n\|\|\|$	*Order*	$\|e^n\|$	*Order*
1/4	5.196970e-03		1.247593e-04	
1/8	1.269027e-03	2.033948e+00	1.449317e-05	3.105703e+00
1/16	3.153325e-04	2.008777e+00	1.767677e-06	3.035446e+00
1/32	7.873437e-05	2.001809e+00	2.227589e-07	2.988299e+00

Table 2.5.23: Orders of convergence for $k = 2, j = 4, l = 4$

h	$\|\|\|e^n\|\|\|$	*Order*	$\|e^n\|$	*Order*
1/4	5.276425e-02		6.808492e-04	
1/8	1.342498e-02	1.974641e+00	8.241034e-05	3.046438e+00
1/16	3.371586e-03	1.993420e+00	1.012732e-05	3.024572e+00
1/32	8.439626e-04	1.998177e+00	1.328451e-06	2.930436e+00

Table 2.5.24: Orders of convergence for $k = 3, j = 1, l = 1$

h	$\|\|\|e^n\|\|\|$	*Order*	$\|e^n\|$	*Order*
1/4	1.235269e-01		1.485070e-02	
1/8	4.253941e-02	1.537953e+00	2.061305e-03	2.848901e+00
1/16	1.808968e-02	1.233633e+00	3.432200e-04	2.586353e+00
1/32	8.601552e-03	1.072498e+00	7.111218e-05	2.270965e+00

Table 2.5.25: Orders of convergence for $k = 3, j = 2, l = 2$

h	$\|\|\|e^n\|\|\|$	$Order$	$\|e^n\|$	$Order$
1/4	1.048823e-02		7.276300e-04	
1/8	1.866607e-03	2.490281e+00	6.014785e-05	3.596620e+00
1/16	4.035579e-04	2.209570e+00	6.163514e-06	3.286688e+00
1/32	9.652462e-05	2.063807e+00	8.686333e-07	2.826934e+00

Table 2.5.26: Orders of convergence for $k = 3, j = 3, l = 3$

h	$\|\|\|e^n\|\|\|$	$Order$	$\|e^n\|$	$Order$
1/4	8.712987e-04		4.796983e-05	
1/8	6.345320e-05	3.779402e+00	1.581963e-06	4.922340e+00
1/16	5.576661e-06	3.508220e+00	5.637940e-08	4.810404e+00
1/32	6.010604e-07	3.213820e+00	5.462806e-09	3.367454e+00

Table 2.5.27: Orders of convergence for $k = 3, j = 4, l = 4$

h	$\|\|\|e^n\|\|\|$	$Order$	$\|e^n\|$	$Order$
1/4	4.710535e-04		8.416242e-06	
1/8	5.781054e-05	3.026486e+00	4.870973e-07	4.110894e+00
1/16	7.207176e-06	3.003827e+00	2.990930e-08	4.025544e+00
1/32	9.014071e-07	2.999183e+00	5.234441e-09	2.514487e+00

Table 2.5.28: Orders of convergence for $k = 4, j = 2, l = 2$

h	$\|\|\|e^n\|\|\|$	$Order$	$\|e^n\|$	$Order$
1/4	1.659611e-02		1.913745e-03	
1/8	2.746179e-03	2.595348e+00	1.336710e-04	3.839640e+00
1/16	5.644401e-04	2.282533e+00	1.117750e-05	3.580018e+00
1/32	1.323725e-04	2.092217e+00	1.258791e-06	3.150486e+00

Table 2.5.29: Orders of convergence for $k = 4, j = 3, l = 2$

h	$\|\|\|e^n\|\|\|$	$Order$	$\|e^n\|$	$Order$
1/4	1.475717e-02		1.880159e-03	
1/8	1.839962e-03	3.003668e+00	1.154356e-04	4.025694e+00
1/16	2.298950e-04	3.000629e+00	7.199269e-06	4.003094e+00
1/32	2.881565e-05	2.996050e+00	6.649049e-07	3.436630e+00

Table 2.5.30: Orders of convergence for $k = 4, j = 3, l = 3$

h	$\|\|\|e^n\|\|\|$	*Order*	$\|e^n\|$	*Order*
1/4	1.036100e-03		6.412737e-05	
1/8	9.113811e-05	3.506965e+00	2.618642e-06	4.614049e+00
1/16	9.779329e-06	3.220247e+00	1.323056e-07	4.306873e+00
1/32	1.166344e-06	3.067742e+00	9.121470e-09	3.858464e+00

Table 2.5.31: Orders of convergence for $k = 4, j = 4, l = 4$

h	$\|\|\|e^n\|\|\|$	*Order*	$\|e^n\|$	*Order*
1/4	7.096379e-05		3.3648980e-06	
1/8	2.503069e-06	4.825313e+00	7.895302e-08	5.412998e+00
1/16	1.067212e-07	4.551780e+00	2.582612e-09	4.934091e+00
1/32	2.247073e-08	2.247728e+00	1.988624e-10	3.698988e+00

Tables for Computational Results for Cranck-Nicolson Scheme

Here, we have provided numerical results for some combinations of weak Galerkin spaces in Tables 2.5.32-2.5.36. Interested individuals can draw their conclusions by reading these numerical results.

Table 2.5.32: Order of convergence with projection based stabilizer.

$(\mathcal{P}_1(K),\ \mathcal{P}_0(\partial K),\ [\mathcal{P}_0(K)]^2)$			$(\mathcal{P}_2(K),\ \mathcal{P}_2(\partial K),\ [\mathcal{P}_0(K)]^2)$	
h	$\|e_h^n\|$	Order	$\|e_h^n\|$	Order
1/2	2.168718e-01	-	1.208324e+00	-
1/4	5.240178e-02	2.049154e+00	1.837478e+00	-6.047200e-01
1/8	1.307873e-02	2.002393e+00	2.008965e+00	-1.287254e-01
1/16	3.268995e-03	2.000100e+00	2.049637e+00	-2.891566e-02
1/32	8.171921e-04	2.024246e+00	2.059648e+00	-7.029334e-03
1/64	2.042943e-04	2.000027e+00	2.062140e+00	-1.745005e-03

Table 2.5.33: Order of convergence with projection based stabilizer.

$(\mathcal{P}_2(K),\ \mathcal{P}_1(\partial K),\ \left[\mathcal{P}_1(K)\right]^2)$			$(\mathcal{P}_3(K),\ \mathcal{P}_2(\partial K),\ \left[\mathcal{P}_2(K)\right]^2)$	
h	$\|e_h^n\|$	Order	$\|e_h^n\|$	Order
1/2	4.742297e-02	-	1.011605e-02	-
1/4	6.114685e-03	2.955236e+00	6.690979e-04	3.918285e+00
1/8	7.700643e-04	2.989227e+00	4.238467e-05	3.980603e+00
1/16	9.641000e-05	2.997724e+00	2.657405e-06	3.995453e+00
1/32	1.205529e-05	2.999516e+00	1.662053e-07	3.998980e+00
1/64	1.470435e-06	3.035351e+00	1.072824e-08	3.953481e+00

Table 2.5.34: Order of convergence with projection based stabilizer.

$(\mathcal{P}_4(K),\ \mathcal{P}_1(\partial K),\ \left[\mathcal{P}_2(K)\right]^2)$			$(\mathcal{P}_4(K),\ \mathcal{P}_3(\partial K),\ \left[\mathcal{P}_3(K)\right]^2)$	
h	$\|e_h^n\|$	Order	$\|e_h^n\|$	Order
1/2	2.501580e-01	-	1.758334e-03	-
1/4	7.047045e-02	1.827749e+00	5.825571e-05	4.915665e+00
1/8	1.815161e-02	1.956921e+00	1.847714e-06	4.978586e+00
1/16	4.572101e-03	1.989168e+00	5.7959655e-08	4.994549e+00
1/32	1.145178e-03	1.997286e+00	1.792593e-09	5.014929e+00
1/64	2.864292e-04	1.999321e+00	6.003574e-11	4.900082e+00

Table 2.5.35: Order of convergence with element-boundary based stabilizer.

$(\mathcal{P}_1(K),\ \mathcal{P}_1(\partial K),\ \left[\mathcal{P}_0(K)\right]^2)$			$(\mathcal{P}_2(K),\ \mathcal{P}_1(\partial K),\ \left[\mathcal{P}_1(K)\right]^2)$	
h	$\|e_h^n\|$	Order	$\|e_h^n\|$	Order
1/2	1.999280e-01	-	4.423827e-02	-
1/4	4.949678e-02	2.014074e+00	6.474764e-03	2.772396e+00
1/8	1.242308e-02	1.994312e+00	1.117428e-03	2.534646e+00
1/16	3.109217e-03	1.998400e+00	2.373067e-04	2.235357e+00
1/32	7.774973e-04	1.999642e+00	5.638894e-05	2.073269e+00
1/64	1.943859e-04	1.999914e+00	1.390757e-05	2.019542e+00

Table 2.5.36: Order of convergence with element-boundary based stabilizer.

$(\mathcal{P}_3(K),\ \mathcal{P}_1(\partial K),\ [\mathcal{P}_1(K)]^2)$			$(\mathcal{P}_3(K),\ \mathcal{P}_3(\partial K),\ [\mathcal{P}_2(K)]^2)$	
h	$\|e_h^n\|$	Order	$\|e_h^n\|$	Order
1/2	1.123773e-01	-	1.003671e-02	-
1/4	1.476136e-02	2.928453e+00	6.621477e-04	3.921989e+00
1/8	2.061161e-03	2.840297e+00	4.189261e-05	3.982386e+00
1/16	3.432408e-04	2.586164e+00	2.625530e-06	3.996015e+00
1/32	7.108107e-05	2.271684e+00	1.641935e-07	3.999140e+00
1/64	1.672330e-05	2.087606e+00	1.027354e-08	3.998391e+00
$(\mathcal{P}_4(K),\ \mathcal{P}_1(\partial K),\ [\mathcal{P}_1(K)]^2)$			$(\mathcal{P}_4(K),\ \mathcal{P}_4(\partial K),\ [\mathcal{P}_4(K)]^2)$	
h	$\|e_h^n\|$	Order	$\|e_h^n\|$	Order
1/2	8.853779e-01	-	1.998017e-04	-
1/4	4.968041e-01	8.336163e-01	3.355287e-06	5.895988e+00
1/8	2.556154e-01	9.587023e-01	5.483753e-08	5.935128e+00
1/16	1.287233e-01	9.897016e-01	9.517105e-10	5.848496e+00
1/32	6.447653e-02	9.974272e-01	2.047374e-11	5.538676e+00
1/64	3.225264e-02	9.993569e-01	5.401416e-13	5.244293e+00

3

Error Estimate in WG-FEMs for Parabolic Equations Under Low Regularity Assumptions

In the previous chapter, we have carried out the convergence analysis for sufficiently smooth solution to the parabolic problem (1.1.1)-(1.1.2) with respect to $L^\infty(L^2)$ and $L^\infty(H^1)$ norms. This chapter is devoted to $L^2(L^2)$ norm and $L^2(H^1)$ norm error analysis when the exact solution $u \in L^2(0,T;H^{k+1}(\Omega)) \cap H^1(0,T;H^{k-1}(\Omega))$, for some $k \geq 1$. More precisely, we consider the weak Galerkin finite element approximations of second order linear parabolic problems (1.1.1)-(1.1.2) in two dimensional convex polygonal domains under the low regularities of the solutions. Optimal order error estimates in $L^2(L^2)$ and $L^2(H^1)$ norms are shown to hold for both the spatially discrete continuous time and the discrete time weak Galerkin finite element schemes. We have derived $\mathrm{O}(h^{k+1})$ in $L^2(L^2)$ norm and $\mathrm{O}(h^k)$ in $L^2(H^1)$ norm for finite element partitions with the arbitrary shape of polygons with certain shape regularity. The fully discrete scheme is based on first order in time Euler method. Numerical experiments are reported for several test cases to justify our theoretical convergence results.

3.1 Introduction

To begin with, let us first recall the second order linear parabolic problem of the form

$$u_t - \nabla \cdot (\alpha \nabla u) = f \quad \text{in } \Omega \times (0,T], \tag{3.1.1}$$

with initial and Dirichlet boundary condition

$$u(x,0) = u^0(x) \ \text{ in } \Omega; \quad u = 0 \quad \text{on } \partial\Omega \times (0,T], \tag{3.1.2}$$

This chapter published online in *Appl. Numer. Math. 162: 81-105, 2021.*

where $\Omega \subset \mathbb{R}^2$ is a convex polygonal domain with boundary $\partial\Omega$. We assume that the coefficient matrix $\alpha = (\alpha_{ij}(x))_{2\times 2} \in [L^\infty(\Omega)]^{2^2}$ is symmetric and uniformly positive definite in Ω. The initial function $u^0 : \Omega \to \mathbb{R}$ and the forcing function $f : \Omega \times [0, T] \to \mathbb{R}$ are assumed to be smooth functions in their respective domains of definition, and T is the finite terminal observation time.

The objective of this work is to study the convergence of weak Galerkin finite element methods for linear parabolic equations under low regularity of the solutions with polygonal meshes. The classical finite element approximations of linear parabolic equations have been studied extensively, [111] contains a comprehensive list of references. It is known fact that the order of convergence of finite element approximations depends on the smoothness of a solution. Under the low regularity of solutions, the convergence analysis has remained a major part of the mathematical study up to the present day. To derive optimal $\mathrm{O}(h^{k+1})$ $(k \geq 1)$ in the L^2 norm for WG-FEM, the minimum regularity assumption on u should be $u \in H^1(0, T; H^{k+1}(\Omega))$ (for instance, see [35, 77, 132]). In this chapter, we indeed have shown the convergence of WG finite element solution to the true solution at an optimal rate in both the $L^2(H^1)$ and $L^2(L^2)$ norms for the WG finite element space $(\mathcal{P}_k(K),\ \mathcal{P}_k(\partial K),\ \left[\mathcal{P}_{k-1}(K)\right]^2)$ under the assumption that $u \in L^2(0, T; H^{k+1}(\Omega)) \cap H^1(0, T; H^{k-1}(\Omega))$. The key element of our proof is the use of L^2 projection instead of the usual elliptic projection. To best of our knowledge, WG-FEM for the parabolic equation under low regularity has not been studied earlier. Our results are intended to enhance the numerical analysis of linear parabolic equations with polygonal meshes under low regularity assumptions. Classical finite element methods for parabolic problems under low regularity can be traced back in [20, 21, 110].

We recall following regularity result for the initial boundary value problem (3.1.1)-(3.1.2) (see, [86], p. 287, Theorem 2.10).

Theorem 3.1.1. *Assume that $f \in L^2(0, T; H^{k-1}(\Omega))$ and $\psi \in H^k(\Omega)$ for some $k \geq 1$. Then the solution of (3.1.1)-(3.1.2) satisfies*

$$u \in L^2(0, T; H^{k+1}(\Omega)) \cap H^1(0, T; H^{k-1}(\Omega)).$$

The remaining part of this chapter is organized as follows. In Section 3.2, we review the definitions of weak gradient with its discrete analogs in suitable polynomial spaces and derive an error equation. Section 3.3 is devoted to the optimal order error estimates of semidiscrete WG-FEM algorithm. In Section 3.4, a backward Euler scheme is proposed and optimal a priori error bounds in $L^2(H^1)$ norm and $L^2(L^2)$ norm are established. Section 3.5 focuses on some numerical results that confirm the convergence theory developed in earlier section.

3.2 Semidiscrete Approximation

This section deals with spatially discrete scheme for the parabolic problem (3.1.1)-(3.1.2).

Let $\mathcal{T}_h$ be the finite element discretization of Ω as described in Chapter 1. Based on the discretization $\mathcal{T}_h$, for $k \geq 1$, we define following weak Galerkin finite element space

$$\mathcal{V}_h = \{v_h = \{v_0, v_b\} : \ v_h|_K \in \mathcal{V}(k, k-1, K), \ [v_h]_e = 0, \ \forall e \in \mathcal{F}_h^0, \ K \in \mathcal{T}_h\}. \tag{3.2.1}$$

Here, $[v_h]_e = [v_b]$ denotes the jump of $v_h \in \prod_{K\in\mathcal{T}_h} \mathcal{V}(k, k-1, K)$ across an interior edge $e \in \mathcal{F}_h^0$ and $\mathcal{V}(k, k-1, K)$ is the local weak Galerkin space as defined in (1.4.5). Denote by $\mathcal{V}_h^0$ the subspace of $\mathcal{V}_h$ consisting of all finite element functions with vanishing boundary value

$$\mathcal{V}_h^0 = \{v_h \in \mathcal{V}_h : v_b|_{\partial\Omega} = 0\}. \tag{3.2.2}$$

For each $v_h = \{v_0, v_b\} \in \mathcal{V}_h$, we recall its discrete weak gradient $(\nabla_w v_h) \in [\mathcal{P}_{k-1}(K)]^2$ that satisfies the following equation

$$(\nabla_w v_h, \mathbf{q})_K = -\int_K v_0(\nabla \cdot \mathbf{q})dK + \int_{\partial K} v_b(\mathbf{q}\cdot\mathbf{n})ds \ \ \forall \mathbf{q} \in [\mathcal{P}_{k-1}(K)]^2, \tag{3.2.3}$$

where $\mathbf{n}$ is the unit outward normal to ∂K.

For each element $K \in \mathcal{T}_h$ and edge $e \in \mathcal{F}_h$, operators $Q_0 : L^2(K) \to \mathcal{P}_k(K)$ and $Q_b : L^2(e) \to \mathcal{P}_k(e)$ are the usual L^2 projections. For any $\phi \in H^1(K)$, we write $Q_h\phi = \{Q_0\phi, Q_b\phi\}$. In addition to Q_h, let $\mathbb{Q}_h : [L^2(K)]^2 \to [\mathcal{P}_{k-1}(K)]^2$ be an another local L^2 projection. For the L^2 projections, we have following results (Lemma 4.1, [123]).

Lemma 3.2.1. *Let $\mathcal{T}_h$ be a finite element partition of Ω satisfying the shape regularity assumption as specified in [123]. Then, for $v \in H^{k+1}(\Omega)$, we have*

$$\sum_{K\in\mathcal{T}_h} \left(\|v - Q_0 v\|_K^2 + h_K^2\|\nabla(v - Q_0 v)\|_K^2\right) \ \leq \ Ch^{2k+2}\|v\|_{k+1}^2,$$

$$\sum_{K\in\mathcal{T}_h} \left(\|\nabla v - \mathbb{Q}_h(\nabla v)\|_K^2 + h_K^2\|\nabla(\nabla v - \mathbb{Q}_h(\nabla v))\|_K^2\right) \ \leq \ Ch^{2k}\|v\|_{k+1}^2.$$

The following identity will be frequently used in our analysis (cf. [121])

$$\nabla_w(Q_h\phi) = \mathbb{Q}_h(\nabla\phi) \ \ \forall \phi \in H^1(K). \tag{3.2.4}$$

Further, for $\phi \in H^1(K)$, we use definitions of L^2 projections Q_0 and Q_b to have

$$\begin{aligned} \|Q_0\phi - Q_b\phi\|_{\partial K}^2 &= \langle Q_0\phi - Q_b\phi, Q_0\phi - Q_b\phi\rangle_{\partial K} \\ &= \langle Q_0\phi - Q_b\phi, Q_0\phi - \phi\rangle_{\partial K} \\ &\leq \|Q_0\phi - Q_b\phi\|_{\partial K}\|Q_0\phi - \phi\|_{\partial K}. \end{aligned} \tag{3.2.5}$$

Now, we recall the bilinear map $\mathcal{A}_w : \mathcal{V}_h^0 \times \mathcal{V}_h^0 \to \mathbb{R}$ given by

$$\mathcal{A}_w(w_h, v_h) = \sum_{K\in\mathcal{T}_h} \big(\alpha\nabla_w w_h, \nabla_w v_h\big)_K + \mathcal{S}(w_h, v_h) \ \ \forall w_h,\ v_h \in \mathcal{V}_h^0. \tag{3.2.6}$$

Here, for $w_h = \{w_0, w_b\},\ v_h = \{v_0, v_b\} \in \mathcal{V}_h^0$, the stabilizer $\mathcal{S}(\cdot,\cdot)$ is defined as

$$\mathcal{S}(w_h, v_h) = \sum_{K\in\mathcal{T}_h} h_K^{-1}\langle w_0 - w_b, v_0 - v_b\rangle_{\partial K}. \tag{3.2.7}$$

The finite element space $\mathcal{V}_h^0$ is a normed linear space with a triple-bar norm given by (cf. [121])

$$|||v_h|||^2 = \sum_{K\in\mathcal{T}_h} \|\alpha^{\frac{1}{2}}\nabla_w v_h\|_K^2 + \sum_{K\in\mathcal{T}_h} h_K^{-1}\|v_0 - v_b\|_{\partial K}^2 = \mathcal{A}_w(v_h, v_h). \tag{3.2.8}$$

Further, the following Poincaŕe-type inequality holds true (cf. [90])

$$\|v_0\| \le C|||v_h|||,\ v_h = \{v_0, v_b\} \in \mathcal{V}_h^0. \tag{3.2.9}$$

For any $\phi \in H_0^1(\Omega)$, it is easy to notice that

$$\|\phi\|_{1,h}^2 = \sum_{K\in\mathcal{T}_h} \|\nabla\phi\|_K^2 = \|\nabla\phi\|^2. \tag{3.2.10}$$

Remark 3.2.1. *For any $\phi \in H^{k+1}(\Omega)$, Lemma 3.2.1 and inequality (3.2.5) yield following discrete H^1 norm error estimate*

$$\begin{aligned}
\|Q_h\phi - \phi\|_{1,h}^2 &= \sum_{K\in\mathcal{T}_h} \Big(\|\nabla(Q_0\phi - \phi)\|_K^2 + h_K^{-1}\|Q_0\phi - Q_b\phi\|_{\partial K}^2\Big) \\
&\le Ch^{2k}\|\phi\|_{k+1}^2 + C\sum_{K\in\mathcal{T}_h} h_K^{-1}\|Q_0\phi - \phi\|_{\partial K}^2 \\
&\le Ch^{2k}\|\phi\|_{k+1}^2 + C\sum_{K\in\mathcal{T}_h} \Big(h_K^{-2}\|Q_0\phi - \phi\|_K^2 + \|\nabla(Q_0\phi - \phi)\|_K^2\Big) \\
&\le Ch^{2k}\|\phi\|_{k+1}^2.
\end{aligned} \tag{3.2.11}$$

For a time dependent weak function $v_h : [0,T] \to \mathcal{V}_h^0$, we write $v_h(t) := \{v_0(t), v_b(t)\}$ and $v_{ht}(t) := \{v_0'(t), v_b'(t)\}$. For simplicity, we use $v_h = \{v_0, v_b\}$ for $v_h(t)$ and $v_{ht} = \{v_0', v_b'\}$ for $v_{ht}(t)$.

The semidiscrete weak Galerkin finite element approximation to (3.1.1)-(3.1.2) is defined as follows: Find $u_h : [0,T] \to \mathcal{V}_h^0$ satisfying both $u_h(0) = Q_h u^0$ and following equation

$$(u_{ht}, v_0) + \mathcal{A}_w(u_h, v_h) = (f, v_0) \ \ \forall v_h = \{v_0, v_b\} \in \mathcal{V}_h^0. \tag{3.2.12}$$

We now split our semidiscrete error $u-u_h$ using L^2 projection Q_h as an intermediate operator. We write

$$u - u_h = (u - Q_h u) + (Q_h u - u_h).$$

For our convenience, we define

$$e_h := \{e_0, e_b\} = u_h - Q_h u. \tag{3.2.13}$$

Error e_h is characterized in the following result, which is key for our convergence analysis.

Lemma 3.2.2. *Suppose error e_h is defined by (3.2.13). Then, for all $v_h = \{v_0, v_b\} \in \mathcal{V}_h^0$, we have*

$$(e_{ht}, v_0) + \mathcal{A}_w(e_h, v_h) = l_1(u, v_h) + l_2(u, v_h) + \mathcal{S}(Q_h u, v_h), \tag{3.2.14}$$

where bilinear forms $l_1(\cdot,\cdot)$ and $l_2(\cdot,\cdot)$ are given by

$$\begin{aligned} l_1(u, v_h) &= \sum_{K\in\mathcal{T}_h} \langle (\alpha\nabla u - \mathbb{Q}_h(\alpha\nabla u))\cdot \mathbf{n}, v_0 - v_b\rangle_{\partial K}, \\ l_2(u, v_h) &= \sum_{K\in\mathcal{T}_h} (\alpha\mathbb{Q}_h(\nabla u) - \mathbb{Q}_h(\alpha\nabla u), \nabla_w v_h)_K. \end{aligned}$$

Proof. For any $v_h = \{v_0, v_b\} \in \mathcal{V}_h^0$, we test equation (3.1.1) against v_0 on each element $K \in \mathcal{T}_h$ to obtain

$$\begin{aligned} (f, v_0) &= (u_t, v_0) - \sum_{K\in\mathcal{T}_h} (\nabla\cdot(\alpha\nabla u), v_0)_K \\ &= (u_t, v_0) + \sum_{K\in\mathcal{T}_h} (\alpha\nabla u, \nabla v_0)_K - \sum_{K\in\mathcal{T}_h} \langle \alpha\nabla u\cdot\mathbf{n}, v_0\rangle_{\partial K} \\ &= (u_t, v_0) + \sum_{K\in\mathcal{T}_h} (\alpha\nabla u, \nabla v_0)_K - \sum_{K\in\mathcal{T}_h} \langle \alpha\nabla u\cdot\mathbf{n}, v_0 - v_b\rangle_{\partial K}, \end{aligned} \tag{3.2.15}$$

where we have used the divergence theorem and the fact that

$$\sum_{K\in\mathcal{T}_h} \langle \alpha\nabla u\cdot\mathbf{n}, v_b\rangle_{\partial K} = 0.$$

Then integration by parts together with definition (1.4.9) for weak gradient and L^2 projection $\mathbb{Q}_h$ yield

$$\begin{aligned} (\mathbb{Q}_h(\alpha\nabla u), \nabla_w v_h)_K &= -(v_0, \nabla\cdot(\mathbb{Q}_h(\alpha\nabla u)))_K + \langle v_b, \mathbb{Q}_h(\alpha\nabla u)\cdot\mathbf{n}\rangle_{\partial K} \\ &= (\nabla v_0, \mathbb{Q}_h(\alpha\nabla u))_K - \langle v_0 - v_b, \mathbb{Q}_h(\alpha\nabla u)\cdot\mathbf{n}\rangle_{\partial K} \\ &= (\nabla v_0, \alpha\nabla u)_K - \langle v_0 - v_b, \mathbb{Q}_h(\alpha\nabla u)\cdot\mathbf{n}\rangle_{\partial K}. \end{aligned} \tag{3.2.16}$$

Combining (3.2.15), (3.2.16) and (3.2.4), we have

$$\begin{aligned}(f, v_0) &= (Q_h u_t, v_0) + \sum_{K\in\mathcal{T}_h} (\mathbb{Q}_h(\alpha\nabla u), \nabla_w v_h)_K \\ &\quad + \sum_{K\in\mathcal{T}_h} \langle v_0 - v_b, (\mathbb{Q}_h(\alpha\nabla u) - \alpha\nabla u)\cdot \mathbf{n}\rangle_{\partial K} \\ &= (Q_h u_t, v_0) + \sum_{K\in\mathcal{T}_h} (\alpha\mathbb{Q}_h(\nabla u), \nabla_w v_h)_K - l_2(u, v_h) - l_1(u, v_h) \\ &= ((Q_h u)_t, v_0) + \sum_{K\in\mathcal{T}_h} (\alpha\nabla_w Q_h u, \nabla_w v)_K - l_2(u, v_h) - l_1(u, v_h). \quad (3.2.17)\end{aligned}$$

Adding $\mathcal{S}(Q_h u, v_h)$ to both sides of the above equation gives

$$((Q_h u)_t, v_0) + \mathcal{A}_w(Q_h u, v_h) = (f, v_0) + l_1(u, v_h) + l_2(u, v_h) + \mathcal{S}(Q_h u, v_h). \quad (3.2.18)$$

Subtracting (3.2.12) from (3.2.18) leads to desire result. □

Lemma 3.2.3. *Assume that $\mathcal{T}_h$ is shape regular discretization of Ω. Then, for $u \in H^{k+1}(\Omega)$ and $v_h = \{v_0, v_b\} \in \mathcal{V}_h^0$, we have*

$$\begin{aligned}|l_1(u, v_h)| &\le C(\|\alpha\|_{k,\infty}) h^k \|u\|_{k+1} |||v_h|||, \\ |l_2(u, v_h)| &\le C(\|\alpha\|_{1,\infty}) h^{k+1} \|u\|_{k+1} |||v_h|||, \\ |\mathcal{S}(Q_h u, v_h)| &\le C h^k \|u\|_{k+1} |||v_h|||,\end{aligned}$$

where $C(\|\alpha\|_{k,\infty})$ is a positive constant depending on $\|\alpha\|_{k,\infty}$-the element-wise $W^{k,\infty}$ norm of the coefficient matrix α.

Proof. For first estimate, we use trace inequality (1.4.19) and Lemma 3.2.1 to have

$$\begin{aligned}|l_1(u, v)| &\le \sum_{K\in\mathcal{T}_h} \|\alpha\nabla u - \mathbb{Q}_h(\alpha\nabla u)\|_{\partial K} \|v_0 - v_b\|_{\partial K} \\ &\le C\Big(\sum_{K\in\mathcal{T}_h} h_K \|\alpha\nabla u - \mathbb{Q}_h(\alpha\nabla u)\|_{\partial K}^2\Big)^{\frac{1}{2}} \left(\sum_{K\in\mathcal{T}_h} h_K^{-1} \|v_0 - v_b\|_{\partial K}^2\right)^{\frac{1}{2}} \\ &\le C\left(\sum_{K\in\mathcal{T}_h} \left(\|\alpha\nabla u - \mathbb{Q}_h(\alpha\nabla u)\|_K^2 + h_K^2 \|\nabla(\alpha\nabla u - \mathbb{Q}_h(\alpha\nabla u))\|_K^2\right)\right)^{\frac{1}{2}} \\ &\quad \times \left(\sum_{K\in\mathcal{T}_h} \left(\|\alpha^{\frac{1}{2}}\nabla_w v_h\|_K^2 + h_K^{-1} \|v_0 - v_b\|_{\partial K}^2\right)\right)^{\frac{1}{2}} \\ &\le C(\|\alpha\|_{k,\infty}) h^k \|u\|_{k+1} |||v_h|||. \quad (3.2.19)\end{aligned}$$

Let $\bar{\alpha}$ be the average of α on each element $K \in \mathcal{T}_h$. Then, we have (see, page 2118 in [123])

$$\|\alpha - \bar{\alpha}\|_{L^\infty(\Omega)} \leq Ch\|\nabla\alpha\|_{L^\infty(\Omega)}. \tag{3.2.20}$$

Then, using the definition of $\mathbb{Q}_h$ operator, Lemma 3.2.1 and estimate (3.2.20), we obtain

$$\begin{aligned}
|l_2(u,v)| &= \Big|\sum_{K\in\mathcal{T}_h}(\alpha\mathbb{Q}_h(\nabla u) - \alpha\nabla u, \nabla_w v_h)_K\Big| \\
&= \Big|\sum_{K\in\mathcal{T}_h}(\mathbb{Q}_h(\nabla u) - \nabla u, (\alpha-\bar{\alpha})\nabla_w v_h)_K\Big| \\
&\leq \sum_{K\in\mathcal{T}_h}\Big|(\mathbb{Q}_h(\nabla u) - \nabla u, (\alpha-\bar{\alpha})\nabla_w v_h)_K\Big| \\
&\leq Ch\|\alpha\|_{1,\infty}\sum_{K\in\mathcal{T}_h}\Big|(\mathbb{Q}_h(\nabla u) - \nabla u, \nabla_w v_h)_K\Big| \\
&\leq C(\|\alpha\|_{1,\infty})h^{k+1}\|u\|_{k+1}|||v_h|||.
\end{aligned} \tag{3.2.21}$$

Using the definition of Q_b operator and trace inequality (1.4.19), we obtain

$$\begin{aligned}
|S(Q_h u, v_h)| &= \Big|\sum_{K\in\mathcal{T}_h} h_K^{-1}\langle Q_0 u - Q_b u, v_0 - v_b\rangle_{\partial K}\Big| \\
&= \Big|\sum_{K\in\mathcal{T}_h} h_K^{-1}\langle Q_0 u - u, v_0 - v_b\rangle_{\partial K}\Big| \\
&\leq \Big(\sum_{K\in\mathcal{T}_h} h_K^{-1}\|Q_0 u - u\|_{\partial K}^2\Big)^{\frac{1}{2}}\Big(\sum_{K\in\mathcal{T}_h} h_K^{-1}\|v_0 - v_b\|_{\partial K}^2\Big)^{\frac{1}{2}} \\
&\leq \Big(\sum_{K\in\mathcal{T}_h}\Big(h_K^{-2}\|Q_0 u - u\|_K^2 + \|\nabla(Q_0 u - u)\|_K^2\Big)\Big)^{\frac{1}{2}}|||v||| \\
&\leq Ch^k\|u\|_{k+1}|||v_h|||. \quad \square
\end{aligned} \tag{3.2.22}$$

3.3 Semidiscrete Error Analysis

This section deals with the error analysis for the spatially discrete scheme (3.2.12). Optimal order of convergence in both $L^2(L^2)$ and $L^2(H^1)$ norms are established.

Theorem 3.3.1. *Let $u \in L^2(0,T;H^{k+1}(\Omega))$ be the solution of (3.1.1)-(3.1.2) and u_h be the solution of (3.2.12). Then, we have*

$$\Big(\int_0^T \|u - u_h\|_{1,h}^2 dt\Big)^{\frac{1}{2}} \leq Ch^k\Big(\int_0^T \|u\|_{k+1}^2 ds\Big)^{\frac{1}{2}}.$$

Proof. By letting $v_h = e_h$ in (3.2.14), we have

$$\frac{1}{2}\frac{d}{dt}(e_0, e_0) + |||e_h|||^2 = l_1(u, e_h) + l_2(u, e_h) + \mathcal{S}(Q_h u, e_h).$$

By integration over the time period $[0, t]$, we get

$$\frac{1}{2}\|e_0(t)\|^2 + \int_0^t |||e_h|||^2 ds \leq \int_0^t |l_1(u, e)| ds + \int_0^t |l_2(u, e)| ds + \int_0^t |\mathcal{S}(Q_h u, e_h)| ds.$$

Here, we have used the fact that $e_h(0) = 0$. It then follows from Lemma 3.2.3 that

$$\frac{1}{2}\|e_0(t)\|^2 + \int_0^t |||e_h|||^2 ds \leq Ch^{2k} \int_0^t \|u\|_{k+1}^2 ds + \frac{1}{2}\int_0^t |||e_h|||^2 ds. \tag{3.3.1}$$

Hence, we have

$$\|e_0(t)\|^2 + \int_0^t |||e_h|||^2 ds \leq Ch^{2k} \int_0^t \|u\|_{k+1}^2 ds. \tag{3.3.2}$$

Now, triangle inequality, Lemma 3.2.1, estimates (3.2.11) and (3.3.2) lead to desire result. □

Remark 3.3.1. *Theorem 3.3.1 is analogous to Theorem 4.2 in [132]. It is worth to note that Theorem 4.2 in [132] is derived under the assumption that the coefficient matrix α is piecewise constants with respect to the finite element discretization.*

Next, for the L^2 norm error estimate, we now consider the following auxiliary problem: For every $t \in [0, T]$, find $z(t) \in H_0^1(\Omega) \cap H^2(\Omega)$ such that

$$-\nabla \cdot (\alpha \nabla z(t)) = e_h(t). \tag{3.3.3}$$

Then, we may define $z_h(t) \in \mathcal{V}_h^0$ as the solution to following discrete elliptic problem

$$\mathcal{A}_w(z_h(t), v_h) = (e_h(t), v_h) \ \ \forall v_h \in \mathcal{V}_h^0, \ \ t \in (0, T]. \tag{3.3.4}$$

Setting $v_h = z_h$ in (3.3.4) and using the estimate (3.2.9), we obtain

$$|||z_h||| \leq C\|e_h\|. \tag{3.3.5}$$

Clearly, z_h is the weak Galerkin finite element approximation to z and satisfies following estimates (see, Theorem 4.10 in [121])

$$\|Q_h z - z_h\|_{1,h} \leq Ch\|z\|_2. \tag{3.3.6}$$

Now, we combine estimates (3.2.11) and (3.3.6) to obtain

$$\|z - z_h\|_{1,h} \leq \|z - Q_h z\|_{1,h} + \|Q_h z - z_h\|_{1,h} \leq Ch\|z\|_2 \leq Ch\|e_h\|. \tag{3.3.7}$$

Here, we have used the standard a priori estimate for elliptic problem.

Setting $v_h = e_h$ in (3.3.4) and further using identity (3.2.14), we have

$$\begin{aligned} \|e_h\|^2 &= \mathcal{A}_w(z_h, e_h) \\ &= l_1(u, z_h) + l_2(u, z_h) + \mathcal{S}(Q_h u, z_h) - (e_{ht}, z_h). \end{aligned} \tag{3.3.8}$$

Differentiating (3.3.4) with respect to t, we obtain

$$\mathcal{A}_w(z_{ht}, v_h) = (e_{ht}, v_h) \quad \forall v_h \in \mathcal{V}_h^0.$$

Thus, we have

$$\frac{1}{2}\frac{d}{dt}\mathcal{A}_w(z_h, z_h) = \mathcal{A}_w(z_{ht}, z_h) = (e_{ht}, z_h),$$

which together with (3.3.8), we arrive at

$$\|e_h\|^2 = l_1(u, z_h) + l_2(u, z_h) + \mathcal{S}(Q_h u, z_h) - \frac{1}{2}\frac{d}{dt}\mathcal{A}_w(z_h, z_h). \tag{3.3.9}$$

Hence, integrating (3.3.9) from 0 to T we obtain

$$\begin{aligned} \int_0^T \|e_h\|^2 ds + \frac{1}{2}|||z_h(T)|||^2 \leq & \int_0^T |l_1(u, z_h)| ds + \int_0^T |l_2(u, z_h)| ds \\ & + \int_0^T |\mathcal{S}(Q_h u, z_h)| ds + \frac{1}{2}|||z_h(0)|||^2. \end{aligned} \tag{3.3.10}$$

Taking $t \to 0$, it now follows from (3.3.4) that

$$|||z_h(0)|||^2 = A(z_h(0), z_h(0)) = (e_h(0), z_h(0)) = 0$$

and hence, estimate (3.3.10) reduces to

$$\int_0^T \|e_h\|^2 ds \leq \int_0^T |l_1(u, z_h)| ds + \int_0^T |l_2(u, z_h)| ds + \int_0^T |\mathcal{S}(Q_h u, z_h)| ds. \tag{3.3.11}$$

Arguing as in (3.2.19) and using estimate (3.3.7), we obtain

$$\begin{aligned} |l_1(u, z_h)| &\leq C(\|\alpha\|_{k,\infty}) h^k \|u\|_{k+1} \left(\sum_{K \in \mathcal{T}_h} h_K^{-1} \|z_0 - z_b\|_{\partial K}^2 \right)^{\frac{1}{2}} \\ &\leq C(\|\alpha\|_{k,\infty}) h^k \|u\|_{k+1} \left(\sum_{K \in \mathcal{T}_h} h_K^{-1} \|(z_0 - z) - (z_b - z)\|_{\partial K}^2 \right)^{\frac{1}{2}} \\ &\leq C(\|\alpha\|_{k,\infty}) h^k \|u\|_{k+1} \|z_h - z\|_{1,h} \\ &\leq C(\|\alpha\|_{k,\infty}) h^{k+1} \|u\|_{k+1} \|e_h\|. \end{aligned} \tag{3.3.12}$$

Similarly, we have

$$\begin{aligned}|\mathcal{S}(Q_h u, z_h)| &\leq Ch^k\|u\|_{k+1}\Big(\sum_{K\in\mathcal{T}_h} h_K^{-1}\|(z_0-z)-(z_b-z)\|_{\partial K}^2\Big)^{\frac{1}{2}}\\ &\leq Ch^k\|u\|_{k+1}\|z_h-z\|_{1,h}\\ &\leq Ch^{k+1}\|u\|_{k+1}\|e_h\|. \end{aligned} \tag{3.3.13}$$

For $l_2(u, z_h)$, we use Lemma 3.2.3 to have

$$\begin{aligned}|l_2(u,z_h)| &\leq C(\|\alpha\|_{1,\infty})h^{k+1}\|u\|_{k+1}|||z_h|||\\ &\leq C(\|\alpha\|_{1,\infty})h^{k+1}\|u\|_{k+1}\|e_h\|. \end{aligned} \tag{3.3.14}$$

Here, we have used the estimate (3.3.5).

Now, we use the estimates (3.3.12)-(3.3.14) in (3.3.11) to have

$$\int_0^T \|e_h\|^2 ds \leq Ch^{2(k+1)}\int_0^T \|u\|_{k+1}^2 ds. \tag{3.3.15}$$

Thus we have proved the following optimal $L^2(0,T;L^2(\Omega))$ norm estimate.

Theorem 3.3.2. *Let $u \in L^2(0,T;H^{k+1}(\Omega))$ be the solution of (3.1.1)-(3.1.2) and u_h be the solution of (3.2.12). Then, we have*

$$\Big(\int_0^T \|u-u_h\|^2 dt\Big)^{\frac{1}{2}} \leq Ch^{k+1}\Big(\int_0^T \|u\|_{k+1}^2 dt\Big)^{\frac{1}{2}}.$$

Remark 3.3.2. *In literature, concerning the convergence of WG-FEM for parabolic problems, $O(h^{k+1})$ with respect to L^2 norm is derived under the assumption that $u \in H^1(0,T;H^{k+1}(\Omega))$ (see, e.g., Theorem 4.6 in [132] and Theorem 4.4 in [77]). In Theorem 3.3.2, we indeed have proved $O(h^{k+1})$ order error estimates under low regularity assumption $u \in L^2(0,T;H^{k+1}(\Omega))$. We note that the assumption $u \in L^2(0,T;H^{k+1}(\Omega))$, for $u^0 \in H^k(\Omega)$ and $f \in L^2(0,T;H^{k-1})$ (cf. Theorem 2.10 in [86]), is essentially leads to $u \in H^1(0,T;H^{k-1}(\Omega))$. In this work, it is implicitly assumed that $u \in L^2(0,T;H^{k+1}(\Omega)) \cap H^1(0,T;H^{k-1}(\Omega))$.*

3.4 Fully Discrete Scheme

We now turn our attention to fully discrete scheme based on first order backward time discretization. We have extended the classical finite element error analysis technique (cf. [20, 110]) to WG-FEMs with low regularity. It is worth to note that the algorithms presented in [20, 110] are only valid for linear finite elements with triangular meshes.

Optimal order error estimates in $L^2(L^2)$ and $L^2(H^1)$ norms are shown to hold even if the solution $u \in L^2(0,T;H^{k+1}(\Omega)) \cap H^1(0,T;H^1(\Omega))$.

First we divide the time interval $J = [0,T]$ into M equally spaced sub intervals $I_n = (t_{n-1}, t_n]$, $n = 1, 2, \ldots, M$ with $t_0 = 0$, and $t_M = T$ and $\tau = t_n - t_{n-1}$, the time step. For a sequence $\{\omega^n\}_{n=0}^N \subset L^2(\Omega)$, we define

$$\partial_\tau \omega^n = \frac{\omega^n - \omega^{n-1}}{\tau}, \quad n = 1, 2, \ldots, M.$$

Also, for a continuous mapping $\phi : [0,T] \to L^2(\Omega)$, we define $\phi^n = \phi(., t_n)$, $0 \le n \le M$. Further, for a given Banach space $\mathcal{B}$ and some function $\xi \in L^2(0,T;\mathcal{B})$, we write

$$\overline{\xi}^{\,n} = \tau^{-1} \int_{t_{n-1}}^{t_n} \xi(x,t)dt. \tag{3.4.1}$$

With the above notation, we now introduce the fully discrete weak Galerkin finite element approximation to the problem (3.1.1)-(3.1.2): Let $U_h^0 = Q_h u^0$ and $U_h^n = \{U_0^n, U_b^n\} \in \mathcal{V}_h^0$ be the fully discrete solution of u at $t = t_n$ which we shall define through the following scheme

$$(\partial_\tau U_h^n, v_h) + \mathcal{A}_w(U_h^n, v_h) = (\overline{f}^{\,n}, v_h) \;\; \forall v_h \in \mathcal{V}_h^0, \;\; n = 1, \ldots, M. \tag{3.4.2}$$

Here, $\overline{f}^{\,n}$ is defined as in (3.4.1).

For our convenience, we define a piecewise constant function $U_{h,\tau}$ in time by

$$U_{h,\tau}(x,t) = U_h^n(x) \;\; \forall t \in I_n, \;\; n = 1, 2, \ldots, M. \tag{3.4.3}$$

As a standard error analysis trick, an intermediate operator $\overline{Q}_\tau : (0,T] \to \mathcal{V}_h^0$ is introduced and defined as

$$\overline{Q}_\tau|_{I_n} = \overline{Q}_\tau^{\,n} := \{\overline{Q}_0^{\,n}, \overline{Q}_b^{\,n}\}, \;\; n = 1, 2, \ldots, M, \tag{3.4.4}$$

where

$$\overline{Q}_0^{\,n} = \frac{1}{\tau} \int_{I_n} Q_0 u dt \quad \text{and} \quad \overline{Q}_b^{\,n} = \frac{1}{\tau} \int_{I_n} Q_b u dt, \;\; n = 1, \ldots, M.$$

It is easy to notice from the definition of L^2 projection that

$$\overline{Q}_0^{\,n} = Q_0 \overline{u}^{\,n} \quad \text{and} \quad \overline{Q}_b^{\,n} = Q_b \overline{u}^{\,n}, \;\; n = 1, 2, \ldots, M,$$

and hence,

$$\overline{Q}_\tau^{\,n} = Q_h \overline{u}^{\,n}, \;\; n = 1, 2, \ldots, M. \tag{3.4.5}$$

We now present the main results of this section in the following theorems.

Theorem 3.4.1. *Suppose u and $U_{h,\tau}$ are the solutions of (3.1.1)-(3.1.2) and (3.4.2), respectively. Then, for $u \in L^2(0,T;H^{k+1}(\Omega)) \cap H^1(0,T;L^2(\Omega))$, we have*

$$\left(\int_0^T \|u - U_{h,\tau}\|^2 dt \right)^{\frac{1}{2}} \leq C(\tau + h^{k+1}) \left\{ \|u\|_{L^2(0,T;H^{k+1}(\Omega))} + \|u_t\|_{L^2(0,T;L^2(\Omega))} \right\}.$$

Theorem 3.4.2. *Suppose u and $U_{h,\tau}$ are the solutions of (3.1.1)-(3.1.2) and (3.4.2), respectively. Then, for $u \in L^2(0,T;H^{k+1}(\Omega)) \cap H^1(0,T;H^1(\Omega))$, we have*

$$\left(\int_0^T |||u - U_{h,\tau}|||^2 \right)^{\frac{1}{2}} \leq C(\tau + h^{k}) \left\{ \|u\|_{L^2(0,T;H^{k+1}(\Omega))} + \|u_t\|_{L^2(0,T;H^1(\Omega))} \right\}.$$

The proofs of the above theorems require some preparations. For the Theorem 3.4.1, we appeal to parabolic duality. A backward problem is considered as follows: Find $z_h^n = \{z_0^n, z_b^n\} \in \mathcal{V}_h^0$ such that

$$(-\partial_\tau z_h^n, v_h) + \mathcal{A}_w(z_h^{n-1}, v_h) = (\overline{Q}_\tau^{\,n} - U_h^n, v_h) \quad \forall v_h \in \mathcal{V}_h^0,\ 1 \leq n \leq M, \tag{3.4.6}$$

with $z_h^M = 0$.

Regarding the stability of z_h^n, we have the following result.

Lemma 3.4.1. *For z_h^n satisfying (3.4.6), we obtain*

$$\max_{1\leq n\leq M} |||z_h^{n-1}|||^2 + \sum_{n=1}^{M} \tau \|\partial_\tau z_h^n\|^2 \leq C \sum_{n=1}^{M} \tau \|\overline{Q}_\tau^{\,n} - U_h^n\|^2.$$

Proof. Setting $v_h = -\tau \partial_\tau z_h^n$ in (3.4.6), we have

$$\frac{\tau}{2} \|\partial_\tau z_h^n\|^2 + \mathcal{A}_w(z_h^{n-1}, z_h^{n-1} - z_h^n) \leq C\tau \|\overline{Q}_\tau^{\,n} - U_h^n\|^2. \tag{3.4.7}$$

It is easy to verify that

$$\begin{aligned} \mathcal{A}_w(z_h^{n-1}, z_h^{n-1} - z_h^n) &= \frac{\tau^2}{2} \mathcal{A}_w(\partial_\tau z_h^n, \partial_\tau z_h^n) \\ &\quad - \frac{1}{2} \mathcal{A}_w(z_h^n, z_h^n) + \frac{1}{2} \mathcal{A}_w(z_h^{n-1}, z_h^{n-1}). \end{aligned}$$

This combine with (3.4.7) yields

$$\frac{1}{2}\tau \|\partial_\tau z_h^n\|^2 - \frac{1}{2} \mathcal{A}_w(z_h^n, z_h^n) + \frac{1}{2} \mathcal{A}_w(z_h^{n-1}, z_h^{n-1}) \leq C\tau \|\overline{Q}_\tau^{\,n} - U_h^n\|^2$$

and then summing over n from $n = l$ to $n = M$ yields

$$\sum_{n=l}^{M} \tau \|\partial_\tau z_h^n\|^2 + \mathcal{A}_w(z_h^{l-1}, z_h^{l-1}) \leq C \sum_{n=1}^{M} \tau \|\overline{Q}_\tau^{\,n} - U_h^n\|^2, \quad 1 \leq l \leq M-1.$$

Finally, coercivity of the bilinear map $\mathcal{A}_w(\cdot,\cdot)$ leads to desire result. □

Remark 3.4.1. *Note that $z_h^{n-1} \in \mathcal{V}_h^0$ can be recognized as a weak Galerkin approximation to $z^{n-1} \in H^2(\Omega) \cap H_0^1(\Omega)$ satisfying following elliptic equation*

$$-\nabla \cdot (\alpha \nabla z^{n-1}) = \big(\overline{Q}_\tau^{\,n} - U_h^n\big) + \partial_\tau z_h^n.$$

Then, arguing as in (3.3.7), we obtain

$$\|z^{n-1} - z_h^{n-1}\|_{1,h} \leq Ch\big\{\|\overline{Q}_\tau^{\,n} - U_h^n\| + \|\partial_\tau z_h^n\|\big\},$$

which together with Lemma 3.4.1 yields

$$\begin{aligned}\sum_{n=1}^{M} \|z^{n-1} - z_h^{n-1}\|_{1,h}^2 &\leq Ch^2 \sum_{n=1}^{M} \big\{\|\overline{Q}_\tau^{\,n} - U_h^n\|^2 + \|\partial_\tau z_h^n\|^2\big\} \\ &\leq Ch^2 \sum_{n=1}^{M} \|\overline{Q}_\tau^{\,n} - U_h^n\|^2. \end{aligned} \tag{3.4.8}$$

Proof of Theorem 3.4.1. Choose $v_h = \tau(\overline{Q}_\tau^{\,n} - U_h^n) \in V_h^0$ in (3.4.6) to have

$$\begin{aligned}\tau\|\overline{Q}_\tau^{\,n} - U_h^n\|^2 &= \tau(-\partial_\tau z_h^n, \overline{Q}_\tau^{\,n} - U_h^n) + \tau \mathcal{A}_w(z_h^{n-1}, \overline{Q}_\tau^{\,n} - U_h^n) \\ &= \tau(-\partial_\tau z_h^n, \overline{Q}_\tau^{\,n} - u^n) + \tau(-\partial_\tau z_h^n, u^n - U_h^n) \\ &\quad + \tau \mathcal{A}_w(z_h^{n-1}, \overline{Q}_\tau^{\,n} - U_h^n). \end{aligned} \tag{3.4.9}$$

From equation (3.2.18), for all $v_h = \{v_0, v_b\} \in \mathcal{V}_h^0$ and $1 \leq n \leq M$, we obtain

$$\begin{aligned}&(\partial_\tau u^n, v_h) + \tau^{-1} \int_{I_n} \mathcal{A}_w(Q_h u, v_h) dt \\ &= (\overline{f}^{\,n}, v_h) + l_1(\overline{u}^{\,n}, v_h) + l_2(\overline{u}^{\,n}, v_h) + \mathcal{S}(\overline{Q}_\tau^{\,n}, v_h). \end{aligned} \tag{3.4.10}$$

Using the definition (3.2.6) for the bilinear map $\mathcal{A}_w(\cdot,\cdot)$, we obtain

$$\begin{aligned}\tau^{-1} \int_{I_n} \mathcal{A}_w(Q_h u, v_h) dt &= \tau^{-1} \int_{I_n} \sum_{K \in \mathcal{T}_h} (\alpha \nabla_w Q_h u, v_h)_K dt \\ &\quad + \tau^{-1} \int_{I_n} \sum_{K \in \mathcal{T}_h} \langle Q_0 u - Q_b u, v_0 - v_b \rangle_{\partial K} dt \\ &= \sum_{K \in \mathcal{T}_h} (\alpha \tau^{-1} \int_{I_n} \nabla_w Q_h u dt, v_h)_K \\ &\quad + \sum_{K \in \mathcal{T}_h} \langle \overline{Q}_0^{\,n} - \overline{Q}_b^{\,n}, v_0 - v_b \rangle_{\partial K}. \end{aligned} \tag{3.4.11}$$

Again, using the identity (3.2.4), we arrive at

$$\begin{aligned}\int_{I_n}\nabla_w Q_h u dt &= \int_{I_n}\mathbb{Q}_h(\nabla u)dt\\ &= \mathbb{Q}_h\Big(\int_{I_n}\nabla u dt\Big)\\ &= \mathbb{Q}_h\bigg(\nabla\Big(\int_{I_n} u dt\Big)\bigg)\\ &= \tau\mathbb{Q}_h\nabla\overline{u}^{\,n} = \tau\nabla_w Q_h\overline{u}^{\,n} = \tau\nabla_w\overline{Q}_\tau^{\,n},\end{aligned}$$

which together with (3.4.11) yields

$$\begin{aligned}\tau^{-1}\int_{I_n}\mathcal{A}_w(Q_h u, v_h)dt &= \sum_{K\in\mathcal{T}_h}(\alpha\nabla_w\overline{Q}_\tau^{\,n}, v_h)_K\\ &\quad+\sum_{K\in\mathcal{T}_h}\langle\overline{Q}_0^{\,n}-\overline{Q}_b^{\,n}, v_0-v_b\rangle_{\partial K}\\ &= \mathcal{A}_w(\overline{Q}_\tau^{\,n}, v_h).\end{aligned}\tag{3.4.12}$$

Using (3.4.12) in (3.4.10), we obtain

$$(\partial_\tau u^n, v_h)+\mathcal{A}_w(\overline{Q}_\tau^{\,n}, v_h) = (\overline{f}^{\,n}, v_h)+l_1(\overline{u}^{\,n}, v_h)+l_2(\overline{u}^{\,n}, v_h)+\mathcal{S}(\overline{Q}_\tau^{\,n}, v_h).\tag{3.4.13}$$

Now setting $v_h = z_h^{n-1}$ both in (3.4.2) and (3.4.13), then subtracting one from another, we obtain

$$\begin{aligned}(\partial_\tau(u^n-U_h^n), z_h^{n-1})+\mathcal{A}_w(\overline{Q}_\tau^{\,n}-U_h^n, z_h^{n-1}) &= l_1(\overline{u}^{\,n}, z_h^{n-1})+l_2(\overline{u}^{\,n}, z_h^{n-1})\\ &\quad+\mathcal{S}(\overline{Q}_\tau^{\,n}, z_h^{n-1}),\end{aligned}\tag{3.4.14}$$

which together with (3.4.9) yields

$$\begin{aligned}&\sum_{n=1}^{M}\tau\|\overline{Q}_\tau^{\,n}-U_h^n\|^2\\ &=\sum_{n=1}^{M}\tau(-\partial_\tau z_h^n, \overline{Q}_\tau^{\,n}-u^n)+\sum_{n=1}^{M}\tau l_1(\overline{u}^{\,n}, z_h^{n-1})\\ &\quad+\sum_{n=1}^{M}\tau l_2(\overline{u}^{\,n}, z_h^{n-1})+\sum_{n=1}^{M}\tau\mathcal{S}(\overline{Q}_\tau^{\,n}, z_h^{n-1})\\ &\quad-\sum_{n=1}^{M}\tau\Big\{(\partial_\tau z_h^n, u^n-U_h^n)+(\partial_\tau(u^n-U_h^n), z_h^{n-1})\Big\}\\ &:= I_1+I_2+I_3+I_4+I_5.\end{aligned}\tag{3.4.15}$$

We now estimate each term separately. For the term I_1, we use Cauchy-Schwarz inequality, Lemma 3.2.1 and Lemma 3.4.1 to have

$$\begin{aligned}
|I_1| &\leq \sum_{n=1}^{M} \tau(-\partial_\tau z_h^n, \overline{Q}_\tau{}^n - \overline{u}{}^n) + \sum_{n=1}^{M} \tau(-\partial_\tau z_h^n, \overline{u}{}^n - u^n) \\
&\leq \sum_{n=1}^{M} \tau\|\partial_\tau z_h^n\|\|\overline{Q}_\tau{}^n - \overline{u}{}^n\| + \sum_{n=1}^{M} \tau\|\partial_\tau z_h^n\|\|\overline{u}{}^n - u^n\| \\
&\leq \left(\sum_{n=1}^{M} \tau\|\partial_\tau z_h^n\|^2\right)^{\frac{1}{2}} \\
&\quad \times \left[\left(\sum_{n=1}^{M} \tau\|\overline{Q}_\tau^n - \overline{u}{}^n\|^2\right)^{\frac{1}{2}} + \left(\sum_{n=1}^{M} \tau\|\overline{u}{}^n - u^n\|^2\right)^{\frac{1}{2}}\right] \\
&\leq C\left(\sum_{n=1}^{M} \tau\|\partial_\tau z_h^n\|^2\right)^{\frac{1}{2}} \\
&\quad \times \left[\left(\sum_{n=1}^{M} \tau h^{2(k+1)}\|\overline{u}{}^n\|_{k+1}^2\right)^{\frac{1}{2}} + \left(\sum_{n=1}^{M} \tau^2 \int_{I_n} \|u_t\|^2 dt\right)^{\frac{1}{2}}\right] \\
&\leq C(\tau + h^{k+1})\left(\|u\|_{L^2(H^{k+1})} + \|u_t\|_{L^2(L^2)}\right) \\
&\quad \times \left(\sum_{n=1}^{M} \tau\|\overline{Q}_\tau^n - U_h^n\|^2\right)^{\frac{1}{2}}. \qquad (3.4.16)
\end{aligned}$$

Here, we have used following facts

$$\|\overline{u}{}^n\|_{k+1} \leq \frac{1}{\tau}\int_{I_n} \|u\|_{k+1} dt \leq \frac{1}{\tau^{\frac{1}{2}}}\Big(\int_{I_n} \|u\|_{k+1}^2 dt\Big)^{\frac{1}{2}} \qquad (3.4.17)$$

and

$$\tau\|\bar{u}^n - u^n\|^2 \leq \tau^2 \int_{I_n} \|u_t\|^2 dt. \qquad (3.4.18)$$

For the estimate (3.4.18), we first note that $|u(t) - u^n|^2 \leq (t_n - t_{n-1})\int_{I_n} |u_t|^2 dt, \quad t \in I_n = (t_{n-1}, t_n]$, so that

$$\int_{I_n} |u(t) - u^n|^2 dt \leq \tau^2 \int_{I_n} |u_t|^2 dt, \quad t \in I_n = (t_{n-1}, t_n]. \qquad (3.4.19)$$

Now, the estimate (3.4.19) and definition (3.4.1) yield

$$|\overline{u}{}^n - u^n|^2 \leq \frac{1}{\tau}\int_{I_n} |u(t) - u^n|^2 dt \leq \tau \int_{I_n} |u_t|^2 dt.$$

Then integrating over Ω leads to estimate (3.4.18).

Arguing as in (3.3.12) and using estimate (3.4.8), it now follows that

$$\begin{aligned}
I_2 &\leq \sum_{n=1}^{M} |\tau l_1(\overline{u}^{\,n}, z_h^{n-1})| \\
&\leq \sum_{n=1}^{M} \left\{ C\tau h^k \|\overline{u}^{\,n}\|_{k+1} \Big(\sum_{K\in\mathcal{T}_h} h_K^{-1} \|z_0^{n-1} - z_b^{n-1}\|_{\partial K}^2 \Big)^{\frac{1}{2}} \right\} \\
&\leq \sum_{n=1}^{M} \left\{ C\tau h^k \|\overline{u}^{\,n}\|_{k+1} \times \Big(\sum_{K\in\mathcal{T}_h} h_K^{-1} \|(z_0^{n-1} - z^{n-1}) - (z_b^{n-1} - z^{n-1})\|_{\partial K}^2 \Big)^{\frac{1}{2}} \right\} \\
&\leq \sum_{n=1}^{M} C\tau h^k \|\overline{u}^{\,n}\|_{k+1} \|z_h^{n-1} - z^{n-1}\|_{1,h} \\
&\leq Ch^k \Big(\sum_{n=1}^{M} \tau \|\overline{u}^{\,n}\|_{k+1}^2 \Big)^{\frac{1}{2}} \Big(\sum_{n=1}^{M} \tau \|z_h^{n-1} - z^{n-1}\|_{1,h}^2 \Big)^{\frac{1}{2}} \\
&\leq Ch^{k+1} \|u\|_{L^2(H^{k+1})} \Big(\sum_{n=1}^{M} \tau \|\overline{Q}_\tau^{\,n} - U_h^n\|^2 \Big)^{\frac{1}{2}}. \qquad (3.4.20)
\end{aligned}$$

For I_3, we use Lemma 3.2.3 and Lemma 3.4.1 to have

$$\begin{aligned}
I_3 &\leq \sum_{n=1}^{M} |\tau l_2(\overline{u}^{\,n}, z_h^{n-1})| \leq \sum_{n=1}^{M} C\tau h^{k+1} \|\overline{u}^{\,n}\|_{k+1} |||z_h^{n-1}||| \\
&\leq Ch^{k+1}\tau^{\frac{1}{2}} \Big(\sum_{n=1}^{M} \tau \|\overline{u}^{\,n}\|_{k+1}^2 \Big)^{\frac{1}{2}} \Big(\sum_{n=1}^{M} |||z_h^{n-1}|||^2 \Big)^{\frac{1}{2}} \\
&\leq Ch^{k+1}\tau^{\frac{1}{2}} \Big(\sum_{n=1}^{M} \tau \|\overline{u}^{\,n}\|_{k+1}^2 \Big)^{\frac{1}{2}} \Big(M \max_{0\leq l\leq M-1} |||z_h^{l}|||^2 \Big)^{\frac{1}{2}} \\
&\leq Ch^{k+1}\tau^{\frac{1}{2}} \Big(\sum_{n=1}^{M} \tau \|\overline{u}^{\,n}\|_{k+1}^2 \Big)^{\frac{1}{2}} \Big(\frac{T}{\tau} \max_{0\leq l\leq M-1} |||z_h^{l}|||^2 \Big)^{\frac{1}{2}} \\
&\leq Ch^{k+1} \|u\|_{L^2(H^{k+1})} \Big(\sum_{n=1}^{M} \tau \|\overline{Q}_\tau^{\,n} - U_h^n\|^2 \Big)^{\frac{1}{2}}. \qquad (3.4.21)
\end{aligned}$$

Arguing as in (3.3.13) and using the fact that $\overline{Q}_\tau^{\,n} = Q_h \overline{u}^{\,n}$, we obtain

$$\begin{aligned}
I_4 &= \sum_{n=1}^{M} \tau \mathcal{S}(\overline{Q}_\tau^{\,n}, z_h^{n-1}) \leq Ch^k \sum_{n=1}^{M} \tau \|\overline{u}^{\,n}\|_{k+1} \|z_h^{n-1} - z^{n-1}\|_{1,h} \\
&\leq Ch^k \Big(\sum_{n=1}^{M} \tau \|\overline{u}^{\,n}\|_{k+1}^2 \Big)^{\frac{1}{2}} \Big(\sum_{n=1}^{M} \tau \|z_h^{n-1} - z^{n-1}\|_{1,h}^2 \Big)^{\frac{1}{2}} \\
&\leq Ch^{k+1} \|u\|_{L^2(H^{k+1})} \Big(\sum_{n=1}^{M} \tau \|\overline{Q}_\tau^{\,n} - U_h^n\|^2 \Big)^{\frac{1}{2}}. \qquad (3.4.22)
\end{aligned}$$

In the last inequality, we have used estimate (3.4.8).

For the term I_5, use the following identity

$$\sum_{n=1}^{M}(\phi_n-\phi_{n-1})\xi_n=\phi_M\xi_M-\phi_0\xi_0-\sum_{n=1}^{M}\phi_{n-1}(\xi_n-\xi_{n-1}),$$

with $\phi_n=z_h^n$ and $\xi_n=u^n-U_h^n$, to obtain

$$\begin{aligned}-I_5 &= \sum_{n=1}^{M}\tau\Big\{(\partial_\tau z_h^n,u^n-U_h^n)+(\partial_\tau(u^n-U_h^n),z_h^{n-1})\Big\}\\ &= -(z_h^0,u^0-U_h^0)=-(z_h^0,u^0-Q_hu^0)=0. \end{aligned}\tag{3.4.23}$$

By simple calculation, it follows that

$$\begin{aligned}&\int_0^T\|u-U_{h,\tau}\|^2dt\\ &\le C\left(\int_0^T\|u-\overline{u}^{\,n}\|^2dt+\int_0^T\|\overline{u}^{\,n}-\overline{Q}_\tau^{\,n}\|^2dt+\int_0^T\|\overline{Q}_\tau^{\,n}-U_{h,\tau}\|^2dt\right)\\ &\le C\left(\tau^2\|u_t\|^2_{L^2(L^2(\Omega))}+\sum_{n=1}^{M}\Big\{\tau\|\overline{u}^{\,n}-\overline{Q}_\tau^{\,n}\|^2+\tau\|\overline{Q}_\tau^{\,n}-U_h^n\|^2\Big\}\right)\\ &\le C\left(\tau^2\|u_t\|^2_{L^2(L^2(\Omega))}+h^{2(k+1)}\|u\|^2_{L^2(H^{k+1}(\Omega))}+\sum_{n=1}^{M}\tau\|\overline{Q}_\tau^{\,n}-U_h^n\|^2\right).\end{aligned}\tag{3.4.24}$$

Now, we combine the estimates (3.4.15)-(3.4.24) to derive the desired result. This completes the rest of the proof. □

For discrete H^1 norm estimate, like in L^2 norm estimate, we consider an another auxiliary problem: For $1\le n\le M$, find $w_h^n\in V_h^0$ such that

$$(-\partial_\tau w_h^n,v_h)+\mathcal{A}_w(w_h^{n-1},v_h)=\mathcal{A}_w(\overline{Q}_\tau^{\,n}-U_h^n,v_h)\ \forall v_h\in\mathcal{V}_h^0,\ w_h^M=0.\tag{3.4.25}$$

The following lemma is concerned about the stability of w_h satisfying (3.4.25).

Lemma 3.4.2. *Suppose w_h^n satisfy* (3.4.25). *Then, we have*

$$\max_{1\le n\le M}\|w_h^{n-1}\|^2+\sum_{n=1}^{M}\tau|||w_h^{n-1}|||^2\ \le\ \sum_{n=1}^{M}\tau|||\overline{Q}_\tau^{\,n}-U_h^n|||^2\tag{3.4.26}$$

and

$$\sum_{n=1}^{M}\tau\|\partial_\tau w_h^n\|^2_{H^{-1}(\Omega)}\ \le\ \sum_{n=1}^{M}\tau|||\overline{Q}_\tau^{\,n}-U_h^n|||^2\tag{3.4.27}$$

hold true.

Proof. Inequality (3.4.26) can be obtained by setting $v_h = w_h^{n-1}$ in (3.4.25) and using the standard arguments. We omit the details.

Using the definition of w_h^n in (3.4.25), we obtain

$$\begin{aligned}
\|\partial_\tau w_h^n\|_{H^{-1}(\Omega)} &= \sup_{\phi\in H_0^1(\Omega)}\left\{\frac{(\partial_\tau w_h^n,\phi)}{\|\phi\|_1}\,:\,\phi\neq 0\right\}\\
&= \sup_{\phi\in H_0^1(\Omega)}\left\{\frac{\sum_{K\in\mathcal{T}_h}(\partial_\tau w_h^n, Q_h\phi)_K}{\|\phi\|_1}\,:\,\phi\neq 0\right\}\\
&\le C\Big(|||w_h^{n-1}||| + |||\overline{Q}_\tau^{\,n} - U_h^n|||\Big)\\
&\quad\times \sup_{\phi\in H_0^1(\Omega)}\left\{\frac{|||Q_h\phi|||}{\|\phi\|_1}\,:\,\phi\neq 0\right\}. \qquad (3.4.28)
\end{aligned}$$

Then, use the fact that $|||\cdot|||$ norm and discrete H^1 norm are equivalent to have

$$\begin{aligned}
|||Q_h\phi|||^2 \le C\|Q_h\phi\|_{1,h}^2 &= C\sum_{K\in\mathcal{T}_h}(\|\nabla Q_0\phi\|_K^2 + h_K^{-1}\|Q_0\phi - Q_b\phi\|_{\partial K}^2)\\
&\le C\sum_{K\in\mathcal{T}_h}(\|\nabla(Q_0\phi-\phi)\|_K^2 + \|\nabla\phi\|_K^2 + h_K^{-1}\|Q_0\phi-\phi\|_{\partial K}^2)\\
&\le C\sum_{K\in\mathcal{T}_h}(\|\phi\|_{1,K}^2 + h_K^{-2}\|Q_0\phi-\phi\|_K^2 + \|\nabla(Q_0\phi-\phi)\|_K^2)\\
&\le C\sum_{K\in\mathcal{T}_h}\|\phi\|_{1,K}^2. \qquad (3.4.29)
\end{aligned}$$

Additionally, here, we have applied error estimates for the L^2 projection (e.g., see Lemma 4.1 in [123]). This with (3.4.26) and (3.4.28) gives (3.4.27). □

Proof of Theorem 3.4.2. Set $v_h = \tau(\overline{Q}_\tau^{\,n} - U_h^n)$ in (3.4.25) to obtain

$$\begin{aligned}
\sum_{n=1}^M \tau|||\overline{Q}_\tau^{\,n} - U_h^n|||^2 &= \sum_{n=1}^M \tau(-\partial_\tau w_h^n, \overline{Q}_\tau^{\,n} - U_h^n) + \sum_{n=1}^M \tau\mathcal{A}_w(w_h^{n-1}, \overline{Q}_\tau^{\,n} - U_h^n)\\
&= \sum_{n=1}^M \tau(-\partial_\tau w_h^n, \overline{Q}_\tau^{\,n} - u^n) + \sum_{n=1}^M \tau(-\partial_\tau w_h^n, u^n - U_h^n)\\
&\quad + \sum_{n=1}^M \tau\mathcal{A}_w(w_h^{n-1}, \overline{Q}_\tau^{\,n} - U_h^n)\\
&= \sum_{n=1}^M \tau(-\partial_\tau w_h^n, \overline{Q}_\tau^{\,n} - u^n) + \sum_{n=1}^M \tau l_1(\overline{u}^{\,n}, w_h^{n-1})\\
&\quad + \sum_{n=1}^M \tau l_2(\overline{u}^{\,n}, w_h^{n-1}) + \sum_{n=1}^M \tau\mathcal{S}(\overline{Q}_\tau^{\,n}, w_h^{n-1})\\
&\quad - \sum_{n=1}^M \tau\Big\{(\partial_\tau w_h^n, u^n - U_h^n) + (\partial_\tau(u^n - U_h^n), w_h^{n-1})\Big\}. \qquad (3.4.30)
\end{aligned}$$

Further, arguing as in equation (3.4.23), we obtain

$$\sum_{n=1}^{M}\tau\Big\{(\partial_\tau w_h^n, u^n - U_h^n) + (\partial_\tau(u^n - U_h^n), w_h^{n-1})\Big\} = 0,$$

which together with (3.4.30) leads to following equation

$$\begin{aligned}\sum_{n=1}^{M}\tau\big|\!\big|\!\big|\overline{Q}_\tau{}^n - U_h^n\big|\!\big|\!\big|^2 &= \sum_{n=1}^{M}\tau(-\partial_\tau w_h^n, \overline{Q}_\tau{}^n - u^n) + \sum_{n=1}^{M}\tau l_1(\overline{u}{}^n, w_h^{n-1}) \\ &\quad + \sum_{n=1}^{M}\tau l_2(\overline{u}{}^n, w_h^{n-1}) + \sum_{n=1}^{M}\tau\mathcal{S}(\overline{Q}_\tau{}^n, w_h^{n-1}) \\ &:= II_1 + II_2 + II_3 + II_4. \end{aligned} \tag{3.4.31}$$

For the term II_1, we first observe that

$$\begin{aligned}&\tau(-\partial_\tau w_h^n, \overline{Q}_\tau{}^n - u^n) \\ &= \sum_{K\in\mathcal{T}_h}\tau(-\partial_\tau w_h^n, \overline{Q}_\tau{}^n - u^n)_K \\ &\le \tau\sum_{K\in\mathcal{T}_h}\|\partial_\tau w_h^n\|_{H^{-1}(K)}\|\overline{Q}_\tau{}^n - u^n\|_{1,K} \\ &\le \tau\sum_{K\in\mathcal{T}_h}\|\partial_\tau w_h^n\|_{H^{-1}(K)}\Big\{\|\overline{Q}_\tau{}^n - \overline{u}{}^n\|_{1,K} + \|\overline{u}{}^n - u^n\|_{1,K}\Big\}.\end{aligned}$$

Arguing as deriving (3.4.18), we can deduce

$$\|\nabla(\bar{u}^n - u^n)\|^2 \le \tau\int_{I_n}\|\nabla u_t\|^2 dt. \tag{3.4.32}$$

Now, use the fact that $\overline{Q}_\tau{}^n = Q_h\overline{u}{}^n$ and Lemma 3.2.1 together with estimate (3.4.32) to have

$$\tau(-\partial_\tau w_h^n, \overline{Q}_\tau{}^n - u^n) \le \tau^{\frac{1}{2}}\|\partial_\tau w_h^n\|_{H^{-1}(\Omega)}\Big\{\tau^{\frac{1}{2}}h^k\|\overline{u}{}^n\|_{k+1} + \tau\|u_t\|_{L^2(I_n;H^1(\Omega))}\Big\},$$

and hence,

$$\begin{aligned}II_1 &= \sum_{n=1}^{M}\tau(-\partial_\tau w_h^n, \overline{Q}_\tau{}^n - u^n) \\ &\le C(\tau + h^k)\left(\sum_{n=1}^{M}\tau\|\partial_\tau w_h^n\|^2_{H^{-1}(\Omega)}\right)^{\frac{1}{2}}\big(\|u\|_{L^2(H^{k+1}(\Omega))} + \|u_t\|_{L^2(H^1(\Omega))}\big) \\ &\le C(\tau + h^k)\left(\sum_{n=1}^{M}\tau\big|\!\big|\!\big|\overline{Q}_\tau{}^n - U_h^n\big|\!\big|\!\big|^2\right)^{\frac{1}{2}} \\ &\quad \times\Big(\|u\|_{L^2(H^{k+1}(\Omega))} + \|u_t\|_{L^2(H^1(\Omega))}\Big).\end{aligned} \tag{3.4.33}$$

Here, we have used Lemma 3.4.2 and the estimate (3.4.17).

For the second term in (3.4.31), we use Lemma 3.2.3, Lemma 3.4.2 and the estimate (3.4.17) to have

$$\begin{aligned} II_2 &= \sum_{n=1}^{M} \tau l_1(\overline{u}^{\,n}, w_h^{n-1}) \\ &\leq Ch^k \sum_{n=1}^{M} \tau \|\overline{u}^{\,n}\|_{k+1} |||w_h^{n-1}||| \\ &\leq Ch^k \Big(\sum_{n=1}^{M} \tau \|\overline{u}^{\,n}\|_{k+1}^2 \Big)^{\frac{1}{2}} \Big(\sum_{n=1}^{M} \tau |||w_h^{n-1}|||^2 \Big)^{\frac{1}{2}} \\ &\leq Ch^k \|u\|_{L^2(H^{k+1}(\Omega))} \left(\sum_{n=1}^{M} \tau |||\overline{Q}_\tau^{\,n} - U_h^n|||^2 \right)^{\frac{1}{2}}. \end{aligned} \tag{3.4.34}$$

Similarly, we arrive at

$$\begin{aligned} II_3 &= \sum_{n=1}^{M} \tau l_2(\overline{u}^{\,n}, w_h^{n-1}) \\ &\leq Ch^{k+1} \sum_{n=1}^{M} \tau \|\overline{u}^{\,n}\|_{k+1} |||w_h^{n-1}||| \\ &\leq Ch^{k+1} \Big(\sum_{n=1}^{M} \tau \|\overline{u}^{\,n}\|_{k+1}^2 \Big)^{\frac{1}{2}} \Big(\sum_{n=1}^{M} \tau |||w_h^{n-1}|||^2 \Big)^{\frac{1}{2}} \\ &\leq Ch^{k+1} \|u\|_{L^2(H^{k+1}(\Omega))} \left(\sum_{n=1}^{M} \tau |||\overline{Q}_\tau^{\,n} - U_h^n|||^2 \right)^{\frac{1}{2}} \end{aligned} \tag{3.4.35}$$

and

$$\begin{aligned} II_4 &= \sum_{n=1}^{M} \tau \mathcal{S}(\overline{Q}_\tau^{\,n}, w_h^{n-1}) \\ &\leq Ch^k \sum_{n=1}^{M} \tau \|\overline{u}^{\,n}\|_{k+1} |||w_h^{n-1}||| \\ &\leq Ch^k \Big(\sum_{n=1}^{M} \tau \|\overline{u}^{\,n}\|_{k+1}^2 \Big)^{\frac{1}{2}} \Big(\sum_{n=1}^{M} \tau |||w_h^{n-1}|||^2 \Big)^{\frac{1}{2}} \\ &\leq Ch^k \|u\|_{L^2(H^{k+1}(\Omega))} \left(\sum_{n=1}^{M} \tau |||\overline{Q}_\tau^{\,n} - U_h^n|||^2 \right)^{\frac{1}{2}}. \end{aligned} \tag{3.4.36}$$

Again it is easy to verify that

$$\begin{aligned}
&\int_0^T \|u - U_{h,\tau}\|_{1,h}^2 dt \\
&\leq C\left(\int_0^T \|u - \overline{u}^n\|_{1,h}^2 dt + \int_0^T \|\overline{u}^n - \overline{Q}_\tau^n\|_{1,h}^2 dt + \int_0^T |||\overline{Q}_\tau^n - U_{h,\tau}|||^2 dt \right) \\
&\leq C\left(\int_0^T \|\nabla(u - \overline{u}^n)\|^2 dt + \sum_{n=1}^M \left\{ \tau\|\overline{u}^n - \overline{Q}_\tau^n\|_{1,h}^2 + \tau|||\overline{Q}_\tau^n - U_h^n|||^2 \right\} \right) \\
&\leq C\left(\tau^2 \|u_t\|_{L^2(H^1(\Omega))}^2 + h^{2k}\|u\|_{L^2(H^{k+1}(\Omega))}^2 + \sum_{n=1}^M \tau|||\overline{Q}_\tau^n - U_h^n|||^2 \right).
\end{aligned}$$

Finally, Theorem 3.4.2 follows immediately from above inequality and estimates (3.4.33)-(3.4.36). □

Remark 3.4.2. *Theorems 3.4.1-3.4.2 are the extensions of Theorems 4.8-4.9 in [132]. It is worth to note that Theorems 4.8-4.9 in [132] have discussed the convergence of fully discrete solution under the assumption that* $u \in H^1(0,T;H^{k+1}(\Omega)) \cap H^2(0,T;L^2(\Omega))$. *In our proofs, we have ensured the same optimal order convergence under the assumption that solution* $u \in L^2(0,T;H^{k+1}(\Omega)) \cap H^1(0,T;H^1(\Omega))$.

3.5 Numerical Section

In this section, we will explore the results of computations for the parabolic problem (3.1.1)-(3.1.2) in $\Omega \times J$, where $\Omega \subset \mathbb{R}^2$ and $J = [0,1]$. To test the flexibility of the WG method, parabolic problems are solved on finite element partitions with different kinds of configuration, including triangular mesh, rectangular mesh, and polygonal mesh. While the Examples 3.5.1-3.5.3 deal with discontinuous solutions with smooth coefficients, Example 3.5.4 is carried out for discontinuous solutions with discontinuous coefficients. Example 3.5.5 compares the use of different meshes with discontinuous solution. Higher order numerical methods that work well for problems with low regularity in the solution has remained a major part of the mathematical study up to the present day. It is worthwhile to note that the numerical examples presented in [77] and [132] assume sufficiently smooth solutions.

Let $U_{h,\tau}$ be the weak Galerkin solution defined by (3.4.3). Then, we have calculated the following error

$$e_h := \overline{Q}_\tau^n - U_{h,\tau} = Q_h\overline{u}^n - U_{h,\tau}$$

with respect to average triple-bar norm and the L^2 norm. More precisely, the errors are presented with respect to $L^2(J;|||\cdot|||)$ and $L^2(J;L^2(\Omega))$ norms through tables and error plots for the WG space $(\mathcal{P}_k(K),\ \mathcal{P}_k(\partial K),\ \left[\mathcal{P}_{k-1}(K)\right]^2)$ with time step $\tau = \mathrm{O}(h^{k+1})$.

Example 3.5.1. Consider the problem (3.1.1)-(3.1.2) in $\Omega \times J = (0,1)^2 \times J$. Numerical solution is compared with the following exact solution

$$u(x,y,t) = \begin{cases} \exp(-t)\sin(2\pi x)\sin(2\pi y), & \text{if } \ x \leq 0.5, \\ \exp(-t)\sin(\pi x)\sin(\pi y)\sin(\pi x + \pi y - t), & \text{otherwise.} \end{cases}$$

The right-hand side f and initial condition u^0 are determined from the choice for u and the variable diffusion-coefficient

$$\alpha = \begin{bmatrix} 1 & xy \\ xy & x^2y^2 + 1 \end{bmatrix}.$$

Here, we can easily see that both u and u_t are discontinuous along the line $x = 0.5$. We have used triangular mesh in this Example. First, we uniformly partition the domain into $n \times n$ sub rectangles and then divide each rectangular element by the diagonal line with a negative slope. The mesh size is denoted by $h = 1/n$. The errors with respect to $L^2(H^1)$ norm and $L^2(L^2)$ norm for linear and quadratic WG spaces are reported in Table 3.5.1 and Table 3.5.2, respectively. Figure 3.5.1, for $k = 1$ and $k = 2$, shows that the rate of convergence are $\mathrm{O}(h^k)$ and $\mathrm{O}(h^{k+1})$ with respect to $L^2(H^1)$ norm and $L^2(L^2)$ norm, respectively.

Table 3.5.1: Order of convergence for $k = 1$ with time step $\tau = 10^{-4}$

h	$L^2(J; \lvert\lvert\lvert e_h \rvert\rvert\rvert)$	Order	$L^2(J; \lVert e_h \rVert)$	Order
1/4	1.406842e+00		1.821684e-01	
1/8	7.143323e-01	9.777931e-01	4.766399e-02	1.934301e+00
1/16	3.565919e-01	1.002321e+00	1.199687e-02	1.990242e+00
1/32	1.781393e-01	1.001268e+00	3.003124e-03	1.998122e+00

Example 3.5.2. For our second numerical Example in $(0,1)^2 \times J$, we select the data appearing in (3.1.1)-(3.1.2) by setting the exact solution as

$$u(x,y,t) = \begin{cases} \exp(-t)\sin(2\pi x)\sin(2\pi y), & \text{if } \ x \leq 0.5, \\ t^2\cos(t)\sin(\pi x)\sin(\pi y), & \text{otherwise,} \end{cases}$$

Table 3.5.2: Order of convergence for $k = 2$ with time step $\tau = 10^{-4}$

h	$L^2(J; \|\|\|e_h\|\|\|)$	Order	$L^2(J; \|e_h\|)$	Order
1/4	5.680487e-01		4.952508e-02	
1/8	1.534120e-01	1.888603e+00	6.476731e-03	2.934822e+00
1/16	4.136305e-02	1.890997e+00	8.243902e-04	2.973867e+00
1/32	1.255650e-02	1.719908e+00	1.082086e-04	2.929513e+00

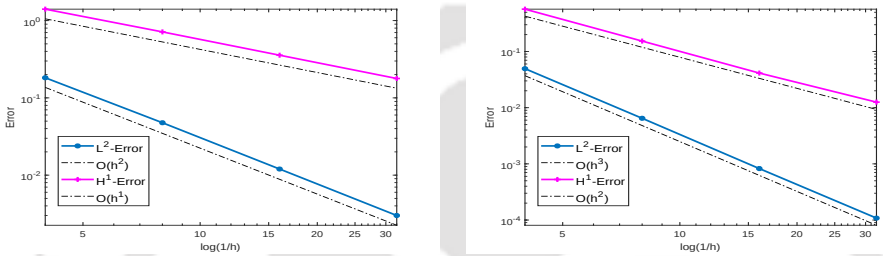

Figure 3.5.1: Log-log plots for WG-spaces $(\mathcal{P}_1, \mathcal{P}_1, [\mathcal{P}_0]^2)$ (left) and $(\mathcal{P}_2, \mathcal{P}_2, [\mathcal{P}_1]^2)$ (right) in Example 3.5.1

and the diffusion-coefficient

$$\alpha = \begin{bmatrix} 1 & 0 \\ 0 & 1 \end{bmatrix}.$$

In this Example, we have used uniform rectangular mesh. The errors with respect to $L^2(H^1)$ norm and $L^2(L^2)$ norm for different WG spaces are reported in Table 3.5.3, Table 3.5.4 and Table 3.5.5. It is clear from Figure 3.5.2 that we have achieved optimal order of convergence in both $L^2(H^1)$ norm and $L^2(L^2)$ norm, which confirm the theoretical prediction as proved in Theorem 3.4.1 and Theorem 3.4.2.

Table 3.5.3: Order of convergence for $k = 1$ with time step $\tau = 10^{-4}$

h	$L^2(J; \|\|\|e_h\|\|\|)$	Order	$L^2(J; \|e_h\|)$	Order
1/4	5.470442e-01		6.927764e-02	
1/8	2.755674e-01	9.892519e-01	1.758557e-02	1.977998e+00
1/16	1.379793e-01	9.979536e-01	4.408994e-03	1.995871e+00
1/32	6.901197e-02	9.995333e-01	1.100828e-03	2.001861e+00

Table 3.5.4: Order of convergence for $k = 2$ with time step $\tau = 10^{-4}$

h	$L^2(J; \|\|\|e_h\|\|\|)$	Order	$L^2(J; \|e_h\|)$	Order
1/4	1.037132e-01		8.752664e-03	
1/8	2.630818e-02	1.979016e+00	1.102222e-03	2.989307e+00
1/16	6.600814e-03	1.994795e+00	1.378105e-04	2.999658e+00
1/32	1.651862e-03	1.998551e+00	1.742393e-05	2.983543e+00

Table 3.5.5: Order of convergence for $k = 3$ with time step $\tau = 10^{-5}$

h	$L^2(J; \|\|\|e_h\|\|\|)$	Order	$L^2(J; \|e_h\|)$	Order
1/4	1.337790e-02		9.695897e-04	
1/8	1.701945e-03	2.974595e+00	6.148203e-05	3.979138e+00
1/16	2.137171e-04	2.993410e+00	3.867133e-06	3.990829e+00
1/32	2.678218e-05	2.996357e+00	3.927503e-07	3.299580e+00

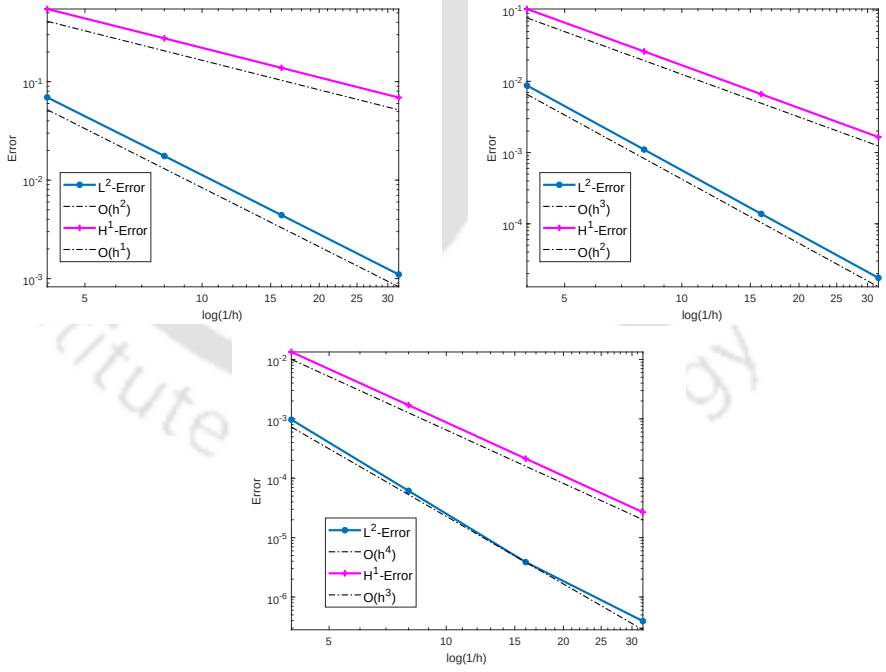

Figure 3.5.2: Log-log plots for WG-spaces $\left(\mathcal{P}_1, \mathcal{P}_1, \left[\mathcal{P}_0\right]^2\right)$ (top left), $\left(\mathcal{P}_2, \mathcal{P}_2, \left[\mathcal{P}_1\right]^2\right)$ (top right) and $\left(\mathcal{P}_3, \mathcal{P}_3, \left[\mathcal{P}_2\right]^2\right)$ (bottom) in Example 3.5.2.

Example 3.5.3. For our third numerical Example, we consider the problem (3.1.1)-(3.1.2) in $(0,1)^2 \times J$. The right-hand side f and initial data u^0 are determined from the choice for u given by

$$u(x,y,t) = \begin{cases} \exp(-t)xy(x-1)(y-1)(x-0.5), & \text{if } x \leq 0.5, \\ t^2\cos(t)\sin(\pi x)\sin(\pi y), & \text{otherwise} \end{cases}$$

and the diffusion coefficient

$$\alpha = \begin{bmatrix} 1 & 0 \\ 0 & 1 \end{bmatrix}.$$

In this Example, we have used polygonal meshes. A typical polygonal mesh is presented in Figure 3.5.3 for $h = \frac{1}{8}$. The $L^2(H^1)$ norm and $L^2(L^2)$ norm errors for various h are reported in Tables 3.5.6-3.5.8. Figure 3.5.3 shows the order of convergence in both L^2 and H^1 norms which consolidates our theoretical findings.

Table 3.5.6: Order of convergence for $k = 1$ with time step $\tau = 10^{-4}$

h	$L^2(J;\|\|\|e_h\|\|\|)$	Order	$L^2(J;\|e_h\|)$	Order
1/4	1.590247e-01		1.864766e-02	
1/8	8.144667e-02	9.653229e-01	4.800009e-03	1.957885e+00
1/16	4.095904e-02	9.916739e-01	1.208733e-03	1.989541e+00
1/32	2.050872e-02	9.979441e-01	3.030617e-04	1.995813e+00

Table 3.5.7: Order of convergence for $k = 2$ with time step $\tau = 10^{-4}$

h	$L^2(J;\|\|\|e_h\|\|\|)$	Order	$L^2(J;\|e_h\|)$	Order
1/4	3.044458e-02		2.553227e-03	
1/8	7.795970e-03	1.965385e+00	3.262544e-04	2.968253e+00
1/16	1.960830e-03	1.991264e+00	4.110424e-05	2.988638e+00
1/32	4.912277e-04	1.997001e+00	5.435414e-06	2.918825e+00

Table 3.5.8: Order of convergence for $k = 3$ with time step $\tau = 10^{-5}$

h	$L^2(J; \|\|\|e_h\|\|\|)$	Order	$L^2(J; \|e_h\|)$	Order
1/4	3.938913e-03		2.849781e-04	
1/8	5.046945e-04	2.964315e+00	1.822870e-05	3.966568e+00
1/16	6.351037e-05	2.990346e+00	1.167715e-06	3.964451e+00
1/32	8.030599e-06	2.983413e+00	1.199279e-07	3.283449e+00

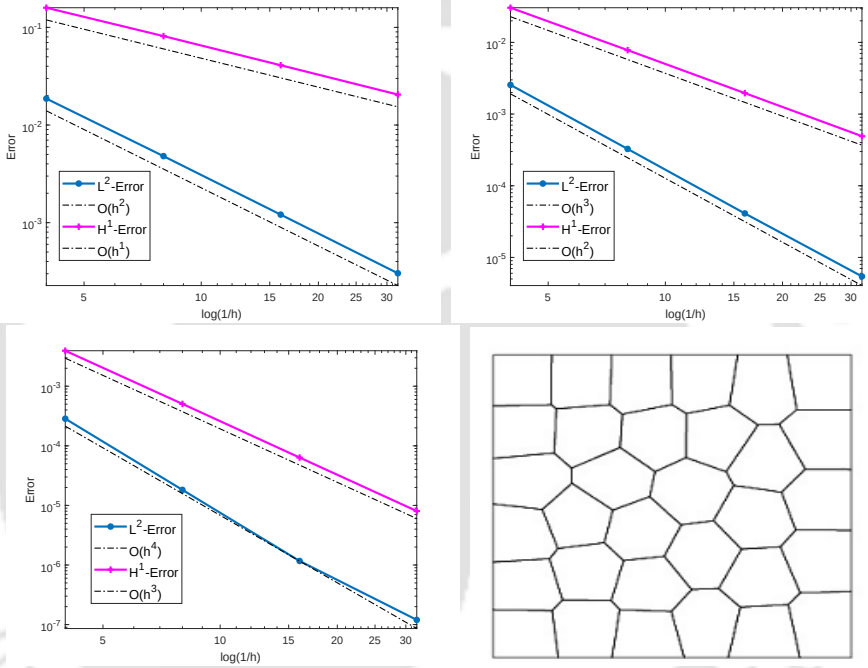

Figure 3.5.3: Log-log plots for WG-spaces $\left(\mathcal{P}_1, \mathcal{P}_1, \left[\mathcal{P}_0\right]^2\right)$ (top left), $\left(\mathcal{P}_2, \mathcal{P}_2, \left[\mathcal{P}_1\right]^2\right)$ (top right) and $\left(\mathcal{P}_3, \mathcal{P}_3, \left[\mathcal{P}_2\right]^2\right)$ (bottom left) in Example 3.5.3, with a polygonal mesh (bottom right).

Example 3.5.4. This test problem arises from the modeling of heat transfer in biological media with discontinuous coefficients. More precisely, we have considered Pennes model (cf. [98]), which is described by a differential equation of parabolic type. In this Example, we consider following parabolic equation

$$\sigma u_t - \nabla \cdot (\alpha \nabla u) = f \tag{3.5.1}$$

in $\Omega \times J$, where $\Omega = (-1, 1) \times (0, 1)$ and $J = [0, 1]$. Coefficient functions σ and α are positive and piecewise constants, which correspond to the Pennes model, are given by

(cf. [31])

$$(\sigma, \alpha) = \begin{cases} (4.08, 0.0052) & \text{in } x \leq 0, \\ (3.06, 0.0021) & \text{in } x > 0. \end{cases}$$

We select f and initial data u^0 by setting the exact solution as

$$u(x, y, t) = \begin{cases} t^2 \cos(t) \cos(\pi x) \sin(\pi y) & \text{if } x \leq 0, \\ t \sin(2\pi x) \sin(\pi y) & \text{if } x > 0. \end{cases}$$

In biological system, it is natural to have heterogeneity in the underlying medium as properties of biological media vary between different layers. Normally, problems involving heterogeneity in the underlying media are referred to as interface problems. Since the solution and coefficients are discontinuous across the line $x = 0$, the performance of WG-FEMs depends on the quality of underlying finite element partition (cf. [92]). Our numerical results are based on the uniform triangular meshes for $k = 1$ and $k = 2$ such that grid line exactly follow the line $x = 0$. The errors with respect to $L^2(H^1)$ norm and $L^2(L^2)$ norm for linear and quadratic WG spaces are reported in Table 3.5.9 and Table 3.5.10, respectively. Figure 3.5.4 indicates desirable rates of convergence for this parabolic problem with discontinuous coefficients. The proposed fully discrete scheme can be easily extended for the numerical approximation of parabolic interface problems. To the best of our knowledge, $L^2(L^2)$ norm and $L^2(H^1)$ norm error estimates of WG-FEMs for parabolic interface problems under the solution regularity $u \in L^2(0, T; H^{k+1}(\Omega)) \cap H^1(0, T; H^1(\Omega))$ are missing.

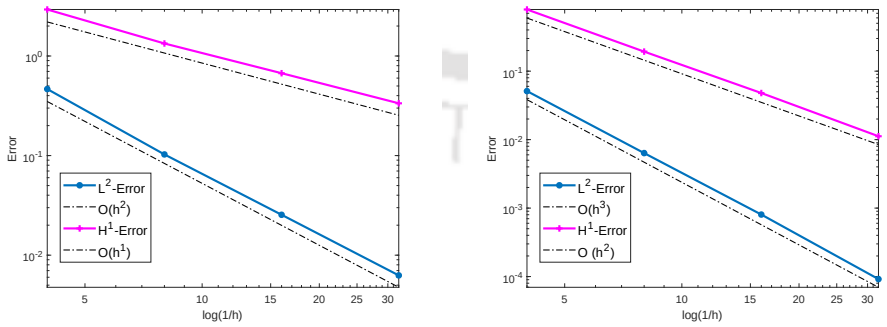

Figure 3.5.4: Log-log plots for WG-spaces $\left(\mathcal{P}_1, \mathcal{P}_1, \left[\mathcal{P}_0\right]^2\right)$ (top left) and $\left(\mathcal{P}_2, \mathcal{P}_2, \left[\mathcal{P}_1\right]^2\right)$ (top right) in Example 3.5.4.

Table 3.5.9: Order of convergence for $k = 1$ with time step $\tau = 10^{-4}$

h	$L^2(J; \|\|\|e_h\|\|\|)$	Order	$L^2(J; \|e_h\|)$	Order
1/4	2.93129e+00		4.65798e-01	
1/8	1.33587e+00	1.13376	1.02728e-01	2.18088
1/16	6.71807e-01	0.991661	2.54458e-02	2.01333
1/32	3.34983e-01	1.00396	6.26613e-03	2.02178

Table 3.5.10: Order of convergence for $k = 2$ with time step $\tau = 10^{-5}$

h	$L^2(J; \|\|\|e_h\|\|\|)$	Order	$L^2(J; \|e_h\|)$	Order
1/4	7.95396e-01		5.11442e-02	
1/8	1.92958e-01	2.04339	6.35741e-03	3.00806
1/16	4.79256e-02	2.00942	8.04763e-04	2.98180
1/32	1.12038e-02	2.09680	9.17893e-05	3.13217

Example 3.5.5. Present numerical Example compares the effect of triangular mesh, rectangular mesh, and polygonal mesh. For this purpose, we consider the IBVP (3.1.1)-(3.1.2) in $(0,1)^2 \times J$ with the exact solution

$$u(x,t) = \begin{cases} t^2 \cos(t) \sin(2\pi x) \sin(\pi y) & \text{if } \ x \leq 0.5, \\ te^{-t} \sin(\pi x) \sin(\pi y) & \text{Otherwise.} \end{cases}$$

The right-hand side f and initial condition u^0 are determined from the choice for u and the diffusion-coefficient

$$\alpha = \begin{bmatrix} 1 & 0 \\ 0 & 1 \end{bmatrix}.$$

Convergence results for $k = 1$ with respect to both $L^2(H^1)$ norm and $L^2(L^2)$ norm for the triangular mesh, rectangular mesh and polygonal mesh are presented in Table 3.5.11, Table 3.5.12 and Table 3.5.13, respectively. In practice, allowing arbitrary shape in a finite element partition provides a convenient flexibility in both numerical approximation and mesh generation. Especially, we have fewer elements and we could evaluate integrals and solve the resulting linear systems in more expedited manner (cf. [64]). However, one disadvantage is that instead of integrals of polynomials on the reference element, we

may have to evaluate integrals of rational functions (cf. [133]). It would be challenging to develop weak Galerkin solver using polygonal meshes for parabolic equation with weak Galerkin space $(\mathcal{P}_k(K),\ \mathcal{P}_j(\partial K),\ \left[\mathcal{P}_l(K)\right]^2)$, where $k \geq 1$, $j \geq 0$ and $l \geq 0$ are arbitrary integers.

Table 3.5.11: Convergence with $k = 1$ and time step $\tau = 10^{-4}$ on triangular mesh

h	$L^2(J;\|\|\|e_h\|\|\|)$	Order	$L^2(J;\|e_h\|)$	Order
1/4	3.047318e-01		3.565084e-02	
1/8	1.384530e-01	1.138144e+00	8.077301e-03	2.141991e+00
1/16	6.528944e-02	1.084474e+00	1.896970e-03	2.090177e+00
1/32	3.161147e-02	1.046401e+00	4.580316e-04	2.050178e+00
1/64	1.554168e-02	1.024306e+00	1.124297e-04	2.026424e+00
1/128	7.704123e-03	1.012439e+00	2.784458e-05	2.013555e+00

Table 3.5.12: Convergence with $k = 1$ and time step $\tau = 10^{-4}$ on rectangular mesh

h	$L^2(J;\|\|\|e_h\|\|\|)$	Order	$L^2(J;\|e_h\|)$	Order
1/4	7.766676e-02		3.298235e-02	
1/8	3.763046e-02	1.045396e+00	9.699506e-03	1.765711e+00
1/16	1.870251e-02	1.008669e+00	2.530535e-03	1.938469e+00
1/32	9.339713e-03	1.001782e+00	6.395063e-04	1.984412e+00
1/64	4.668508e-03	1.000417e+00	1.603105e-04	1.996090e+00
1/128	2.334088e-03	1.000102e+00	4.010480e-05	1.999022e+00

Table 3.5.13: Convergence with $k = 1$ and time step $\tau = 10^{-4}$ on polygonal mesh

h	$L^2(J;\|\|\|e_h\|\|\|)$	Order	$L^2(J;\|e_h\|)$	Order
1/4	1.23242e+00		1.80416e-01	
1/8	8.00726e-01	0.622113e+00	7.95315e-02	1.181729e+00
1/16	3.75299e-01	1.093268e+00	1.79971e-02	2.143761e+00
1/32	1.88814e-01	0.991074e+00	4.52827e-03	1.990732e+00
1/64	9.4442e-02	0.999465e+00	1.14796e-03	1.979887e+00
1/128	4.67715e-02	1.013798e+00	2.80293e-04	2.034064e+00

4

Weak Galerkin Finite Element Methods for Parabolic Problems with L^2 Initial Data

In the previous chapter, we have discussed the convergence of WG-FEM for the parabolic problem (1.1.1)-(1.1.2) when the true solution $u \in L^2(0,T;H^{k+1}(\Omega)) \cap H^1(0,T;H^{k-1}(\Omega))$, for some $k \geq 1$. Such regularity demands source function $f \in L^2(0,T;H^{k-1}(\Omega))$ and initial data $u^0 \in H^k(\Omega)$. For the non-smooth initial data, it is not straight forward to extend the error analysis techniques presented in the previous chapters. The main goal of this chapter is to analyze the weak Galerkin finite element methods for second order linear parabolic problems with L^2 initial data, both in a spatially semidiscrete case and in a completely discrete case based on the backward Euler method. We have established optimal L^2 error estimates of order $\mathrm{O}(h^2/t)$ for semisdiscrete scheme. Subsequently, the results are extended for fully discrete scheme. The error analysis has been carried out on polygonal meshes for discontinuous piecewise polynomials in finite element partitions. Finally, numerical experiments confirm our theoretical convergence results and efficiency of the scheme.

4.1 Introduction

To begin with, let us first recall the second order linear parabolic problem of the form

$$u_t - \nabla \cdot (\alpha \nabla u) = f \quad \text{in } \Omega \times (0,T], \tag{4.1.1}$$

with initial and Dirichlet boundary condition

$$u(x,0) = u^0(x) \ \text{ in } \Omega; \quad u = 0 \quad \text{on } \partial\Omega \times (0,T], \tag{4.1.2}$$

where $\Omega \subset \mathbb{R}^2$ is a convex polygonal domain with boundary $\partial\Omega$. We assume that the coefficient matrix $\alpha = (\alpha_{ij}(x))_{2\times 2} \in [L^\infty(\Omega)]^{2^2}$ is symmetric and uniformly positive

This chapter is under review in *Numer. Algorithms.*

definite in Ω. The initial function $u^0 : \Omega \to \mathbb{R}$ and the forcing function $f : \Omega \times [0, T] \to \mathbb{R}$ are assumed to be smooth functions in their respective domains of definition, and T is the finite terminal observation time.

The standard weak formulation of the problem (4.1.1)-(4.1.2) is stated as follows: Find $u : [0, \infty) \to H_0^1(\Omega)$ such that

$$\begin{aligned} (u_t, v) + \mathcal{A}(u, v) &= (f, v) \quad \forall v \in H_0^1(\Omega), \text{ and} \\ u(0) &= u^0 \text{ in } \Omega, \end{aligned} \tag{4.1.3}$$

where $\mathcal{A}(\cdot, \cdot)$ is a bilinear form on $H_0^1(\Omega) \times H_0^1(\Omega)$ and given by

$$\mathcal{A}(u, v) = \int_\Omega \alpha \nabla u \cdot \nabla v dx.$$

Classical finite element methods for parabolic problems with non-smooth initial data have been studied broadly so far, an extensive literature for the same can be obtained from [85, 100, 111]. We are well aware of the fact that the higher order of convergence of finite element approximations depends on the higher smoothness of the true solutions, which demands higher regularity of the initial functions. The main concern of this work is to study the convergence of weak Galerkin finite element approximations for homogeneous equation with non-smooth initial data using polygonal meshes. The error analysis is highly motivated by the fact that the solutions of parabolic problem have the so-called smoothing property (cf. [85]). That is, the solution is smooth for positive time t, even when the initial data are not H^1 regular. In previous chapter, we have shown the convergence of WG finite element solution to the true solution at an optimal rate in $L^2(L^2)$ norm under the assumption that $u \in L^2(0, T; H^{k+1}(\Omega)) \cap H^1(0, T; H^{k-1}(\Omega))$. In the case of piecewise linear WG-FEM (i.e., $k = 1$), the optimal error estimate requires the initial value to be in H^1 (see, Theorem 3.3.2) and for L^2 initial data error analysis in Theorem 3.3.2 leads to sub-optimal order of convergence in $L^2(L^2)$ norm (see, Remark 4.2.1). In fact, optimal $L^\infty(L^2)$ error estimate in [35] for linear weak Galerkin elements demand initial data $u^0 \in H^3(\Omega)$ (see, Remark 4.2.3). In this work, assuming initial data in L^2, we have shown the convergence of WG finite element solution to the true solution at an optimal rate in L^2 norm on WG finite element space $(\mathcal{P}_1,\ \mathcal{P}_1,\ \mathcal{P}_0^2)$ (see, Theorem 4.2.2 and Theorem 4.3.1). The non-smooth data error analysis heavily depends on the newly derived optimal L^2 norm error estimates with smooth initial data $u^0 \in H_0^1 \cap H^2$ (see, Lemma 4.2.9 and Lemma 4.3.1). The obtained results intend to enhance the numerical analysis of linear parabolic equations on polygonal meshes with non-smooth initial data. To best of our knowledge, on the smoothing property of the WG-FEM for the parabolic equation has not been studied earlier.

We end this section with the following existence and uniqueness result for the problem (4.1.3) (see, [45], p. 378, Theorem 3).

Theorem 4.1.1. *Assume that $f \in L^2(\Omega)$ and $u^0 \in L^2(\Omega)$. Then the solution of (4.1.3) satisfies*

$$u \in L^2(0,T;H_0^1(\Omega)) \cap H^1(0,T;H^{-1}(\Omega)).$$

The rest of this work is organized as follows. Section 4.2 is concerned with the error analysis of semidiscrete WG finite element algorithm. In Section 4.3, backward Euler scheme is proposed and optimal a priori error bounds in $L^\infty(L^2)$ norm is established. Section 4.4 discusses several numerical Examples which demonstrates the robustness of the WG-FEMs.

4.2 Error Analysis for the Semidiscrete Scheme

This section deals with the error analysis for the spatially discrete scheme. Optimal order of convergence in $L^\infty(L^2)$ norm is established when the initial data of the solution is non-smooth.

Let $\mathcal{V}_h$ be the weak Galerkin finite element space defined by (3.2.1) based on the finite element discretization $\mathcal{T}_h$ of Ω as described in Chapter 1. For each $v_h = \{v_0, v_b\} \in \mathcal{V}_h$, we recall its discrete weak gradient $(\nabla_w v_h) \in [\mathcal{P}_{k-1}(K)]^2$ that satisfies the following equation

$$(\nabla_w v_h, \mathbf{q})_K = -\int_K v_0(\nabla \cdot \mathbf{q})dK + \int_{\partial K} v_b(\mathbf{q}\cdot\mathbf{n})ds \;\; \forall \mathbf{q} \in [\mathcal{P}_{k-1}(K)]^2. \tag{4.2.1}$$

Next, we recall the bilinear map $\mathcal{A}_w(\cdot,\cdot)$ on $\mathcal{V}_h \times \mathcal{V}_h$, which is defined as follows

$$\mathcal{A}_w(w_h, v_h) := \sum_{K\in\mathcal{T}_h} \left(\alpha\nabla_w u_h, \nabla_w v_h\right)_K + \mathcal{S}(w_h, v_h) \;\; \forall w_h, v_h \in \mathcal{V}_h, \tag{4.2.2}$$

where the stabilizer is as defined in (3.2.7). More precisely, for $w_h = \{w_0, w_b\}$, $v_h = \{v_0, v_b\} \in \mathcal{V}_h$, the stabilizer $\mathcal{S}(\cdot,\cdot)$ is defined as

$$\mathcal{S}(w_h, v_h) = \sum_{K\in\mathcal{T}_h} h_K^{-1}\langle w_0 - w_b, v_0 - v_b\rangle_{\partial K}. \tag{4.2.3}$$

For each element $K \in \mathcal{T}_h$, Q_0 and Q_b are the usual L^2 projection operators onto $\mathcal{P}_k(K)$ and $\mathcal{P}_k(\partial K)$, respectively. We shall combine Q_0 with Q_b by writing $Q_h = \{Q_0, Q_b\}$. More precisely, for $w \in H^1(K)$, we have $Q_h w = \{Q_0 w, Q_b w\}$.

We recall following crucial approximation properties for local projections Q_0. For details, we refer to (Lemma 4.1, [123]).

Lemma 4.2.1. *Let $\mathcal{T}_h$ be a finite element partition of Ω satisfying the shape regularity assumption as specified in [123]. Then, for $v \in H^{k+1}(\Omega)$, we have*

$$\sum_{K\in\mathcal{T}_h}\Big(\|v-Q_0v\|_K^2+h_K^2\|\nabla(v-Q_0v)\|_K^2\Big)\le Ch^{2(k+1)}\|v\|_{k+1}^2.$$

Recall that the weak finite element space $\mathcal{V}_h^0$ is a normed linear space with a triple-bar norm given by (cf. [121])

$$|||v_h|||^2=\sum_{K\in\mathcal{T}_h}\|\alpha^{\frac{1}{2}}\nabla_w v_h\|_K^2+\sum_{K\in\mathcal{T}_h}h_K^{-1}\|v_0-v_b\|_{\partial K}^2=\mathcal{A}_w(v_h,v_h). \tag{4.2.4}$$

A time-dependent weak function $v_h:[0,T]\to\mathcal{V}_h$ is written as $v_h(t):=\{v_0(t),v_b(t)\}$ and subsequently we define $v_{ht}(t):=\{v_0'(t),v_b'(t)\}$, where '$\prime$' denotes the time derivatives. For simplicity, we use $v_h=\{v_0,v_b\}$ for $v_h(t)$ and $v_{ht}=\{v_0',v_b'\}$ for $v_{ht}(t)$. It is easy to note from the definition of weak gradient (1.4.4) that $(\nabla_w v_h)'=\nabla_w v_h'$ and $(\nabla_w v_h)|_{t=0}=\nabla_w v_h(0)$ for all $v_h\in\mathcal{V}_h$.

The semidiscrete weak Galerkin finite element approximation for (4.1.1)-(4.1.2) is to find $u_h(t)=\{u_0(t),u_b(t)\}\in\mathcal{V}_h^0$ satisfying $u_h(0)=\{Q_0u^0,Q_b(Q_0u^0)\}$ such that

$$(u_{ht},v_0)+\mathcal{A}_w(u_h,v_h)=(f,v_0)\quad\forall v_h=\{v_0,v_b\}\in\mathcal{V}_h^0,\ t>0, \tag{4.2.5}$$

where the bilinear map $\mathcal{A}_w(\cdot,\cdot)$ is as defined in (4.2.2).

The following result deals with the existence and uniqueness of the WG solution u_h.

Theorem 4.2.1. *For each $h\in(0,h_0]$, there exists a function $u_h\in C^1(0,T;\mathcal{V}_h^0)$ satisfying (4.2.5).*

Proof. For a given element $K\in\{\mathcal{T}_h\}_{0<h\le h_0}$, let $\{\phi_{0,i}:\ i=1,2,\dots,N_0\}$ be a set of basis functions for $\mathcal{P}_k(K)$ and $\{\phi_{b,i}:\ i=1,2,\dots,N_b\}$ be a set of basis function for $\mathcal{P}_k(e)$. Then every $v_h=\{v_0,v_b\}\in\{\mathcal{V}_h^0\}_{0<h\le h_0}$ can be written as

$$v_h|_K=\left\{\sum_{i=1}^{N_0}d_{0,i}(t)\phi_{0,i},\sum_{j=1}^{N_b}d_{b,j}(t)\phi_{b,j}\right\},$$

where $d_{0,i},\ d_{b,j}:(0,T]\to\mathbb{R}$ are the coefficient functions for $1\le i\le N_0$ and $1\le j\le N_b$. For $1\le i\le N_0+N_b$, we write $\hat{\phi}_{i,h}=\{\hat{\phi}_{0,i},\hat{\phi}_{b,i}\}$ with

$$\begin{aligned}\hat{\phi}_{0,i}&=\phi_{0,i}\ \text{ for } 1\le i\le N_0\quad\&\quad\hat{\phi}_{0,i}=0\ \text{ for }\ N_0+1\le i\le N_0+N_b,\\ \hat{\phi}_{b,i}&=0\ \text{ for }\ 1\le i\le N_0\quad\&\quad\hat{\phi}_{b,i}=\phi_{b,i-N_0}\ \text{ for }\ N_0+1\le i\le N_0+N_b,\end{aligned}$$

and similarly to capture the unknown coefficient functions, we define

$$\hat{d}_{i,h}=d_{0,i}\ \text{ for } 1\le i\le N_0\ \ \&\ \ \hat{d}_{i,h}=d_{b,i-N_0}\ \text{ for } N_0+1\le i\le N_0+N_b.$$

Then, we seek our semidiscrete solution $u_h = \{u_0, u_b\} \in \mathcal{V}_h^0$ such that

$$u_h|_K = \sum_{i=1}^{N_0+N_b} \hat{d}_{i,h}(t)\hat{\phi}_{i,h} = \left\{ \sum_{i=1}^{N_0+N_b} \hat{d}_{i,h}(t)\hat{\phi}_{0,i}, \sum_{j=1}^{N_0+N_b} \hat{d}_{j,h}(t)\hat{\phi}_{b,j} \right\}, \quad K \in \mathcal{T}_h.$$

Now, set $v_h = \hat{\phi}_{j,h},\ j = 1, 2, \ldots, N_0 + N_b$ in (4.2.5) to obtain

$$\begin{aligned} &\left(\sum_{i=1}^{N_0+N_b} \hat{d}'_{i,h}(t)\hat{\phi}_{0,i}, \hat{\phi}_{0,j} \right) + \mathcal{A}_w \left(\sum_{i=1}^{N_0+N_b} \hat{d}_{i,h}(t)\hat{\phi}_{i,h}, \hat{\phi}_{j,h} \right) \\ &= (f, \hat{\phi}_{0,j}), \quad j = 1, \ldots, N_0 + N_b. \end{aligned}$$

We can rearrange the above equations as

$$\begin{aligned} &\sum_{i=1}^{N_0+N_b} \hat{d}'_{i,h}(t)\big(\hat{\phi}_{0,i}, \hat{\phi}_{0,j}\big) + \sum_{i=1}^{N_0+N_b} \hat{d}_{i,h}(t)\mathcal{A}_w\big(\hat{\phi}_{i,h}, \hat{\phi}_{j,h}\big) \\ &= (f, \hat{\phi}_{0,j}),\ j = 1, \ldots, N_0 + N_b. \end{aligned}$$

On each element K, the local stiffness matrix $\mathcal{A}_K$ associated with the bilinear map $\mathcal{A}_w(\cdot, \cdot)$ defined by (4.2.2) can thus be written as a block matrix

$$\mathcal{A}_K = \begin{bmatrix} \mathcal{A}_{0,0} & \mathcal{A}_{0,b} \\ \mathcal{A}_{b,0} & \mathcal{A}_{b,b} \end{bmatrix}, \tag{4.2.6}$$

where $\mathcal{A}_{0,0}$ is a $N_0 \times N_0$, $\mathcal{A}_{0,b}$ is a $N_0 \times N_b$, $\mathcal{A}_{b,0}$ is a $N_b \times N_0$, and $\mathcal{A}_{b,b}$ is a $N_b \times N_b$ matrices. More precisely, these matrices are given by

$$\mathcal{A}_{0,0} = [\mathcal{A}_w(\phi_{0,j}, \phi_{0,i})_K]_{i,j}, \quad \mathcal{A}_{0,b} = [\mathcal{A}_w(\phi_{0,j}, \phi_{b,i})_K]_{i,j}$$

$$\mathcal{A}_{b,0} = [\mathcal{A}_w(\phi_{b,j}, \phi_{0,i})_K]_{i,j}, \quad \mathcal{A}_{b,b} = [\mathcal{A}_w(\phi_{b,j}, \phi_{b,i})_K]_{i,j},$$

where i, j are the row and column indices, respectively.

We denote by

$$\hat{d}_{h,0} = [\hat{d}_{1,h}(0), \ldots, \hat{d}_{N_0+N_b,h}(0)]^T$$

the components of given initial approximation $u_h(0)$. Then, for our semidiscrete solution, we need to find unknown vector $\hat{d}_h(t) = [\hat{d}_{1,h}(t), \ldots, \hat{d}_{N_0+N_b,h}(t)]^T$ such that

$$\begin{cases} \mathcal{C}_K \hat{d}'_h(t) + \mathcal{A}_K \hat{d}_h(t) = F_K(t) \ \text{ for } \ t \in (0, T], \\ \hat{d}_h(0) = \hat{d}_{h,0}, \end{cases} \tag{4.2.7}$$

where the coefficient matrix C_K is given by

$$\mathcal{C}_K = [\mathcal{C}_{j,i}], \quad \mathcal{C}_{j,i} = (\hat{\phi}_{j,h}, \hat{\phi}_{i,h})_K, \quad 1 \le i, j \le N_0 + N_b$$

and the source vector is given by

$$F_K = [F_1, \ldots, F_{N_0+N_b}], \quad F_j = (f, \hat{\phi}_{j,h})_K, \quad 1 \le i, j \le N_0 + N_b.$$

For all $t \in J = (0, T]$, it is easy note that

$$|(\hat{\phi}_{i,h}, \hat{\phi}_{j,h})| \le \|\hat{\phi}_{i,h}\|\|\hat{\phi}_{j,h}\|, \quad |(f, \hat{\phi}_{j,h})| \le \|f\|\|\hat{\phi}_{j,h}\| \quad \&$$
$$|\mathcal{A}_w(\hat{\phi}_{i,h}, \hat{\phi}_{j,h})| \le C\|\hat{\phi}_{i,h}\|_{1,h}\|\hat{\phi}_{j,h}\|_{1,h}.$$

Furthermore, for any $v \in \mathbb{R}^{N_0+N_b} \setminus \{\mathbf{0}\}$, we have

$$v^T C_K v = (\hat{v}, \hat{v})_K > 0, \quad \hat{v} = \sum_{i=1}^{N_0+N_b} v_i \hat{\phi}_{0,i}.$$

Hence, the matrix C_K is invertible for all $t \in J$ and the equation (4.2.7) can be restated as

$$\begin{cases} \hat{d}_h'(t) + \mathcal{C}_K^{-1}\mathcal{A}_K \hat{d}_h(t) = \mathcal{C}_K^{-1} F_K(t), \\ \hat{d}_h(0) = \hat{d}_{h,0}. \end{cases}$$

Now, the existence of the solution $u_h \in C^1(0, T; \mathcal{V}_h^0)$ follows from the standard ODE theory. This completes the rest of the proof. □

We have adopted following few results from [85] to state some a priori bounds for the solution u satisfying (4.1.3) under appropriate regularity assumptions on the initial data u^0 and source function f.

Lemma 4.2.2. *Let u satisfies (4.1.1). If $u^0 \in L^2(\Omega)$ and $f \in L^2(\Omega)$, then*

$$\|u(t)\|^2 + \int_0^t \|u(s)\|_1^2 ds \le C\Big(\|u^0\|^2 + \int_0^t \|f(s)\|^2 ds\Big).$$

Moreover, when $u^0 \in H_0^1(\Omega)$ and $f \in L^2(\Omega)$, we have

$$\|u(t)\|_1^2 + \int_0^t \{\|u_s(s)\|^2 + \|u(s)\|_2^2\} ds \le C\Big(\|u^0\|_1^2 + \int_0^t \|f(s)\|^2 ds\Big).$$

Lemma 4.2.3. *Let u satisfies (4.1.1) with $f = 0$, and let $0 \le i, j, s \le 2$. If $0 \le s + 2j - i \le 2$, then*

$$t^i \Big\| \frac{\partial^j u}{\partial t^j}(t) \Big\|_s^2 \le C\|u^0\|_{s+2j-i}^2.$$

Further, if $0 \le s + 2j - i - 1 \le 2$, then

$$\int_0^t \vartheta^i \Big\| \frac{\partial^j u}{\partial \vartheta^j}(\vartheta) \Big\|_s^2 d\vartheta \le C\|u^0\|_{s+2j-i-1}^2.$$

In the following Lemmas, we have proved basic stability results for the weak Galerkin solution u_h satisfying (4.2.5).

Lemma 4.2.4. *Assume that u_h is a solution of (4.2.5). Let $f \in L^2(\Omega)$ and $u^0 \in L^2(\Omega)$ with initial approximation $u_h(0) = (Q_0u^0, Q_b(Q_0u^0))$, then*

$$\|u_h(t)\|^2 + \int_0^t \|u_h\|_{1,h}^2 \leq C\Big(\|u_h(0)\|^2 + \int_0^t \|f(s)\|^2 ds\Big). \tag{4.2.8}$$

Proof. Taking $v_h = u_h$ in (4.2.5), we get

$$\frac{1}{2}\frac{d}{dt}\|u_h(t)\|^2 + \mathcal{A}_w(u_h, u_h) = (f, u_h).$$

Now, integrate the above equation with respect to t to obtain

$$\frac{1}{2}\|u_h(t)\|^2 + \int_0^t \mathcal{A}_w(u_h, u_h)ds = \frac{1}{2}\|u_h(0)\|^2 + \int_0^t (f, u_h)ds$$

Then, Young's inequality and (1.4.15) leads to

$$\begin{aligned}\frac{1}{2}\|u_h(t)\|^2 + \int_0^t \|u_h\|_{1,h}^2 ds \;\leq\; & \frac{1}{2}\|u_h(0)\|^2 + C_\nu \int_0^t \|f(s)\|^2 ds \\ & + C(\nu)\int_0^t \|u_h(s)\|^2 ds,\end{aligned}$$

for some $\nu > 0$. Finally, suitable $\nu > 0$ and (3.2.9) yield desired result. □

Lemma 4.2.5. *Assume that u_h is a solution of (4.2.5). Let $f = 0$ and $u^0 \in L^2(\Omega)$ with initial approximation $u_h(0) = (Q_0u^0, Q_b(Q_0u^0))$, then*

$$t\|u_h(t)\|_{1,h}^2 + \int_0^t s\|u_{hs}\|^2 ds \leq C\|u_h(0)\|^2. \tag{4.2.9}$$

Proof. Setting $v_h = u_{ht}$ in (4.2.5), we get

$$\|u_{ht}(t)\|^2 + \frac{1}{2}\frac{d}{dt}\mathcal{A}_w(u_h, u_h) = 0.$$

Multiplying above equation by t, we obtain

$$t\|u_{ht}(t)\|^2 + \frac{1}{2}\frac{d}{dt}\{t\mathcal{A}_w(u_h(t), u_h(t))\} = \frac{1}{2}\mathcal{A}_w(u_h, u_h).$$

Then, integrate above equation over $[0, t]$ to get

$$t\|u_h(t)\|_{1,h}^2 + \int_0^t s\|u_{hs}(s)\|^2 ds \leq C\int_0^t \|u_h(s)\|_{1,h}^2 ds,$$

which together with estimate (4.2.8) yields (4.2.9). □

Lemma 4.2.6. *Assume that u_h is a solution of (4.2.5). Let $f = 0$ and $u^0 \in H_0^1(\Omega) \cap H^2(\Omega)$ with suitable initial approximation $u_h(0) \in \mathcal{V}_h^0$, then*

$$\|u_{ht}\|^2 + \int_0^t \|u_{hs}\|_{1,h}^2 ds \leq C\|u_{ht}(0)\|^2. \tag{4.2.10}$$

Further, if $u_0 \in L^2(\Omega)$ and $f = 0$ with $u_h(0) = (Q_0u^0, Q_b(Q_0u^0))$, then

$$t^2\|u_{ht}(t)\|^2 + \int_0^t s^2\|u_{hs}\|_{1,h}^2 ds \leq C\|u_h(0)\|^2. \tag{4.2.11}$$

Proof. We differentiate (4.2.5) with respect to time t to obtain

$$(u_{htt}, v_h) + \mathcal{A}_w(u_{ht}, v_h) = 0.$$

Now, set $v_h = u_{ht}$ in the above equation to have

$$\frac{1}{2}\frac{d}{dt}\|u_{ht}\|^2 + \mathcal{A}_w(u_{ht}, u_{ht}) = 0. \tag{4.2.12}$$

Integrating above equation from 0 to t and applying (1.4.15), we arrive at (4.2.10).

In the case $u^0 \in L^2(\Omega)$, like earlier, we multiply (4.2.12) by t^2 and obtain

$$\frac{1}{2}\frac{d}{dt}\{t^2\|u_{ht}\|^2\} + t^2\mathcal{A}_w(u_{ht}, u_{ht}) = t\|u_{ht}\|^2,$$

which upon integrating over $[0, t]$ leads to

$$t^2\|u_{ht}\|^2 + \int_0^t s^2\mathcal{A}_w(u_{hs}, u_{hs})ds = \int_0^t s\|u_{hs}\|^2 ds.$$

Now, apply the coercive property (1.4.15) to obtain

$$t^2\|u_{ht}\|^2 + \int_0^t s^2\|u_{hs}\|_{1,h}^2 ds \leq C\int_0^t s\|u_{hs}\|^2 ds. \tag{4.2.13}$$

Finally, estimates (4.2.9) and (4.2.13) lead to desire result. □

For the error analysis, we split our semidiscrete error $e_h = u - u_h$ into two components using an intermediate operator. We write

$$e_h = u - u_h := (u - Q_hu) + (Q_hu - u_h).$$

The following estimate for e_h is derived over the time interval $[0, t]$, which is very imperative for our further analysis.

Lemma 4.2.7. *Let $u^0 \in H_0^1(\Omega) \cap H^k(\Omega)$, $r \in \{1, 2\}$ and $f = 0$, then*

$$\int_0^t \|e_h\|^2 ds \leq Cth^{2r}\|u^0\|_r^2. \tag{4.2.14}$$

Proof. To derive L^2 error estimate over the time interval $[0,t]$, we recall the following estimate from earlier work (cf. [34], Theorem 3.2)

$$\int_0^t \|e_h\|^2 ds \leq Ch^{2r} \int_0^t \|u\|_r^2 ds. \tag{4.2.15}$$

Now, apply Lemma 4.2.3 with $i = 0 = j$ and $s = r$ in the above estimate to have

$$\begin{aligned} \int_0^t \|e_h\|^2 ds &\leq Ch^{2r} \int_0^t \|u^0\|_r^2 ds \\ &\leq Cth^{2r} \|u^0\|_r^2. \end{aligned}$$ □

Remark 4.2.1. *For $u^0 \in L^2(\Omega)$ and $f = 0$, let u solves (4.1.1)-(4.1.2). Then, from the Lemma 4.2.2, we have $u \in L^2(0,T;H^1(\Omega))$. As as consequence, we obtain*

$$\int_0^t \|e_h\|^2 ds \leq Ch^2 \int_0^t \|u\|_1^2 ds. \tag{4.2.16}$$

Here, we have used (4.2.15) with $r = 1$. Finally, a priori estimate in Lemma 4.2.2 yields

$$\int_0^t \|e_h\|^2 ds \leq Ch^2 \|u^0\|^2. \tag{4.2.17}$$

Clearly, $L^2(L^2)$ error estimate (4.2.17) is not optimal for non-smooth initial data u^0. The rest of section is devoted in deriving optimal $L^\infty(L^2)$ norm estimate for the WG finite element approximation with $u^0 \in L^2(\Omega)$.

Next, we have applied elliptic projection to derive optimal L^2 error estimates. For $w \in H^2(\Omega) \cap H_0^1(\Omega)\}$, we define

$$f_w = -\nabla \cdot (\alpha \nabla w) \text{ in } \Omega.$$

Now, define $\mathcal{E}_h : H^2(\Omega) \cap H_0^1(\Omega) \to \mathcal{V}_h^0$ by

$$\mathcal{A}_w(\mathcal{E}_h w, v_h) = (f_w, v_0) \ \ \forall v_h = \{v_0, v_b\} \in \mathcal{V}_h^0. \tag{4.2.18}$$

It is easy to observe from the definition of elliptic projection and equation (4.2.5) that

$$(u_{ht}, v_h) + \mathcal{A}_w(u_h - \mathcal{E}_h u, v_h) = (f, v_h) + (\nabla \cdot (a \nabla u), v_h) = (u_t, v_h), \tag{4.2.19}$$

for all $v_h = \{v_0, v_b\} \in \mathcal{V}_h^0$. Here, we have used equation (4.1.1).

Remark 4.2.2. *For $u^0 \in H_0^1(\Omega) \cap H^2(\Omega)$ and $f = 0$ with $u_h(0) = \mathcal{E}_h u^0$, identity (4.2.19) yields*

$$(u_{ht}(0), v_h) = \ (u_t(0), v_h) \ \ \forall v_h = \{v_0, v_b\} \in \mathcal{V}_h^0,$$

which implies

$$\|u_{ht}(0)\| \leq \|u_t(0)\| \leq C\|u^0\|_2. \tag{4.2.20}$$

Hence, apriori estimate (4.2.10) reduces to

$$\|u_{ht}\|^2 + \int_0^t \|u_{hs}\|_{1,h}^2 ds \leq C\|u^0\|_2^2. \tag{4.2.21}$$

We can derive following lemma from the Chapter 2 (see, proof of Theorem 2.3.2 and Remark 2.3.3) directly. We omit the details.

Lemma 4.2.8. *For $v \in H^1(0,T; H^{\lambda+1}(\Omega) \cap H_0^1(\Omega))$, $0 \leq \lambda \leq k$, we have*

$$\begin{aligned} \|Q_h v - \mathcal{E}_h v\| + h\|Q_h v - \mathcal{E}_h v\|_{1,h} &\leq Ch^{\lambda+1}\|v\|_{\lambda+1} \quad \text{and} \\ \int_0^t s^2 \Big(\|(v - Q_h v)_t\|^2 + \|\big(Q_h v - \mathcal{E}_h v\big)_t\|^2 \Big) ds &\leq Ch^{2(\lambda+1)} \int_0^t s^2 \|v_t\|_{\lambda+1}^2 ds. \end{aligned}$$

Corollary 4.2.1. *For $u^0 \in H_0^1(\Omega) \cap H^2(\Omega)$ and $f = 0$, Lemma 4.2.3 and Lemma 4.2.8 yield*

$$\begin{aligned} \|u - Q_h u\| + \|Q_h u - \mathcal{E}_h u\| &\leq Ch^2\|u\|_2 \leq Ch^2\|u^0\|_2 \quad \text{and} \\ \int_0^t s^2 \Big(\|(u - Q_h u)_t\|^2 + \|\big(Q_h u - \mathcal{E}_h u\big)_t\|^2 \Big) ds &\leq Ch^4 \int_0^t s^2 \|u_t\|_2^2 ds \leq Ch^2 t \|u^0\|_2^2. \end{aligned}$$

Remark 4.2.3. *Theorem 3.1.2 in [35] and Lemma 4.2.1, for the weak Galerkin space $(\mathcal{P}_1(K),\ \mathcal{P}_1(\partial K),\ \big[\mathcal{P}_0(K)\big]^2)$, yields*

$$\|(u - u_h)(t)\|^2 \leq Ch^4 \left(\|u\|_2^2 + \int_0^t \|u_t\|_2^2 d\vartheta \right), \tag{4.2.22}$$

which demands $u \in H^1(0,T; H^2(\Omega))$. Again, due to Theorem 2.10 in [86], solution $u \in H^1(0,T; H^2(\Omega))$ provided initial data $u^0 \in H^3(\Omega)$. Thus, for $u^0 \in H_0^1(\Omega) \cap H^2(\Omega)$, we can not directly use estimate (4.2.22).

Next result illustrates optimal $L^\infty(L^2)$ norm error estimate for the semidiscrete approximation on linear weak Galerkin space $(\mathcal{P}_1(K),\ \mathcal{P}_1(\partial K),\ \big[\mathcal{P}_0(K)\big]^2)$ with $u^0 \in H_0^1(\Omega) \cap H^2(\Omega)$.

Lemma 4.2.9. *If $u^0 \in H_0^1(\Omega) \cap H^2(\Omega)$ and $f = 0$, then*

$$\|e_h(t)\| \leq Ch^2\|u^0\|_2. \tag{4.2.23}$$

Proof. First, we split our error into three components and we write

$$e_h = u - u_h = (u - Q_h u) + (Q_h u - \mathcal{E}_h u) + (\mathcal{E}_h u - u_h) := \rho + \eta + \xi, \tag{4.2.24}$$

where $\rho := u - Q_h u$, $\eta := Q_h u - \mathcal{E}_h u$ and $\xi := \mathcal{E}_h u - u_h$.

According to the definition of projection $\mathcal{E}_h u$, we have

$$\begin{aligned}(\xi_t, v_h) + \mathcal{A}_w(\xi, v_h) &= (\mathcal{E}_h u_t, v_h) + \mathcal{A}_w(\mathcal{E}_h u, v_h) - (u_{ht}, v_h) - \mathcal{A}_w(u_h, v_h)\\ &= -(\eta_t, v_h) - (\rho_t, v_h).\end{aligned}$$

Choose $v_h = \xi$ to have

$$\frac{1}{2}\frac{d}{dt}\|\xi\|^2 + \mathcal{A}_w(\xi, \xi) = -(\eta_t, \xi) - (\rho_t, \xi). \tag{4.2.25}$$

Multiplying (4.2.25) by t, we get

$$\frac{1}{2}\frac{d}{dt}\{t\|\xi\|^2\} + t\mathcal{A}_w(\xi, \xi) = -t(\eta_t, \xi) - t(\rho_t, \xi) + \frac{1}{2}\|\xi\|^2. \tag{4.2.26}$$

Integration of (4.2.26) over $[0, t]$ yields

$$\frac{t}{2}\|\xi\|^2 + \int_0^t t\mathcal{A}_w(\xi, \xi)ds = -\int_0^t s(\eta_s, \xi)ds - \int_0^t s(\rho_s, \xi)ds + \frac{1}{2}\int_0^t \|\xi\|^2 ds.$$

Next, standard inequality and positive definiteness of $\mathcal{A}_w(\cdot, \cdot)$ lead to

$$\frac{t}{2}\|\xi\|^2 \leq C\int_0^t s^2\{\|\eta_s\|^2 + \|\rho_s\|^2\}ds + C\int_0^t \|\xi\|^2 ds. \tag{4.2.27}$$

Now, from (4.2.24) and estimate (4.2.27), we have

$$\begin{aligned}t\|e_h\|^2 &\leq C\big(t\|\rho\|^2 + t\|\eta\|^2 + t\|\xi\|^2\big)\\ &\leq Ct(\|\rho\|^2 + \|\eta\|^2) + C\int_0^t \|\xi\|^2 ds + C\int_0^t s^2(\|\eta_t\|^2 + \|\rho_t\|^2)ds.\\ &\leq Ct(\|\rho\|^2 + \|\eta\|^2) + C\int_0^t \big(\|\eta\|^2 + s^2\|\eta_t\|^2\big)ds\\ &\quad + C\int_0^t \big(\|\rho\|^2 + s^2\|\rho_t\|^2\big)ds + C\int_0^t \|e_h\|^2 ds.\end{aligned} \tag{4.2.28}$$

Finally, Lemma 4.2.7 and Corollary 4.2.1 yield

$$t\|e_h(t)\|^2 \leq Cth^4\|u^0\|_2^2. \quad \square$$

Next, we proceed for the error analysis with non-smooth initial data.

Lemma 4.2.10. *If $u^0 \in L^2$ and $f \equiv 0$. Then, for $t > 0$, we have*

$$\|e_h(t)\| \leq C\frac{h}{t^{1/2}}\|u^0\|. \tag{4.2.29}$$

Proof. We first recall the estimate (4.2.28)

$$\begin{aligned} t\|e_h\|^2 &\leq Ct(\|\rho\|^2 + t\|\eta\|^2) + C\int_0^t \big(\|\eta\|^2 + s^2\|\eta_t\|^2\big)ds \\ &\quad + C\int_0^t \big(\|\rho\|^2 + s^2\|\rho_t\|^2\big)ds + C\int_0^t \|e_h\|^2 ds. \end{aligned} \tag{4.2.30}$$

Then apply Lemma 4.2.8 with $\lambda = 0$ to arrive at

$$t\|e_h\|^2 \leq Ch^2 t\|u\|_1^2 + Ch^2\int_0^t \big(\|u\|_1^2 + s^2\|u_t\|_1^2\big)ds + C\int_0^t \|e_h\|^2 ds.$$

Then, using Lemmas 4.2.2-4.2.3 and estimate (4.2.17), we obtain

$$t\|e_h\|^2 \leq Ch^2\|u^0\|^2.$$

This completes the rest of proof. □

To obtain optimal $L^\infty(L^2)$ norm error estimate, we now use parabolic dual argument considering a backward problem. For fixed $t > 0$ and $g \in L^2(\Omega)$, define $w : [0, t) \to H_0^1(\Omega)$ by

$$\begin{aligned} (\phi, w_s) - \mathcal{A}(\phi, w) &= 0 \quad \forall \phi \in H_0^1(\Omega), \quad s \leq t, \\ w(t) &= g, \end{aligned} \tag{4.2.31}$$

and define $w_h = \{w_0, w_b\} : [0, t) \to \mathcal{V}_h^0$ by

$$\begin{aligned} (v_0, w_{hs}) - \mathcal{A}_w(v_h, w_h) &= 0 \ \ \forall v_h = \{v_0, v_b\} \in \mathcal{V}_h^0, \ \ s \leq t, \\ w_h(t) &= g_h. \end{aligned} \tag{4.2.32}$$

Then, by construction, we have

$$\frac{d}{ds}\{(u, w) - (u_h, w_h)\} = (f, w - w_h). \tag{4.2.33}$$

Integrating above from 0 to t and setting $\tilde{e}_h := w - w_h$, we obtain

$$\begin{aligned} (u(t), w(t)) - (u_h(t), w_h(t)) &= (u^0, w(0)) - (u_h(0), w_h(0)) \\ &\quad + \int_0^t (f, \tilde{e}_h)ds. \end{aligned} \tag{4.2.34}$$

Further, if $u_h(0) = (Q_0u^0, Q_b(Q_0u^0)$ and $g_h = (Q_0g, Q_b(Q_0g))$, we arrive at following crucial identity

$$(e_h(t), g) = (u^0, \tilde{e}_h(0)) + \int_0^t (f, \tilde{e}_h)ds. \tag{4.2.35}$$

Lemma 4.2.11. *If $u^0 \in L^2$ and $f = 0$, then*

$$\|e_h(t)\|_{-2} \leq Ch^2\|u^0\|. \tag{4.2.36}$$

Proof. From the equation (4.2.35) with $f = 0$, we have

$$(e_h(t), g) = (u^0, \tilde{e}_h(0)).$$

Thus, applying estimate (4.2.23) to the backward error $\tilde{e}_h(t)$ yields

$$|(e_h(t), g)| \leq Ch^2\|u^0\|\|g\|_2, \quad g \in H_0^1(\Omega) \cap H^2(\Omega).$$

Then, definition (1.2.1) with $m = 2$ leads to desire estimate. □

Now, we are in a position to discuss the main result of this section.

Theorem 4.2.2. *Let u be the solution of (4.1.1)-(4.1.2) and $u_h \in \mathcal{V}_h^0$ be the solution of (4.2.5). Assume that $u^0 \in L^2(\Omega)$ and $f = 0$, then there is a positive constant C independent of h such that*

$$\|e_h(t)\| \leq C\frac{h^2}{t}\|u^0\|, \quad t > 0. \tag{4.2.37}$$

Proof. Integrating the equation (4.2.33) from $t/2$ to t and using the fact $g_h = (Q_0 g, Q_b(Q_0 g))$, we get

$$\begin{aligned}
(e_h(t), g) &= \left(u\left(\tfrac{t}{2}\right), w\left(\tfrac{t}{2}\right)\right) - \left(u_h\left(\tfrac{t}{2}\right), w_h\left(\tfrac{t}{2}\right)\right) \\
&= \left(e_h\left(\tfrac{t}{2}\right), w\left(\tfrac{t}{2}\right)\right) - \left(e_h\left(\tfrac{t}{2}\right), \tilde{e}_h\left(\tfrac{t}{2}\right)\right) \\
&\quad + \left(u\left(\tfrac{t}{2}\right), \tilde{e}_h\left(\tfrac{t}{2}\right)\right) \\
&\leq \left\|e_h\left(\tfrac{t}{2}\right)\right\|_{-2}\left\|w\left(\tfrac{t}{2}\right)\right\|_2 + \left\|e_h\left(\tfrac{t}{2}\right)\right\|\left\|\tilde{e}_h\left(\tfrac{t}{2}\right)\right\| \\
&\quad + \left\|u\left(\tfrac{t}{2}\right)\right\|_2\left\|\tilde{e}_h\left(\tfrac{t}{2}\right)\right\|_{-2}.
\end{aligned} \tag{4.2.38}$$

Applying estimate (4.2.36) for the terms $\|e_h(\frac{t}{2})\|_{-2}$ and $\|\tilde{e}_h(\frac{t}{2})\|_{-2}$, we obtain

$$\left\|e_h\left(\frac{t}{2}\right)\right\|_{-2} \leq Ch^2\|u^0\| \quad \& \quad \left\|\tilde{e}_h\left(\frac{t}{2}\right)\right\|_{-2} \leq Ch^2\|g\|. \tag{4.2.39}$$

Further, using estimate (4.2.29) for the terms $\left\|e_h\left(\frac{t}{2}\right)\right\|$ and $\|\tilde{e}_h\left(\frac{t}{2}\right)\|$, we get

$$\left\|e_h\left(\frac{t}{2}\right)\right\| \leq C\frac{h}{t^{1/2}}\|u^0\| \quad \& \quad \left\|\tilde{e}_h\left(\frac{t}{2}\right)\right\| \leq C\frac{h}{t^{1/2}}\|g\|. \tag{4.2.40}$$

Again, Lemma 4.2.3 gives us

$$\left\|u\left(\frac{t}{2}\right)\right\|_2 \leq \frac{C}{t}\|u_0\| \quad \text{and} \quad \left\|w\left(\frac{t}{2}\right)\right\|_2 \leq \frac{C}{t}\|g\|. \tag{4.2.41}$$

Finally, $g = e_h(t)$ and estimates (4.2.38)-(4.2.41) lead to desire result. □

4.3 Error Analysis for the Fully Discrete Scheme

In this section, we have extended the classical finite element error analysis technique [85] to WG-FEMs with L^2 initial data for first order backward time fully discrete scheme. It is worth to note that the algorithms presented in [85] are only valid for linear finite elements with triangular meshes. Optimal order error estimates in $L^\infty(L^2)$ norm are shown to hold even if the initial data is in $L^2(\Omega)$.

First, we divide the time interval $J = [0, T]$ into M equally spaced sub intervals $I_n = (t_{n-1}, t_n]$, $n = 1, 2, \ldots, M$ with $t_0 = 0$, and $t_M = T$ and $\tau = t_n - t_{n-1}$, the time step. For a continuous mapping $\chi : [0, T] \to L^2(\Omega)$, we define $\chi^n = \chi(., t_n)$. Then, for a sequence $\{\omega^n\}_{n=0}^M \subset L^2(\Omega)$, we define

$$\partial_\tau \omega^n = \frac{\omega^n - p^{n-1}}{\tau}, \quad n \geq 1.$$

We now introduce the fully discrete weak Galerkin finite element approximation to the problem (4.1.1)-(4.1.2). Let $U_h^0 = (Q_0 u^0, Q_b(Q_0 u^0))$ and $U_h^n = \{U_0^n, U_b^n\} \in \mathcal{V}_h^0$ be the fully discrete solution of u at $t = t_n$, which we have defined through the following scheme

$$(\partial_\tau U_h^n, v_0) + \mathcal{A}_w(U_h^n, v_h) = (\overline{f}^{\,n}, v_0) \;\; \forall v_h = \{v_0, v_b\} \in \mathcal{V}_h^0, \;\; n \geq 1, \tag{4.3.1}$$

where

$$\overline{f}^{\,n} = \tau^{-1} \int_{t_{n-1}}^{t_n} f(x, t) dt. \tag{4.3.2}$$

We now present the main result of this section in the following theorem.

Theorem 4.3.1. *Suppose u and U_h^n be the solution of (4.1.1)-(4.1.2) and (4.3.1), respectively. In addition, assume that initial data $u^0 \in L^2(\Omega)$ and $f = 0$. Then, we have*

$$\|U_h^n - u^n\| \leq C \frac{(h^2 + \tau)}{t_n} \|u^0\|. \tag{4.3.3}$$

To prove the above theorem, following preparations are required. Similar to (1.2.1), we have used the following discrete negative norm

$$\|\chi\|_{-1,h} := \sup_{0 \neq v_h \in \mathcal{V}_h^0} \frac{(\chi, v_h)}{\|v_h\|_{1,h}}.$$

Remark 4.3.1. *By differentiating (4.2.5) with respect to t for $f = 0$, we obtain*

$$(u_{htt}, v_h) + \mathcal{A}_w(u_{ht}, v_h) = 0 \;\; \forall v_h = \{v_0, v_b\} \in \mathcal{V}_h^0.$$

Now, apply continuity and coercivity properties of $A_w(\cdot,\cdot)$ to have

$$(u_{htt}, v_h) \leq C\|u_{ht}\|_{1,h}\|v_h\|_{1,h} \ \ \forall v_h = \{v_0, v_b\} \in \mathcal{V}_h^0,$$

which yields

$$\sup_{0\neq v_h\in\mathcal{V}_h^0} \frac{(u_{htt}, v_h)}{\|v_h\|_{1,h}} \leq C\|u_{ht}\|_{1,h},$$

so that we obtain

$$\|v_{htt}\|_{-1,h} \leq C\|u_{ht}\|_{1,h}. \tag{4.3.4}$$

Now, for the fully discrete error analysis, we split our error into two components using semidiscrete solution as follows

$$U_h^n - u^n := (U_h^n - u_h^n) + (u_h^n - u^n). \tag{4.3.5}$$

The rest of the section is devoted in analyzing error bounds for the first component in (4.3.5).

Lemma 4.3.1. *If $f = 0$ and $u^0 \in H_0^1(\Omega) \cap H^2(\Omega)$, then we have*

$$\|u_h^n - U_h^n\| \leq C\tau\|u_{ht}(0)\|.$$

Proof. Setting $t = t_{n+1}$ in (4.2.5), we obtain

$$(\partial_\tau u_h^{n+1}, v_0) + \mathcal{A}_w(u_h^{n+1}, v_h) = (\zeta^{n+1}, v_0) \ \ \forall v_h = \{v_0, v_b\} \in \mathcal{V}_h^0,$$

where $\zeta^{n+1} := \partial_\tau u_h^{n+1} - u_{ht}^{n+1}$.

Let $\xi^n = u_h^n - U_h^n \in \mathcal{V}_h^0$, then it is easy to note that

$$(\partial_\tau \xi^{n+1}, v_0) + \mathcal{A}_w(\xi^{n+1}, v_h) = (\zeta^{n+1}, v_0) \ \ \forall v_h = \{v_0, v_b\} \in \mathcal{V}_h^0, \tag{4.3.6}$$

with $\xi^0 = 0$.

Set $v_h = \xi^{n+1}$ in (4.3.6) and apply Young's inequality with suitable $\nu > 0$ in the right hand side to obtain

$$\begin{aligned}
&\|\xi^{n+1}\|^2 + 2\tau\mathcal{A}_w(\xi^{n+1}, \xi^{n+1}) + \|\xi^{n+1} - \xi^n\|^2 \\
&= \|\xi^n\|^2 + 2\tau(\zeta^{n+1}, \xi^{n+1}) \\
&\leq \|\xi^n\|^2 + C_\nu\tau\|\zeta^{n+1}\|_{-1,h}^2 + C(\nu)\tau\|\xi^{n+1}\|_{1,h}^2 \\
&\leq \|\xi^n\|^2 + C_\nu\tau\|\zeta^{n+1}\|_{-1,h}^2 + C(\nu)\tau\mathcal{A}_w(\xi^{n+1}, \xi^{n+1}).
\end{aligned} \tag{4.3.7}$$

Note that, in the above estimate, we have used following fact

$$(\partial_\tau \xi^{n+1}, \xi^{n+1}) = \frac{1}{2\tau}(\|\xi^{n+1}\|^2 - \|\xi^n\|^2) + \frac{1}{2\tau}\|\xi^{n+1} - \xi^n\|^2.$$

Then, we sum (4.3.7) over n from 1 to l so that

$$\|\xi^{l+1}\|^2 \leq C\tau \sum_{m=1}^{l+1} \|\zeta^m\|^2_{-1,h}, \quad 1 \leq l \leq M-1. \tag{4.3.8}$$

Now, by Taylor's theorem

$$\zeta^m = \frac{1}{\tau}\int_{t_{m-1}}^{t_m} (s - t_{m-1}) u_{hss}(s) ds. \tag{4.3.9}$$

Hence

$$\|\zeta^m\|^2_{-1,h} \leq \frac{\tau}{3}\int_{t_{m-1}}^{t_m} \|u_{hss}(s)\|^2_{-1,h} ds. \tag{4.3.10}$$

Thus, combining (4.3.4) and (4.3.8), we get

$$\|\xi^{l+1}\|^2 \leq C\tau^2 \int_0^{t_{l+1}} \|u_{hs}(s)\|^2_{1,h} ds. \tag{4.3.11}$$

Now, apply (4.2.10) leads us to

$$\|\xi^{l+1}\|^2 \leq C\tau^2 \|u_{ht}(0)\|^2. \quad \square$$

Let $\{F^j\}_{j=1}^M \subset \mathcal{V}_h^0$, and $\{z_h^m\}_{m=1}^M \subset \mathcal{V}_h^0$ be the solution of the discrete time backward problem

$$(v_0, \partial_\tau z_h^m) - \mathcal{A}_w(v_h, z_h^{m-1}) = (v_0, F^m) \ \ \forall v_h = \{v_0, v_b\} \in \mathcal{V}_h^0, \tag{4.3.12}$$

with $z_h^M = 0$.

Regarding the stability of z_h^m, we have the following result.

Lemma 4.3.2. *For z_h^m satisfying (4.3.12), we obtain*

$$\max_{1\leq m\leq M} \|z_h^{m-1}\|^2_{1,h} + \sum_{m=1}^M \tau\|\partial_\tau z_h^m\|^2 \leq C\sum_{m=1}^M \tau\|F^m\|^2.$$

Proof. Setting $v_h = \tau\partial_\tau z_h^m$ in (4.3.12) and applying Cauchy-Schwarz inequality, we have

$$\tau\|\partial_\tau z_h^m\|^2 + \mathcal{A}_w(z_h^{m-1} - z_h^m, z_h^{m-1}) \leq \|\tau\partial_\tau z_h^m\|\|F^m\|.$$

Next, applying Young's inequality for suitable $\nu > 0$, we arrive at

$$\tau\|\partial_\tau z_h^m\|^2 + \mathcal{A}_w(z_h^{m-1} - z_h^m, z_h^{m-1}) \leq C_\nu\tau\|\partial_\tau z_h^m\|^2 + C(\nu)\tau\|F^m\|^2.$$

Now, selecting $\nu > 0$ appropriately leads us

$$\tau\|\partial_\tau z_h^m\|^2 + \mathcal{A}_w(z_h^{m-1} - z_h^m, z_h^{m-1}) \le C\tau\|F^m\|^2. \tag{4.3.13}$$

It is easy to verify that

$$\begin{aligned}\mathcal{A}_w(z_h^{m-1} - z_h^m, z_h^{m-1}) &= \frac{\tau^2}{2}\mathcal{A}_w(\partial_\tau z_h^m, \partial_\tau z_h^m) \\ &\quad -\frac{1}{2}\mathcal{A}_w(z_h^m, z_h^m) + \frac{1}{2}\mathcal{A}_w(z_h^{m-1}, z_h^{m-1}).\end{aligned}$$

This combine with (4.3.13) yields

$$\tau\|\partial_\tau z_h^m\|^2 - \frac{1}{2}\mathcal{A}_w(z_h^m, z_h^m) + \frac{1}{2}\mathcal{A}_w(z_h^{m-1}, z_h^{m-1}) \le C\tau\|F^m\|^2,$$

and then summing over m from $m = l$ to $m = M$ yields

$$\sum_{m=l}^{M}\tau\|\partial_\tau z_h^m\|^2 + \mathcal{A}_w(z_h^{l-1}, z_h^{l-1}) \le C\sum_{m=l}^{M}\tau\|F^m\|^2, \quad 1 \le l \le M-1.$$

This completes the rest of proof. □

Lemma 4.3.3. *If $f = 0$ and $u^0 \in L^2(\Omega)$, then we have*

$$\|u_h^n - U_h^n\| \le C\frac{\tau^{1/2}}{t_n^{1/2}}\|u_h(0)\|.$$

Proof. We multiply (4.3.7) by $t_{n+1} = t_n + \tau$ to obtain

$$t_{n+1}\|\xi^{n+1}\|^2 \le t_n\|\xi^n\|^2 + \tau\|\xi^n\|^2 + C\tau t_{n+1}\|\zeta^{n+1}\|_{-1,h}^2. \tag{4.3.14}$$

Sum (4.3.14) over n from 1 to l with $1 \le l \le M-1$ to have

$$\begin{aligned}t_{l+1}\|\xi^{l+1}\|^2 &\le \sum_{n=1}^{l}\tau\|\xi^n\|^2 + C\tau\sum_{n=1}^{l}t_{n+1}\|\zeta^{n+1}\|_{-1,h}^2 \\ &= \sum_{n=1}^{l}\tau\|\xi^n\|^2 + C\tau^2\sum_{n=1}^{l}\|\zeta^{n+1}\|_{-1,h}^2 + C\tau\sum_{n=1}^{l}t_n\|\zeta^{n+1}\|_{-1,h}^2 \\ &= \sum_{n=1}^{l}\tau\|\xi^n\|^2 + C\tau^2\sum_{n=1}^{l}\|\zeta^{n+1}\|_{-1,h}^2 \\ &\quad +C\sum_{m=2}^{l+1}\frac{t_{m-1}}{m-1}t_{m-1}\|\zeta^m\|_{-1,h}^2.\end{aligned} \tag{4.3.15}$$

In order to estimate $\sum_{m=1}^{l}\tau\|\xi^m\|^2$, let $\{z_h^m\}_{m=0}^M \subset \mathcal{V}_h^0$ be the solution of (4.3.12) with $F^m = \xi^m$. Set $v_h = \xi^m$ in (4.3.12) to obtain

$$\begin{aligned}\|\xi^m\|^2 &= (\xi^m, \partial_\tau z_h^m) - \mathcal{A}_w(\xi^m, z_h^{m-1}) \\ &= \partial_\tau(\xi, z_h)^m - (\partial_\tau \xi^m, z_h^{m-1}) - \mathcal{A}_w(\xi^m, z_h^{m-1}) \\ &= \partial_\tau(\xi, z_h)^m - (\zeta^m, z_h^{m-1}). \end{aligned} \tag{4.3.16}$$

Here, we have used (4.3.6). Since $z_h^M = 0$, we obtain by summing (4.3.16)

$$\sum_{m=1}^{M}\tau\|\xi^m\|^2 = -\sum_{m=1}^{M}\tau(\zeta^m, z_h^{m-1}).$$

Now, apply Cauchy-Schwarz inequality and then Young's inequality to have

$$\begin{aligned}\sum_{m=1}^{M}\tau\|\xi^m\|^2 &\le \sum_{m=1}^{M}\tau\|\zeta^m\|_{-1,h}\|z_h^{m-1}\|_{1,h} \\ &\le \max_{1\le m\le M}\|z_h^{m-1}\|_{1,h}\sum_{m=1}^{M}\tau\|\zeta^m\|_{-1,h}. \\ &\le C_\nu \max_{1\le m\le M}\|z_h^{m-1}\|_{1,h}^2 + C(\nu)\Big(\sum_{m=1}^{M}\tau\|\zeta^m\|_{-1,h}\Big)^2,\end{aligned}$$

where ν is a suitable positive real number. It then follows from Lemma 4.3.2 with $F^m = \xi^m$ that

$$\begin{aligned}\sum_{m=1}^{M}\tau\|\xi^m\|^2 &\le C\Big(\sum_{m=1}^{M}\tau\|\zeta^m\|_{-1,h}\Big)^2 \\ &\le C\tau^2\|\zeta^1\|_{-1,h}^2 + C\Big(\sum_{m=2}^{M}\frac{\tau^2}{t_{m-1}^2}\Big)\Big(\sum_{m=2}^{M}t_{m-1}^2\|\zeta^m\|_{-1,h}^2\Big) \\ &\le C\tau^2\|\zeta^1\|_{-1,h}^2 + C\sum_{m=2}^{M}t_{m-1}^2\|\zeta^m\|_{-1,h}^2.\end{aligned}$$

In the last term, we have used that

$$\sum_{m=2}^{M}\frac{\tau^2}{t_{m-1}^2} = \sum_{m=2}^{M}\frac{\tau^2}{\tau^2(m-1)^2} = \sum_{m=2}^{M}\frac{1}{(m-1)^2} \le \frac{\pi^2}{6}.$$

Hence, it follows from (4.3.15) that

$$t_{l+1}\|\xi^{l+1}\|^2 \le C\tau^2\|\zeta^1\|_{-1,h}^2 + C\sum_{m=2}^{M}t_{m-1}^2\|\zeta^m\|_{-1,h}^2, \tag{4.3.17}$$

for $1 \leq l \leq M-1$. Now from (4.3.9) to get

$$\begin{aligned}\tau^2\|\zeta^1\|^2_{-1,h} &= \Big\|\int_0^\tau s u_{hss}(s)ds\Big\|^2_{-1,h}\\ &\leq \tau\int_0^\tau s^2\|u_{hss}(s)\|^2_{-1,h}ds\\ &\leq C\tau\int_0^\tau s^2\|u_{hs}(s)\|^2_{1,h}ds\\ &\leq C\tau\|u_h(0)\|^2. \end{aligned} \tag{4.3.18}$$

Here, we have used estimate (4.2.11) and estimate (4.3.4). Also, from (4.3.10),

$$\begin{aligned} t^2_{m-1}\|\zeta^m\|^2_{-1,h} &\leq \frac{\tau}{3}t^2_{m-1}\int_{t_{m-1}}^{t_m}\|u_{hss}(s)\|^2_{-1,h}ds\\ &\leq \frac{\tau}{3}\int_{t_{m-1}}^{t_m} s^2\|u_{hss}(s)\|^2_{-1,h}ds\\ &\leq C\tau\int_{t_{m-1}}^{t_m} s^2\|u_{hs}(s)\|^2_{1,h}ds. \end{aligned}$$

Hence,

$$\begin{aligned}\sum_{m=2}^{M} t^2_{m-1}\|\zeta^m\|^2_{-1,h} &\leq C\tau\int_0^{t_M} s^2\|u_{hs}(s)\|^2_{1,h}ds\\ &\leq C\tau\|u_h(0)\|^2. \end{aligned} \tag{4.3.19}$$

Now, combining estimates (4.3.17)-(4.3.19), we obtain

$$t_{l+1}\|\xi^{l+1}\|^2 \leq C\tau\|u_h(0)\|^2, \;\; 1 \leq l \leq M-1, \tag{4.3.20}$$

which completes the rest of the proof. □

Like earlier, we use parabolic duality argument for the optimal L^2 norm error estimate with non-smooth data. For any fixed $t_n > 0$ $(1 \leq n \leq M)$ and any function $\psi_h \in \mathcal{V}_h^0$, define $w_h(s) \in \mathcal{V}_h^0$ to be the continuous time weak Galerkin solution of the backward problem

$$(v_0, w_{hs}) - \mathcal{A}_w(v_h, w_h) = 0 \quad \forall v_h = \{v_0, v_b\} \in \mathcal{V}_h^0, \;\; s \leq t_n, \tag{4.3.21}$$

with $w_h(t_n) = \psi_h$.

Let $\{W_h^m\}_{m=0}^n \subset \mathcal{V}_h^0$ be the solution of discrete time backward problem

$$(v_0, \partial_\tau W_h^m) - \mathcal{A}_w(v_h, W_h^{m-1}) = 0 \quad \forall v_h = \{v_0, v_b\} \in \mathcal{V}_h^0, \;\; 1 \leq m \leq n, \tag{4.3.22}$$

with $W_h^n = \psi_h$.

Now, from the discrete analogue of (4.2.33), we have (see, Appendix)

$$\partial_\tau\{(u_h, w_h) - (U_h, W_h)\}^m = 0. \tag{4.3.23}$$

Sum (4.3.23) over m from $1 \le m \le n$, we obtain

$$(\xi^n, \psi_h) = (u_h(0), w_h(0) - W_h^0). \tag{4.3.24}$$

Also, by Lemma 4.3.1 applied to $w_h(t_m) - W_h^m$ with time reversed, we get

$$(\xi^n, \psi_h) \le \|u_h(0)\|\|w_h(0) - W_h^0\| \le C\tau\|u_h(0)\|\|w_{ht}(t_n)\|. \tag{4.3.25}$$

Lemma 4.3.4. *If $f = 0$ and $u^0 \in L^2(\Omega)$, then*

$$\|u_h^n - U_h^n\| \le \frac{C\tau}{t_n}\|u_h(0)\|. \tag{4.3.26}$$

Proof. Summing (4.3.23) over $m = q+1, \ldots, n$ with $q = [n/2]$ and setting $\psi_h = \xi^n$, we obtain

$$\begin{aligned}\|\xi^n\|^2 &= (\xi^q, w_h^q) + (U_h^q, (w_h - W_h)^q)\\ &= -(\xi^q, (w_h - W_h)^q) + (\xi^q, w_h^q) + (u_h^q, (w_h - W_h)^q).\end{aligned}$$

Next, apply Cauchy-Schwarz inequality to obtain

$$\|\xi^n\|^2 \le \|\xi^q\|\|(w_h - W_h)^q\| + \|\xi^q\|\|w_h^q\| + \|u_h^q\|\|(w_h - W_h)^q\|. \tag{4.3.27}$$

Now by Lemma 4.3.3, we obtain

$$\|(w_h - W_h)^q\| \le \frac{C\tau^{1/2}}{t_q^{1/2}}\|w_h(t_n)\|.$$

In the above relation, multiplying and dividing by $(t_n - t_q)^{1/2}$, we get

$$\|(w_h - W_h)^q\| \le \frac{C\tau^{1/2}}{(t_n - t_q)^{1/2}}\|w_h(t_n)\|.$$

Here, we have used the fact that

$$\frac{(t_n - t_q)^{1/2}}{t_q^{1/2}} = \Big(\frac{t_n}{t_q} - 1\Big)^{1/2} = (\frac{n}{[n/2]} - 1)^{1/2} \le \sqrt{2}.$$

Now, we multiply and divide $t_n^{1/2}$, we have

$$\|(w_h - W_h)^q\| \le \frac{Ct_n^{1/2}\tau^{1/2}}{t_n^{1/2}\Big(t_n - t_q\Big)^{1/2}}\|w_h(t_n)\| \le \frac{C\tau^{1/2}}{t_n^{1/2}}\|\xi^n\|. \tag{4.3.28}$$

Here, we have used the fact that

$$\frac{t_n^{1/2}}{(t_n - t_q)^{1/2}} = \Big(\frac{n}{n - [n/2]}\Big)^{1/2} \leq \sqrt{2}.$$

It follows by (4.3.25) with time reversed and (4.2.11) that

$$(\xi^q, w_h^q) \leq C\tau \|u_h(0)\| \|w_{ht}(t_q)\| \leq \frac{C\tau}{t_n} \|u_h(0)\| \|\xi^n\|, \tag{4.3.29}$$

and

$$(u_h^q, (w_h - W_h)^q) \leq C\tau \|w_h(t_n)\| \|u_{ht}(t_q)\| \leq \frac{C\tau}{t_n} \|u_h(0)\| \|\xi^n\|. \tag{4.3.30}$$

Now, estimates (4.3.28)-(4.3.30) together with (4.3.27) leads to

$$\|\xi^n\| \leq \frac{C\tau^{1/2}}{t_n^{1/2}} \|\xi^q\| + \frac{C\tau}{t_n} \|u_h(0)\| \leq \frac{C\tau}{t_n} \|u_h(0)\|. \quad \square \tag{4.3.31}$$

4.4 Numerical Section

In this section, we have tested various numerical Examples for the parabolic problem (4.1.1)-(4.1.2) in $\Omega \times J$, where $\Omega \subset \mathbb{R}^2$ and $J = (0, T]$. Finite element partitions with different kinds of configurations like triangular, rectangular and polygonal meshes are used for solving parabolic problems to confirm the flexibility of WG method. These numerical results demonstrate that the scheme is robust and accurate. All computations are carried out using the MATLAB software.

For a given finite number of successive iterations (indexed by i), let e_i be the error corresponding to the $L^\infty(L^2)$-norm on the i-th iteration, and h_i is corresponding mesh size. Then expected order of convergence (EOC) can be defined by

$$EOC(e_i) = \log\Big(\frac{e_{i+1}}{e_i}\Big) / \log\Big(\frac{h_{i+1}}{h_i}\Big).$$

Let U_h^n be the weak Galerkin solution defined by (4.3.1). Then, we have calculated the following error

$$e_h^n := Q_h u(x, t_n) - U_h^n$$

at final time $t_n = T$ with respect to L^2-norm for the linear WG space of the form $(\mathcal{P}_1(K),\ \mathcal{P}_1(\partial K),\ \big[\mathcal{P}_0(K)\big]^2)$.

Example 4.4.1. Non-smooth data with triangular mesh: This Example is derived from (cf. Exercise 3.7, page 171, [6]). Consider the problem (4.1.1)-(4.1.2) in $\Omega \times J$, where $\Omega = (0, 2) \times (0, 2)$. The exact solution of the given problem defined as

$$u(x,y,t) = \frac{200}{\pi^2}\sum_{i,j=1}^{\infty}\frac{1}{ij}\{1+(-1)^{i+1}\}\{1-\cos(\frac{j\pi}{2})\}\exp\{-\pi^2 t(\frac{i^2+j^2}{36})\} \times \sin(\frac{i\pi x}{2})\sin(\frac{j\pi y}{2}),$$

with initial data

$$u^0 = \begin{cases} 50 \text{ if } y \leq 1, \\ 0 \text{ otherwise.} \end{cases}$$

The right-hand side f cab be evaluated from the exact solution u and the diffusion-coefficient

$$\alpha = \begin{bmatrix} 1/9 & 0 \\ 0 & 1/9 \end{bmatrix}.$$

Triangular mesh is used in this Example, which is depicted in Figure 4.4.1. The domain is uniformly partitioned into $n \times n$ sub rectangles in such a way that each rectangular element is further divided into two triangles using a diagonal line with negative slop, where the mesh size is $h = 1/n$. The errors with respect to $L^\infty(L^2)$ norm for linear WG space is reported in Table 4.4.1 at final time $T = 1$.

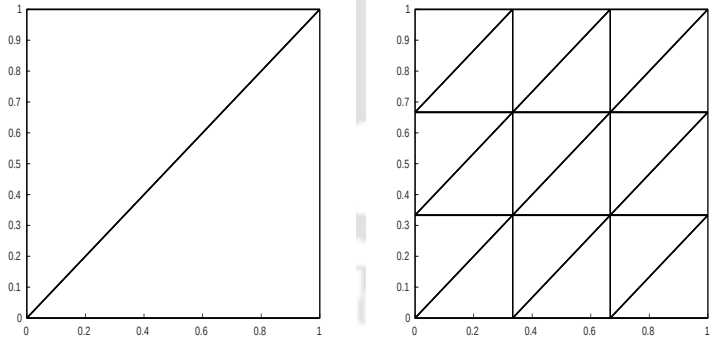

Figure 4.4.1: An initial triangular mesh with $h = 1/2$ (left), and its refinement with $h = 1/8$ (right).

Example 4.4.2. Non-smooth data with polygonal mesh: We consider a second order parabolic equation on a two-dimensional domain $\Omega \times J$, where $\Omega = (0,1) \times (0,1)$ for which the exact solution possesses non smooth initial data. The Example discussed

here is extracted from [15]

$$\begin{aligned} u_t - \frac{1}{12}\Delta u &= 0 \text{ in } \Omega \times J, \\ u &= 0 \text{ on } \partial\Omega \times J, \\ u(x,y,0) &= u^0 \text{ in } \Omega. \end{aligned} \tag{4.4.1}$$

We select the data appearing in (4.4.1) by setting the exact solution,

$$u(x,y,t) = \frac{8}{\pi^2}\sum_{i,j=0}^{\infty} c_i c_j \exp\{-\pi^2 t\frac{(2i+1)^2+(2j+1)^2}{12}\} \times \sin(\pi x(2i+1))\sin(\pi y(2j+1)),$$

where

$$c_i = \begin{cases} (-1)^{(i/2)}(2i+1)^{-1} & \text{if } i \text{ is even}, \\ (-1)^{(i+1)/2}(2i+1)^{-1} & \text{otherwise}, \end{cases}$$

with initial data

$$u^0 = \begin{cases} 1 & \text{if } 1/4 \le x, y \le 3/4, \\ 0 & \text{otherwise}. \end{cases}$$

In this Example, we have used polygonal meshes. A typical polygonal mesh and its refinement is depicted in Figure 4.4.2. The errors with respect to $L^\infty(L^2)$-norm for linear WG space is represented in Table 4.4.1 at final time $T = 1$. We have achieved optimal order of convergence in $L^\infty(L^2)$-norm, which confirms the theoretical prediction as proved in Theorem 4.3.1. This can be observed from Table 4.4.1.

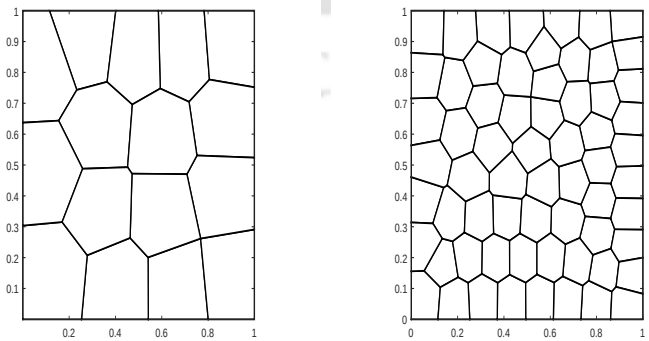

Figure 4.4.2: An initial polygonal mesh (left), and its refinement (right).

Table 4.4.1: The history of $L^\infty(L^2)$ error convergence with time step $\tau = h^2$.

Example 4.4.1 (Triangular mesh)			Example 4.4.2 (Polygonal mesh)	
h	$\|e_h^n\|$	EOC	$\|e_h^n\|$	EOC
1/4	7.127644e-01	-	3.303126e-03	-
1/8	1.762327e-01	2.015943e+00	8.109071e-04	2.026224e+00
1/16	4.407500e-02	1.999450e+00	2.021031e-04	2.004445e+00
1/32	1.102763e-02	1.998837e+00	5.049565e-05	2.000861e+00
1/64	2.757641e-03	1.999617e+00	1.262222e-05	2.000194e+00
1/128	6.894597e-04	1.999896e+00	3.155453e-06	2.000047e+00

Example 4.4.3. Non-smooth data with rectangular mesh: In the following Example, we choose $\Omega = (0,1) \times (0,1)$. We select the data appearing in (4.1.1)-(4.1.2) by setting the exact solution, which we have taken from [6] as

$$u(x,y,t) = \frac{400}{\pi^2} \sum_{i,j=1}^{\infty} \frac{1}{ij} \{1 - \cos(\frac{i\pi}{2})\}\{1 - \cos(\frac{j\pi}{2})\} \exp(-\pi^2 t(\frac{i^2+j^2}{12})) \times \sin(i\pi x) \sin(j\pi y),$$

with initial data

$$u^0 = \begin{cases} 100 & \text{if } x, y \leq 1/2, \\ 0 & \text{otherwise,} \end{cases}$$

and diffusion-coefficient

$$\alpha = \begin{bmatrix} 1/12 & 0 \\ 0 & 1/12 \end{bmatrix}.$$

In this Example, we have used rectangular mesh as shown in Figure 4.4.3. The errors with respect to $L^\infty(L^2)$-norm for linear WG space is reported in Table 4.4.2 at final time $T = 1$.

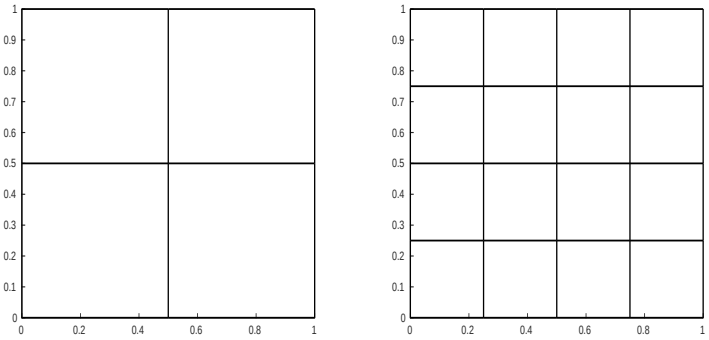

Figure 4.4.3: An initial rectangular mesh with $h = 1/2$ (left), and its refinement with $h = 1/4$ (right).

Table 4.4.2: $L^\infty(L^2)$ error convergence with time step $\tau = h^2$.

h	$\|e_h^n\|$	EOC
1/4	3.915363e+00	-
1/8	8.092984e-01	2.274402e+00
1/16	1.893695e-01	2.095468e+00
1/32	4.647979e-02	2.026528e+00
1/64	1.156529e-02	2.006802e+00
1/128	2.887895e-03	2.001711e+00

Example 4.4.4. Comparison among smooth data and non smooth data: We consider a two dimensional heat transfer equation with homogeneous boundary conditions. The solution of model problem represents the temperature distribution in a thin rectangular plate. Temperature distribution of the insulated edges of plate is kept zero.

$$(\mathbf{P}^*)\begin{cases} u_t - \alpha\Delta u = 0 \ \text{ in } \ \Omega \times J, \\ u(x,0) = u^0, \ \text{ in } \ \Omega, \\ u(x,t) = 0 \quad \text{on } \partial\Omega \times J, \end{cases}$$

where α denotes the thermal diffusivity and $\Omega = (0,1) \times (0,1)$.

Here, we would check the behavior of given solution with smooth and non-smooth data. For non-smooth data, we have opted the same exact solution, diffusion coefficient α, and initial data u^0 as given in Example 4.4.3, whereas for the smooth data, we have taken exact solution from (cf. Exercise 3.7, page 171, [6]) as

$$u(x,y,t) = \frac{1600}{\pi^2} \sum_{i,j=\text{odd}}^{\infty} \frac{\sin(i\pi x)\sin(j\pi y)}{ij} \times \exp(-\pi^2 t(\frac{i^2+j^2}{3}))$$

with initial data $u^0 = 100$, and the thermal diffusion-coefficient

$$\alpha = \begin{bmatrix} 1/3 & 0 \\ 0 & 1/3 \end{bmatrix}.$$

The uniform triangular mesh is used as taken in Example 4.4.1. The error with respect to $L^\infty(L^2)$ norm for linear WG space is represented in Table 4.4.3 at final time $T = 1$. We have obtained optimal order of convergence in $L^\infty(L^2)$ norm as shown in Table 4.4.3. Figure 4.4.4 show the temperature distribution in the plat at $t = 1$ for smooth initial data. Further, Figure 4.4.5 and Figure 4.4.6 shows the temperature distribution in the plat at various time level $t = 0.01,\ 1,\ 5,\ 10$ with a fix time step $\tau = 0.002$, when initial data is non-smooth. It can be demonstrated from the Figures 4.4.5 - 4.4.6 that when time t increases, then solution decays to zero. Here, we can observe from Table 4.4.3 that when non-smooth initial data u^0 appeared in $(\mathbf{P}^*)$, it's convergence behavior is same as smooth initial data, and we have achieved optimal rate of convergence in $L^\infty(L^2)$-norm.

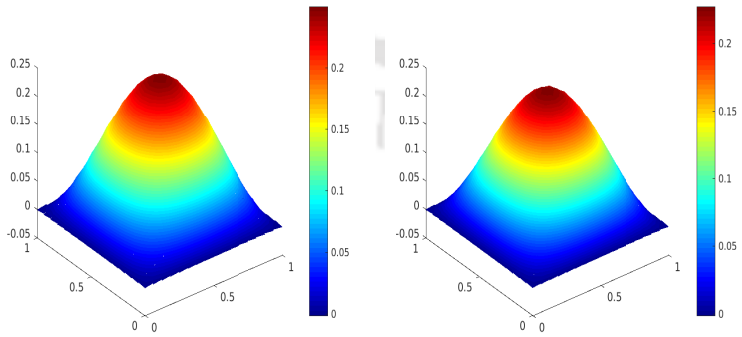

Figure 4.4.4: WG solution plot (left), exact solution plot (right) at $t = 1$ in Example 4.4.4 for smooth initial data.

Table 4.4.3: The history of $L^\infty(L^2)$ error convergence with time step $\tau = h^2$.

	Smooth data		Non-smooth data	
h	$\|e_h^n\|$	EOC	$\|e_h^n\|$	EOC
1/2	6.929241e-01	-	1.435194e+00	-
1/4	2.222611e-01	1.640442e+00	3.429445e-01	2.065199e+00
1/8	4.778263e-02	2.217698e+00	8.387519e-02	2.031659e+00
1/16	1.124189e-02	2.087601e+00	2.085701e-02	2.007712e+00
1/32	2.763636e-03	2.024246e+00	5.207374e-03	2.001905e+00
1/64	6.879407e-04	2.006212e+00	1.301416e-03	2.000474e+00
1/128	1.717990e-04	2.001562e+00	3.155453e-04	2.044163e+00

Example 4.4.5. Non-smooth data on rectangular mesh with Hanging nodes: In this Example, we solve the same problem as in Example 4.4.2 on rectangular mesh with hanging nodes in the finite element partition. The initial mesh is shown as in Figure 4.4.7 (Left). The mesh on the right in Figure 4.4.7 is generated by uniform refinement procedure. It should be pointed out that the initial mesh has a hanging nodes A, B, C and D. For the finite element partition $\mathcal{T}_h$ with hanging nodes, we notice that the WG algorithm is still hold on this refinements. The errors with respect to $L^\infty(L^2)$ norm for linear WG space is reported in Table 4.4.4 at final time $T = 1$.

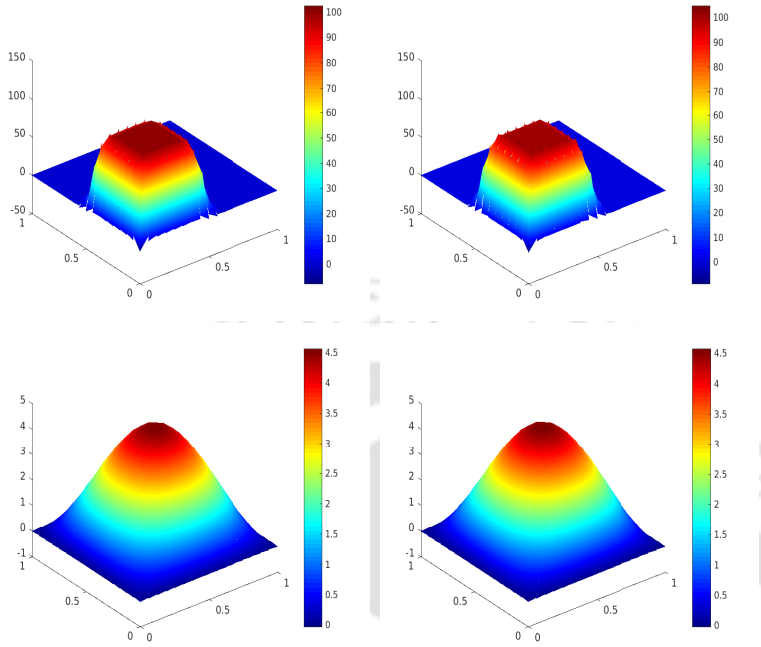

Figure 4.4.5: WG solution plot (top left), exact solution plot (top right) at $t = 0.01$ and WG solution plot (bottom left), exact solution plot (bottom right) at $t = 1$ in Example 4.4.4 for non-smooth initial data

Table 4.4.4: $L^\infty(L^2)$ error convergence with time step $\tau = h^2$.

h	$\|e_h^n\|$	EOC
1/4	3.918887e-01	-
1/8	1.554516e-01	1.333979e+00
1/16	4.764673e-02	1.706016e+00
1/32	1.271481e-02	1.905868e+00
1/64	3.234341e-03	1.974966e+00
1/128	7.590261e-04	2.091250e+00

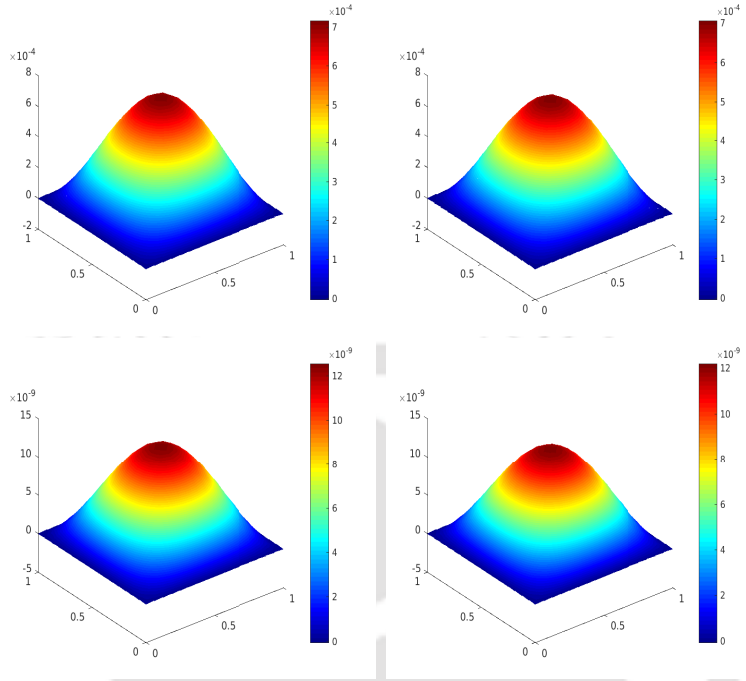

Figure 4.4.6: WG solution plot (top left), exact solution plot (top right) at $t = 5$ and WG solution plot (bottom left), exact solution plot (bottom right) at $t = 10$ in Example 4.4.4 for non-smooth initial data.

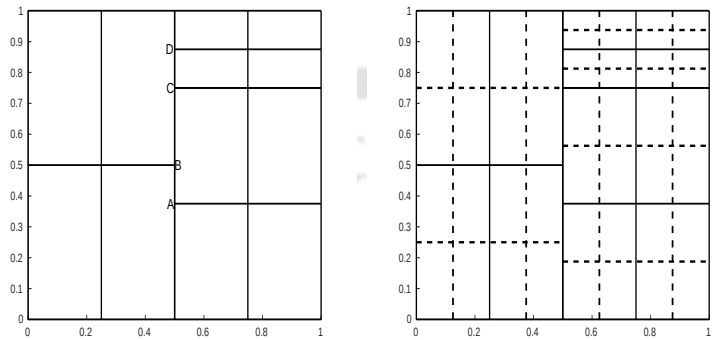

Figure 4.4.7: An initial rectangular mesh with Hanging nodes (left), and its refinement (right).

5

L^2 Estimates of WG-FEMs for Second-Order Wave Equations with Polygonal Meshes

This chapter is devoted to the a priori error analysis in WG-FEM for the linear wave model problem (1.1.3)-(1.1.4). Typical semidiscrete and fully discrete schemes are presented for a finite element discretization with polygonal meshes. The fully discrete space-time finite element discretizations is based on implicit second order Newmark scheme. For sufficiently smooth solutions, optimal order error estimate in the $L^\infty(L^2)$ norm is shown to hold as $O(h^{k+1} + \tau^2)$, where h is the mesh size and τ the time step. An extensive set of numerical experiments are conducted to demonstrate the robustness, reliability, flexibility, and accuracy of the proposed method.

5.1 Introduction

To begin with, let us first recall the second order wave equation. Let $\Omega \subset \mathbb{R}^2$ be a convex polygonal domain with boundary $\partial\Omega$. In Ω, we consider following wave equation

$$u_{tt}(x,t) - \nabla \cdot (\alpha(x)\nabla u(x,t)) = f(x,t) \ \text{ in } \Omega \times (0,T], \tag{5.1.1}$$

with initial and boundary conditions

$$u(x,0) = u^0(x),\ u_t(x,0) = v^0(x) \text{ in } \Omega;\ \text{ and } \ u(x,t) = 0 \text{ on } \partial\Omega \times (0,T],\ T < \infty \tag{5.1.2}$$

We assume that the coefficient matrix $\alpha = (\alpha_{ij}(x))_{2\times 2} \in [L^\infty(\Omega)]^{2^2}$ is symmetric and uniformly positive definite in Ω. We are well aware of the fact that the rate of convergence of finite element approximations depends on the 'smoothness' of a solution.

This chapter is under review in *Appl. Numer. Math.*

Throughout this analysis, coefficient α, initial functions $\{u^0, v^0\}$ and the load term f are assumed to be sufficiently smooth in their respective domains of definition so that solution u belongs to desired Sobolev space. For the related regularity results, we refer to [45, 82]. Additional regularity assumptions were made throughout this Chapter to carry out the convergence analysis.

The present work is aimed to analyze weak Galerkin finite element method for second-order linear wave equation, where we have reported both semidiscrete and fully discrete schemes. The fully discrete space-time finite element discretizations can be revised as the Crank-Nicolson discretization of the reformulation of the governing equation in the first-order system, as in Baker [7]. The error estimates in L^2 norm are new (see, Theorem 5.2.1 and Theorem 5.3.1), which are based on the use of the Ritz projection. Both the algorithm and error estimates are discussed for variable coefficient, while most existing work (see, [58]) assumed piecewise constant coefficients. An enormous set of numerical illustrations have been considered and described for the establishment of the efficient WG method in scientific computing. These experiments suggest that the WG scheme is the decisive and efficient numerical technique to examine such type of problems. For the relevant literature on the numerical study to hyperbolic problems, we refer to Section 1.3.

The rest of the chapter is divided as follows. In Section 5.2, we discuss the weak Galerkin finite element discretization and described the error estimates for the semidiscrete scheme. The error analysis for the fully discrete scheme is reported in Section 5.3. Section 5.4 focuses on numerical examples.

5.2 Error Analysis for the Semidiscrete Scheme

This section deals with the error analysis for the spatially discrete scheme. Optimal order of convergence in $L^\infty(L^2)$ norm is established.

Let $\mathcal{V}_h$ be the weak Galerkin finite element space defined by (3.2.1) based on the finite element discretization $\mathcal{T}_h$ of Ω as described in Chapter 1. For each $v_h = \{v_0, v_b\} \in \mathcal{V}_h$, recall its discrete weak gradient $(\nabla_w v_h) \in [\mathcal{P}_{k-1}(K)]^2$ that satisfies the following equation

$$(\nabla_w v_h, \mathbf{q})_K = -\int_K v_0(\nabla \cdot \mathbf{q})dK + \int_{\partial K} v_b(\mathbf{q}\cdot\mathbf{n})ds \;\; \forall \mathbf{q} \in [\mathcal{P}_{k-1}(K)]^2. \tag{5.2.1}$$

Next, we recall the bilinear map $\mathcal{A}_w(\cdot,\cdot)$ on $\mathcal{V}_h \times \mathcal{V}_h$, which is defined as follows

$$\mathcal{A}_w(w_h, v_h) := \sum_{K\in\mathcal{T}_h} \left(\alpha\nabla_w u_h, \nabla_w v_h\right)_K + \mathcal{S}(w_h, v_h) \;\; \forall w_h, v_h \in \mathcal{V}_h, \tag{5.2.2}$$

where the stabilizer $\mathcal{S}(\cdot,\cdot)$ is given by

$$\mathcal{S}(w_h, v_h) = \sum_{K\in\mathcal{T}_h} h_K^{-1}\langle w_0 - w_b, v_0 - v_b\rangle_{\partial K}. \tag{5.2.3}$$

For each element $K \in \mathcal{T}_h$, denote by Q_0 the usual L^2 projection operator from $L^2(K)$ onto $\mathcal{P}_k(K)$ and by Q_b the L^2 projection from $L^2(e)$ onto $\mathcal{P}_k(e)$ for any $e \in \mathcal{F}_h$. We shall combine Q_0 with Q_b by writing $\mathcal{Q}_h = \{Q_0, Q_b\}$. In addition to $\mathcal{Q}_h$, let $\mathbb{Q}_h$ be an another local L^2 projection from $[L^2(K)]^2$ onto $[\mathcal{P}_{k-1}(K)]^2$.

We recall following crucial approximation properties for local projections Q_h and $\mathbb{Q}_h$. For details, we refer to (Lemma 4.1, [123]).

Lemma 5.2.1. *Let $\mathcal{T}_h$ be a finite element partition of Ω satisfying the shape regularity assumption as specified in [123]. Then, for $v \in H^{k+1}(\Omega)$, we have*

$$\begin{aligned}
\sum_{K\in\mathcal{T}_h}\Big(\|v - Q_0 v\|_K^2 + h_K^2\|\nabla(v - Q_0 v)\|_K^2\Big) &\leq Ch^{2k+2}\|v\|_{k+1}^2,\\
\sum_{K\in\mathcal{T}_h}\Big(\|\nabla v - \mathbb{Q}_h(\nabla v)\|_K^2 + h_K^2\|\nabla(\nabla v - \mathbb{Q}_h(\nabla v))\|_K^2\Big) &\leq Ch^{2k}\|v\|_{k+1}^2.
\end{aligned}$$

Next, we derive an optimal order of error estimate in L^2-norm, the basic idea applied is to use elliptic projection as in [126]. For $v \in \mathcal{X} = H_0^1(\Omega) \cap H^2(\Omega)$, we define

$$f_v^* = -\nabla\cdot(\alpha\nabla v).$$

Clearly $f_v^* \in L^2(\Omega)$. Define $\mathcal{E}_h : \mathcal{X} \to \mathcal{V}_h^0$ by

$$\mathcal{A}_w(\mathcal{E}_h v, \phi_h) = (f_v^*, \phi_h) \ \ \forall \phi_h \in \mathcal{V}_h^0. \tag{5.2.4}$$

Next, for our convenience, we recall following crucial result. For more details, we refer to Lemma 4.2.8.

Lemma 5.2.2. *For $v \in H_0^1(\Omega) \cap H^{k+1}(\Omega)$, there exists a constant C such that*

$$\begin{aligned}
|||\mathcal{Q}_h v - \mathcal{E}_h v||| &\leq Ch^k\|v\|_{k+1},\\
\|\mathcal{Q}_h v - \mathcal{E}_h v\| &\leq Ch^{k+1}\|v\|_{k+1}.
\end{aligned}$$

A time-dependent weak function $v_h : [0,T] \to \mathcal{V}_h$ is written as $v_h(t) := \{v_0(t), v_b(t)\}$ and subsequently we define $v_{ht}(t) := \{v_0'(t), v_b'(t)\}$, where '$\prime$' denotes the time derivatives. For simplicity, we use $v_h = \{v_0, v_b\}$ for $v_h(t)$ and $v_{ht} = \{v_0', v_b'\}$ for $v_{ht}(t)$.

The continuous-time weak Galerkin finite element approximation to (5.1.1)-(5.1.2) is defined as follows: Find $u_h = \{u_0, u_b\} : [0,T] \to \mathcal{V}_h^0$ satisfying

$$(u_{htt}, v_0) + \mathcal{A}_w(u_h, v_h) = (f, v_0) \ \ \forall v_h = \{v_0, v_b\} \in \mathcal{V}_h^0, \tag{5.2.5}$$

with $u_h(0) = \mathcal{Q}_h u^0$ and $u_{ht}(0) = \mathcal{Q}_h v^0$. Well-posedness of the scheme (5.2.5) can be verified from the fact that weak finite element space $\mathcal{V}_h^0$ is a normed linear space with respect to the triple norm $|||\cdot|||$ defined as

$$|||v_h||| = \sqrt{\mathcal{A}_w(v_h, v_h)}, \ v_h = \{v_0, v_b\} \in \mathcal{V}_h^0.$$

As a standard procedure in finite element method, we split our error $e_h = u_h - \mathcal{Q}_h u$ into two standard components ρ and θ using following relation

$$e_h(t) = u_h(t) - \mathcal{Q}_h u(t) := \theta(t) + \rho(t),$$

where $\theta = u_h - \mathcal{E}_h u$ and $\rho = \mathcal{E}_h u - \mathcal{Q}_h u$. From Lemma 5.2.2, we already have bound for $\rho(t)$. So, we only need to bound $\theta(t)$.

Next, using the definitions of projection operators $\mathcal{E}_h$ and $\mathcal{Q}_h$, we arrive at following important identity

$$\begin{aligned}
&(\theta_{tt}, \phi_h) + \mathcal{A}_w(\theta, \phi_h) \\
&= (u_{htt}, \phi_h) + \mathcal{A}_w(u_h, \phi_h) - ((\mathcal{E}_h u)_{tt}, \phi_h) - \mathcal{A}_w(\mathcal{E}_h u, \phi_h) \\
&= (f, \phi_h) - ((\mathcal{E}_h u)_{tt}, \phi_h) + (\nabla \cdot (\alpha \nabla u), \phi_h) \\
&= (u_{tt}, \phi_h) - ((\mathcal{E}_h u)_{tt}, \phi_h) \\
&= (\mathcal{Q}_h u_{tt}, \phi_h) - ((\mathcal{E}_h u)_{tt}, \phi_h) \\
&= ((\mathcal{Q}_h u)_{tt}, \phi_h) - ((\mathcal{E}_h u)_{tt}, \phi_h) = -(\rho_{tt}, \phi_h)
\end{aligned} \tag{5.2.6}$$

for all $\phi_h \in \mathcal{V}_h^0$.

Now, for some suitable $\xi \in (0, T)$, we define

$$\hat{\theta}(., t) = \int_t^\xi \theta(., s) ds, \ \ 0 \le t \le T.$$

Clearly, we observe that

$$\hat{\theta}(\xi) = 0 \ \text{ and } \ \hat{\theta}_t = -\theta(., t), \ t \in [0, T]. \tag{5.2.7}$$

Now, set $\phi_h = \hat{\theta}$ in (5.2.6), integrate between 0 to ξ with respect to the variable t to obtain

$$\begin{aligned}
&- \int_0^\xi (\theta_t, \hat{\theta}_t) ds + (\theta_t(\xi), \hat{\theta}(\xi)) - (\theta_t(0), \hat{\theta}(0)) + \int_0^\xi \mathcal{A}_w(\theta, \hat{\theta}) ds \\
&= \int_0^\xi (\rho_t, \hat{\theta}_t) ds - (\rho_t(\xi), \hat{\theta}(\xi)) + (\rho_t(0), \hat{\theta}(0)).
\end{aligned}$$

Using (5.2.7), we have

$$\int_0^\xi \frac{1}{2}\frac{d}{dt}\|\theta(t)\|^2 dt - (\theta_t(0), \hat{\theta}(0)) - \int_0^\xi \frac{1}{2}\frac{d}{dt}\mathcal{A}_w(\hat{\theta}, \hat{\theta})dt$$
$$= -\int_0^\xi (\rho_t, \theta)dt + (\rho_t(0), \hat{\theta}(0)).$$

Since θ is continuous in the time variable, we select ξ such that $\|\theta(\xi)\| = \max_{0\le t\le T}\|\theta(t)\|$. Then observe that $e_{ht}(0) = 0$, which together with Young's inequality gives

$$\begin{aligned}
&\frac{1}{2}\|\theta(\xi)\|^2 + \frac{1}{2}\mathcal{A}_w(\hat{\theta}(0), \hat{\theta}(0)) \\
&= \frac{1}{2}\|\theta(0)\|^2 + (e_{ht}(0), \hat{\theta}(0)) - \int_0^\xi (\rho_t, \theta)dt \\
&\le \frac{1}{2}\|\theta(0)\|^2 + \max_{0\le t\le T}\|\theta(t)\| \int_0^\xi \|\rho_t\|dt \\
&\le \frac{1}{2}\|\theta(0)\|^2 + \|\theta(\xi)\|\sqrt{T}\|\rho_t\|_{L^2(L^2)} \\
&\le \frac{1}{2}\|\theta(0)\|^2 + \frac{1}{2\epsilon}\|\theta(\xi)\|^2 + \frac{\epsilon}{2}T\|\rho_t\|^2_{L^2(L^2)},
\end{aligned} \tag{5.2.8}$$

for some $\epsilon > 0$. Again, it follows from [36] that

$$\rho_t = \mathcal{E}_h u_t - \mathcal{Q}_h u_t.$$

Then, as a consequence of Lemma 5.2.2, we obtain

$$\|\rho_t\| \le Ch^{k+1}\|u_t\|_{k+1}. \tag{5.2.9}$$

Now, combine estimates (5.2.8)-(5.2.9) to obtain

$$\|\theta(\xi)\|^2 \le Ch^{2(k+1)}\big(\|u^0\|^2_{k+1} + \|u_t\|^2_{L^2(H^{k+1})}\big).$$

Thus we have proved the following optimal $L^\infty(L^2)$ norm estimate.

Theorem 5.2.1. *Let u and u_h be the solutions of problems (5.1.1)-(5.1.2) and (5.2.5), respectively. Assume that the solution of (5.1.1)-(5.1.2) is so regular that $u_t \in H^{k+1}(\Omega)\cap H_0^1(\Omega)$. Then there exists a constant C such that*

$$\|u(t) - u_h(t)\| \le Ch^{k+1}\Big\{\|u^0\|_{k+1} + \|u\|_{k+1} + \|u_t\|_{L^2(H^{k+1})}\Big\}, \quad t \in [0, T].$$

5.3 Error Analysis for the Fully Discrete Scheme

In this section, we are now going to formulate a fully discrete weak Galerkin finite element scheme to approximate the solution of the problem (5.1.1)-(5.1.2). Optimal a priori error estimate in $L^\infty(L^2)$ norm is derived.

We first divide the time interval $J = [0, T]$ into N equally spaced subintervals by the following points

$$0 = t_0 < t_1 < ... < T_N = T$$

with $t_n = n\tau$, $\tau = \frac{T}{N}$ being the time step. Let $I_n = (t_{n-1}, t_n]$ be the n-th subinterval. For a sequence $\{\gamma^n\}_{n=0}^N \subset L^2(\Omega)$, we define

$$\partial_\tau \gamma^n = \frac{\gamma^{n+1} - \gamma^n}{\tau} \quad \text{and} \quad \gamma^{n+\frac{1}{2}} = \frac{1}{2}(\gamma^{n+1} + \gamma^n), \;\; n = 0, 1, \ldots, N-1.$$

Also, for a continuous mapping $\zeta : [0, T] \to L^2(\Omega)$, we define $\zeta^n = \zeta(., t_n)$, $0 \le n \le N$. Then the fully discrete weak Galerkin finite element approximation to the problem (5.1.1)-(5.1.2) is defined as follows: Find $U^n = \{U_0^n, U_b^n\} \in \mathcal{V}_h^0$ such that

$$\partial_\tau U^n = p^{n+\frac{1}{2}} \;\text{ for }\; n = 0,\; 1, \ldots, N-1 \tag{5.3.1}$$

and

$$(\partial_\tau p^n, \phi_0) + \mathcal{A}_w(U^{n+\frac{1}{2}}, \phi_h) = (f^{n+\frac{1}{2}}, \phi_0) \;\; \forall \phi_h \in \mathcal{V}_h^0, \tag{5.3.2}$$

with $U^0 = \mathcal{Q}_h u^0$ and $p^0 = \mathcal{Q}_h v^0$.

The following Lemma gives the existence and uniqueness of the fully discrete solution U^n of u^n in terms of the auxiliary variable p^n.

Lemma 5.3.1. *There exists a unique sequence $\{U^n\}_{n=0}^N \subset \mathcal{V}_h^0$ and a corresponding unique sequence $\{p^n\}_{n=0}^N \subset \mathcal{V}_h^0$ which satisfies (5.3.1)-(5.3.2).*

Proof. From (5.3.1), we have

$$U^{n+1} = \frac{\tau}{2}(p^{n+1} + p^n) + U^n. \tag{5.3.3}$$

Using (5.3.3) in (5.3.2), we get

$$\mathcal{A}_w\tau(p^{n+1}, \phi_h) = \mathcal{F}^n(\phi_h) \;\; \forall \phi_h \in \mathcal{V}_h^0, \tag{5.3.4}$$

where $\mathcal{A}_w\tau$ is the bilinear form given by

$$\mathcal{A}_w\tau(w_h, v_h) = (w_h, v_h) + \frac{\tau^2}{4}\mathcal{A}_w(w_h, v_h) \;\; \forall w_h, v_h \in \mathcal{V}_h^0$$

and $\mathcal{F}^n$ is the linear functional given by

$$\mathcal{F}^n(v_h) = (p^n, v_h) - \frac{\tau^2}{4}\mathcal{A}_w(p^n, v_h) - \tau\mathcal{A}_w(U^n, v_h) + \tau(f^{n+\frac{1}{2}}, v_h) \ \ \forall v_h \in \mathcal{V}_h^0.$$

Due to the positive definiteness of bilinear form $\mathcal{A}_w$, there exists uniquely defined $p^{n+1} \in \mathcal{V}_h^0$ satisfying equation (5.3.4) and subsequently U^{n+1} exists uniquely for $n = 0, 1, \ldots, N-1$. This completes the rest of the proof. □

Later on, we will need the following results. The proofs involve the use of Taylor's series and standard arguments, and therefore, details are omitted.

Lemma 5.3.2. *For any $v \in H^3(J; L^2(\Omega))$, we have*

$$\|\partial_\tau v^n - v_t^{n+\frac{1}{2}}\|^2 \leq C\tau^3 \int_{t_n}^{t_{n+1}} \|v_{ttt}\|^2 dt. \tag{5.3.5}$$

In order to compute the error between U^n and u^n, we first establish the error $\xi^n := U^n - \mathcal{E}_h u^n$, for $1 \leq n \leq N$. To do so, first we introduce following notations

$$\mathcal{P}^n := p^n - \mathcal{E}_h u_t^n \ \text{ and } \ \eta^n := u^n - \mathcal{E}_h u^n.$$

Now, for the error ξ^n, we have the following result.

Lemma 5.3.3. *Let u and U^n be the solutions of Problem (5.1.1)-(5.1.2) and (5.3.1)-(5.3.2), respectively. Assume that $u \in H^1(J; H^{k+1}(\Omega)) \cap H^4(J; L^2(\Omega))$. Then, we have*

$$\begin{aligned}\max_{0\leq n\leq N} \|\xi^n\|^2 \ &\leq \ Ch^{2(k+1)}\Big(\|u^0\|_{k+1}^2 + \|u_t\|^2_{L^2(H^{k+1}(\Omega))}\Big) \\ &\quad + C\tau^4\Big(\|u_{tttt}\|^2_{L^2(L^2(\Omega))} + \|u_{ttt}\|^2_{L^2(L^2(\Omega))}\Big).\end{aligned}$$

Proof. For each $\phi_h = \{\phi_0, \phi_b\} \in \mathcal{V}_h^0$, combining scheme (5.3.2) with the definition of $\mathcal{E}_h$, we have

$$\begin{aligned}&(\partial_\tau \mathcal{P}^n, \phi_0) + \mathcal{A}_w(\xi^{n+\frac{1}{2}}, \phi_h) \\ &= (\partial_\tau p^n, \phi_0) + \mathcal{A}_w(U^{n+\frac{1}{2}}, \phi_h) - (\partial_\tau \mathcal{E}_h u_t^n, \phi_0) + (\nabla\cdot(a\nabla u^{n+\frac{1}{2}}), \phi_0) \\ &= \big\{(\partial_\tau p^n, \phi_0) + \mathcal{A}_w(U^{n+\frac{1}{2}}, \phi_h) - (f^{n+\frac{1}{2}}, \phi_0)\big\} + (u_{tt}^{n+\frac{1}{2}}, \phi_0) - (\partial_\tau \mathcal{E}_h u_t^n, \phi_0) \\ &= (u_{tt}^{n+\frac{1}{2}}, \phi_0) - (\partial_\tau \mathcal{E}_h u_t^n, \phi_0) \\ &= (u_{tt}^{n+\frac{1}{2}} - \partial_\tau u_t^n + \partial_\tau u_t^n - \partial_\tau \mathcal{E}_h u_t^n, \phi_0).\end{aligned} \tag{5.3.6}$$

Writing $\omega^n := \partial_\tau u_t^n - u_{tt}^{n+\frac{1}{2}}$, we have the following error equation

$$(\partial_\tau \mathcal{P}^n, \phi_0) + \mathcal{A}_w(\xi^{n+\frac{1}{2}}, \phi_h) = (\partial_\tau \eta_t^n - \omega^n, \phi_0) \ \ \forall \phi_h \in \mathcal{V}_h^0. \tag{5.3.7}$$

It is easy to observe that

$$\partial_\tau \xi^n = \mathcal{P}^{n+\frac{1}{2}} + \partial_\tau \eta^n - \eta_t^{n+\frac{1}{2}} - \sigma^n, \tag{5.3.8}$$

where $\sigma^n := \partial_\tau u^n - u_t^{n+\frac{1}{2}}$. Substituting $n = 0$ in (5.3.8) and rearranging, we derive

$$\partial_\tau \xi^0 = \mathcal{P}^0 + \frac{\tau}{2}\partial_\tau \mathcal{P}^0 + \partial_\tau \eta^0 - \eta_t^{\frac{1}{2}} - \sigma^0. \tag{5.3.9}$$

Further, for $1 \le n \le N-1$, we can easily derive

$$\partial_\tau \xi^n = \mathcal{P}^0 + \frac{\tau}{2}\sum_{k=0}^{n} \partial_\tau \mathcal{P}^k + \frac{\tau}{2}\sum_{k=0}^{n-1} \partial_\tau \mathcal{P}^k + \partial_\tau \eta^n - \eta_t^{n+\frac{1}{2}} - \sigma^n. \tag{5.3.10}$$

Now, we define a sequence $\{\alpha^n\}_{n=0}^N$ such that $\alpha^0 = 0$ and

$$\alpha^n = \tau \sum_{k=0}^{n-1} \xi^{n+\frac{1}{2}}, \;\; 1 \le n \le N.$$

Then, we note that

$$\alpha^{\frac{1}{2}} = \frac{1}{2}\tau \xi^{\frac{1}{2}} \tag{5.3.11}$$

and

$$\alpha^{n+\frac{1}{2}} = \frac{\tau}{2}\Big\{ \sum_{k=0}^{n} \xi^{k+\frac{1}{2}} + \sum_{k=0}^{n-1} \xi^{k+\frac{1}{2}} \Big\}, \;\; 1 \le n \le N-1. \tag{5.3.12}$$

Next, using the identities (5.3.7), (5.3.9) and (5.3.11), we get for each $\phi_h \in \mathcal{V}_h^0$

$$\begin{aligned}
&(\partial_\tau \xi^0, \phi_0) + \mathcal{A}_w(\alpha^{\frac{1}{2}}, \phi_h) \\
&= (\mathcal{P}^0 + \partial_\tau \eta^0 - \eta_t^{\frac{1}{2}} - \sigma^0, \phi_0) + \frac{\tau}{2}\big\{(\partial_\tau \mathcal{P}^0, \phi_0) + \mathcal{A}_w(\xi^{\frac{1}{2}}, \phi_h)\big\} \\
&= (\mathcal{P}^0 + \partial_\tau \eta^0 - \eta_t^{\frac{1}{2}} - \sigma^0, \phi_0) + \frac{\tau}{2}(\partial_\tau \eta_t^0 - \omega^0, \phi_0) \\
&= (\mathcal{P}^0 - \eta_t^0, \phi_0) + (\partial_\tau \eta^0 - \sigma^0 - \frac{\tau}{2}\omega^0, \phi_0).
\end{aligned}$$

Further, using the fact that

$$(\mathcal{P}^0 - \eta_t^0, \phi_0) = (p^0 - \mathcal{E}_h u_t^0 - u_t^0 + \mathcal{E}_h u_t^0, \phi_0) = (\mathcal{Q}_h \phi - \phi, \phi_0) = 0$$

we arrive at

$$(\partial_\tau \xi^0, \phi_0) + \mathcal{A}_w(\alpha^{\frac{1}{2}}, \phi_h) = (\partial_\tau \eta^0 - \sigma^0 - \frac{\tau}{2}\omega^0, \phi_0) \;\; \forall \phi_h \in \mathcal{V}_h^0. \tag{5.3.13}$$

Similarly, for any $\phi_h \in \mathcal{V}_h^0$ and $1 \le n \le N-1$, from (5.3.7), (5.3.10) and (5.3.12), we have

$$\begin{aligned}
&(\partial_\tau \xi^n, \phi_0) + \mathcal{A}_w(\alpha^{n+\frac{1}{2}}, \phi_h) \\
&= (\mathcal{P}^0 + \partial_\tau \eta^n - \eta_t^{n+\frac{1}{2}} - \sigma^n, \phi_0) + \frac{\tau}{2}\sum_{k=0}^{n-1}\left\{(\partial_\tau \mathcal{P}^k, \phi_0) + \mathcal{A}_w(\xi^{k+\frac{1}{2}}, \phi_h)\right\} \\
&\quad + \frac{\tau}{2}\sum_{k=0}^{n}\left\{(\partial_\tau \mathcal{P}^k, \phi_0) + \mathcal{A}_w(\xi^{k+\frac{1}{2}}, \phi_h)\right\} \\
&= (\mathcal{P}^0 + \partial_\tau \eta^n - \eta_t^{n+\frac{1}{2}} - \sigma^n, \phi_0) + \frac{\tau}{2}\sum_{k=0}^{n-1}(\partial_\tau \eta_t^k - \omega^k, \phi_0) \\
&\quad + \frac{\tau}{2}\sum_{k=0}^{n}(\partial_\tau \eta_t^k - \omega^k, \phi_0) \\
&= (\mathcal{P}^0 + \partial_\tau \eta^n - \eta_t^{n+\frac{1}{2}} - \sigma^n, \phi_0) + (\frac{\tau}{2}\partial_\tau \eta_t^n + \tau\sum_{k=0}^{n-1}\partial_\tau \eta_t^k, \phi_0) \\
&\quad - (\frac{\tau}{2}\sum_{k=0}^{n}\omega^k + \frac{\tau}{2}\sum_{k=0}^{n-1}\omega^k, \phi_0).
\end{aligned}$$

Then, using the identity

$$\frac{\tau}{2}\partial_\tau \eta_t^n + \tau\sum_{k=0}^{n-1}\partial_\tau \eta_t^k = \eta_t^{n+\frac{1}{2}} - \eta_t^0$$

and the fact that $(\mathcal{P}^0 - \eta_t^0, \phi_0) = 0$, we drive

$$(\partial_\tau \xi^n, \phi_0) + \mathcal{A}_w(\alpha^{n+\frac{1}{2}}, \phi_h) = (\partial_\tau \eta^n - \sigma^n - \frac{\tau}{2}\omega^n - \tau\sum_{k=0}^{n-1}\omega^{k+\frac{1}{2}}, \phi_0), \tag{5.3.14}$$

for all $\phi_h \in \mathcal{V}_h^0$. Now, for the sake of brevity, we define

$$\epsilon^n = \begin{cases} \partial_\tau \eta^0 - \sigma^0 - \frac{\tau}{2}\omega^0 & \text{for } n = 0, \\ \partial_\tau \eta^n - \sigma^n - \frac{\tau}{2}\omega^n - \tau\sum_{k=0}^{n-1}\omega^{k+\frac{1}{2}} & \text{for } 1 \le n \le N-1. \end{cases}$$

Then, combining the identities (5.3.13) and (5.3.14), we get

$$(\partial_\tau \xi^n, \phi_0) + \mathcal{A}_w(\alpha^{n+\frac{1}{2}}, \phi_h) = (\epsilon^n, \phi_0), \quad 0 \le n \le N-1 \tag{5.3.15}$$

for all $\phi_h \in \mathcal{V}_h^0$. Then, substituting $\phi_h = \partial_\tau \alpha^n = \frac{\xi^{n+1}+\xi^n}{2}$ in (5.3.15) we obtain

$$\|\xi^{n+1}\|^2 - \|\xi^n\|^2 + |||\alpha^{n+1}|||^2 - |||\alpha^n|||^2 = 2\tau(\epsilon^n, \xi^{n+\frac{1}{2}}).$$

Now, summing over $n = 0$ to $l-1$, $1 \leq l \leq N$, we get

$$\|\xi^l\|^2 - \|\xi^0\|^2 + \left|\left|\left|\alpha^l\right|\right|\right|^2 - \left|\left|\left|\alpha^0\right|\right|\right|^2 = 2\tau \sum_{n=0}^{l-1} (\epsilon^n, \xi^{n+\frac{1}{2}}). \tag{5.3.16}$$

Next, using Young's inequality on the right hand side of (5.3.16) and the fact that $\left|\left|\left|\alpha^l\right|\right|\right| \geq 0$, we obtain

$$\begin{aligned} \|\xi^l\|^2 &\leq \|\xi^0\|^2 + 4T\tau \sum_{n=0}^{l-1} \|\epsilon^n\|^2 + \frac{\tau}{4T} \sum_{n=0}^{l-1} \|\xi^{n+\frac{1}{2}}\|^2 \\ &\leq \|\xi^0\|^2 + 4T\tau \sum_{n=0}^{l-1} \|\epsilon^n\|^2 + \frac{1}{2} \max_{0\leq n\leq N} \|\xi^n\|^2, \end{aligned}$$

which implies

$$\max_{0\leq n\leq N} \|\xi^n\|^2 \leq 2\|\xi^0\|^2 + 8T\tau \sum_{n=0}^{N-1} \|\epsilon^n\|^2. \tag{5.3.17}$$

Now, we shall estimate ϵ^n. For the estimation of ϵ^n, use triangle inequality and Cauchy-Schwarz inequality to have

$$\begin{aligned} \|\epsilon^n\|^2 &\leq \|\partial_\tau \eta^n\|^2 + \|\sigma^n\|^2 + \frac{\tau^2}{4} \|\sum_{k=0}^{n} \omega^k\|^2 + \frac{\tau^2}{4} \|\sum_{k=0}^{n} \omega^k\|^2 \\ &\leq \|\partial_\tau \eta^n\|^2 + \|\sigma^n\|^2 + \frac{\tau^2}{2} N \|\sum_{k=0}^{N-1} \omega^k\|^2 \\ &\leq \|\partial_\tau \eta^n\|^2 + \|\sigma^n\|^2 + \frac{T}{2} \Big(\tau \|\sum_{k=0}^{N-1} \omega^k\|^2\Big). \end{aligned}$$

Summing both sides of the above equation from $n = 0$ to $n = N-1$ and then multiplying the resultant by τ, we obtain

$$\begin{aligned} \tau \sum_{n=0}^{N-1} \|\epsilon^n\|^2 &\leq \tau \sum_{n=0}^{N-1} \|\partial_\tau \eta^n\|^2 + \tau \sum_{n=0}^{N-1} \|\sigma^n\|^2 \\ &\quad + \tau \sum_{n=0}^{N-1} \left(\frac{T}{2} \Big(\tau \|\sum_{k=0}^{N-1} \omega^k\|^2\Big) \right). \end{aligned} \tag{5.3.18}$$

Using Lemma 5.3.2, we have

$$\|\omega^k\|^2 \leq C\tau^3 \int_{t_k}^{t_{k+1}} \|u_{tttt}\|^2 dt.$$

Hence,

$$\tau \sum_{k=0}^{N-1} \|\omega^k\|^2 \leq C\tau^4 \|u_{tttt}\|^2_{L^2(J;L^2(\Omega))}. \tag{5.3.19}$$

Analogously, we can derive

$$\tau \sum_{k=0}^{N-1} \|\sigma^k\|^2 \leq C\tau^4 \|u_{ttt}\|^2_{L^2(J;L^2(\Omega))}. \tag{5.3.20}$$

and

$$\tau \sum_{k=0}^{N-1} \|\eta^k\|^2 \leq C\|\eta_t\|^2_{L^2(J;L^2(\Omega))} \leq Ch^{2(k+1)} \|u_t\|_{L^2(J;H^{k+1}(\Omega))}, \tag{5.3.21}$$

where for the last inequality we have used Lemma 5.2.1 and Lemma 5.2.2.

Using estimates (5.3.19)-(5.3.21) in (5.3.18), we get

$$\begin{aligned} \tau \sum_{n=0}^{N-1} \|\epsilon^n\|^2 \quad \leq \quad & C\Big(\tau^4 \|u_{tttt}\|^2_{L^2(J;L^2(\Omega))} + \tau^4 \|u_{ttt}\|^2_{L^2(J;L^2(\Omega))} \\ & + h^{2(k+1)} \|u_t\|^2_{L^2(J;H^{k+1}(\Omega))}\Big). \end{aligned} \tag{5.3.22}$$

Further, use (5.3.22) in (5.3.17) to obtain

$$\begin{aligned} \max_{0\leq n\leq N} \|\xi^n\|^2 \quad \leq \quad & 2\|\xi^0\|^2 + C\Big(\tau^4 \|u_{tttt}\|^2_{L^2(J;L^2(\Omega))} + \tau^4 \|u_{ttt}\|^2_{L^2(J;L^2(\Omega))} \\ & + h^{2(k+1)} \|u_t\|^2_{L^2(J;H^{k+1}(\Omega))}\Big). \end{aligned} \tag{5.3.23}$$

Finally, a simple application of Lemma 5.2.2 proves Lemma 5.3.3. □

Now, we are in a position to state the main result of this section.

Theorem 5.3.1. *Let u and U^n be the solutions of Problem (5.1.1)-(5.1.2) and (5.3.1)-(5.3.2), respectively. Assume that $u \in H^1(J; H^{k+1}(\Omega)) \cap H^4(J; L^2(\Omega))$. Then, we have*

$$\max_{0\leq n\leq N} \|u^n - U^n\| \leq \tilde{C}(u^0, u)\big(h^{k+1} + \tau^2\big),$$

where $\tilde{C}(u^0, u) = \|u^0\|_{k+1} + \|u\|_{L^\infty(H^{k+1}(\Omega))} + \|u_t\|_{L^2(H^{k+1}(\Omega))} + \|u\|_{H^4(L^2(\Omega))}$.

Proof. Applying triangle inequality to

$$u^n - U^n = u^n - \mathcal{Q}_h u^n + \mathcal{Q}_h u^n - \mathcal{E}_h u^n + \mathcal{E}_h u^n - U^n,$$

followed by Lemma 5.2.1, Theorem 5.2.1 and Lemma 5.3.3 leads to

$$\begin{aligned} \|u^n - U^n\|^2 \quad \leq \quad & Ch^{2(k+1)}\Big(\|u^0\|^2_{k+1} + \|u^n\|^2_{k+1} + \|u_t\|^2_{L^2(H^{k+1}(\Omega))}\Big) \\ & + C\tau^4\Big(\|u_{tttt}\|^2_{L^2(L^2(\Omega))} + \|u_{ttt}\|^2_{L^2(L^2(\Omega))}\Big). \end{aligned}$$

This completes the rest of the proof. □

Remark 5.3.1. *For the time discretization, the simplest scheme consists of using the classical leapfrog scheme with three time levels. The fully discrete numerical solution to the wave equation (5.1.1)-(5.1.2) is then defined by finding the sequence* $\{U^n\}_{n=0}^N \in \mathcal{V}_h^0$ *such that*

$$\left(\bar{\partial}_{tt}U^n, v_h\right) + \mathcal{A}(U^n, v_h) = (f^n, v_h)\ \forall v_h \in \mathcal{V}_h^0,\ n = 1,\ 2, \ldots, N-1,$$

where

$$\bar{\partial}_{tt}U^n = \frac{U^{n+1} - 2U^n + U^{n-1}}{\tau^2}.$$

This scheme yields a second-order accuracy in time direction which is generally not sufficient for a higher-order finite element method. As a stability constraint, the scheme requires to choose $\tau = O(h)$*. Although Crank-Nicolson type scheme is implicit in nature, but, we do not have stability restriction on mesh parameters. It is found in [65] that the implicit procedure results in less dispersive solutions than the explicit one, which is advantageous for the numerical solution in very oscillatory media.*

It would be interesting to extend the results presented in Chapter 5 to a more general Newmark scheme

$$\left(\bar{\partial}_{tt}U^n, v_h\right) + \mathcal{A}_w(U^{n,\theta,\gamma}, v_h) = (f^{n,\theta,\gamma}, v_h)\ \forall v_h \in \mathcal{V}_h^0,$$

where

$$\begin{aligned}\bar{\partial}_{tt}U^n &= \frac{U^{n+1} - 2U^n + U^{n-1}}{\tau^2},\\ U^{n,\theta,\gamma} &= \theta U^{n+1} + \left(\frac{1}{2} - 2\theta + \gamma\right)U^n + \left(\frac{1}{2} + \theta - \gamma\right)U^{n-1}.\end{aligned}$$

Here, $\gamma,\ \theta \geq 0$ *are free parameters. Above scheme reduces to explicit when* $\theta = 0$ *and* $\gamma = \frac{1}{2}$.

5.4 Numerical Section

In this section, we shall illustrate several numerical Examples to validate the theoretical results for the hyperbolic problem (5.1.1)-(5.1.2) in $\Omega \times J$, where $\Omega \subset \mathbb{R}^2$ and $J = (0, 1]$. To test the flexibility of the WG method, hyperbolic problems are solved on finite element partitions with different kind of configurations, including triangular, rectangular, and polygonal meshes. In Example 5.4.1 and Example 5.4.2, smooth solutions with smooth coefficient and non-smooth coefficient are discussed, respectively. Example 5.4.3 and Example 5.4.4 explain the singularity of the solutions with convex domain

and non-convex domain, respectively. Further, H-shaped domain is discussed in Example 5.4.5. We have verified our theoretical results for anisotropic problem in Example 5.4.6 and singularly perturbed problem with boundary layers in Example 5.4.7. At last, in Example 5.4.8, a second-order wave equation has been considered with degenerate diffusion coefficients.

Let U^n be the weak Galerkin solution defined by (5.3.1) and (5.3.2). Then, we have calculated following error

$$e_h := Q_h u(x, t_N) - U^N$$

at final time $t_N = T$ with respect to L^2-norm. More precisely, the errors are presented with respect to L^2-norm through tables and error plots for the WG space

$$(\mathcal{P}_k(K), \mathcal{P}_k(\partial K), [\mathcal{P}_{k-1}(K)]^2)$$

with time step $\tau = \mathrm{O}(h^k)$.

We try to understand the behavior of true errors obtained in Theorem 5.3.1 on different meshes with uniform time steps and have observed experimental order of convergence (EOC) for each quantity of interest. The EOC is defined as follows: For a given finite sequence of successive runs (indexed by i), the EOC of the corresponding sequence of quantity of interest $e(i)$ (L^2 error) itself is a sequence defined by

$$\mathrm{EOC}(e(i)) = \frac{\log\Big(e(i+1)/e(i)\Big)}{\log\Big(h(i+1)/h(i)\Big)} \tag{5.4.1}$$

where $h(i)$ denotes the mesh size of the run i.

Example 5.4.1. Smooth solution with smooth coefficient: This example is taken from [52]. Consider the problem (5.1.1)-(5.1.2) in $\Omega \times J$, where $\Omega = (0,1)^2$. Numerical solution is compared with the following exact solution

$$u(x, y, t) = t^2 \sin(\pi x) \sin(\pi y).$$

The right-hand side f, initial condition u^0 and v^0 are determined from the choice for u and the diffusion-coefficient $a = I$. The above solution explains our all theoretical regularity assumptions. In this Example, triangular mesh is used. We have done uniform partitioning of the domain into $n \times n$ sub rectangles which is followed by dividing each rectangular element by the diagonal line with a negative slope, where the mesh size is $h = 1/n$. The L^2-norm errors for linear, quadratic, and cubic WG spaces at final time $T = 1$ are reported in Tables 5.4.1-5.4.2, which shows that the rate convergence of the order $\mathrm{O}(h^{k+1})$ in L^2 norm for $k = 1,\ 2,\ 3$.

Table 5.4.1: Example 5.4.1. The history of L^2 error convergence on triangular mesh

	$k=1,\ \ \tau=h$		$k=2,\ \ \tau=h^2$	
h	$\|e_h\|$	EOC	$\|e_h\|$	EOC
1/2	3.160843e-01	-	1.110369e-01	-
1/4	1.023902e-01	1.626232e+00	1.592060e-02	2.802072e+00
1/8	2.839685e-02	1.850275e+00	2.025394e-03	2.974621e+00
1/16	7.311000e-03	1.957590e+00	2.551498e-04	2.988786e+00
1/32	1.841533e-03	1.989161e+00	3.191920e-05	2.998848e+00
1/64	4.612530e-04	1.997277e+00	3.990720e-06	2.999703e+00
1/128	1.140937e-04	2.015339e+00	4.702395e-07	3.085182e+00

Example 5.4.2. Smooth solution with non-smooth coefficient: We consider the following IBVP

$$\begin{cases} \gamma u_{tt} - \nabla \cdot (\beta \nabla u) = f \ \ \text{in } \Omega \times J, \\ u(x,0) = u^0, \quad u_t(x,0) = v^0 \ \ \text{in } \ \Omega, \\ u(x,t) = 0 \quad \text{on } \partial\Omega \times J, \end{cases}$$

where $\Omega = (0,1)^2$. The data appearing in the above problem are selected by setting the exact solution as

$$u(x,y,t) = t^2 \exp(-t) \sin(\pi x) \sin(\pi y)$$

and the coefficients, which are discontinuous along the circle $x^2 + y^2 = 1/4$, are given by

$$(\gamma, \beta) = \begin{cases} (1, 1500) & \text{in } \ x^2 + y^2 \le 1/4, \\ (10, 3000) & \text{else.} \end{cases}$$

A large variation in the coefficients is a common occurrence in study of acoustic wave

Table 5.4.2: Example 5.4.1. The history of L^2 error convergence on triangular mesh

$k = 3, \quad \tau = h^3$

h	$\|e_h\|$	EOC
1/2	2.689181e-02	-
1/4	1.793403e-03	3.906395e+00
1/8	1.137499e-04	3.978763e+00
1/16	7.133565e-06	3.995098e+00
1/32	4.461914e-07	3.998889e+00
1/64	2.738926e-08	4.025981e+00

propagation through heterogeneous media in geophysical prospecting (cf. [10]). Our numerical results are based on the uniform triangular meshes for $k = 1$ and $k = 2$, and polygonal mesh for $k = 1$.The errors with respect to L^2 norm for different WG spaces at final time $T = 1$ are reported in Tables 5.4.3-5.4.4. These tables also suggest that we have achieved optimal order of convergence in L^2 norm, which confirm the theoretical prediction as proved in Theorem 5.3.1.

Example 5.4.3. Low regular solution with convex domain: We consider a hyperbolic equation on a two-dimensional domain, for which the exact solution possesses a corner singularity in spatial direction. The Example discussed here is extracted from [127] with minor modifications. For simplicity, we take $\Omega = (0, 1)^2$ and let the exact solution be given by

$$u(x, y, t) = t^2 \exp(-t)xy(1 - x)(1 - y)r^{-2+\gamma},$$

where $r = \sqrt{x^2 + y^2}$ and $\gamma \in (0, 1]$ is a constant. Clearly, we have

$$u \in H_0^1(\Omega) \cap C^\infty(J; H^{1+\gamma-\varepsilon}(\Omega)) \quad \text{and} \quad u \notin C^\infty(J; H^{1+\gamma}(\Omega)),$$

where ε is a positive real number. The elements; $\left(\mathcal{P}_1, \mathcal{P}_1, \left[\mathcal{P}_0\right]^2\right)$, along with uniform triangular meshes are used for numerical discretization. This Example is numerically

Table 5.4.3: Example 5.4.2. The history of L^2 error convergence on triangular mesh

	$k=1,\ \ \tau=h$		$k=2,\ \ \tau=h^2$	
h	$\|e_h\|$	EOC	$\|e_h\|$	EOC
1/2	1.104800e-02	-	2.691773e-03	-
1/4	2.861880e-03	1.948749e+00	3.396372e-04	2.986491e+00
1/8	7.058120e-04	2.019608e+00	4.077137e-05	3.058366e+00
1/16	1.742732e-04	2.017933e+00	5.004021e-06	3.026397e+00
1/32	4.278779e-05	2.026079e+00	6.194159e-07	3.014108e+00
1/64	1.087677e-05	1.975949e+00	7.425173e-08	3.060412e+00
1/128	2.630438e-06	2.047875e+00	1.037842e-08	2.838837e+00

Table 5.4.4: Example 5.4.2. The history of L^2 error convergence on polygonal mesh

	$k=1,\ \ \tau=h$	
h	$\|e_h\|$	EOC
1/2	1.175354e-02	-
1/4	3.194154e-03	1.879590e+00
1/8	7.995092e-04	1.998247e+00
1/16	1.987951e-04	2.007832e+00
1/32	4.934780e-05	2.010225e+00
1/64	1.224992e-05	2.010214e+00
1/128	2.839435e-06	2.109096e+00

testified with $\gamma = 1/2$ and $\gamma = 1/8$. Table 5.4.5 represents the order of convergence in L^2-norm. Note that L^2 error act similarly as anticipated by theory in theorem 5.3.1; i.e., the L^2 error converge with rate given by $O(h^{\gamma+1})$, which decays when γ tends to 0. This happens because of the low regularity of the solution u. Also, we have used higher order polynomial approximations reported in Table 5.4.6, but the accuracy is only about order $O(h^{1+\gamma})$, which is as expected due to low regularity of the solution. Figure 5.4.1 represents the WG solution and exact solution at final time.

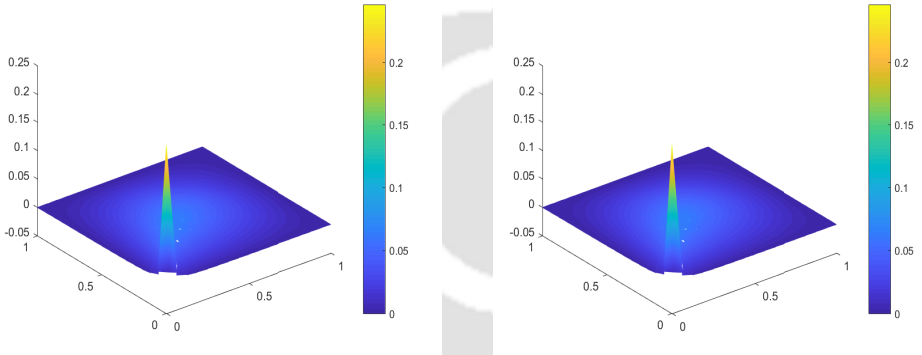

Figure 5.4.1: Surface plots for WG solution (left) and exact solution (right) at final time $t_N = 1$ in Example 5.4.3.

Example 5.4.4. Singular solution with non-convex domain: In this Example, which is adopted from [52], we consider the two-dimensional hyperbolic equation on the L-shaped domain $\Omega = (0,1)^2 \setminus [1/2,1)^2$. The source term f, initial data u^0 and v^0 are determined from the choice of u and diffusion coefficient a, where

$$u = t^2 r^\gamma \sin(\gamma\theta), \quad \gamma \in (0,1] \ \ \& \ \ \alpha = I.$$

Although u is smooth in time (and can even be integrated exactly in time), it has a spatial singularity at the origin, such that $u \in C^\infty(J; H^{1+\gamma}(\Omega))$. Therefore, this Example helps in proving the sharpness of the regularity assumptions of our theoretical results. We do not anticipate the order of accuracy $O(h^{1+k})$ for L^2 error in this Example. Indeed, in Table 5.4.7, we have observed the order of accuracy $1+\gamma$ in L^2 error for $\gamma = 1/4$ and $\gamma = 2/3$ along with uniform rectangular meshes. Figure 5.4.2 (bottom left) shows that the accuracy of L^2 error decreases to 1, when γ tends to zero. On the other hand, when the value of γ increases to 1, the WG method produces better convergence rates and accuracy (bottom right of Figure 5.4.2).

Table 5.4.5: Example 5.4.3. Orders of convergence for $k = 1$ with time step $\tau = h$

	$\gamma = 1/2$		$\gamma = 1/8$	
h	$\|e_h\|$	EOC	$\|e_h\|$	EOC
1/2	1.169748e-01	-	3.324833e-01	-
1/4	4.690373e-02	1+0.318423e+00	1.695260e-01	0.9717751e+00
1/8	1.609453e-02	1+0.543132e+00	7.547393e-02	1+0.167456e+00
1/16	5.694236e-03	1+0.498996e+00	3.451423e-02	1+0.128787e+00
1/32	2.021886e-03	1+0.493801e+00	1.584318e-02	1+0.123329e+00
1/64	7.173313e-04	1+0.494990e+00	7.273297e-03	1+0.123181e+00
1/128	2.541346e-04	1+0.497047e+00	3.336602e-03	1+0.124230e+00

Table 5.4.6: Example 5.4.3. Orders of convergence for $k = 2$ with time step $\tau = h^2$

	$\gamma = 1/2$		$\gamma = 1/8$	
h	$\|e_h\|$	EOC	$\|e_h\|$	EOC
1/2	8.011995e-02	-	0.2737947e+00	-
1/4	2.524920e-02	1+0.665924e+00	1.131524e-01	1+0.274828e+00
1/8	8.846819e-03	1+0.513007e+00	5.190337e-02	1+0.124367e+00
1/16	3.116419e-03	1+0.505270e+00	2.375428e-02	1+0.127640e+00
1/32	1.100946e-03	1+0.501146e+00	1.089435e-02	1+0.124608e+00
1/64	3.803752e-04	1+0.533248e+00	5.0018327e-03	1+0.123051e+00

Table 5.4.7: Example 5.4.4. Orders of convergence for $k = 1$ with time step $\tau = h$

	$\gamma = 1/4$		$\gamma = 2/3$	
h	$\|e_h\|$	EOC	$\|e_h\|$	EOC
1/2	9.100011e-03	-	7.645603e-03	-
1/4	5.155180e-03	0.8198457e+00	3.833580e-03	0.9959379e-01
1/8	2.237644e-03	1+0.204042e+00	1.343874e-03	1+0.512295e+00
1/16	9.445873e-04	1+0.244224e+00	4.409452e-04	1+0.607726e+00
1/32	3.976334e-04	1+0.248245e+00	1.420867e-04	1+0.633828e+00
1/64	1.672416e-04	1+0.249505e+00	4.535879e-05	1+0.647318e+00

Example 5.4.5. Smooth solution with H-shaped domain: To demonstrate the efficiency and robustness of the weak Galerkin methods on a non-convex H-shaped domain, we consider the wave equation (5.1.1)-(5.1.2) with constant speed $a = I$ in a computational domain $\Omega \times J$, where Ω consists of two (0.3×2) rectangles connected by a narrow 0.4×0.15 channel. The data appearing in the problem (5.1.1)-(5.1.2) are selected by setting the exact solution as

$$u(x, y, t) = t^2 \exp(-t) \sin(\pi x) \sin(\pi y).$$

The order of convergence for L^2 error at the final time T is evaluated for the linear WG space $(\mathcal{P}_1(K),\ \mathcal{P}_1(\partial K),\ \left[\mathcal{P}_0(K)\right]^2)$ based on uniform rectangular mesh with mesh-size $h = 1/n$, where $n = 2, 4, 8, 16, 32, 64$. An initial mesh is depicted in figure 5.4.3. A circular wave is initiated in the left region, which propagates outward until it affect on the right boundary. Then, a fraction of the wave creates a hole in the channel and produces a spherical outgoing wave as it approaches the opposite right field. Further reflection occurs when the wave moves back and forth in and out of the channel, latter generating several circular waves in the left and right domains. In Figure 5.4.4, contour plots of the numerical solution are shown at different times $t = 0.25, 1$. Finally, we verified that the L^2 error which we have obtained in theorem 5.3.1 achieved second-

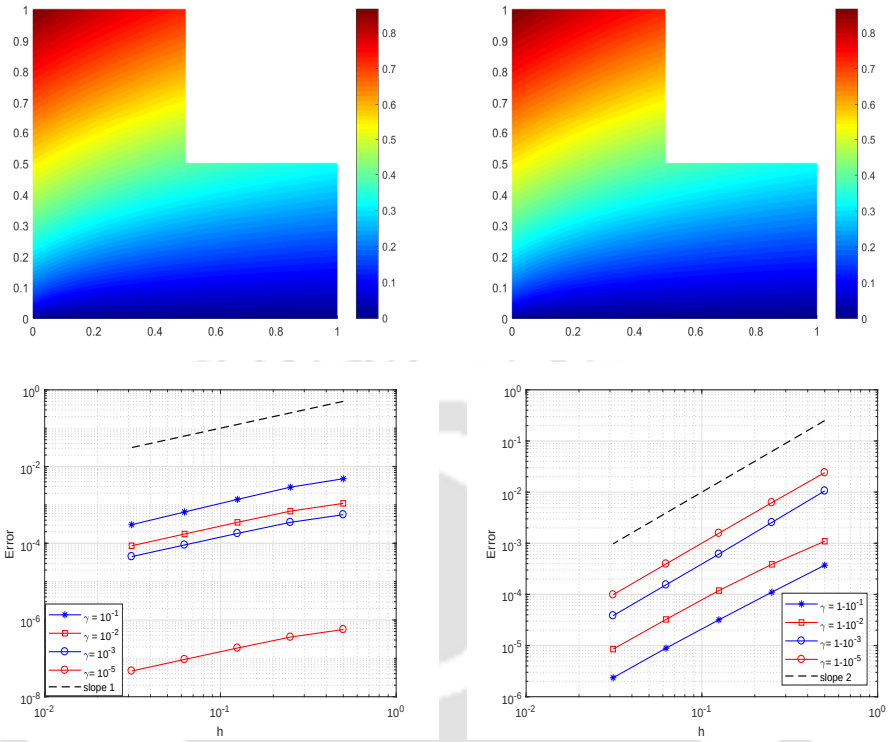

Figure 5.4.2: Contour plots for exact solution (top left), WG solution (top right) at time $t = 1$, and log-log plot of the L^2 norm versus the mesh size at time $t = 1$ (bottom) in Example 5.4.4.

order of convergence in L^2-norm. In Figure 5.4.5, we follow the rate of convergence with various mesh levels and time step $\tau = h$ at $t = 0.25, 0.5, 1$.

Example 5.4.6. An anisotropic problem: This Example is governed by differential equation which has arisen from modeling of fluid flow in porous media with anisotropic permeability. The Example discussed here is selected from [79] (Example 2) with minor changes. We consider a two-dimensional linear hyperbolic problem with an anisotropy, which is given by following equation

$$u_{tt} - \nabla \cdot (a \nabla u) = f \quad \text{in } (0,1)^2 \times (0,T],\ T < \infty,$$

with suitable initial and boundary conditions. The permeability tensor a is given by

$$a = \begin{bmatrix} \lambda^2 & 0 \\ 0 & 1 \end{bmatrix} \quad \text{for} \quad \lambda \neq 0,$$

$\lambda^2 : 1$, which is the ratio of two positive eigenvalues of the 2×2 permeability tensor a,

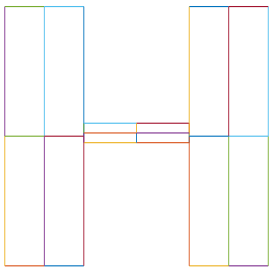

Figure 5.4.3: Initial mesh with $h = 1/2$

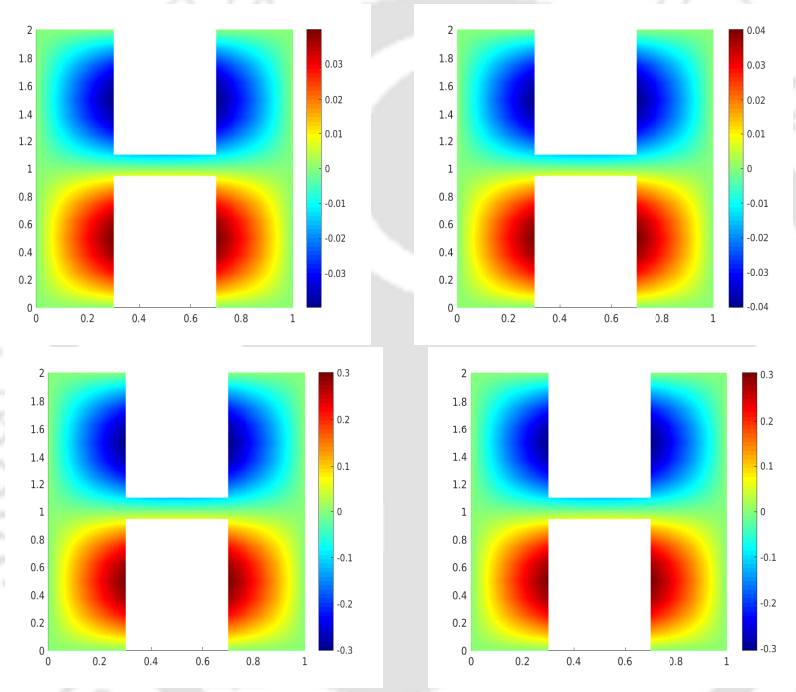

Figure 5.4.4: Contour plots for exact solution at $t = 0.25$ (top left) and at $t = 1$ (bottom left), WG solution at $t = 0.25$ (top right) and at $t = 1$ (bottom right) in Example 5.4.5.

is the anisotropy for this test Example. The exact solution for this Example is given by

$$u(x, y) = t^2 \exp(-t) \exp\left(\frac{(x - x_c)^2 + (y - y_c)^2}{2\sigma^2}\right),$$

where $(x_c, y_c) = (0.5, 0.5)$ and $\sigma^2 = 1$. The load function f and initial data u^0, v^0 can be calculated appropriately.

In order to apply the weak Galerkin method on an anisotropic problem, the rectangular mesh was formed by dividing the domain into $\lambda^2 n \times n$ sub-rectangles with mesh size $h = 1/n$. Two case with $\lambda = 3$ and $\lambda = 9$ were tested, the results for the same with optimal order of accuracy is shown in Tables 5.4.8 . The numerical experiment suggests

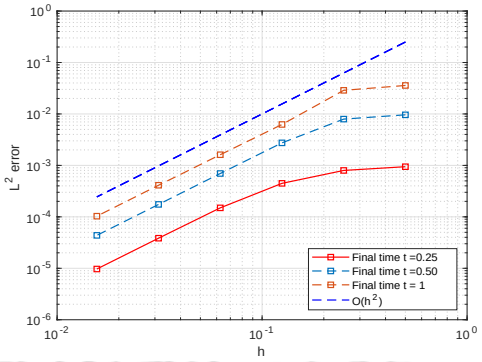

Figure 5.4.5: Log-log plot of the L^2 norm versus the mesh size at different time levels in Example 5.4.5.

that the weak Galerkin method can be easily used to handle anisotropic problems and meshes.

Table 5.4.8: Example 5.4.6. Orders of convergence for $k = 1$ with time step $\tau = h$

	$\lambda = 3$		$\lambda = 9$	
h	$\|e_h\|$	EOC	$\|e_h\|$	EOC
1/2	4.672784e-02	-	4.088648e-02	-
1/4	8.900946e-03	2.392252e+00	1.057090e-02	1.951526e+00
1/8	2.581968e-03	1.785487e+00	2.550441e-03	2.051279e+00
1/16	5.811225e-04	2.151557e+00	6.144093e-04	2.053475e+00
1/32	1.539353e-04	1.916518e+00	1.538812e-04	1.997383e+00
1/64	3.788106e-05	2.022776e+00	3.840375e-05	2.002497e+00

Example 5.4.7. Singularly perturbed problem with boundary layers: Consider the following singularly perturbed 2D hyperbolic equation

$$u_{tt} - \varepsilon \Delta u = f \ \text{ in } (0,1)^2 \times (0,1].$$

This Example is considered with different values of ε, which is motivated by the Examples in [32]. The initial data u^0, v^0 and the load function f are selected by setting the exact solution as

$$u(x, y, t) = t^2 \exp(-t)\phi(x)\phi(y),$$

where $\phi(s) = m_1 + m_2 s + \exp(-\frac{1-s}{\varepsilon})$, $m_1 = -\exp(-1/\varepsilon)$, $m_2 = -1 - m_1$. The test problem has two boundary layers along $x = 1$ and $y = 1$.

The L^2 error and order of convergence for WG solution U^n at the final time $t_N = 1$ are evaluated for linear elements on uniform rectangular meshes with $h = 1/n$, which are illustrated in Table 5.4.9. Here, we observed that the order of convergence in L^2 norm is of second-order in time for both $\varepsilon = 1$ and $\varepsilon = 10^{-10}$. Figure 5.4.6 shows that when $\varepsilon = 10^{-10} \lll h$, the numerical solutions do not indicate factitious oscillations near the boundary layers $x = 1$ and $y = 1$.

Table 5.4.9: Example 5.4.7. Orders of convergence for $k = 1$ with time step $\tau = h$

	$\varepsilon = 1$		$\varepsilon = 10^{-10}$	
h	$\|e_h\|$	EOC	$\|e_h\|$	EOC
1/2	1.208067e-03	-	7.331059e-03	-
1/4	4.307413e-04	1.487807e+00	2.103734e-03	1.801070e+00
1/8	1.161648e-04	1.890649e+00	5.430122e-04	1.953895e+00
1/16	2.981440e-05	1.962092e+00	1.368221e-04	1.988683e+00
1/32	7.502611e-06	1.990545e+00	3.427194e-05	1.997202e+00
1/64	1.879151e-06	1.997312e+00	8.571266e-06	1.999448e+00

Example 5.4.8. Degenerate diffusion coefficient: In the following Example, we have considered the diffusion coefficient a, which is singular at certain domain points. In the present case, the mixed finite element method may not be applicable due to

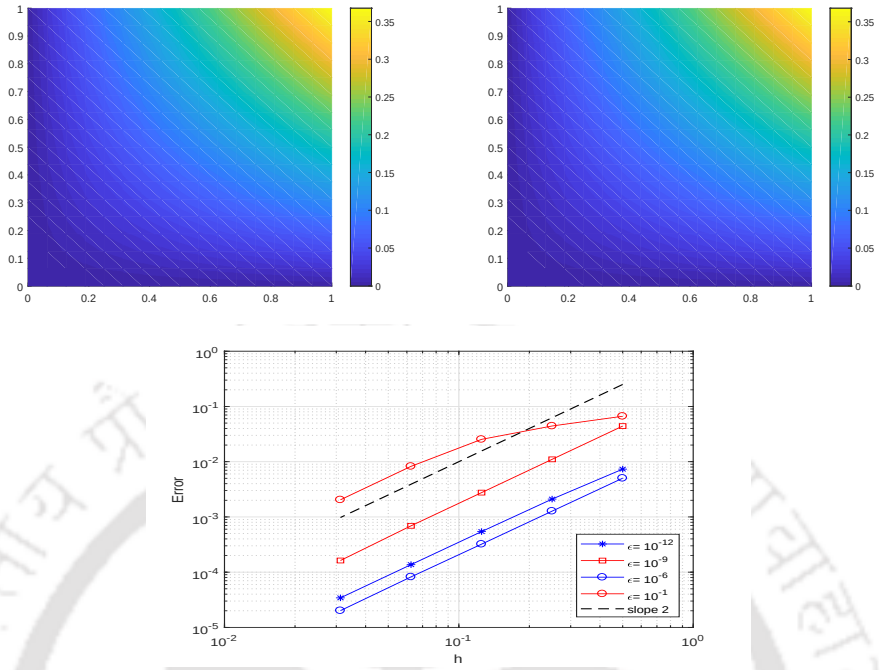

Figure 5.4.6: Contour plots for WG solution (top left), exact solution (top right) at $t = 1$ for $\varepsilon = 10^{-10}$ and log-log plot of the L^2 norm versus the mesh size at time $t = 1$ (bottom) in Example 5.4.7.

the degeneracy of diffusion coefficient (cf. [89]). We consider the following hyperbolic problem in a two-dimensional domain $\Omega = (0, 1)^2$

$$u_{tt} - \nabla \cdot (\beta \nabla u) = f \ \text{ in } \ \Omega \times (0, T], \ T < \infty, \tag{5.4.2}$$

with initial and boundary conditions given by (5.1.2).

The data appearing in the above problem was selected for the exact solution

$$u(x, y, t) = \exp(-t) \sin(t^2) \sin(\pi x) \sin(\pi y)$$

with the diffusion coefficient $\beta = xy$, which leads to degeneracy at the origin. For the finite element partitions, we have used triangular and rectangular uniform meshes with mesh size $h = 1/n$. When the diffusion coefficient matrix a in equation (5.1.1) is not uniformly positive definite on the given domain, we observed that the WG approximation for linear polynomial has optimal order of convergence in L^2-norm at final time $T = 1$, however, the L^2 error does not achieve its optimal order upon using the higher degrees of polynomials. The results for the same are represented in Tables 5.4.10-5.4.11. Interestingly, the numerical experiments in [89] for degenerated elliptic problems with

linear elements show that the weak Galerkin method converges with a rate of $O(h^{1.25})$ in L^2-norm. The theory for observed convergence behavior still needs to be explored in the future.

Table 5.4.10: Example 5.4.8. Order of convergence for $k = 1$ with time step $\tau = h$

	Triangular mesh		Rectangular mesh	
h	$\|e_h\|$	EOC	$\|e_h\|$	EOC
1/2	4.601996e-02	-	4.556321e-02	-
1/4	1.939664e-02	1.246453e+00	1.788823e-02	1.348859e+00
1/8	5.306794e-03	1.869894e+00	4.896286e-03	1.869251e+00
1/16	1.334486e-03	1.991556e+00	1.244662e-03	1.975933e+00
1/32	3.313538e-04	2.009840e+00	3.109424e-04	2.001035e+00
1/64	8.225470e-05	2.010202e+00	7.748119e-05	2.004729e+00
1/128	2.045350e-05	2.007750e+00	1.875632e-05	2.046469e+00

Table 5.4.11: Example 5.4.8. Order of convergence on triangular mesh

	$k=2,\ \ \tau=h^2$		$k=3,\ \ \tau=h^3$	
h	$\|e_h\|$	EOC	$\|e_h\|$	EOC
1/2	2.917535e-02	-	2.480945e-02	-
1/4	1.211002e-02	1.268548e+00	1.217084e-02	1.027460e+00
1/8	5.354976e-03	1.177250e+00	5.538107e-03	1.135964e+00
1/16	2.142023e-03	1.321906e+00	2.222993e-03	1.316889e+00
1/32	8.184210e-04	1.388059e+00	8.902596e-04	1.320205e+00
1/64	3.112014e-04	1.394995e+00	3.520743e-04	1.338346e+00
1/128	1.200837e-04	1.373836e+00	1.382716e-04	1.348375e+00

6

WG-FEMs for General Linear Second Order Hyperbolic Equation with Variable Coefficients on Polygonal Meshes

This chapter is concerned with a priori error analysis of weak Galerkin finite element approximations to a general linear second order hyperbolic equation (1.1.5) with variable coefficients on polygonal meshes.

The convergence analysis is carried out for the semidiscrete and fully discrete weak Galerkin approximations. Following Baker [7], Crank-Nicolson scheme is applied for the temporal discretization after reformulating the governing equation as first-order system. Optimal order of convergence in $L^\infty(L^2)$ norm is derived for the fully discrete solution. Several numerical experiments are performed in a two-dimensional setting that illustrates our theoretical convergence findings.

6.1 Introduction

To start with, let us first recall the general linear second order hyperbolic equation. Let Ω be a convex polygonal domain in $\mathbb{R}^2$ with boundary $\partial\Omega$. In Ω, we consider following general linear second order hyperbolic equation

$$\gamma u_{tt} - \nabla \cdot (\alpha \nabla u) - \nabla \cdot (\beta \nabla u_t) + \sigma u_t = f(x,t) \ \text{ in } \Omega \times (0,T], \tag{6.1.1}$$

with initial and boundary conditions;

$$u(x,0) = u^0, \ u_t(x,0) = v^0 \text{ in } \Omega; \ u(x,t) = 0 \text{ on } \partial\Omega \times (0,T]. \tag{6.1.2}$$

This chapter is submitted for publication. in *IMA J. Numer. Anal.*

We assume that the coefficient matrices $\alpha = (\alpha_{ij}(x))_{2\times 2}$ and $\beta = (\beta_{ij}(x))_{2\times 2}$ are in $[L^\infty(\Omega)]^{2\times 2}$, which are symmetric and uniformly positive definite in Ω. The damping coefficients $\gamma = \gamma(x)$ and $\sigma = \sigma(x)$ are non-negative real valued functions defined on Ω. The initial data $\{u^0(x), v^0(x)\}$ and the forcing term f are assumed to be smooth functions in their respective domains of definition, and T is the finite terminal observation time. For the related existence and uniqueness results for the problem (6.1.1)-(6.1.2), we refer to [118, 119].

Equation (6.1.1)-(6.1.2) is provoked by numerous applications of nonlinear hyperbolic problems in medicine and industrial fields like acoustics, fluid mechanics, astrophysics, aerodynamics, and high intensity focused ultrasound by appropriate selection of the damping coefficients. As a model, we consider following Westervelt's quasi-linear wave equation

$$(1 - 2ku)u_{tt} - c^2\Delta u - b\Delta u_t = 2ku_t^2 \tag{6.1.3}$$

with acoustic pressure u. In (6.1.3), the constant c denotes the speed of sound, b is the sound diffusivity, and $k = \beta_a/\lambda,\ \lambda = \varrho c^2$ is the bulk modulus, ϱ is the mass density and β_a the coefficient of nonlinearity of the medium. For more detailed discussion, we refer to [4, 93, 94] and references therein. Although substantial work has been dedicated to their analytical studies [47, 93] and their numerical treatment via finite element procedure (cf. [4, 47, 60, 61, 94, 108] just to name a few), rigorous error analysis for finite element methods of nonlinear acoustic phenomena is still largely unexplored in the literature. Recently, a priori error estimates for the classical finite element approximation of Westervelt's quasi-linear strongly damped wave equation (6.1.3) with linear elements have been discussed in [94]. Then, a high-order discontinuous Galerkin (DG) method for the equation (6.1.3) has been carried out in [4]. It is worthwhile to note that only the semidiscrete scheme (space discretization) has been discussed in [4, 94]. The fully discrete scheme (space-time discretization) error analysis is still open. A priori error analysis in [94] for the equation (6.1.3) heavily depends on a linearized problem

$$\begin{cases} \gamma(x,t)u_{tt} - \nabla\cdot(\alpha\nabla u) - \nabla\cdot(\beta\nabla u_t) + \sigma(x,t)u_t = f(x,t), & \text{in } \Omega\times(0,T],\ T<\infty, \\ u = 0, & \text{on } \partial\Omega\times(0,T], \\ (u,u_t) = (u^0,v^0), & \text{on } \Omega\times\{t=0\}. \end{cases} \tag{6.1.4}$$

Upon changing $\sigma := \sigma(x,t)$ and $\gamma := \gamma(x,t)$ in equation (6.1.1), it represents a linearized Westervelt's equation, which has several applications including treatment of kidney and bladder stones via thermal therapy, ultrasound cleaning and sonochemistry. When $\sigma = 0$, the equation (6.1.1) describes the wave propagation phenomena of actual

vibration through a viscoelastic medium representing a viscoelastic wave equation [81]. For instance, during the heat conduction in memory materials [53], gas diffusion [134], propagation of sound through viscous media [103]. Upon $\sigma \neq 0$, Lim et al. [78] concerned an accurate and efficient numerical algorithm for solving viscous and nonviscous wave equations. In this study, attention is restricted to assume the coefficient $\gamma(x) = 1$ for all $x \in \Omega$. There are plenty of literature available for the convergence analysis for the general linear second order hyperbolic equation via finite element algorithm (*cf.* [13, 57, 62, 73, 96] just to name a few). Recently, WG-FEM for the viscoelastic wave equation has been discussed in [125]. Convergence analysis has been carried out for both semidiscrete scheme and fully discrete scheme in H^1 norm. The fully discrete scheme is based on backforward Euler scheme.

In this chapter, we concentrate on developing and analyzing a WG finite element method for the general linear second order hyperbolic equation with variable coefficients. The main aspect of our proof is the use of a non-standard elliptic type projection operator instead of the usual elliptic projection. The error estimates in energy norm and L^2 norm are new (see, Theorem 6.2.3, Theorem 6.2.2 and Theorem 6.3.1). More precisely, we have achieved $\mathrm{O}(h^k)$ and $\mathrm{O}(h^{k+1})$ for the WG space $(\mathcal{P}_k(K), \mathcal{P}_k(\partial K), [\mathcal{P}_{k-1}(K)]^2)$ in energy norm and L^2 norm, respectively. Further, semidiscrete error analysis have been extended for a fully discrete scheme. The fully discrete space-time finite element discretizations can be reinterpreted as the Crank-Nicolson discretization of the reformulation of the governing equation in the first-order system, as in Baker [7]. Both algorithms and error estimates are discussed for variable coefficient. It is worth to note that only H^1 norm error estimate has been discussed in [125]. The L^2 analysis with variable coefficients adds more challenge than one would imagine (see, Chapter 2), and this work fills a gap in existing literature. Several numerical experiments have been reported and described in order to establish the efficiency of the WG method in scientific computing. Our obtained results intent to enhance the numerical analysis technique of the general linear hyperbolic equations. To best of our knowledge, the WG finite element method for the general linear second order hyperbolic equation with variable coefficients has not been illustrated yet.

To conclude the introduction, we describe the lineup of this chapter. In Section 6.2, we recall the weak Galerkin discretization and concern to the error estimates of semi discrete WG-FEMs algorithm. Further, in Section 6.3, a Newmark second order scheme is proposed and optimal a priori error bounds in $L^\infty(H^1)$ norm and $L^\infty(L^2)$ norm are established, whereas, section 6.4 discusses several numerical examples which demonstrates the robustness of the WG-FEMs.

6.2 Error Analysis for the Semidiscrete Scheme

This section deals with the error analysis for the spatially discrete scheme. Optimal order of convergence in $L^\infty(L^2)$ norm and $L^\infty(H^1)$ norm are established.

Let $\mathcal{V}_h$ be the weak Galerkin finite element space defined by (3.2.1) based on the finite element discretization $\mathcal{T}_h$ of Ω as described in Chapter 1. For each $v_h = \{v_0, v_b\} \in \mathcal{V}_h$, recall that the discrete weak gradient $(\nabla_w v_h) \in [\mathcal{P}_{k-1}(K)]^2$ satisfies following equation

$$(\nabla_w v_h, \mathbf{q})_K = -\int_K v_0(\nabla \cdot \mathbf{q})dK + \int_{\partial K} v_b(\mathbf{q}\cdot\mathbf{n})ds \;\; \forall \mathbf{q} \in [\mathcal{P}_{k-1}(K)]^2. \tag{6.2.1}$$

Using the weak function defined by (1.4.3), we define a bilinear map $\mathcal{B} : \mathcal{V}_h \times \mathcal{V}_h \to \mathbb{R}$, which is being consider in this work as

$$\mathcal{B}(w_h, v_h) := \sum_{K\in\mathcal{T}_h} (\sigma w_h, v_h)_K \quad \forall\, w_h, v_h \in \mathcal{V}_h. \tag{6.2.2}$$

Next, for the WG approximation, we define bilinear maps $\mathcal{A}_{r,w} : \mathcal{V}_h \times \mathcal{V}_h \to \mathbb{R}$ $(r = 1, 2)$, involving discrete weak gradient operator ∇_w, by

$$\mathcal{A}_{1,w}(w_h, v_h) := \sum_{K\in\mathcal{T}_h} \left(\alpha\nabla_w w_h, \nabla_w v_h\right)_K + \mathcal{S}(w_h, v_h), \;\; \forall\, w_h, v_h \in \mathcal{V}_h \tag{6.2.3}$$

and

$$\mathcal{A}_{2,w}(w_h, v_h) := \sum_{K\in\mathcal{T}_h} \left(\beta\nabla_w w_h, \nabla_w v_h\right)_K + \mathcal{S}(w_h, v_h), \;\; \forall w_h, v_h \in \mathcal{V}_h, \tag{6.2.4}$$

where the stabilizer $\mathcal{S}(\cdot,\cdot)$ is defined as

$$\mathcal{S}(w_h, v_h) = \sum_{K\in\mathcal{T}_h} h_K^{-1}\langle w_0 - w_b, v_0 - v_b\rangle_{\partial K}. \tag{6.2.5}$$

For any $v_h \in \mathcal{V}_h$, the energy norm is defined as

$$|||v_h|||^2 = \sum_{K\in\mathcal{T}_h} \|\nabla_w v_h\|_K^2 + \sum_{K\in\mathcal{T}_h} h_K^{-1}\|v_0 - v_b\|_{\partial K}^2. \tag{6.2.6}$$

In (cf. [90], Lemma 7.2), it can easily proved that for $(r = 1, 2)$, there exist constants $\sigma_*, \sigma^* > 0$ such that

$$\sigma_*|||v_h|||^2 \le \mathcal{A}_{r,w}(v_h, v_h) \le \sigma^*|||v_h|||^2 \quad \forall v_h \in \mathcal{V}_h. \tag{6.2.7}$$

For each element $K \in \mathcal{T}_h$, denote by Q_0 the usual L^2 projection operator from $L^2(K)$ onto $\mathcal{P}_k(K)$ and by Q_b the L^2 projection from $L^2(e)$ onto $\mathcal{P}_k(e)$ for any $e \in \mathcal{F}_h$. We shall combine Q_0 with Q_b by writing $\mathcal{Q}_h = \{Q_0, Q_b\}$. In addition to $\mathcal{Q}_h$, let $\mathbb{Q}_h$ be another local L^2 projection from $[L^2(K)]^2$ onto $[\mathcal{P}_{k-1}(K)]^2$.

We recall following crucial approximation properties for local projections $\mathcal{Q}_h$ and $\mathbb{Q}_h$. For details, we refer to (cf. Lemma 4.1, [123]).

Lemma 6.2.1. *Let $\mathcal{T}_h$ be a finite element partition of Ω satisfying the shape regularity assumption as specified in (cf. [123]). Then, for $v \in H^{k+1}(\Omega)$, we have*

$$\sum_{K\in\mathcal{T}_h}\Big(\|v-Q_0v\|_K^2+h_K^2\|\nabla(v-Q_0v)\|_K^2\Big) \leq Ch^{2k+2}\|v\|_{k+1}^2,$$
$$\sum_{K\in\mathcal{T}_h}\Big(\|\nabla v-\mathbb{Q}_h(\nabla v)\|_K^2+h_K^2\|\nabla(\nabla v-\mathbb{Q}_h(\nabla v))\|_K^2\Big) \leq Ch^{2k}\|v\|_{k+1}^2.$$

A time-dependent weak function $v_h : [0,T] \to \mathcal{V}_h$ is written as $v_h(t) := \{v_0(t), v_b(t)\}$ and subsequently we define $v_h'(t) := \{v_0'(t), v_b'(t)\}$, where '$\prime$' denotes the time derivatives. For simplicity, we use $v_h = \{v_0, v_b\}$ for $v_h(t)$ and $v_h' = \{v_0', v_b'\}$ for $v_h'(t)$. Similar remarks hold for other higher order time derivatives.

The continuous-time weak Galerkin finite element approximation to (6.1.1)-(6.1.2) is defined as follows: Find $u_h = \{u_0, u_b\} : [0,T] \to \mathcal{V}_h^0$ satisfying

$$(u_h'', \phi_0) + \mathcal{A}_{1,w}(u_h, \phi_h) + \mathcal{A}_{2,w}(u_h', \phi_h) + \mathcal{B}(u_h', \phi_0) = (f, \phi_0), \tag{6.2.8}$$

for all $\phi_h = \{\phi_0, \phi_b\} \in \mathcal{V}_h^0$, where $u_h(0) = \mathcal{Q}_h u^0$ and $u_h'(0) = \mathcal{Q}_h v^0$ are approximations of the initial functions u^0 and v^0.

The following result deals with the existence and and uniqueness of the WG solution u_h. The basic technique is borrowed from [94].

Theorem 6.2.1. *For each $h \in (0, h_0]$, there exist a function $u_h \in C^2(0,T;\mathcal{V}_h^0)$ satisfying (6.2.8).*

Proof. For a given element $K \in \{\mathcal{T}_h\}_{0<h\leq h_0}$, let $\{\phi_{0,i} : \ i = 1, 2, \ldots, N_0\}$ be a set of basis functions for $\mathcal{P}_k(K)$ and $\{\phi_{b,i} : \ i = 1, 2, \ldots, N_b\}$ be a set of basis function for $\mathcal{P}_k(e)$. Then every $v_h = \{v_0, v_b\} \in \{\mathcal{V}_h^0\}_{0<h\leq h_0}$ can be written as

$$v_h|_K = \left\{ \sum_{i=1}^{N_0} d_{0,i}(t)\phi_{0,i}, \sum_{j=1}^{N_b} d_{b,j}(t)\phi_{b,j} \right\},$$

where $d_{0,i},\ d_{b,j} : (0,T] \to \mathbb{R}$ are the coefficient functions for $1 \leq i \leq N_0$ and $1 \leq j \leq N_b$. For $1 \leq i \leq N_0 + N_b$, we write $\hat{\phi}_{i,h} = \{\hat{\phi}_{0,i}, \hat{\phi}_{b,i}\}$ with

$$\hat{\phi}_{0,i} = \phi_{0,i} \ \text{ for } 1 \leq i \leq N_0 \quad \& \quad \hat{\phi}_{0,i} = 0 \ \text{ for } \ N_0 + 1 \leq i \leq N_0 + N_b,$$
$$\hat{\phi}_{b,i} = 0 \ \text{ for } \ 1 \leq i \leq N_0 \quad \& \quad \hat{\phi}_{b,i} = \phi_{b,i-N_0} \ \text{ for } \ N_0 + 1 \leq i \leq N_0 + N_b,$$

and similarly to capture the unknown coefficient functions, we define

$$\hat{d}_{i,h} = d_{0,i} \ \text{ for } 1 \leq i \leq N_0 \ \ \& \ \ \hat{d}_{i,h} = d_{b,i-N_0} \ \text{ for } N_0 + 1 \leq i \leq N_0 + N_b.$$

Then, we seek our semi-discrete solution $u_h = \{u_0, u_b\} \in \mathcal{V}_h^0$ such that

$$u_h|_K = \sum_{i=1}^{N_0+N_b} \hat{d}_{i,h}(t)\hat{\phi}_{i,h} = \left\{ \sum_{i=1}^{N_0+N_b} \hat{d}_{i,h}(t)\hat{\phi}_{0,i}, \sum_{j=1}^{N_0+N_b} \hat{d}_{j,h}(t)\hat{\phi}_{b,j} \right\}, \quad K \in \mathcal{T}_h.$$

Now, set $v_h = \phi_{j,h}, j = 1, 2, \ldots, N_0 + N_b$ in (6.2.8) to obtain

$$\begin{aligned}
&\left(\sum_{i=1}^{N_0+N_b} \hat{d}''_{i,h}(t)\hat{\phi}_{i,h}, \hat{\phi}_{j,h} \right) + \mathcal{A}_{1,w}\left(\sum_{i=1}^{N_0+N_b} \hat{d}_{i,h}(t)\hat{\phi}_{i,h}, \hat{\phi}_{j,h} \right) \\
&+\mathcal{A}_{2,w}\left(\sum_{i=1}^{N_0+N_b} \hat{d}'_{i,h}(t)\hat{\phi}_{i,h}, \hat{\phi}_{j,h} \right) + \mathcal{B}\Big(\sum_{i=1}^{N_0+N_b} \hat{d}'_{i,h}(t)\hat{\phi}_{i,h}, \hat{\phi}_{j,h} \Big) \\
&= (f, \hat{\phi}_{j,h}), \quad j = 1, \ldots, N_0 + N_b.
\end{aligned}$$

We can rearrange the above equation as

$$\begin{aligned}
&\sum_{i=1}^{N_0+N_b} \hat{d}''_{i,h}(t)\big(\hat{\phi}_{i,h}, \hat{\phi}_{j,h}\big) + \sum_{i=1}^{N_0+N_b} \hat{d}_{i,h}(t)\mathcal{A}_{1,w}\big(\hat{\phi}_{i,h}, \hat{\phi}_{j,h}\big) \\
&+ \sum_{i=1}^{N_0+N_b} \hat{d}'_{i,h}(t)\mathcal{A}_{2,w}\big(\hat{\phi}_{i,h}, \hat{\phi}_{j,h}\big) + \sum_{i=1}^{N_0+N_b} \hat{d}'_{i,h}(t)\mathcal{B}\big(\hat{\phi}_{i,h}, \hat{\phi}_{j,h}\big) \\
&= (f, \hat{\phi}_{j,h}), \quad j = 1, \ldots, N_0 + N_b.
\end{aligned}$$

On each element K, the local stiffness matrix $\mathcal{A}_{r,K}$ $(r = 1,\ 2)$ associated with the bilinear maps $\mathcal{A}_{r,w}(\cdot,\cdot)$ defined by (6.2.3)-(6.2.4) can thus be written as a block matrix

$$\mathcal{A}_{r,K} = \begin{bmatrix} \mathcal{A}_{0,0} & \mathcal{A}_{0,b} \\ \mathcal{A}_{b,0} & \mathcal{A}_{b,b} \end{bmatrix}, \tag{6.2.9}$$

where $\mathcal{A}_{0,0}$ is a $N_0 \times N_0$, $\mathcal{A}_{0,b}$ is a $N_0 \times N_b$, $\mathcal{A}_{b,0}$ is a $N_b \times N_0$, and $\mathcal{A}_{b,b}$ is a $N_b \times N_b$ matrices. More precisely, these matrices are given by

$$\mathcal{A}_{0,0} = [\mathcal{A}_{r,w}(\phi_{0,j}, \phi_{0,i})_K]_{i,j}, \quad \mathcal{A}_{0,b} = [\mathcal{A}_{r,w}(\phi_{0,j}, \phi_{b,i})_K]_{i,j}$$

$$\mathcal{A}_{b,0} = [\mathcal{A}_{r,w}(\phi_{b,j}, \phi_{0,i})_K]_{i,j}, \quad \mathcal{A}_{b,b} = [\mathcal{A}_{r,w}(\phi_{b,j}, \phi_{b,i})_K]_{i,j},$$

where i, j are the row and column indices, respectively.

We denote by

$$\hat{d}_{h,0} = [\hat{d}_{1,h}(0), \ldots, \hat{d}_{N_0+N_b,h}(0)]^T$$

and

$$\hat{d}_{h,1} = [\hat{d}'_{1,h}(0), \ldots, \hat{d}'_{N_0+N_b,h}(0)]^T,$$

the components of the given initial approximation $u_h(0)$ and $u_h'(0)$ respectively. Then, for our semi-discrete solution, we need to find unknown vector

$$\hat{d}_h(t) = [\hat{d}_{1,h}(t), \ldots, \hat{d}_{N_0+N_b,h}(t)]^T,\ t \in (0,T]$$

such that

$$\begin{cases} \mathcal{C}_K \hat{d}_h''(t) + \mathcal{A}_{1,K}\hat{d}_h(t) + \mathcal{A}_{2,K}\hat{d}_h'(t) + \mathcal{B}_K \hat{d}_h'(t) = F_K(t) \\ \hat{d}_h(0) = \hat{d}_{h,0}, \ \text{ and } \ \hat{d}_h'(0) = \hat{d}_{h,1}. \end{cases} \tag{6.2.10}$$

The coefficient matrices are given by

$$\mathcal{C}_K = [\mathcal{C}_{i,j}], \quad \mathcal{C}_{i,j} = (\hat{\phi}_{i,h}, \hat{\phi}_{j,h}),$$

$$\mathcal{B}_K = [\mathcal{B}_{i,j}], \quad \mathcal{B}_{i,j} = \mathcal{B}(\hat{\phi}_{i,h}, \hat{\phi}_{j,h}),$$

and the source term is given by

$$F_h = [F_1, \ldots, F_{N_0+N_b}], \quad F_j = (f, \hat{\phi}_{j,h}),$$

with $1 \le i, j \le N_0 + N_b$.

Note that the matrices and right-hand side vectors all are well-defined. Since

$$|(\hat{\phi}_{i,h}, \hat{\phi}_{j,h})| \le \|\hat{\phi}_{i,h}\|\|\hat{\phi}_{j,h}\|, \quad |\mathcal{B}(\hat{\phi}_{i,h}, \hat{\phi}_{j,h})| \le \|\hat{\phi}_{i,h}\|\|\hat{\phi}_{j,h}\|,$$
$$|\mathcal{A}_{r,k}(\hat{\phi}_{i,h}, \hat{\phi}_{j,h})| \le C\|\hat{\phi}_{i,h}\|_{1,h}\|\hat{\phi}_{j,h}\|_{1,h} \ \text{ and } \ |(f, \hat{\phi}_{j,h})| \le \|f\|\|\hat{\phi}_{j,h}\|,$$

for all $t \in J = (0,T]$ and $(r = 1, 2)$.

Furthermore, for any $v \in \mathbb{R}^{N_0+N_b} \setminus \{\mathbf{0}\}$, we have

$$v^T C_K v = (\hat{v}, \hat{v})_K > 0, \ \ \hat{v} = \sum_{i=1}^{N_0+N_b} v_i \hat{\phi}_{0,i}.$$

Hence, the matrix C_K is invertible for all $t \in J$ and the equation (6.2.10) can be restated as:

$$\begin{cases} \hat{d}_h''(t) + \mathcal{C}_K^{-1}\mathcal{A}_{1,K}\hat{d}_h(t) + \mathcal{C}_K^{-1}\mathcal{A}_{2,K}\hat{d}_h'(t) + \mathcal{C}_K^{-1}\mathcal{B}_K\hat{d}_h'(t) = \mathcal{C}_K^{-1}F_K(t) \\ \hat{d}_h(0) = \hat{d}_{h,0}, \ \text{ and } \ \hat{d}_h'(0) = \hat{d}_{h,1}. \end{cases}$$

Now, the existence of the solution $u_h \in C^2(0,T;\mathcal{V}_h^0)$ follows from the standard ODE theory. This complete the rest of the proof. □

As a standard procedure in finite element method, we split our semi-discrete error $u - u_h$ using $\mathcal{Q}_h$ projection as an intermediate operator defined as

$$u - u_h := u - \mathcal{Q}_h u + \mathcal{Q}_h u - u_h.$$

For our convenience, we define

$$e_h = \{e_0, e_b\} = u_h - \mathcal{Q}_h u.$$

Error e_h is characterized in the following result, which is key for our convergence analysis.

Lemma 6.2.2. *For all $\phi_h = \{\phi_0, \phi_b\} \in \mathcal{V}_h^0$, we have*

$$\begin{aligned}
&(e_h'', \phi_0) + \mathcal{A}_{1,w}(e_h, \phi_h) + \mathcal{A}_{2,w}(e_h', \phi_h) + \mathcal{B}(e_h', \phi_0) \\
&= \ell_1(u, \phi_h) + \ell_2(u, \phi_h) + \mathcal{B}(\mathcal{Q}_h u' - u', \phi_0) + \ell_3(u', \phi_h) + \ell_4(u', \phi_h) \\
&\quad + \mathcal{S}(\mathcal{Q}_h u, \phi_h) + \mathcal{S}(\mathcal{Q}_h u', \phi_h),
\end{aligned} \tag{6.2.11}$$

where bilinear forms $\ell_i(\cdot,\cdot)$, $i = 1, 2, 3, 4$ are given by

$$\begin{aligned}
\ell_1(u, \phi_h) &= \sum_{K \in \mathcal{T}_h} \big\langle (\alpha \nabla u - \mathbb{Q}(\alpha \nabla u)) \cdot \mathbf{n}, \phi_0 - \phi_b \big\rangle_{\partial K}, \\
\ell_2(u, \phi_h) &= \sum_{K \in \mathcal{T}_h} (\alpha \mathbb{Q}_h(\nabla u) - \mathbb{Q}_h(\alpha \nabla u), \nabla_w \phi_h)_K, \\
\ell_3(u, \phi_h) &= \sum_{K \in \mathcal{T}_h} \big\langle (\beta \nabla u - \mathbb{Q}(\beta \nabla u)) \cdot \mathbf{n}, \phi_0 - \phi_b \big\rangle_{\partial K}, \\
\ell_4(u, \phi_h) &= \sum_{K \in \mathcal{T}_h} (\beta \mathbb{Q}_h(\nabla u) - \mathbb{Q}_h(\beta \nabla u), \nabla_w \phi_h)_K.
\end{aligned}$$

Proof. On each element $K \in \mathcal{T}_h$, for $\phi_h = \{\phi_0, \phi_b\} \in \mathcal{V}_h^0$, we test equation (6.1.1) against ϕ_0 to arrive at

$$\begin{aligned}
(f, \phi_0) &= (u'', \phi_0) - \sum_{K \in \mathcal{T}_h} (\nabla \cdot (\alpha \nabla u), \phi_0)_K - \sum_{K \in \mathcal{T}_h} (\nabla \cdot (\beta \nabla u'), \phi_0)_K + \mathcal{B}(u', \phi_0) \\
&= (u'', \phi_0) + \sum_{K \in \mathcal{T}_h} (\alpha \nabla u, \nabla \phi_0)_K - \sum_{K \in \mathcal{T}_h} \langle \alpha \nabla u \cdot \mathbf{n}, \phi_0 \rangle_{\partial K} \\
&\quad + \sum_{K \in \mathcal{T}_h} (\beta \nabla u', \nabla \phi_0)_K - \sum_{K \in \mathcal{T}_h} \langle \beta \nabla u \cdot \mathbf{n}, \phi_0 \rangle_{\partial K} + \mathcal{B}(u', \phi_0) \\
&= (u'', \phi_0) + \sum_{K \in \mathcal{T}_h} (\alpha \nabla u, \nabla \phi_0)_K - \sum_{K \in \mathcal{T}_h} \langle \alpha \nabla u \cdot \mathbf{n}, \phi_0 - \phi_b \rangle_{\partial K} \\
&\quad + \sum_{K \in \mathcal{T}_h} (\beta \nabla u', \nabla \phi_0)_K - \sum_{K \in \mathcal{T}_h} \langle \beta \nabla u \cdot \mathbf{n}, \phi_0 - \phi_b \rangle_{\partial K} + \mathcal{B}(u', \phi_0).
\end{aligned} \tag{6.2.12}$$

Here, we have used the divergence theorem and the fact that

$$\sum_{K\in\mathcal{T}_h}\langle\alpha\nabla u\cdot\mathbf{n},\phi_b\rangle_{\partial K}=0 \quad\text{and}\quad \sum_{K\in\mathcal{T}_h}\langle\beta\nabla u\cdot\mathbf{n},\phi_b\rangle_{\partial K}=0.$$

Then integration by part together with definition (1.4.5) for weak gradient and L^2 projection $\mathbb{Q}_h$ yields

$$\begin{aligned}(\mathbb{Q}_h(\alpha\nabla u),\nabla_w\phi_h)_K &= -(\phi_0,\nabla\cdot(\mathbb{Q}_h(\alpha\nabla u)))_K+\langle\phi_b,\mathbb{Q}_h(\alpha\nabla u)\cdot\mathbf{n}\rangle_{\partial K}\\ &= (\nabla\phi_0,\mathbb{Q}_h(\alpha\nabla u))_K-\langle\phi_0-\phi_b,\mathbb{Q}_h(\alpha\nabla u)\cdot\mathbf{n}\rangle_{\partial K}\\ &= (\nabla\phi_0,\alpha\nabla u)_K-\langle\phi_0-\phi_b,\mathbb{Q}_h(\alpha\nabla u)\cdot\mathbf{n}\rangle_{\partial K}. \qquad (6.2.13)\end{aligned}$$

As a consequence of (6.2.13), we get

$$(\mathbb{Q}_h(\beta\nabla u'),\nabla_w\phi_h)_K=(\nabla\phi_0,\beta\nabla u')_K-\langle\phi_0-\phi_b,\mathbb{Q}_h(\beta\nabla u')\cdot\mathbf{n}\rangle_{\partial K}. \qquad (6.2.14)$$

Combining (6.2.12), (6.2.13) and (6.2.14), we have

$$\begin{aligned}(f,v_0) &= (u'',\phi_0)+\sum_{K\in\mathcal{T}_h}(\mathbb{Q}_h(\alpha\nabla u),\nabla_w\phi_h)_K+\mathcal{B}(u',\phi_0)\\ &\quad+\sum_{K\in\mathcal{T}_h}(\mathbb{Q}_h(\beta\nabla u'),\nabla_w\phi_h)_K+\sum_{K\in\mathcal{T}_h}\langle\phi_0-\phi_b,(\mathbb{Q}_h(\alpha\nabla u)-\alpha\nabla u)\cdot\mathbf{n}\rangle_{\partial K}\\ &\quad+\sum_{K\in\mathcal{T}_h}\langle\phi_0-\phi_b,(\mathbb{Q}_h(\beta\nabla u')-\beta\nabla u')\cdot\mathbf{n}\rangle_{\partial K}\\ &= (\mathcal{Q}_hu'',\phi_0)+\sum_{K\in\mathcal{T}_h}(\alpha\nabla_w\mathcal{Q}_hu,\nabla_w\phi_h)_K+\mathcal{B}(\mathcal{Q}_hu',\phi_0)\\ &\quad-\mathcal{B}(\mathcal{Q}_hu'-u',\phi_0)-\ell_1(u,\phi_h)+\sum_{K\in\mathcal{T}_h}(\beta\nabla_w\mathcal{Q}_hu',\nabla_w\phi_h)_K\\ &\quad-\ell_2(u,\phi_h)-\ell_3(u',\phi_h)-\ell_4(u',\phi_h). \qquad (6.2.15)\end{aligned}$$

Adding $\mathcal{S}(\mathcal{Q}_hu,\phi_h)$ and $\mathcal{S}(\mathcal{Q}_hu',\phi_h)$ to both sides of the above equation leads to

$$\begin{aligned}&(\mathcal{Q}_hu'',\phi_0)+\mathcal{A}_{1,w}(\mathcal{Q}_hu,\phi_h)+\mathcal{A}_{2,w}(\mathcal{Q}_hu',\phi_h)+\mathcal{B}(\mathcal{Q}_hu',\phi_0)\\ &=(f,\phi_0)+\ell_1(u,\phi_h)+\ell_2(u,\phi_h)+\ell_3(u',\phi_h)+\ell_4(u',\phi_h)\\ &\quad+\mathcal{B}(\mathcal{Q}_hu'-u',\phi_0)+\mathcal{S}(\mathcal{Q}_hu,\phi_h)+\mathcal{S}(\mathcal{Q}_hu',\phi_h). \qquad (6.2.16)\end{aligned}$$

Subtracting (6.2.16) from (6.2.8) leads us to desire result. □

We recall following crucial estimates for the bilinear maps ℓ_i, $i=1,2,3,4$ and stabilizer term $\mathcal{S}(\cdot,\cdot)$ from earlier work (cf. [34]).

Lemma 6.2.3. *Assume that $\mathcal{T}_h$ is shape regular discretization of computational domain Ω. Then, for $u \in H^{k+1}(\Omega)$ and $\phi_h \in \mathcal{V}_h^0$, we have*

$$|\ell_1(u,\phi_h)| \leq C(\|\alpha\|_{k,\infty})h^k\|u\|_{k+1}|||\phi_h|||, \tag{6.2.17}$$
$$|\ell_2(u,\phi_h)| \leq C(\|\alpha\|_{k,\infty})h^{k+1}\|u\|_{k+1}|||\phi_h|||, \tag{6.2.18}$$
$$|\ell_3(u,\phi_h)| \leq C(\|\beta\|_{k,\infty})h^k\|u\|_{k+1}|||\phi_h|||, \tag{6.2.19}$$
$$|\ell_4(u,\phi_h)| \leq C(\|\beta\|_{k,\infty})h^{k+1}\|u\|_{k+1}|||\phi_h|||, \tag{6.2.20}$$
$$|\mathcal{S}(Q_hu,\phi_h)| \leq Ch^k\|u\|_{k+1}|||\phi_h|||, \tag{6.2.21}$$

where $C(\|\alpha\|_{k,\infty})$ and $C(\|\beta\|_{k,\infty})$ are a positive constant depending on $\|\cdot\|_{k,\infty}$ the element-wise $W^{k,\infty}$ norm of the coefficient matrix α and β.

By letting $v_h = e_h'$ in (6.2.11), we have

$$\frac{1}{2}\frac{d}{dt}\|e_0'\|^2 + \frac{1}{2}\frac{d}{dt}|||e_h|||^2 + |||e_h'|||^2 + \|e_0'\|^2 = \ell_1(u,e_h') + \ell_2(u,e_h')$$
$$+\mathcal{B}(\mathcal{Q}_hu' - u', e_h') + \ell_3(u',e_h') + \ell_4(u',e_h') + \mathcal{S}(\mathcal{Q}_hu,e_h') + \mathcal{S}(\mathcal{Q}_hu',e_h').$$

By integration over the time interval $[0,t]$, we get

$$\frac{1}{2}\|e_0'\|^2 + \int_0^t |||e_h'|||^2 ds + \frac{1}{2}|||e_h|||^2 + \int_0^t \|e_0'\|^2 d \leq \frac{1}{2}\|e_0'(0)\|^2 + \frac{1}{2}|||e_h(0)|||^2 s$$
$$+\int_0^t |\ell_1(u,e')|ds + \int_0^t |\ell_2(u,e')|ds + \int_0^t |\ell_3(u',e_h')|ds + \int_0^t |\ell_4(u',e_h')|ds$$
$$+\int_0^t |\mathcal{B}(\mathcal{Q}_hu' - u', e_0')|ds + \int_0^t |\mathcal{S}(Q_hu,e_h')|ds + \int_0^t |\mathcal{S}(Q_hu',e_h')ds.$$

It then follow from Lemma 6.2.1 and the estimates (6.2.17)-(6.2.21) together with Young's inequality for some appropriate $\nu > 0$ leads to

$$\frac{1}{2}\|e_0'\|^2 + \int_0^t |||e_h'|||^2 ds + |||e_h|||^2 + \int_0^t \|e_0'\|^2 ds \leq C_\nu \int_0^t |||e_h'|||^2 ds$$
$$+ C_\nu \int_0^t \|e_0'\|^2 ds + C(\nu)h^{2k}\int_0^t \Big(\|u\|_{k+1}^2 + \|u'\|_{k+1}^2\Big)ds.$$

Here, we have used the fact that $e_h(0) = u_h(0) - \mathcal{Q}_hu^0 = 0$. As a consequence, we have $e_h'(0) = 0$.

We can rearrange the above equation as

$$|||e_h|||^2 \leq Ch^{2k}\int_0^t \Big(\|u\|_{k+1}^2 + \|u'\|_{k+1}^2\Big)ds. \tag{6.2.22}$$

Finally, Lemma (6.2.1) together with the estimate (6.2.22) leads us to the following point wise $L^\infty(0,T;H^1(\Omega))$ convergence result.

Theorem 6.2.2. *Let $u \in H^1(0,T;H^{k+1}(\Omega))$ be the solution of (6.1.1)-(6.1.2) and $u_h \in H^2(0,T;\mathcal{V}_h^0)$ be the solution of (6.2.8). Then, we have*

$$\|u-u_h\|_{1,h} \le Ch^k\Big(\int_0^T \Big\{\|u\|_{k+1}^2 + \|u'\|_{k+1}^2\Big\}ds\Big)^{\frac{1}{2}}.$$

To get an optimal order of error estimate in L^2 norm, we define a non-standard projection operator, which is crucial for our later error analysis. For $z \in H^1(0,T;\mathcal{X})$, where $\mathcal{X} = H_0^1(\Omega)\cap H^2(\Omega)$, define $\mathcal{E}_h : \mathcal{X} \to \mathcal{V}_h^0$ by

$$\mathcal{A}_{1,w}(\mathcal{E}_h z,\phi_h) + \mathcal{A}_{2,w}((\mathcal{E}_h z)',\phi_h) = (f_z,\phi_0)\ \ \forall \phi_h = \{\phi_0,\phi_b\} \in \mathcal{V}_h^0, \tag{6.2.23}$$

with $(\mathcal{E}_h z)(0) = \mathcal{Q}_h z^0 \in \mathcal{V}_h^0$ and

$$f_z = -\nabla\cdot\big((\alpha\nabla z) + (\beta\nabla z')\big).$$

Note that $\mathcal{E}_h z$ can be recognized as the WG finite element approximation solution applied to following IBVP

$$-\nabla\cdot(\alpha\nabla z) - \nabla\cdot(\beta\nabla z') = f_z \quad \text{in } \Omega\times(0,T], \tag{6.2.24}$$

with boundary condition $z(x,t) = 0$ on $\partial\Omega\times(0,T]$ and initial condition $z(x,0) = z^0$ in Ω.

Remark 6.2.1. *Note that error bounds for the projection operator $\mathcal{E}_h$ satisfying equation (6.2.23) with constant coefficients have been established using WG method in H^1 norm and L^2 norm, (see, cf. [37]). A limitation of this article is the use of constant coefficients which do not occur in some applications. Here, we cannot import those results directly. We need to bound the error $\zeta_u := \mathcal{Q}_h u - \mathcal{E}_h u$ in both energy norm and L^2 norm with variable coefficients, which is illustrated in the next lemma.*

Lemma 6.2.4. *Let $u \in H^1(0,T;H^{k+1}(\Omega))$ be the solution of (6.1.1)-(6.1.2). Let $\mathcal{E}_h u \in H^1(0,T;\mathcal{V}_h^0)$ be the WG solution of the equation (6.2.24). Then, there exists a constant C such that*

$$|||\mathcal{Q}_h u - \mathcal{E}_h u||| \le Ch^k \|u\|_{H^1(0,T;H^{k+1}(\Omega))}, \tag{6.2.25}$$

$$\|\mathcal{Q}_h u - \mathcal{E}_h u\| \le Ch^{k+1}\|u\|_{H^1(0,T;H^{k+1}(\Omega))}. \tag{6.2.26}$$

Proof. Following the analysis used to derive (6.2.16), we obtain

$$\begin{aligned}\mathcal{A}_{1,w}(\mathcal{Q}_h u,\phi_h) + \mathcal{A}_{2,w}((\mathcal{Q}_h u)_t,\phi_h) &= (f_u,\phi_0) + \ell_1(u,\phi_h) + \ell_2(u,\phi_h)\\ &\quad + \mathcal{S}(\mathcal{Q}_h u,\phi_h) + \mathcal{S}(\mathcal{Q}_h u',\phi_h) + \ell_3(u',\phi_h) + \ell_4(u',\phi_h),\end{aligned} \tag{6.2.27}$$

for all $\phi_h = \{\phi_0,\phi_b\} \in \mathcal{V}_h^0$.

Now, subtracting (6.2.23) from the above equation, we arrive at following error relation for ζ_u

$$\begin{aligned}\mathcal{A}_{1,w}(\zeta_u(t),\phi_h)+\mathcal{A}_{2,w}(\zeta_u'(t),\phi_h) &= \ell_1(u,\phi_h)+\ell_2(u,\phi_h)+\ell_3(u',\phi_h)\\ &+\mathcal{S}(\mathcal{Q}_h u,\phi_h)+\mathcal{S}(\mathcal{Q}_h u',\phi_h)+\ell_4(u',\phi_h),\phi_h),\ t\in(0,T]. \end{aligned}\tag{6.2.28}$$

Finally, setting $\phi_h=\zeta_u$ in (6.2.28) and then standard analysis leads to following estimate

$$\begin{aligned}|||\zeta_u(t)|||^2 &\leq C\big(|||\zeta_u(0)|||^2+h^{2k}\|u\|^2_{H^1(0,t;H^{k+1}(\Omega))}\big)\\ &\leq Ch^{2k}\|u\|^2_{H^1(0,t;H^{k+1}(\Omega))}.\end{aligned}\tag{6.2.29}$$

Here, we have used the fact that $\zeta_u(0)=0$.

For the estimate (6.2.26), we define a dual problem that seeks a solution $w\in H^1(0,T;H^2(\Omega))$ such that

$$-\nabla\cdot\big((\alpha\nabla w)-(\beta\nabla w')\big)=\zeta_u \ \text{ in } \ \Omega \tag{6.2.30}$$

and $w(\tau)=0$ for some $\tau\in J=(0,T]$. Assume that there exists a unique solution $w\in H^1(J;H^2(\Omega))$ such that (cf. [3])

$$\|w\|_{H^1(J;H^2(\Omega))}\leq C\|\zeta_u\|_{L^2(J;L^2(\Omega))}. \tag{6.2.31}$$

Multiply the equation (6.2.30) by ζ_u', we get

$$(\zeta_u,\zeta_u')=\big(-\nabla\cdot\big((\alpha\nabla w)-(\beta\nabla w')\big),\zeta_u'\big). \tag{6.2.32}$$

Next, arguing as in (6.2.15), we obtain

$$\begin{aligned}(\zeta_u,\zeta_u') &= \sum_{K\in\mathcal{T}_h}\Big\{(\alpha\nabla_w\mathcal{Q}_h w,\nabla_w\zeta_u')_K-(\beta\nabla_w\mathcal{Q}_h w',\nabla_w\zeta_u')_K\Big\}\\ &\quad -\ell_1(w,\zeta_u')-\ell_2(w,\zeta_u')+\ell_3(w',\zeta_u')+\ell_4(w',\zeta_u'),\end{aligned}\tag{6.2.33}$$

where the bilinear maps $\ell_i(\cdot,\cdot)$ are as defined in Lemma 6.2.2.

Now, integrate equation (6.2.33) in $[0,\tau]$ to obtain

$$\begin{aligned}&\frac{1}{2}\|\zeta_u(\tau)\|^2=\sum_{K\in\mathcal{T}_h}\int_0^\tau\big\{(\alpha\nabla_w\mathcal{Q}_h w,\nabla_w\zeta_u')_K-(\beta\nabla_w\mathcal{Q}_h w',\nabla_w\zeta_u')_K\big\}ds\\ &-\int_0^\tau\ell_1(w,\zeta_u')ds+\int_0^\tau\ell_3(w',\zeta_u')ds-\int_0^\tau\ell_2(w,\zeta_u')ds+\int_0^\tau\ell_4(w',\zeta_u')ds\\ &=\sum_{K\in\mathcal{T}_h}\int_0^\tau\big\{(-\alpha\nabla_w\mathcal{Q}_h w',\nabla_w\zeta_u)_K-(\beta\nabla_w\mathcal{Q}_h w',\nabla_w\zeta_u')_K\big\}ds\\ &+\sum_{K\in\mathcal{T}_h}(\alpha\nabla_w\mathcal{Q}_h w,\nabla_w\zeta_u)_K(0)-\int_0^\tau\ell_1(w,\zeta_u')ds+\int_0^\tau\ell_3(w',\zeta_u')ds.\\ &-\int_0^\tau\ell_2(w,\zeta_u')ds+\int_0^\tau\ell_4(w',\zeta_u')ds.\end{aligned}$$

In the above, we have applied the facts that $(\nabla_w v_h(t))' = \nabla_w v_h'(t)$ and $\nabla_w v_h(t)|_{t=0} = \nabla_w v_h(0)$ for $v_h \in \mathcal{V}_h^0$, and $\zeta_u(0) = 0$. Further, using bilinear maps (6.2.3)-(6.2.4), we can rearrange the above equation as follows

$$\begin{aligned}\frac{1}{2}\|\zeta_u(\tau)\|^2 &= \int_0^\tau \{-\mathcal{A}_{1,w}(\zeta_u, \mathcal{Q}_h w') - \mathcal{A}_{2,w}(\zeta_u', \mathcal{Q}_h w')\}ds + \int_0^\tau \mathcal{S}(\zeta_u, \mathcal{Q}_h w')ds \\ &+ \int_0^\tau \mathcal{S}(\zeta_u', \mathcal{Q}_h w')ds - \int_0^\tau \ell_1(w, \zeta_u')ds + \int_0^\tau \ell_3(w', \zeta_u')ds - \int_0^\tau \ell_2(w, \zeta_u')ds \\ &+ \int_0^\tau \ell_4(w', \zeta_u')ds.\end{aligned}$$

Next, using the error equation (6.2.28), we obtain

$$\begin{aligned}\frac{1}{2}\|\zeta_u(\tau)\|^2 &= -\int_0^\tau \ell_1(u, \mathcal{Q}_h w')ds - \int_0^\tau \ell_3(u', \mathcal{Q}_h w')ds - \int_0^\tau \ell_2(u, \mathcal{Q}_h w')ds \\ &- \int_0^\tau \ell_4(u', \mathcal{Q}_h w')ds - \int_0^\tau \mathcal{S}(\mathcal{Q}_h u, \mathcal{Q}_h w')ds - \int_0^\tau \mathcal{S}(\mathcal{Q}_h u', \mathcal{Q}_h w')ds \\ &+ \int_0^\tau \mathcal{S}(\zeta_u, \mathcal{Q}_h w')ds + \int_0^\tau \mathcal{S}(\zeta_u', \mathcal{Q}_h w')ds - \int_0^\tau \ell_1(w, \zeta_u')ds \\ &+ \int_0^\tau \ell_3(w', \zeta_u')ds - \int_0^\tau \ell_2(w, \zeta_u')ds + \int_0^\tau \ell_4(w', \zeta_u')ds. \qquad (6.2.34)\end{aligned}$$

Now, we apply trace inequality (1.4.19) and Lemma 6.2.1 to obtain

$$\begin{aligned}|\ell_1(u, \mathcal{Q}_h w')| &= \Big| \sum_{K\in\mathcal{T}_h} \langle (\alpha\nabla u - \mathbb{Q}_h(\alpha\nabla u)) \cdot \mathbf{n}, Q_0 w' - Q_b w' \rangle_{\partial K} \Big| \\ &\le \sum_{K\in\mathcal{T}_h} \|\alpha\nabla u - \mathbb{Q}_h(\alpha\nabla u)\|_{\partial K} \|Q_0 w' - Q_b w'\|_{\partial K} \\ &\le C\Big(\sum_{K\in\mathcal{T}_h} h_K \|\alpha\nabla u - \mathbb{Q}_h(\alpha\nabla u)\|_{\partial K}^2 \Big)^{\frac{1}{2}} \times \left(\sum_{K\in\mathcal{T}_h} h_K^{-1} \|Q_0 w' - Q_b w'\|_{\partial K}^2 \right)^{\frac{1}{2}} \\ &\le C\left(\sum_{K\in\mathcal{T}_h} \left(\|\alpha\nabla u - \mathbb{Q}_h(\alpha\nabla u)\|_K^2 + h_K^2 \|\nabla(\alpha\nabla u - \mathbb{Q}_h(\alpha\nabla u))\|_K^2 \right) \right)^{\frac{1}{2}} \\ &\qquad \times \left(\sum_{K\in\mathcal{T}_h} h_K^{-1} \|Q_0 w' - Q_b w'\|_{\partial K}^2 \right)^{\frac{1}{2}} \\ &\le C(\|\alpha\|_{k,\infty}) h^k \|u\|_{k+1} \times \left(\sum_{K\in\mathcal{T}_h} h_K^{-2} \|Q_0 w' - w'\|_K^2 + \|\nabla(Q_0 w' - w')\|_K^2 \right)^{1/2} \\ &\le C(\|\alpha\|_{k,\infty}) h^k \|u\|_{k+1} h \|w'\|_2.\end{aligned}$$

Using the definition of $\mathbb{Q}_h$ operator and Lemma 6.2.1, we obtain

$$\begin{aligned}
|\ell_2(u, \mathcal{Q}_h w')| &= \Big| \sum_{K\in\mathcal{T}_h} (\alpha \mathbb{Q}_h(\nabla u) - \alpha\nabla u, \nabla_w \mathcal{Q}_h w')_K \Big| \\
&= \Big| \sum_{K\in\mathcal{T}_h} (\mathbb{Q}_h(\nabla u) - \nabla u, (\alpha - \bar{\alpha})\nabla_w \mathcal{Q}_h w')_K \Big| \\
&\leq \sum_{K\in\mathcal{T}_h} \Big| (\mathbb{Q}_h(\nabla u) - \nabla u, (\alpha - \bar{\alpha})\nabla_w \mathcal{Q}_h w')_K \Big| \\
&\leq Ch\|\alpha\|_{1,\infty} \sum_{K\in\mathcal{T}_h} \Big| (\mathbb{Q}_h(\nabla u) - \nabla u, \nabla_w \mathcal{Q}_h w')_K \Big| \\
&\leq C(\|\alpha\|_{k,\infty}) h^{k+1} \|u\|_{k+1} \|w'\|_2.
\end{aligned}$$

Here, $\bar{\alpha}$ is the average of α on each element $K \in \mathcal{T}_h$.

Similar arguments yield

$$\begin{aligned}
|\ell_3(u', \mathcal{Q}_h w')| &\leq C(\|\beta\|_{k,\infty}) h^{k+1} \|u'\|_{k+1} \|w'\|_2. \\
|\ell_4(u', \mathcal{Q}_h w')| &\leq C(\|\beta\|_{k,\infty}) h^{k+1} \|u'\|_{k+1} \|w'\|_2. \\
|\mathcal{S}(\mathcal{Q}_h u, \mathcal{Q}_h w')| &\leq Ch^{k+1} \|u\|_{k+1} \|w'\|_2. \\
|\mathcal{S}(\mathcal{Q}_h u', \mathcal{Q}_h w')| &\leq Ch^{k+1} \|u'\|_{k+1} \|w'\|_2,
\end{aligned}$$

and hence,

$$\begin{aligned}
&\int_0^\tau \ell_1(u, \mathcal{Q}_h w')ds + \int_0^\tau \ell_3(u', \mathcal{Q}_h w')ds + \int_0^\tau \ell_2(u, \mathcal{Q}_h w')ds \\
&+ \int_0^\tau \ell_4(u', \mathcal{Q}_h w')ds + \int_0^\tau \mathcal{S}(\mathcal{Q}_h u, \mathcal{Q}_h w')ds + \int_0^\tau \mathcal{S}(\mathcal{Q}_h u', \mathcal{Q}_h w')ds \\
&\leq Ch^{k+1} \|u\|_{H^1(H^{k+1})} \|w\|_{H^1(H^2)} \leq Ch^{k+1} \|u\|_{H^1(H^{k+1})} \|\zeta_u\|_{L^2(L^2)}. \qquad (6.2.35)
\end{aligned}$$

In the last inequality, we have used the a priori estimate (6.2.31). For the other last six terms appearing in equation (6.2.34), we use Lemma 6.2.3 to have

$$|\ell_1(w, \zeta_u')| + |\ell_2(w', \zeta_u')| \leq C(\|\alpha\|_{1,\infty}) h (\|w\|_2 + \|w'\|_2) |||\zeta_u'|||,$$

which together with estimate (6.2.25) yields

$$\begin{aligned}
\int_0^\tau \ell_1(w, \zeta_u')ds + \int_0^\tau \ell_2(w', \zeta_u')ds \leq C(\|\alpha\|_{k+1,\infty}) h^{k+1} \Big(&\|u\|_{H^1(H^{k+1})} \\
&\times \|\zeta_u\|_{L^2(L^2)} \Big). \qquad (6.2.36)
\end{aligned}$$

As a consequence, we get

$$\begin{aligned}
\int_0^\tau \ell_3(w, \zeta_u')ds + \int_0^\tau \ell_4(w', \zeta_u')ds \leq C(\|\beta\|_{k+1,\infty}) h^{k+1} \Big(&\|u\|_{H^1(H^{k+1})} \\
&\times \|\zeta_u\|_{L^2(L^2)} \Big), \qquad (6.2.37)
\end{aligned}$$

and

$$\int_0^\tau \mathcal{S}(\mathcal{Q}_h w, \zeta_u')ds + \int_0^\tau \mathcal{S}(\mathcal{Q}_h w', \zeta_u')ds \leq Ch^{k+1}\|u\|_{H^1(H^{k+1})}\|\zeta_u\|_{L^2(L^2)}. \quad (6.2.38)$$

Combining the estimates (6.2.34)-(6.2.38) and further using Young's inequality, we obtain

$$\frac{1}{2}\|\zeta_u(\tau)\|^2 \leq C_\nu\|\zeta_u\|^2_{L^2(L^2)} + C(\nu)h^{2(k+1)}\|u\|^2_{H^1(H^{k+1})}, \quad (6.2.39)$$

for some $\nu > 0$.

Now, we select τ such that $\|\zeta_u(\tau)\| = \max_{t\in[0,T]}\|\zeta_u(t)\|$ so that $\|\zeta_u\|^2_{L^2(L^2)} \leq T\|\zeta_u(\tau)\|^2$ and subsequently estimate (6.2.39) reduces to

$$\frac{1}{2}\|\zeta_u(\tau)\|^2 \leq C_\nu T\|\zeta_u(\tau)\|^2 + C(\nu)h^{2(k+1)}\|u\|^2_{H^1(H^{k+1})}. \quad (6.2.40)$$

Thus, for suitable $\nu > 0$, we obtain

$$\|\zeta_u(\tau)\|^2 \leq Ch^{2(k+1)}\|u\|^2_{H^1(H^{k+1})}. \quad (6.2.41)$$

This completes the rest of the proof. □

Remark 6.2.2. *A modification in the dual problem that seeks a solution $w \in H^1(J; H^2(\Omega))$ such that*

$$-\nabla\cdot\big((\alpha\nabla w) - (\beta\nabla w')\big) = \zeta_u' \ \text{ in } \ \Omega,$$

with $w(T) = 0$ leads to following estimate

$$\begin{aligned}\|\zeta_u'\|^2_{L^2(0,T;L^2(\Omega))} &= \int_0^T \|(\mathcal{Q}_h u - \mathcal{E}_h u)'\|^2 dt \\ &\leq Ch^{2(k+1)}\|u\|^2_{H^1(0,T;H^{k+1}(\Omega))}. \end{aligned} \quad (6.2.42)$$

We omit the details.

Next, to obtained optimal error estimate in L^2 norm, we split our error $e_h = u_h - \mathcal{Q}_h u$ into two standard components ζ and θ using following relation

$$e_h(t) = u_h(t) - \mathcal{Q}_h u(t) = \theta(t) + \zeta_u(t),$$

where $\theta = u_h - \mathcal{E}_h u$. From Lemma 6.2.4, we already have bound for $\zeta(t)$. We only need to bound $\theta(t)$.

Now, using the definition (6.2.23) for the projection operator $\mathcal{E}_h$ and semidiscrete approximate (6.2.8), we arrive at

$$\begin{aligned}
&(\theta'', \phi_0) + \mathcal{A}_{1,w}(\theta, \phi_h) + \mathcal{A}_{2,w}(\theta', \phi_h) + \mathcal{B}(\theta', \phi_0) \\
&= \Big(\frac{\partial^2 u_h}{\partial t^2}, \phi_0\Big) + \mathcal{A}_{1,w}(u_h, \phi_h) + \mathcal{A}_{2,w}(u_h', \phi_h) + \mathcal{B}(u_h', \phi_0) \\
&\quad -\Big(\frac{\partial^2 \mathcal{E}_h u}{\partial t^2}, \phi_0\Big) - \mathcal{A}_{1,w}(\mathcal{E}_h u, \phi_h) - \mathcal{A}_{2,w}((\mathcal{E}_h u)', \phi_h) - \mathcal{B}((\mathcal{E}_h u)', \phi_0) \\
&= (f, \phi_0) - \Big(\frac{\partial^2 \mathcal{E}_h u}{\partial t^2}, \phi_0\Big) - (-\nabla \cdot (\alpha \nabla u), \phi_h) - (-\nabla \cdot (\beta \nabla u'), \phi_h) \\
&\quad -\mathcal{B}((\mathcal{E}_h u)', \phi_0).
\end{aligned}$$

Further, equation (6.1.1) and L^2 projection Q_h yields following important identity

$$\begin{aligned}
&(\theta'', \phi_0) + \mathcal{A}_{1,w}(\theta, \phi_h) + \mathcal{A}_{2,w}(\theta', \phi_h) + \mathcal{B}(\theta', \phi_0) \\
&= \Big(\frac{\partial^2 u}{\partial t^2}, \phi_0\Big) - \Big(\frac{\partial^2 \mathcal{E}_h u}{\partial t^2}, \phi_0\Big) - \mathcal{B}((\mathcal{E}_h u)', \phi_0) + \mathcal{B}(u', \phi_0) \\
&= \Big(\frac{\partial^2}{\partial t^2}(\mathcal{Q}_h u - \mathcal{E}_h u), \phi_0\Big) - \mathcal{B}((\mathcal{E}_h u)', \phi_0) + \mathcal{B}((\mathcal{Q}_h u)', \phi_0) \\
&\quad -\mathcal{B}((\mathcal{Q}_h u)' - u', \phi_0) \\
&= \Big(\frac{\partial^2}{\partial t^2}(-\zeta_u), \phi_0\Big) - \mathcal{B}(\zeta_u', \phi_0) - \mathcal{B}((\mathcal{Q}_h u)' - u', \phi_0) \ \forall \phi_h = \{\phi_0, \phi_b\} \in \mathcal{V}_h^0,
\end{aligned}$$

which can be rearranged as

$$\begin{aligned}
&\frac{d}{dt}(\theta', \phi_0) - (\theta', \phi_0') + \frac{d}{dt}\mathcal{A}_{2,w}(\theta, \phi_h) - \mathcal{A}_{2,w}(\theta, \phi_h') + \mathcal{A}_{1,w}(\theta, \phi_h) \\
&+\frac{d}{dt}\mathcal{B}(\theta, \phi_0) = \frac{d}{dt}(-\zeta_u', \phi_0) + (\zeta_u', \phi_0') - \frac{d}{dt}\mathcal{B}(\zeta_u, \phi_0) + \mathcal{B}(e_h, \phi_0') \\
&\qquad - \mathcal{B}((\mathcal{Q}_h u)' - u', \phi_0) \ \ \forall \phi_h = \{\phi_0, \phi_b\} \in \mathcal{V}_h^0, \ \ t > 0. \qquad (6.2.43)
\end{aligned}$$

Now, for $0 < \xi \leq T$, we define

$$\hat{\theta}(., t) = \int_t^\xi \theta(., s) ds, \ \ 0 \leq t \leq T.$$

Then, clearly $\hat{\theta}(\xi) = 0$ and $\frac{\partial \hat{\theta}}{\partial t} = -\theta(., t)$, $0 \leq t \leq T$. Now, substituting $\phi_h = \hat{\theta}(t) \in \mathcal{V}_h^0$ in (6.2.43) and making some rearrangement, we get

$$\begin{aligned}
&\frac{1}{2}\frac{d}{dt}(\theta, \theta) + \frac{d}{dt}\mathcal{A}_{2,w}(\theta, \hat{\theta}) + \mathcal{A}_{2,w}(\theta, \theta) - \frac{1}{2}\frac{d}{dt}\mathcal{A}_{1,w}(\hat{\theta}, \hat{\theta}) + \frac{d}{dt}\mathcal{B}(\theta, \hat{\theta}) \\
&+\mathcal{B}(\theta, \theta) = \frac{d}{dt}(-e_h', \hat{\theta}) - (\zeta_u', \theta) - \frac{d}{dt}\mathcal{B}(e_h, \hat{\theta}) - \mathcal{B}(\zeta_u, \theta) \\
&-\mathcal{B}((\mathcal{Q}_h u)' - u', \theta). \qquad (6.2.44)
\end{aligned}$$

Integrating (6.2.44) from 0 to ξ, and using the fact that $\hat{\theta}(\xi) = 0$ and $\theta(0) = 0$, we derive

$$\begin{aligned}
&\frac{1}{2}\|\theta(\xi)\|^2 + \frac{1}{2}\mathcal{A}_{1,w}(\hat{\theta}(0), \hat{\theta}(0)) + \int_0^\xi |||\theta|||^2 \mathrm{ds} + \int_0^\xi \|\theta\|^2 \mathrm{ds} \\
&\leq (e_h'(0), \hat{\theta}(0)) + \mathcal{B}(e_h(0), \hat{\theta}(0)) - \int_0^\xi (\zeta_u', \theta)\mathrm{ds} - \int_0^\xi \mathcal{B}(\zeta_u, \theta)\mathrm{ds} \\
&- \int_0^\xi \mathcal{B}((\mathcal{Q}_h u)' - u', \theta) ds
\end{aligned}$$

Applied Cauchy-Schwarz inequality, Lemma (6.2.4) together with the fact that $e_h(0) = 0$, $e_h'(0) = 0$ and $\mathcal{A}_{1,w}(\hat{\theta}(0), \hat{\theta}(0)) > 0$, yields

$$\begin{aligned}
&\frac{1}{2}\|\theta(\xi)\|^2 + \int_0^\xi |||\theta|||^2 \mathrm{ds} + \int_0^\xi \|\theta\|^2 \mathrm{ds} \\
&\leq \int_0^\xi \|\zeta_u'\| |||\theta||| \mathrm{ds} + \int_0^\xi \|\zeta_u\| |||\theta||| \mathrm{ds} + \int_0^\xi \|(\mathcal{Q}_h u)' - u'\| |||\theta||| \mathrm{ds}. \qquad (6.2.45)
\end{aligned}$$

Since θ is continuous in the time variable, we select ξ such that $\|\theta(\xi)\| = \max_{0\leq t\leq T} \|\theta(t)\|$. Then observe that $\|\hat{\theta}(0)\| \leq \xi \|\theta(\xi)\|$, which together with Young's inequality for some appropriate $\nu > 0$, leads us to

$$\begin{aligned}
\frac{1}{2}\|\theta(\xi)\|^2 + \int_0^\xi |||\theta|||^2 \mathrm{ds} + \int_0^\xi \|\theta\|^2 \mathrm{ds} &\leq \max_{0\leq t\leq T} \|\theta(t)\| \int_0^\xi \Big(\|\zeta_u'\| + \|\zeta_u\| \\
&\quad + \|(\mathcal{Q}_h u)' - u'\| \Big) dt \\
&\leq \|\theta(\xi)\| \sqrt{T} \Big\{ \|\zeta_u'\|_{L^2(L^2)} + \|\zeta_u\|_{L^2(L^2)} + \|(\mathcal{Q}_h u)' - u'\|_{L^2(L^2)}^2 \Big\} \\
&\leq C_\nu \|\theta(\xi)\|^2 + C(\nu) T \Big(\|\zeta_u'\|_{L^2(L^2)}^2 + \|\zeta_u\|_{L^2(L^2)}^2 + \|(\mathcal{Q}_h u)' - u'\|_{L^2(L^2)}^2 \Big).
\end{aligned}$$

We can restate the above equation

$$\|\theta(\xi)\|_{L^\infty(L^2)}^2 \leq C \Big(\|\zeta_u'\|_{L^2(L^2)}^2 + \|\zeta_u\|_{L^2(L^2)}^2 + \|(\mathcal{Q}_h u)' - u'\|_{L^2(L^2)}^2 \Big). \qquad (6.2.46)$$

Then, from the estimate (6.2.42), we obtain

$$\|\zeta_u'\|_{L^2(L^2)} \leq C h^{k+1} \|u\|_{H^1(0,T;H^{k+1}(\Omega))}. \qquad (6.2.47)$$

Finally, using the estimates (6.2.47) in (6.2.46) together with Lemma (6.2.1) leads us to the following optimal error estimate for the semi-discrete solution (6.2.8).

Theorem 6.2.3. *Let u and u_h be the solutions of Problem (6.1.1)-(6.1.2) and (6.2.8), respectively. Assume that $u \in L^2(J; H^{k+1}(\Omega))$ and $\frac{\partial u}{\partial t} \in L^2(J; H^{k+1}(\Omega))$. Then, there is a constant C such that*

$$\|u - u_h\| \leq C h^{k+1} \Big(\|u\|_{L^2(H^{k+1})} + \|\frac{\partial u}{\partial t}\|_{L^2(H^{k+1})} \Big).$$

6.3 Error Analysis for the Fully Discrete Scheme

In this section, we describe a fully discrete weak Galerkin finite element scheme to approximate the solution of the problem (6.1.1)-(6.1.2). We have derived an optimal a priori error estimate in $L^\infty(L^2)$ norm.

We first divide the time interval $J = [0, T]$ into N equally spaced sub intervals by the following points

$$0 = t_0 < t_1 < ... < T_N = T$$

with $t_n = n\tau,\ \tau = \frac{T}{N}$ being the time step. Let $I_n = (t_{n-1}, t_n]$ be the n-th sub-interval. For a sequence $\{\gamma^n\}_{n=0}^N \subset L^2(\Omega)$, we define

$$\partial_\tau \gamma^n = \frac{\gamma^{n+1} - \gamma^n}{\tau} \quad \text{and} \quad \gamma^{n+\frac{1}{2}} = \frac{1}{2}(\gamma^{n+1} + \gamma^n),\ \ n = 0, 1, \ldots, N-1.$$

Also, for a continuous mapping $\psi : [0, T] \to L^2(\Omega)$, we define $\psi^n = \psi(., t_n)$, $0 \le n \le N$. Then the fully discrete weak Galerkin finite element approximation to the problem (6.1.1)-(6.1.2) is defined as follows: Find $U^n = \{U_0^n, U_b^n\} \in \mathcal{V}_h^0$ such that

$$\partial_\tau U^n = p^{n+\frac{1}{2}} \ \text{ for } \ n = 0,\ 1, \ldots, N-1 \tag{6.3.1}$$

and

$$\begin{aligned}(\partial_\tau p^n, \phi_0) + \mathcal{B}(p^{n+\frac{1}{2}}, \phi_0) + \mathcal{A}_{1,w}(U^{n+\frac{1}{2}}, \phi_h) + \mathcal{A}_{2,w}(p^{n+\frac{1}{2}}, \phi_h)& \\ = (f^{n+\frac{1}{2}}, \phi_0)\ \ \forall \phi_h = \{\phi_0, \phi_b\} \in \mathcal{V}_h^0,& \end{aligned} \tag{6.3.2}$$

with $U^0 = \mathcal{Q}_h u^0$ and $p^0 = \mathcal{Q}_h v^0$.

For the well-posedness of the fully discrete scheme (6.3.1)-(6.3.2), we have the following result in terms of the auxiliary variable p^n.

Lemma 6.3.1. *There exists a unique sequence $\{U^n\}_{n=0}^N \subset \mathcal{V}_h^0$ and a corresponding unique sequence $\{p^n\}_{n=0}^N \subset \mathcal{V}_h^0$ satisfying (6.3.1)-(6.3.2).*

Proof. From (6.3.1), we have

$$U^{n+1} = \frac{\tau}{2}(p^{n+1} + p^n) + U^n. \tag{6.3.3}$$

Using (6.3.3) in (6.3.2), we get

$$\begin{aligned}(p^{n+1}, \phi_0) + \frac{\tau}{2}\mathcal{B}(p^{n+1}, \phi_0) + \frac{\tau^2}{4}\mathcal{A}_{1,w}(p^{n+1}, \phi_h)& \\ + \frac{\tau}{2}\mathcal{A}_{2,w}(p^{n+1}, \phi_h) = \mathcal{F}^n(\phi_h)\ \ \forall \phi_h = \{\phi_0, \phi_b\} \in \mathcal{V}_h^0,& \end{aligned} \tag{6.3.4}$$

where, $\mathcal{F}^n$ is the linear functional given by

$$\mathcal{F}^n(\phi_h) = (p^n, \phi_0) - \frac{\tau}{2}\mathcal{B}(p^n, \phi_0) - \frac{\tau^2}{4}\mathcal{A}_{1,w}(p^n, \phi_h) - \frac{\tau}{2}\mathcal{A}_{2,w}(p^n, \phi_h) \\ -\tau\mathcal{A}_{1,w}(U^n, \phi_h) + \tau(f^{n+\frac{1}{2}}, \phi_0) \ \ \forall \phi_h = \{\phi_0, \phi_b\} \in \mathcal{V}_h^0. \tag{6.3.5}$$

Due to the positive definiteness of the bilinear forms $\mathcal{A}_{1,w}$, $\mathcal{A}_{2,w}$, and $\mathcal{B}$, there exists uniquely defined $p^{n+1} \in \mathcal{V}_h^0$ satisfying equation (6.3.4) and subsequently U^{n+1} exists uniquely for $n = 0, 1, \ldots, N-1$. □

Later on, we will need the following results. The proofs involve the use of Taylor's series and standard arguments, and therefore, details are omitted.

Lemma 6.3.2. *For any $v \in H^3(J; L^2(\Omega))$, we have*

$$\|\partial_\tau v^n - v_t^{n+\frac{1}{2}}\|^2 \leq C\tau^3 \int_{t_n}^{t_{n+1}} \|v_{ttt}\|^2 dt. \tag{6.3.6}$$

Further, we need following stability result for the semidiscrete solution.

Lemma 6.3.3. *For any $t \in (0, T]$, let u_h satisfy (6.2.8). Then, we have*

$$\int_0^t \|u_h''''(t)\|^2 ds + \int_0^t |||u_h'''(t)|||^2 ds \leq C\Big(\|u^0\|^2_{H^6(\Omega)} + \|v^0\|^2_{H^6(\Omega)} \\ + \|f\|^2_{H^3(J;H^2(\Omega))}\Big).$$

Proof. Differentiating (6.2.8) twice with respect to time t and substitute $\phi_h = u_h'''(t)$, we have

$$(u_h'''', u_h''') + \mathcal{A}_{1,w}(u_h'', u_h''') + \mathcal{A}_{2,w}(u_h''', u_h''') + \mathcal{B}(u_h''', u_h''') = (f'', u_h''').$$

We can restate the above equation as

$$\frac{1}{2}\frac{d}{dt}\Big(\|u_h'''\|^2 + \mathcal{A}_{1,w}(u_h'', u_h'')\Big) + \mathcal{A}_{2,w}(u''', u''') + \mathcal{B}(u_h''', u_h''') = (f'', u''').$$

Now, integrate the above equation with respect to time from 0 to t and apply Cauchy Schwarz inequality, we get

$$\frac{1}{2}\|u_h'''\|^2 + \frac{1}{2}|||u_h''|||^2 + \int_0^t \|u_h'''\|^2 ds + \int_0^t |||u_h'''|||^2 ds \\ \leq \frac{1}{2}\|u_h'''(0)\|^2 + \frac{1}{2}|||u_h''(0)|||^2 + \frac{1}{2}\Big(\int_0^t \|u_h'''(s)\|^2 ds + \int_0^t \|f''\|^2 ds\Big).$$

We can rearrange the above equation as

$$\int_0^t \|u_h'''(s)\|^2 ds + \int_0^t |||u_h'''(s)|||^2 ds \leq C\Big(\|u_h'''(0)\|^2 + |||u_h'''(0)|||^2 \\ + \int_0^t \|f''(s)\|^2 ds\Big). \tag{6.3.7}$$

Now, we need to bound $\|u_h'''(0)\|^2$ and $|||u_h'''(0)|||^2$ in equation (6.3.7). To this end, taking $t \to 0^+$ in (6.1.1), it follow that

$$\|u''(0)\|_\lambda \leq C\Big(\|u^0\|_{\lambda+2} + \|u'(0)\|_{\lambda+2} + \|f\|_{H^1(H^\lambda)}\Big) \tag{6.3.8}$$

and

$$\|u'''(0)\|_\lambda \leq C\Big(\|u^0\|_{\lambda+4} + \|u'(0)\|_{\lambda+4} + \|f\|_{H^2(H^\lambda)}\Big) \tag{6.3.9}$$

Next, we differentiate (6.2.8) with respect to time t and using the definition of $\mathcal{E}_h$ operator (6.2.23). Then, setting $t \to 0^+$ to have

$$\begin{aligned}(u_h'''(0), \phi_0) &= -\mathcal{A}_{1,w}(u_h'(0), \phi_h) - \mathcal{A}_{2,w}(u_h''(0), \phi_h) - \mathcal{B}(u_h''(0), \phi_0) + (f'(0), \phi_0)\\ &= -\mathcal{A}_{1,w}(\mathcal{E}_h u'(0), \phi_h) - \mathcal{A}_{2,w}(\mathcal{E}_h u''(0), \phi_h) - \mathcal{B}(\mathcal{E}_h u''(0), \phi_0) + (f'(0), \phi_0)\\ &= (\nabla\cdot(\alpha\nabla u'(0), \phi_h)) + (\nabla\cdot(\beta\nabla u''(0)), \phi_h) - \mathcal{B}(\mathcal{E}_h u''(0), \phi_0) + (f'(0), \phi_0)\end{aligned}$$

Now, applying the Cauchy Schwarz inequality together with the estimate (6.3.8) in the above equation with $\lambda = 2$, and we obtained

$$\|u_h'''(0)\| \leq C\Big(\|u^0\|_{H^4(\Omega)} + \|v^0\|_{H^4(\Omega)} + \|f\|_{H^2(J;H^2(\Omega))}\Big). \tag{6.3.10}$$

In the previous estimate, we have used the fact that (cf. [105], Proposition 7.1)

$$\sup_{0\leq t\leq T}\|v(t)\|_{\mathcal{B}} \leq C(T)\|v\|_{H^1(J;\mathcal{B})}\ \forall v \in H^1(J;\mathcal{B}), \tag{6.3.11}$$

for any Banach space $\mathcal{B}$.

As a consequence of estimate (6.3.10) together with standard inverse inequality, estimate (6.3.9) with $\lambda = 2$, and the fact that $\|u\|_{L^2(K)} \leq Ch\|u\|_{2,K}$, we obtain

$$|||u_h'''(0)||| \leq Ch^{-1}\|u_h'''(0)\| \leq C\Big(\|u^0\|_{H^6(\Omega)} + \|v^0\|_{H^6(\Omega)} + \|f\|_{H^2(J;H^2)}\Big). \tag{6.3.12}$$

Again, we are differentiating (6.2.8) thrice with respect to time t and substitute $\phi_h = u_h''''(t)$, we get

$$(u_h'''', u_h'''') + \mathcal{A}_{1,w}(u_h''', u_h'''') + \mathcal{A}_{2,w}(u_h'''', u_h'''') + \mathcal{B}(u_h'''', u_h'''') = (f''', u_h'''').$$

Then, it follows from (6.3.7) that

$$\begin{aligned}\int_0^t \|u_h''''(s)\|^2 ds + \int_0^t |||u_h''''(s)|||^2 ds \leq C\Big(&\|u_h''''(0)\|^2 + |||u_h'''(0)|||^2\\ &+ \int_0^t \|f'''(s)\|^2 ds\Big).\end{aligned} \tag{6.3.13}$$

Here, the term $|||u_h'''(0)|||$ can be bound using the estimate (6.3.12). To the bound $\|u_h''''(0)\|$ and in equation (6.3.13), we follow the step from (6.3.8)-(6.3.12), and we get

$$\|u_h''''(0)\| \leq C\Big(\|u^0\|_{H^6(\Omega)} + \|v^0\|_{H^6(\Omega)} + \|f\|_{H^3(J;H^2(\Omega))}\Big). \ \square$$

In order to compute the error between U^n and u^n, we first established the error for $\xi^n := u_h^n - U^n$, for $1 \leq n \leq N$. To do so, we have the following result.

Lemma 6.3.4. *Let u and U^n be the solutions of problem (6.1.1)-(6.1.2) and the WG approximation (6.3.1)-(6.3.2), respectively. Then, we have*

$$\max_{1\leq n\leq N} \|\xi^n\|^2 \leq C\tau^4\Big(\int_0^T \|u_h''''\|^2 dt + \int_0^T |||u_h'''|||^2 dt\Big).$$

Proof. Substitute $t = t_n$ and $t = t_{n+1}$ in (6.2.8) and then add to have

$$\begin{aligned}&(\partial_\tau u_{ht}^n, \phi_0) + \mathcal{B}(u_{ht}^{n+\frac{1}{2}}, \phi_0) + \mathcal{A}_{1,w}(u_h^{n+\frac{1}{2}}, \phi_h) + \mathcal{A}_{2,w}(u_{ht}^{n+\frac{1}{2}}, \phi_h)\\ &= (f^{n+\frac{1}{2}}, \phi_0) + (\omega^n, \phi_0) \quad \forall \phi_h = \{\phi_0, \phi_b\} \in \mathcal{V}_h^0, \end{aligned} \tag{6.3.14}$$

where $\omega^n := \partial_\tau u_{ht}^n - u_{htt}^{n+\frac{1}{2}}$.

Now, subtracting (6.3.2) from (6.3.14), we have

$$\begin{aligned}&(\partial_\tau \mathcal{P}^n, \phi_0) + \mathcal{B}(\mathcal{P}^{n+\frac{1}{2}}, \phi_0) + \mathcal{A}_{1,w}(\xi^{n+\frac{1}{2}}, \phi_h) + \mathcal{A}_{2,w}(\mathcal{P}^{n+\frac{1}{2}}, \phi_h)\\ &= (\omega^n, \phi_0) \ \ \forall \phi_h = \{\phi_0, \phi_b\} \in \mathcal{V}_h^0, \end{aligned} \tag{6.3.15}$$

with $\mathcal{P}^n := u_{ht}^n - p^n$.

From (6.3.1), it is easy to observe that

$$\partial_\tau \xi^n = \mathcal{P}^{n+\frac{1}{2}} + \partial_\tau u_h^n - u_{ht}^{n+\frac{1}{2}} = \mathcal{P}^{n+\frac{1}{2}} + \alpha^n, \ \alpha^n := \partial_\tau u_h^n - u_{ht}^{n+\frac{1}{2}}, \tag{6.3.16}$$

so that

$$\xi^n = \tau\sum_{k=0}^{n-1} \partial_\tau \xi^k = \tau\sum_{k=0}^{n-1} \mathcal{P}^{k+\frac{1}{2}} + \tau\sum_{k=0}^{n-1} \alpha^k \ \ \& \ \ \mathcal{P}^n = \tau\sum_{k=0}^{n-1} \partial_\tau \mathcal{P}^k.$$

Here, we have used the fact that $\xi^0 = u_h^0 - U^0 = \mathcal{Q}_h u^0 - \mathcal{Q}_h u^0 = 0$ and $\mathcal{P}^0 = u_{ht}^0 - p^0 = \mathcal{Q}_h v^0 - \mathcal{Q}_h v^0 = 0$.

Hence, applying the above relations it follows that

$$\partial_\tau \xi^n = \frac{\tau}{2}\left(\sum_{k=0}^{n} \partial_\tau \mathcal{P}^k + \sum_{k=0}^{n-1} \partial_\tau \mathcal{P}^k\right) + \alpha^n, \tag{6.3.17}$$

$$\xi^{n+\frac{1}{2}} = \frac{\tau}{2}\left(\sum_{k=0}^{n} \mathcal{P}^{k+\frac{1}{2}} + \sum_{k=0}^{n-1} \mathcal{P}^{k+\frac{1}{2}}\right) + \frac{\tau}{2}\left(\sum_{k=0}^{n} \alpha^k + \sum_{k=0}^{n-1} \alpha^k\right). \tag{6.3.18}$$

Now, we define a sequence $\{s^n\}_{n=0}^N$ such that $s^0 = 0$ and

$$s^n = \tau \sum_{k=0}^{n-1} \xi^{k+\frac{1}{2}},\ n = 1, 2, \ldots, N-1,$$

so that

$$s^{n+\frac{1}{2}} = \frac{\tau}{2}\left(\sum_{k=0}^{n} \xi^{k+\frac{1}{2}} + \sum_{k=0}^{n-1} \xi^{k+\frac{1}{2}} \right). \tag{6.3.19}$$

Hence, apply the identities (6.3.17)-(6.3.19) leads us to

$$\begin{aligned}
&(\partial_\tau \xi^n, \phi_0) + \mathcal{B}(\xi^{n+\frac{1}{2}}, \phi_0) + \mathcal{A}_{1,w}(s^{n+\frac{1}{2}}, \phi_h) + \mathcal{A}_{2,w}(\xi^{n+\frac{1}{2}}, \phi_h) \\
&= \frac{\tau}{2} \sum_{k=0}^{n} \Big\{ (\partial_\tau \mathcal{P}^k, \phi_0) + \mathcal{B}(\mathcal{P}^{k+\frac{1}{2}}, \phi_0) + \mathcal{A}_{2,w}(\mathcal{P}^{k+\frac{1}{2}}, \phi_h) \\
&\quad + \mathcal{A}_{1,w}(\xi^{k+\frac{1}{2}}, \phi_h) \Big\} + \frac{\tau}{2} \sum_{k=0}^{n-1} \Big\{ (\partial_\tau \mathcal{P}^k, \phi_0) + \mathcal{B}(\mathcal{P}^{k+\frac{1}{2}}, \phi_0) \\
&\quad + \mathcal{A}_{2,w}(\mathcal{P}^{k+\frac{1}{2}}, \phi_h) + \mathcal{A}_{1,w}(\xi^{k+\frac{1}{2}}, \phi_h) \Big\} + (\alpha^n, \phi_0) \\
&\quad + \frac{\tau}{2} \mathcal{B}\Big(\sum_{k=0}^{n} \alpha^k + \sum_{k=0}^{n-1} \alpha^k, \phi_0 \Big) + \frac{\tau}{2} \mathcal{A}_{2,w}\Big(\sum_{k=0}^{n} \alpha^k + \sum_{k=0}^{n-1} \alpha^k, \phi_h \Big),
\end{aligned}$$

for any $\phi_h = \{\phi_0, \phi_b\} \in \mathcal{V}_h^0$.

Using (6.3.15), for $1 \le n \le N-1$, we derive

$$\begin{aligned}
&(\partial_\tau \xi^n, \phi_0) + \mathcal{B}(\xi^{n+\frac{1}{2}}, \phi_0) + \mathcal{A}_{2,w}(\xi^{n+\frac{1}{2}}, \phi_h) + \mathcal{A}_{1,w}(s^{n+\frac{1}{2}}, \phi_h) \\
&= (\Re_1^n, \phi_0) + \mathcal{B}(\Re_2^n, \phi_0) + \mathcal{A}_{2,w}(\Re_2^n, \phi_h),
\end{aligned} \tag{6.3.20}$$

where

$$\Re_1^n := \frac{\tau}{2}\omega^n + \tau \sum_{k=0}^{n-1} \omega^k + \alpha^n \ \ \& \ \ \Re_2^n := \frac{\tau}{2}\alpha^n + \tau \sum_{k=0}^{n-1} \alpha^k.$$

Substituting $\phi_h = \xi^{n+\frac{1}{2}} = \partial_\tau s^n$ in (6.3.20) and making some rearrangements, we arrive at

$$\begin{aligned}
&(\xi^{n+1}, \xi^{n+1}) + 2\tau \mathcal{B}(\xi^{n+\frac{1}{2}}, \xi^{n+\frac{1}{2}}) + 2\tau \mathcal{A}_{2,w}(\xi^{n+\frac{1}{2}}, \xi^{n+\frac{1}{2}}) \\
&+ \mathcal{A}_{1,w}(s^{n+1}, s^{n+1}) = (\xi^n, \xi^n) + \mathcal{A}_{1,w}(s^n, s^n) + 2\tau(\Re_1^n, \xi^{n+\frac{1}{2}}) \\
&\qquad + 2\tau \mathcal{B}(\Re_2^n, \xi^{n+\frac{1}{2}}) + 2\tau \mathcal{A}_{2,w}(\Re_2^n, \xi^{n+\frac{1}{2}}).
\end{aligned}$$

Next, using Cauchy-Schwarz inequality, together with coercivity (6.2.7), we obtain

$$\begin{aligned}&(\xi^{n+1},\xi^{n+1})+2\tau\|\xi^{n+\frac{1}{2}}\|^2+2\tau\Big|\Big|\Big|\xi^{n+\frac{1}{2}}\Big|\Big|\Big|^2+\mathcal{A}_{1,w}(s^{n+1},s^{n+1})\\&\leq(\xi^n,\xi^n)+\mathcal{A}_{1,w}(s^n,s^n)+2\tau\|\Re_1^n\|\|\xi^{n+\frac{1}{2}}\|+2\tau\|\Re_2^n\|\|\xi^{n+\frac{1}{2}}\|\\&\quad+2\tau|||\Re_2^n|||\Big|\Big|\Big|\xi^{n+\frac{1}{2}}\Big|\Big|\Big|.\end{aligned}$$

Now, applying the Young's inequality with appropriately selecting $\nu>0$ in the above relation, leads us to

$$\begin{aligned}(\xi^{n+1},\xi^{n+1})+\mathcal{A}_{1,w}(s^{n+1},s^{n+1})&\leq(\xi^n,\xi^n)+\mathcal{A}_{1,w}(s^n,s^n)\\&\quad+C(\nu)\tau\Big(\|\Re_1^n\|^2+\|\Re_2^n\|^2+|||\Re_2^n|||^2\Big).\end{aligned}\tag{6.3.21}$$

Summing (6.3.21) from $n=1$ to $n=l-1$ with $2\leq l\leq N$, we obtain

$$\max_{2\leq n\leq N}\|\xi^n\|^2\leq\|\xi^1\|^2+\Big|\Big|\Big|s^1\Big|\Big|\Big|^2+C(\nu)\tau\sum_{n=0}^{l-1}\big(\|\Re_1^n\|^2+|||\Re_2^n|||^2\big).\tag{6.3.22}$$

For estimation of the terms ξ^1 and s^1, we note that

$$s^1=\tau\xi^{\frac{1}{2}}=\frac{\tau}{2}\xi^1\ \ \&\ \ \mathcal{P}^{\frac{1}{2}}=\frac{\mathcal{P}^1}{2}=\frac{\xi^1}{\tau}-\alpha^0.$$

Now, putting $n=0$ in the error equation (6.3.15) and using the above identities, we have

$$\begin{aligned}&\frac{2}{\tau^2}(\xi^1,\phi_0)+\frac{1}{\tau}\mathcal{B}(\xi^1,\phi_0)+\frac{1}{\tau}\mathcal{A}_{2,w}(\xi^1,\phi_h)+\frac{1}{\tau}\mathcal{A}_{1,w}(s^1,\phi_h)\\&=(\omega^0,\phi_0)+\frac{2}{\tau}(\alpha^0,\phi_0)+\mathcal{B}(\alpha^0,\phi_0)+\mathcal{A}_{2,w}(\alpha^0,\phi_h)\ \ \forall\phi_h\in\mathcal{V}_h^0.\end{aligned}\tag{6.3.23}$$

Substituting $\phi_h=\xi^1=\frac{2}{\tau}$ in (6.3.23) together with coercivity (6.2.7), we obtain

$$\|\xi^1\|^2+\Big|\Big|\Big|s^1\Big|\Big|\Big|^2\leq\frac{\tau^2}{2}(\omega^0,\xi^1)+\tau(\alpha^0,\xi^1)+\frac{\tau^2}{2}\mathcal{B}(\alpha^0,\xi^1)+\tau\mathcal{A}_{2,w}(\alpha^0,s^1).$$

Next, use Cauchy-Schwarz and Young's inequality to have

$$\begin{aligned}\|\xi^1\|^2+\Big|\Big|\Big|s^1\Big|\Big|\Big|^2\ \ &\leq\ \ \frac{\tau^4}{4}\|\omega^0\|^2+C_\nu\|\xi^1\|^2+\Big(\tau^2+\frac{\tau^4}{4}\Big)\|\alpha^0\|^2\\&\quad+C_\nu\|\xi^1\|^2+\tau^2\Big|\Big|\Big|\alpha^0\Big|\Big|\Big|^2+C(\nu)\Big|\Big|\Big|s^1\Big|\Big|\Big|^2.\end{aligned}$$

Now, selecting $\nu>0$ appropriately leads us to

$$\|\xi^1\|^2+\Big|\Big|\Big|s^1\Big|\Big|\Big|^2\leq C\Big(\tau^4\|\omega^0\|^2+\tau^2\Big|\Big|\Big|\alpha^0\Big|\Big|\Big|^2\Big).\tag{6.3.24}$$

Combining (6.3.22) and (6.3.24), we have

$$\max_{1\le n\le N}\|\xi^n\|^2 \le C\Big(\tau^4\|\omega^0\|^2+\tau^2|||\alpha^0|||^2+\tau\sum_{n=0}^{l-1}\big(\|\Re_1^n\|^2+|||\Re_2^n|||^2\big)\Big). \tag{6.3.25}$$

Now, we shall estimate both terms $\Re_1^n$ and $\Re_2^n$. For the estimation of $\Re_1^n$, use triangle inequality and Cauchy-Schwarz inequality to have

$$\begin{aligned}\|\Re_1^n\|^2 &\le C\Big(\frac{\tau^2}{4}\|\omega^n\|^2+\tau^2\|\sum_{k=0}^{n-1}\omega^k\|^2+\|\alpha^n\|^2\Big)\\ &\le C\Big(\frac{\tau^2}{4}\|\omega^n\|^2+\tau^2N\sum_{k=0}^{n-1}\|\omega^k\|^2+\|\alpha^n\|^2\Big)\\ &\le C\Big(\frac{\tau^2}{4}\|\omega^n\|^2+\tau\sum_{k=0}^{n-1}\|\omega^k\|^2+\|\alpha^n\|^2\Big).\end{aligned}$$

Then, using Lemma 6.3.2, we obtain

$$\begin{aligned}\|\Re_1^n\|^2 \le C\Bigg(&\tau^5\int_{t_n}^{t_{n+1}}\|u_h''''\|^2dt+\tau^4\int_0^T\|u_h''''\|^2dt\\ &+\tau^3\int_{t_n}^{t_{n+1}}\|u_h'''\|^2dt\Bigg).\end{aligned} \tag{6.3.26}$$

The following estimate for $\Re_2^n$ is achieved using the same technique as used for deriving $\Re_1^n$

$$|||\Re_2^n|||^2 \le C\left(\tau^5\int_{t_n}^{t_{n+1}}|||u_h'''|||^2dt+\tau^4\int_0^T|||u_h'''|||^2dt\right). \tag{6.3.27}$$

Finally, using (6.3.26)-(6.3.27) in (6.3.25), we obtain

$$\max_{1\le n\le N}\|\xi^n\|^2 \le C\tau^4\left(\int_0^T\|u_h''''\|^2dt+\int_0^T|||u_h'''|||^2dt\right). \quad \square$$

Now, the following Theorem state the optimal $L^\infty(L^2)$ error result.

Theorem 6.3.1. *Let u and U^n be the solutions of a general linear second order hyperbolic equation (6.1.1)-(6.1.2) and the weak Galerkin approximation (6.3.1)-(6.3.2), respectively. Assume that $u^0\in H^6(\Omega)\cap H_0^1(\Omega)$, $v^0\in H^6(\Omega)\cap H_0^1(\Omega)$ and $f\in H^3(J;H^2(\Omega))$. Further, Assume that $u_t\in L^2(0,T;H^{k+1}(\Omega))$, then we have*

$$\max_{0\le n\le N}\|u^n-U^n\| \le C(u)\Big(h^{k+1}+\tau^2\Big),$$

where $C(u)=C\left\{\|u^0\|^2_{H^6(\Omega)}+\|v^0\|^2_{H^6(\Omega)}+\|f\|^2_{H^3(H^2(\Omega))}+\|u_t\|^2_{L^2(H^{k+1}(\Omega))}\right\}^{\frac{1}{2}}$.

Proof. Applying the triangle inequality to

$$u^n - U^n = u^n - u_h^n + u_h^n - U^n,$$

followed by Theorem 6.2.3, Lemma 6.3.3 and Lemma 6.3.4 leads to desire result. □

6.4 Numerical Section

This section is devoted to documentation of numerical results that demonstrate the performance of the weak Galerkin method. We shall illustrate various types of numerical examples to validate the theoretical convergence results for the general linear second order hyperbolic equation (6.1.1)-(6.1.2) in $\Omega \times J$, where $\Omega \subset \mathbb{R}^2$ and $J = (0, 1]$. To examine the flexibility and efficiency of the WG method, equation (6.1.1)-(6.1.2) is solved on finite element partitions with different kind of configurations, including triangular, rectangular, and polygonal meshes. In example 6.4.1 and example 6.4.2, we have discussed smooth solutions with smooth coefficient for higher order of convergence using uniform triangular and rectangular meshes, respectively. In example 6.4.3 and example 6.4.4, we have verified our theoretical results for smooth solutions with discontinuous coefficients. Further, in the example 6.4.5, we have shown that the WG algorithm is valid on a rectangular mesh with hanging nodes. At last, in example 6.4.6, we have verified the weak Galerkin algorithm for linearized Westervelt's equation.

Let U^n be the weak Galerkin solution defined by (6.3.1) and (6.3.2). In order to illustrate the convergence history of the WG approach in term of the discetization error, we have calculated following error

$$e_h := Q_h u(x, t_n) - U^n$$

at final time $t_n = T$ with respect to energy norm and L^2-norm. More precisely, the errors are reported with respect to energy norm and L^2-norm through tables and error plots for the WG space

$$(\mathcal{P}_k(K), \mathcal{P}_k(\partial K), [\mathcal{P}_{k-1}(K)]^2)$$

with time step $\tau = O(h^k)$.

We recall the EOC formula from (5.4.1)

$$EOC(e_i) = \log\left(\frac{e_{i+1}}{e_i}\right) / \log\left(\frac{h_{i+1}}{h_i}\right).$$

Example 6.4.1. Smooth solution with smooth coefficient: Consider the problem (6.1.1)-(6.1.2) in $\Omega \times J$, where $\Omega = (0, 1) \times (0, 1)$. Numerical solution is compared with the following exact solution

$$u = \exp(-t)\sin(\pi x)\sin(\pi y)\sin(\pi x + \pi y - t),$$

with coefficients selected as $\sigma = xy + 1$ and

$$\beta(x,y) = \begin{bmatrix} 2 & x^4+y^2+1 \\ x^4+y^2+1 & 5 \end{bmatrix} = \alpha(x,y)$$

The load term f, initial data and boundary data are determined from the choice for u. Here, we have done uniform partitioning of the domain into $n \times n$ sub rectangles which is followed by dividing each rectangular element by the diagonal line with a negative slope, where the mesh size is $h = 1/n$. the initial mesh and its refinement is depicted in Figure 6.4.1. The $L^\infty(H^1)$-norm and $L^\infty(L^2)$-norm errors for linear, quadratic, and cubic WG spaces at final time $T = 1$ are reported in Table 6.4.1, Table 6.4.2 and Table 6.4.3 respectively, which shows that the rate of convergence $\mathrm{O}(h^k)$ in energy norm and $\mathrm{O}(h^{k+1})$ in L^2-norm.

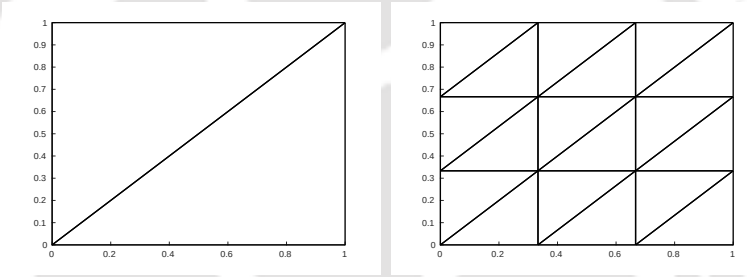

Figure 6.4.1: An initial triangular mesh for $h = 1/2$ (left), and its refinement for $h = 1/8$ (right) in Example 6.4.1.

Example 6.4.2. Smooth solution with smooth coefficient: In this example, we consider the problem (6.1.1)-(6.1.2) in $\Omega \times J$, where $\Omega = (0,1) \times (1,2)$. Numerical solution is compared with the following exact solution

$$u(x,y,t) = \frac{t^2}{4}\exp(-t)\sin(\pi x)\sin(\pi y).$$

The given data are extracted from the true solution $u(x,y,t)$ with coefficients $\alpha = I = \beta$ and $\sigma = 1$. Here, we have done uniform partitioning of the domain into $n \times n$ sub rectangles with the mesh size is $h = 1/n$ as shown in Figure 6.4.2. The order of convergence for the WG spaces $k = 1, k = 2$ and $k = 3$ are reported in Table 6.4.4, Table 6.4.5 and Table 6.4.6, respectively. It showed that we have obtained optimal order of accuracy in energy norm and L^2 norm.

Table 6.4.1: The history of convergence for $k = 1$ in Example 6.4.1 with $\tau = h$.

h	$\|\|\|e_h\|\|\|$	EOC	$\|e_h\|$	EOC
1/2	5.300783e+00	-	1.225644e+00	-
1/4	3.265425e+00	6.989345e-01	3.990989e-01	1.618722e+00
1/8	1.644638e+00	9.895008e-01	1.004111e-01	1.990828e+00
1/16	8.196299e-01	1.004726e+00	2.494270e-02	2.009229e+00
1/32	4.093588e-01	1.001607e+00	6.222854e-03	2.002969e+00
1/64	2.046177e-01	1.000435e+00	1.554877e-03	2.000776e+00

Table 6.4.2: The history of convergence for $k = 2$ in Example 6.4.1 with $\tau = h^2$.

h	$\|\|\|e_h\|\|\|$	EOC	$\|e_h\|$	EOC
1/2	3.930725e+00	-	6.743611e-01	-
1/4	1.313912e+00	1.580926e+00	1.146874e-01	2.555815e+00
1/8	3.479775e-01	1.916803e+00	1.494999e-02	2.939490e+00
1/16	8.840514e-02	1.976792e+00	1.880920e-03	2.990634e+00
1/32	2.247328e-02	1.975920e+00	2.355679e-04	2.997224e+00
1/64	5.427014e-03	2.049980e+00	3.002644e-05	2.971837e+00

Example 6.4.3. Smooth solution with discontinuous coefficients: In this example, we intend to describe the weak Galerkin algorithm for discontinuous coefficients and concerned with higher order of convergence. To do so, we extract this example from [42] with some modification. We consider the following IBVP

$$u_{tt} - \alpha\Delta u - \beta\Delta u_t + \sigma u_t = f(x,t) \text{ in } \Omega \times J, \tag{6.4.1}$$

Table 6.4.3: The history of convergence for $k = 3$ in Example 6.4.1 with $\tau = h^3$.

h	$\|\|\|e_h\|\|\|$	EOC	$\|e_h\|$	EOC
1/2	3.488819e-01	-	4.539509e-01	-
1/4	2.549791e-02	3.774288e+00	6.380849e-02	2.830716e+00
1/8	1.682029e-03	3.922105e+00	8.305679e-03	2.941578e+00
1/16	1.111836e-04	3.919187e+00	1.082756e-03	2.939390e+00
1/32	1.783426e-05	3.029996e+00	1.642762e-07	4.000133e+00
1/64	2.170264e-06	3.038708e+00	1.002437e-08	4.034540e+00

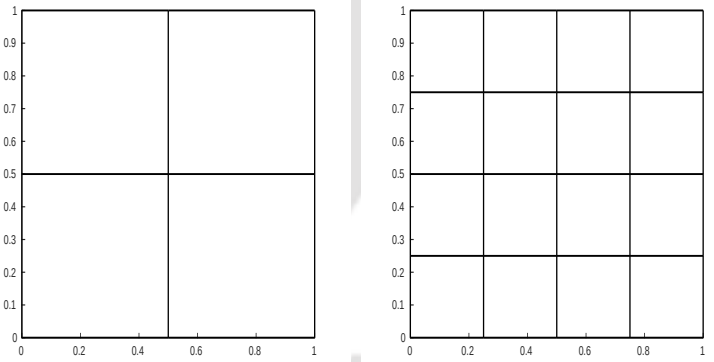

Figure 6.4.2: An initial rectangular mesh for $h = 1/2$ (left), and its refinement $h = 1/4$ (right) in Example 6.4.2.

where $\Omega = (-1, 1) \times (-1, 1)$ and $J = (0, 1]$. The exact solution is same as considered in Example 6.4.2. The finite element partitioning is taken as triangulation for this example. Then, we select the data appearing in the above problem from the choice of u with the following physical coefficients, which we select from [115] to mark the significance of our

Table 6.4.4: The history of convergence for $k = 1$ in Example 6.4.2 with $\tau = h$.

h	$\|\|\|e_h\|\|\|$	EOC	$\|e_h\|$	EOC
1/2	1.431993e-01	-	3.150822e-02	-
1/4	8.870199e-02	6.909856e-01	1.058595e-02	1.573578e+00
1/8	4.654081e-02	9.304701e-01	2.830319e-03	1.903113e+00
1/16	2.354612e-02	9.830072e-01	7.193964e-04	1.976106e+00
1/32	1.180758e-02	9.957759e-01	1.805937e-04	1.994039e+00
1/64	5.908106e-03	9.989455e-01	4.519507e-05	1.998511e+00

Table 6.4.5: The history of convergence for $k = 2$ in Example 6.4.2 with $\tau = h^2$.

h	$\|\|\|e_h\|\|\|$	EOC	$\|e_h\|$	EOC
1/2	7.852199e-02	-	1.212402e-02	-
1/4	2.350025e-02	1.740421e+00	1.547427e-03	2.969925e+00
1/8	6.193307e-03	1.923894e+00	1.792455e-04	3.109862e+00
1/16	1.571053e-03	1.978978e+00	2.162321e-05	3.051284e+00
1/32	2 3.942429e-04	1.994575e+00	.674470e-06	3.015256e+00
1/64	9.865421e-05	1.998632e+00	3.333852e-07	3.003991e+00

model problem.

$$(\sigma, \beta, \alpha) = \left(\frac{C_E^2}{\alpha_E}, \alpha_e, C_E^2\right)$$
$$= \begin{cases} \left(1.2 \times 10^{12}, 1.2 \times 10^{-4}, 1.44 \times 10^{8}\right) & \text{if } y \leq x^2, \\ \left(1.2 \times 10^{12}, 1.6 \times 10^{-4}, 1.96 \times 10^{8}\right) & \text{if } y > x^2. \end{cases}$$

Table 6.4.6: The history of convergence for $k = 3$ in Example 6.4.2 with $\tau = h^3$.

h	$\|\|\|e_h\|\|\|$	EOC	$\|e_h\|$	EOC
1/2	2.564515e-02	-	3.440849e-03	-
1/4	3.664079e-03	2.807163e+00	2.340275e-04	3.878014e+00
1/8	4.777053e-04	2.939257e+00	1.469980e-05	3.992809e+00
1/16	6.043065e-05	2.982768e+00	9.179877e-07	4.001178e+00
1/32	7.577334e-06	2.995518e+00	5.735284e-08	4.000537e+00
1/64	1.006832e-06	2.911867+00	3.570521e-09	4.005658e+00

Dual-phase-lag (DPL) model is being commonly used in the study of heat transport in metallic films during ultra-fast laser heating [99, 114]. Here C_E represents the equivalent thermal wave speed, α_E denotes the equivalent thermal diffusivity and α_e is the electron thermal diffusivity of the material. Our numerical results are based on the uniform triangular meshes for $k = 1$, $k = 2$, and $k = 3$ at final time $T = 1$. It is clear from Table 6.4.7 - Table 6.4.9 that we have achieved optimal order of convergence in both L^2 and H^1 norms, which consolidates our theoretical findings in Theorem 6.3.1.

Example 6.4.4. Smooth solution with discontinuous coefficient: In this example, we apply the WG algorithm on the thermal wave model of bio heat transfer. To do this, we extract this example from [42] with the modification. We consider the problem (6.4.1) in $\Omega \times J$, where $\Omega = (-1, 1) \times (-1, 1)$ and $J = (0, 1]$. The exact solution is same as in Example 6.4.2.

The set of physical coefficients that corresponds to the thermal wave model of bio heat transfer is given by

$$(\sigma, \beta, \alpha) = \begin{cases} \left(0.4325,\ 2.31 \times 10^{-4},\ 2.7199 \times 10^{-9}\right) & \text{if } x \leq 0, \\ \left(0.6050,\ 3.39 \times 10^{-4},\ 7.5520 \times 10^{-9}\right) & \text{if } x > 0. \end{cases}$$

Table 6.4.7: The history of convergence for $k = 1$ in Example 6.4.3 with $\tau = h$.

h	$\|\|\|e_h\|\|\|$	EOC	$\|e_h\|$	EOC
1/2	7.199183e-01	-	5.992461e-03	-
1/4	6.378199e-01	0.174683e+00	1.533555e-03	1.966268e+00
1/8	3.643214e-01	0.807937e+00	3.849478e-04	1.994144e+00
1/16	1.720768e-01	1.082158e+00	9.632205e-05	1.998725e+00
1/32	8.321841e-02	1.005901e+00	2.408562e-05	1.992948e+00
1/64	4.130842e-02	1.010466e+00	6.102753e-06	1.980639e+00

Table 6.4.8: The history of convergence for $k = 2$ in Example 6.4.3 with $\tau = h^2$.

h	$\|\|\|e_h\|\|\|$	EOC	$\|e_h\|$	EOC
1/2	5.495252e-03	-	1.533907e-03	-
1/4	1.526038e-03	1.848394e+00	9.632145e-05	3.993211e+00
1/8	3.994701e-04	1.933631e+00	6.021723e-06	3.999609e+00
1/16	1.085833e-04	1.879285e+00	3.763639e-07	3.999976e+00
1/32	2.738173e-05	1.987516e+00	2.840531e-08	3.727895e+00
1/64	6.845041e-06	2.000082e+00	2.301433e-09	3.625556e+00

Our numerical results are based on the uniform rectangular mesh; see Figure 6.4.2 and polygonal meshes; see Figure 6.4.3 for linear WG space. To support the fact that our numerical algorithm is consistent, the physical coefficients for the thermal wave model of bio heat transfer are chosen. The results are clearly reported in Table 6.4.10 and Table 6.4.11.

Table 6.4.9: The history of convergence for $k = 3$ in Example 6.4.3 with $\tau = h^3$.

h	$\|\|\|e_h\|\|\|$	EOC	$\|e_h\|$	EOC
1/2	5.808203e-02	-	3.849604e-04	-
1/4	9.464643e-03	2.617472e+00	6.021732e-06	5.998388e+00
1/8	1.327746e-03	2.833569e+00	1.409964e-07	5.416448e+00
1/16	1.729794e-04	2.940307e+00	3.842533e-09	5.197456e+00
1/32	2.461127e-05	2.813209e+00	1.520771e-10	4.659182e+00
1/64	3.173622e-06	2.955116e+00	8.571124e-12	4.149174e+00

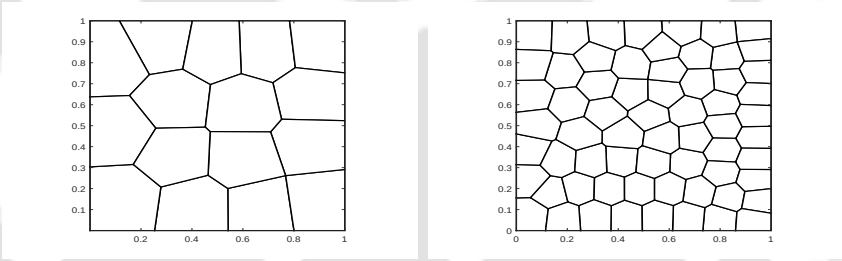

Figure 6.4.3: Initial polygonal mesh with 16 elements (left), with its refinement (right) in Example 6.4.4.

Example 6.4.5. Smooth solution on rectangular mesh with hanging nodes: In this example, we intend to describe the weak Galerkin algorithm on rectangular mesh with hanging nodes and concerned with higher order of convergence. We solve the problem (6.1.1)-(6.1.2) in $\Omega = (0, 1)^2$ with exact solution

$$u(x, y, t) = t^2 \exp(-t) \sin(4\pi x) \sin(4\pi y).$$

The initial mesh is as shown in Figure 6.4.4 (Left). The mesh on the right in Figure 6.4.4 is generated by uniform refinement procedure. It should be pointed out that the initial mesh has a hanging nodes A, B, C and D. Here, we notice that the WG algorithm is still hold on these refinements for the finite element partition $\mathcal{T}_h$ with hanging nodes. The errors with respect to energy norm and $L^\infty(L^2)$ norm for $k = 1$ and $k = 2$ WG spaces are reported in Table 6.4.12 and Table 6.4.13 at final time $T = 1$.

Table 6.4.10: EOC on polygonal mesh in Example 6.4.4 with $\tau = h$.

h	$\|\|\|e_h\|\|\|$	EOC	$\|e_h\|$	EOC
1/4	1.529574e-01	-	9.394611e-05	-
1/8	1.092285e-01	4.857806e-01	4.498886e-05	1.062266e+00
1/16	5.655569e-02	9.496055e-01	1.226609e-05	1.874893e+00
1/32	2.847330e-02	9.900624e-01	3.133530e-06	1.968814e+00
1/64	1.425905e-02	9.977315e-01	7.876408e-07	1.992179e+00
1/128	6.953621e-03	1.036041e+00	2.015728e-07	1.966236e+00

Table 6.4.11: EOC on rectangular mesh in Example 6.4.4 with $\tau = h$.

h	$\|\|\|e_h\|\|\|$	EOC	$\|e_h\|$	EOC
1/4	1.053425e-01	-	5.267267e-02	-
1/8	9.135125e-02	2.055908e-01	4.072098e-02	3.712824e-01
1/16	4.017812e-02	1.185014e+00	1.781938e-02	1.192325e+00
1/32	1.906449e-02	1.075522e+00	5.321198e-03	1.743624e+00
1/64	9.458835e-03	1.011154e+00	1.395924e-03	1.930530e+00
1/128	4.723998e-03	1.001654e+00	3.561065e-04	1.970840e+00

Example 6.4.6. Smooth solution with variable coefficients: In this example, we numerically verified that the equation (6.1.1)-(6.1.2) can be easily extended to following linearized Westervelt's equation with variable coefficients.

$$\gamma(x,t)u'' - \nabla \cdot (\alpha \nabla u' + \beta \nabla u) + \sigma(x,t)u' = f(x,t) \ \text{ in } \Omega \times (0,T], \tag{6.4.2}$$

Table 6.4.12: The history of convergence for $k = 1$ in Example 6.4.5 with $\tau = h$.

h	$\|\|\|e_h\|\|\|$	EOC	$\|e_h\|$	EOC
1/2	5.930691e-01	-	3.517309e-01	-
1/4	1.496784e-01	1.232606e+00	3.868829e-01	6.163031e-01
1/8	2.159354e-01	8.412975e-01	4.662808e-02	1.682595e+00
1/16	1.117858e-01	9.498628e-01	1.249606e-02	1.899726e+00
1/32	5.640954e-02	9.867256e-01	3.182036e-03	1.973451e+00
1/64	2.827087e-02	9.966230e-01	7.992421e-04	1.993246e+00

Table 6.4.13: The history of convergence for $k = 2$ in Example 6.4.5 with $\tau = h^2$.

h	$\|\|\|e_h\|\|\|$	EOC	$\|e_h\|$	EOC
1/2	4.372093e-01	-	2.890906e-01	-
1/4	1.506811e-01	1.536825e+00	5.849087e-02	2.305238e+00
1/8	4.637199e-02	1.700173e+00	9.985819e-03	2.550258e+00
1/16	1.123354e-02	2.045441e+00	1.190625e-03	3.068162e+00
1/32	2.763521e-03	2.023233e+00	1.452761e-04	3.034849e+00
1/64	6.875541e-04	2.006962e+00	1.802853e-05	3.010443e+00

where $\Omega = (0, 1) \times (0, 1)$. It is worth to note that only semi-discrete error analysis has been discussed in [94] and its provides a scope for the generalization of these works to higher order of accuracy methods. The source term appearing in the above problem is

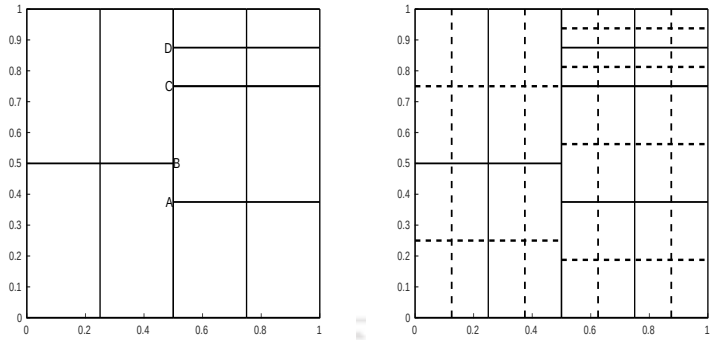

Figure 6.4.4: An initial rectangular mesh with Hanging nodes (left), and its refinement (right).

selected by setting the exact solution as

$$u = \exp(-t)\sin(\pi x)\sin(\pi y)\sin(\pi x + \pi y - t),$$

with coefficients choosing as $\sigma = x^2y + t$, and $\gamma = xyt^2$.

The coefficient matrices are selected as

$$\beta(x,y) = \begin{bmatrix} 1 & x^2y \\ x^2y & xy^2+1 \end{bmatrix} \text{ and } \alpha(x,y) = \begin{bmatrix} 1 & xy \\ xy & x^2y^2+1 \end{bmatrix}$$

Here, we have implemented the equation (6.4.2) with linear and quadratic weak Galerkin approximation space at final time $T = 1$. It is clear from Tables 6.4.14-6.4.15 that we have obtained optimal order of convergence in both L^2 and H^1 norms. Here, we have a future scope to explore these observations by mathematical analysis tools.

Table 6.4.14: The history of convergence for $k = 1$ in Example 6.4.6 with $\tau = h$.

h	$\|\|\|e_h\|\|\|$	EOC	$\|e_h\|$	EOC
1/2	1.328119e+00	-	1.821328e-01	-
1/4	8.105636e-01	7.123875e-01	6.035559e-02	1.593431e+00
1/8	4.097090e-01	9.843259e-01	1.535190e-02	1.975070e+00
1/16	2.048214e-01	1.000233e+00	3.642146e-03	2.075556e+00
1/32	1.030327e-01	9.912643e-01	1.052915e-03	1.790399e+00
1/64	5.204751e-02	9.852012e-01	2.711302e-04	1.957331e+00

Table 6.4.15: The history of convergence for $k = 2$ in Example 6.4.6 with $\tau = h^2$.

h	$\|\|\|e_h\|\|\|$	EOC	$\|e_h\|$	EOC
1/2	9.662629e-01	-	8.386915e-02	-
1/4	3.252471e-01	1.570879e+00	1.615244e-02	2.376388e+00
1/8	8.811055e-02	1.884150e+00	2.172036e-03	2.894632e+00
1/16	2.713964e-02	1.698913e+00	3.325462e-04	2.707421e+00
1/32	7.326731e-03	1.889160e+00	4.552291e-05	2.868890e+00

7

Conclusions and Extensions

In this thesis, we have considered recently developed higher order weak Galerkin finite element methods for the time dependent problems on polygonal meshes . We believe that the work in this thesis could be a first step, but a crucial step for the error analysis of the WG-FEMs for time dependent problems with complex geometry. Our aim is to derived a priori error estimates in suitable norms for the weak Galerkin approximation solution that appeared in the WG formulation. Moreover, the theoretical results are supported by numerical experiments.

7.1 Critical Review of the Results

In the following, we highlight the critical review of the results obtained in each chapter.

In Chapter 2, we have described a systematic numerical study on WG-FEMs for second order linear parabolic problems by allowing polynomial approximations with various degrees for each local element. Our results are intended to extend the numerical analysis of WG-FEMs for elliptic problems [J. Sci. Comput., 74 (2018), 1369-1396] to parabolic problems. This article is only concerned about the discrete H^1 norm convergence. To best of our knowledge, optimal error estimates in L^2 norm for elliptic problems on general WG finite element space $(\mathcal{P}_k(K),\ \mathcal{P}_j(\partial K),\ \left[\mathcal{P}_l(K)\right]^2)$ with arbitrary non-negative integers $\{k,\ j,\ l\}$ have not been established earlier. Therefore, first we developed an a priori bound to obtain optimal convergence in the L^2 norm. Thereafter, we have derived both semidiscrete and fully discrete error estimates established in $L^\infty(L^2)$ and $L^\infty(H^1)$ norms for a general WG element $(\mathcal{P}_k(K),\ \mathcal{P}_j(\partial K),\ \left[\mathcal{P}_l(K)\right]^2)$, where $k \geq 1$, $j \geq 0$ and $l \geq 0$ are arbitrary integers. The fully discrete space-time discretization is based on the first order backward Euler and second order Crank-Nicolson schemes. At the end of this chapter, we have performed various numerical experiments that justify the robustness, reliability and accuracy of WG-FEMs.

In previous chapter, we noticed that to derive optimal $\mathrm{O}(h^{k+1})$ $(k \geq 1)$ in the L^2 norm for WG-FEMs, the minimum regularity assumption on the exact solution u is that $u \in H^1(0,T;H^{k+1}(\Omega))$. In chapter 3, we proceed to discuss the WG algorithm to the parabolic problems, when the solution $u \in L^2(0,T;H^{k+1}(\Omega)) \cap H^1(0,T;H^{k-1}(\Omega))$. Such regularity holds where forcing function $f \in L^2(0,T;H^{k-1}(\Omega))$ and initial function $u^0 \in H^k(\Omega)$ for some $k \geq 1$. The error estimates in $L^2(H^1)$ norm are derived for variable diffusion coefficient α, while most existing work (except [121]) assumed piecewise constant diffusion. Thereafter, we have discussed optimal order error estimates in $L^2(L^2)$ norm for both the spatially discrete continuous time and the discrete time weak Galerkin finite element schemes with variable coefficient. In existing literature, the optimal L^2 error convergence results of WG-FEMs for parabolic problems are derived under the assumption that $u \in H^1(0,T;H^{k+1}(\Omega))$ (see, e.g., Theorem 4.6 in [132] and Theorem 4.4 in [77]). Here, we have proved $\mathrm{O}(h^{k+1})$ order error estimates indeed the true solution of the given problem (3.1.1)-(3.1.2) is in $L^2(0,T;H^{k+1}(\Omega))$. The fully discrete scheme is based on first order in time Euler method. The numerical experiments are comprehensive and the results support the theory very well.

In Chapter 4, we have developed WG-FEMs for solving linear parabolic equations with non-smooth initial data on polygonal meshes. The optimal order of convergence in the $L^\infty(L^2)$ norm is proved in both semidiscrete and full-discrete WG schemes for linear WG space (see, Theorem 4.2.2 and Theorem 4.3.1). We have also derived stability of the semidiscrete solution and established some estimates which played crucial role to proving the optimal convergence rate. The error analysis is highly motivated by the fact that the solutions of parabolic problem have the so-called smoothing property (cf. [85]). That is, the solution is smooth for positive time t, even when the initial data are not H^1 regular. In chapter 3, we have proved the convergence of WG finite element solution to the true solution at an optimal rate in $L^2(L^2)$ norm under the assumption that $u \in L^2(0,T;H^{k+1}(\Omega)) \cap H^1(0,T;H^{k-1}(\Omega))$. In the case of piecewise linear WG-FEM (i.e., $k = 1$), the optimal error estimate requires the initial value to be in H^1 (see, Theorem 3.3.2). In this chapter, we have shown the convergence of WG finite element solution to the true solution at an optimal rate in L^2 norm on WG finite element space $(\mathcal{P}_1,\ \mathcal{P}_1,\ \mathcal{P}_0^2)$ (see, Theorem 4.2.2 and Theorem 4.3.1) with L^2 initial data. The $L^\infty(L^2)$ norm error analysis heavily depends on the newly derived optimal L^2 norm error estimates with smooth initial data $u^0 \in H_0^1 \cap H^2$ (see, Lemma 4.2.9 and Lemma 4.3.1) with parabolic duality argument. Finally, numerical results are reported to confirm our theoretical convergence finding.

In chapter 5, we have analyzed an optimal order of convergence in $L^\infty(L^2)$ norm

for the second-order wave equation on arbitrary polygons or polyhedral meshes. We have developed both semi-discrete and fully discrete WG schemes, and studied their associated error analysis. The fully discrete space-time finite element discretizations can be revised as the Crank-Nicolson discretization of the reformulation of the governing equation in the first-order system, as in Baker [7]. Numerical examples have been demonstrated using various degrees of polynomials in the WG spaces. Our numerical results cover the broad scope of various applied problems under one umbrella, including discontinuous coefficients, singularly perturbed, the flow of fluid in porous media with anisotropy and the low regular problem with non-convex domain. These experiments suggest that the WG scheme is the decisive and efficient numerical technique to examine such type of problems.

In last chapter, we described WG-FEMs for general linear second order hyperbolic equation with variable coefficients on polygonal meshes. The discretization in space using the weak Galerkin method and in time, we have applied the implicit second order Newmark scheme. At first, we derived a result for the well-posedness of weak Galerkin scheme (see, Theorem, 6.2.1). Next, we have established optimal order of convergence with respect to $L^\infty(H^1)$ norm and $L^\infty(L^2)$ norm (see, Theorem 6.2.3, Theorem 6.2.2 and Theorem 6.3.1). For the $L^\infty(H^1)$ norm error estimate of the semidiscrete solution, the splitting technique has been used, where the L^2 projection Q_h of the exact solution has used to split the error into two parts. In fact, apart from the standard error splitting technique, the newly derived error equation (6.2.2) is also critical. The $L^\infty(L^2)$ norm error analysis is based on a non-standard elliptic type projection operator instead of the usual elliptic projection. To get optimal error in $L^\infty(L^2)$ norm, first we established a priori bounded for non standard elliptic projection (see, Lemma 6.2.4). Finally, we have achieved $\mathrm{O}(h^k)$ and $\mathrm{O}(h^{k+1})$ for the WG space $(\mathcal{P}_k(K), \mathcal{P}_k(\partial K), [\mathcal{P}_{k-1}(K)]^2)$ in energy norm and L^2 norm, respectively. We have also proved stability of the semidiscrete solution which is very crucial to prove the optimal convergence rate of the fully discrete solution (see, Lemma 6.3.3). Several numerical experiments are performed in a two-dimensional setting that illustrates our theoretical convergence findings.

7.2 Extensions and Remarks

In this section, we have mentioned some potential extensions of our findings. Here, we are briefly proposing some unexplored problems which can be considered as future scope of the thesis work.

WG-FEMs for Westervelt's Equation: We can extended the weak Galerkin algorithm to following linearized Westervelt's equation with variable coefficients

$$\gamma(x,t)u'' + \sigma(x,t)u' - \nabla\cdot(\epsilon\nabla u' + \beta\nabla u) = f(x,t) \text{ in } \Omega\times(0,T],$$

where $\Omega\subset\mathbb{R}^2$ is a bounded and convex domain. It this thesis, we have numerically verified the above equation in Example 6.4.6. The extension of this theory with high order of accuracy on polygonal mesh can be extend as future work for the Westervelt's quasi-linear acoustic wave equation

$$c^{-2}u'' - \nabla\cdot\big(\alpha(x)\nabla u(x,t) + \beta(x)\nabla u'\big) = \gamma(u^2)'' \text{ in } (0,T]\times\Omega. \tag{7.2.1}$$

This is widely used to simulate high-intensity focused ultrasound fields generated by medical ultrasound transducers.

Stabilizer Free Weak Galerkin (SFWG) Methods: The stabilization term is one of the major complexity of the WG-FEMs and other discontinuous Galerkin finite element methods. This term is often used in finite element formulation with discontinuous approximations to implement the connection of discontinuous functions across element boundaries, which makes their implementation and analysis difficult. As an alternative approach to overcome the programming difficulties without compromising the order of accuracy, Ye and Zhang [130] developed a stabilizer free weak Galerkin (SFWG) finite element method for solving a second order elliptic equation on polytopal meshes. This method is much simpler than the standard WG-FEMs with fewer coefficients and high orders of accuracy on polytopal/polyhedral meshes. Recently, we have analyzed SFWG finite element methods for the second-order Sobolev equation [68]. The main aspect of our proof is the use of a non-standard elliptic type projection operator that we have discussed in chapter 6 instead of the usual elliptic projection. We have obtained convergence rates two orders higher than the optimal convergence rates in the triple bar norm and L^2-norm. More precisely, we have achieved supercloseness property for the WG space $(\mathbb{P}_k(K), \mathbb{P}_{k+1}(\partial K), [\mathbb{P}_{k+1}(K)]^2)$ in energy norm and L^2 norm. We proceed further to study the supercloseness property for the SFWG finite element methods that can be applied to solve the second order wave equation. An unconditionally stable second order Newmark scheme is adopted to analyze the fully discrete scheme, whereas the spatial discretization is analyzed by the SFWG algorithm. From this method, we have obtained a convergence rate which is two orders higher than the optimal convergence rate in $L^\infty(L^2)$ norm for the corresponding SFWG solution [67]. We can extend the SFWG methods to the general linear hyperbolic problems (6.1.1)-(6.1.2), which have

many applications in medical sciences. Further, we would like extend the stabilizer free WG algorithms for the following Cahn-Hilliard equation with non-smooth initial data (cf. [44, 124])

$$u_t - \Delta(-\Delta u + \phi(u)) = 0 \quad x \in \Omega \subset \mathbb{R}^3, \;\; t > 0,$$

together with appropriate boundary conditions.

Mixed WG-FEMs for Interface Problems: The present work can be extended to solve a typical two-dimensional (2D) elliptic interface problem

$$\begin{aligned} \mathbf{q} + \beta \nabla u &= 0 \quad \text{in } \Omega \\ \nabla \cdot \mathbf{q} &= f \quad \text{in } \Omega \\ u &= 0 \quad \text{on } \partial\Omega \\ \big[u\big] = u|_{\Omega_1} - u|_{\Omega_2} = \psi, \;\; \big[\mathbf{q}\cdot\mathbf{n}\big] = \mathbf{q}\cdot\mathbf{n}_1 + \mathbf{q}\cdot\mathbf{n}_2 &= -\phi \quad \text{along } \Gamma, \end{aligned}$$

where $\Omega = \Omega_1 \cup \Omega_2$, $\Gamma = \Omega_1 \cap \Omega_2$, and $\mathbf{n}_1$ and $\mathbf{n}_2$ denote unit outward normal of Ω_1 and Ω_2. The coefficient function $\beta(x)$ is assumed to be positive and piecewise constant across Γ, i.e., $\beta(x) = \beta_k$ for $x \in \Omega_k$, $k = 1, 2$. Across the interface Γ, the source function $f : \Omega \to \mathbb{R}$ can be singular. Jump functions $\psi : \Gamma \to \mathbb{R}$ and $\phi : \Gamma \to \mathbb{R}$ are given.

Although different finite element algorithms are developed for elliptic interface problems, surprisingly, there has been much less research on mixed finite element methods for interface problems with non-homogeneous jump conditions.

Weak Galerkin Solver with Polygonal Meshes: The only omission in the scope of this thesis is a numerical investigation to develop weak Galerkin solver for parabolic equation on polygonal meshes using weak Galerkin space $(\mathcal{P}_k(K),\ \mathcal{P}_j(\partial K),\ \big[\mathcal{P}_l(K)\big]^2)$ with arbitrary non-negative integers $\{k,\ j,\ l\}$. In practice, allowing arbitrary shape in a finite element partition provides a convenient flexibility in both numerical approximation and mesh generation. Especially, we have much less elements and we could evaluate integrals and solve the resulting linear systems in more expedited manner. However, one disadvantage is that instead of integrals of polynomials on the reference element, we may have to evaluate integrals of rational functions. It would be very interesting to develop weak Galerkin solver for PDEs with weak Galerkin space $(\mathcal{P}_k(K),\ \mathcal{P}_j(\partial K),\ \big[\mathcal{P}_l(K)\big]^2)$, where $k \geq 1$, $j \geq 0$ and $l \geq 0$ are arbitrary integers, for polygonal meshes.

Bibliography

[1] R. Adams and J. Fournier, *Sobolev Spaces, sec. ed*, Academic Press, Amsterdam, 2003.

[2] A. AL-Taweel and L. Mu, *A new upwind weak Galerkin finite element method for linear hyperbolic equations*, J. Comput. Appl. Math., 390 (2021), p. 113376.

[3] H. Ammari, D. Chen, and J. Zou, *Well-posedness of an electric interface model and its finite element approximation*, Math. Models Methods Appl. Sci., 26 (2016), pp. 601–625.

[4] P. F. Antonietti, I. Mazzieri, M. Muhr, V. Nikolić, and B. Wohlmuth, *A high-order discontinuous Galerkin method for nonlinear sound waves*, J. Comput. Phys., 415 (2020), p. 109484.

[5] D. N. Arnold, F. Brezzi, B. Cockburn, and L. D. Marini, *Unified analysis of discontinuous Galerkin methods for elliptic problems*, SIAM J. Numer. Anal., 39 (2002), pp. 1749–1779.

[6] N. Asmar, *Partial Differential Equations with Fourier Series and Boundary Value Problems: Third Edition*, Dover Books on Mathematics, Dover Publications, 2017.

[7] G. A. Baker, *Error estimates for finite element methods for second order hyperbolic equations*, SIAM J. Numer. Anal., 13 (1976), pp. 564–576.

[8] G. A. Baker and V. A. Dougalis, *On the L^∞ convergence of Galerkin approximations for second-order hyperbolic equations*, Math. Comp., 34 (1980), pp. 401–424.

[9] G. A. Baker, V. A. Dougalis, and S. M. Serbin, *High order accurate two-step approximations for hyperbolic equations*, RAIRO. Analyse numérique, 13 (1979), pp. 201–226.

[10] A. Bamberger, R. Glowinski, and Q. H. Tran, *A domain decomposition method for the acoustic wave equation with discontinuous coefficients and grid*

change, SIAM J. Numer. Anal., 34 (1997), pp. 603–639.

[11] G. I. Barenblatt, I. P. Zheltov, and I. Kochina, *Basic concepts in the theory of seepage of homogeneous liquids in fissured rocks [strata]*, J. Appl. Math. Mech., 24 (1960), pp. 1286–1303.

[12] G. R. Barrenechea, F. Brezzi, A. Cangiani, and E. H. Georgoulis, *Building bridges: connections and challenges in modern approaches to numerical partial differential equations*, vol. 114, Springer, 2016.

[13] M. Basson, B. Stapelberg, and N. F. J. van Rensburg, *Error estimates for semi-discrete and fully discrete Galerkin finite element approximations of the general linear second-order hyperbolic equation*, Numer. Funct. Anal. Optim., 38 (2017), pp. 466–485.

[14] L. Beirão da Veiga, F. Brezzi, A. Cangiani, G. Manzini, L. D. Marini, and A. Russo, *Basic principles of virtual element methods*, Math. Methods Appl. Sci., 23 (2013), pp. 199–214.

[15] J. Bramble, J. Pasciak, P. Sammon, and V. Thomee, *Incomplete iterations in multistep backward difference methods for parabolic problems with smooth and nonsmooth data*, Math. Comp., 52 (1989).

[16] F. Brezzi, J. Douglas, and L. D. Marini, *Two families of mixed finite elements for second order elliptic problems*, Numer. Math., 47 (1985), pp. 217–235.

[17] E. Burman, O. Duran, A. Ern, and M. Steins, *Convergence analysis of hybrid high-order methods for the wave equation*, J. Sci. Comput., 87 (2021), pp. 1–30.

[18] A. Cangiani, Z. Dong, and E. H. Georgoulis, *hp-version space-time discontinuous Galerkin methods for parabolic problems on prismatic meshes*, SIAM J. Sci. Comput., 39 (2017), pp. A1251–A1279.

[19] A. Cangiani, E. H. Georgoulis, and P. Houston, *hp-version discontinuousGalerkin methods on polygonal and polyhedral meshes*, Math. Methods Appl. Sci., 24 (2014), pp. 2009–2041.

[20] Z. Chen and J. Zou, *Finite element methods and their convergence for elliptic and parabolic interface problems*, Numer. Math., 79 (1998), pp. 175–202.

[21] K. Chrysafinos and L. S. Hou, *Error estimates for semidiscrete finite element approximations of linear and semilinear parabolic equations under minimal regularity assumptions*, SIAM J. Numer. Anal., 40 (2002), pp. 282–306.

[22] K. Chrysafinos and N. J. Walkington, *Error estimates for discontinuous Galerkin approximations of implicit parabolic equations*, SIAM J. Numer. Anal., 43 (2006), pp. 2478–2499.

[23] ——, *Error estimates for the discontinuous Galerkin methods for parabolic equations*, SIAM J. Numer. Anal., 44 (2006), pp. 349–366.

[24] H. E. Cline, R. D. Watkins, G. R. Russell, and K. H. Hynynen, *Ultrasound transducer with focused ultrasound refraction plate*, 1999. US Patent 5,873,845.

[25] B. Cockburn, D. A. Di Pietro, and A. Ern, *Bridging the hybrid high-order and hybridizable discontinuous Galerkin methods*, ESAIM Math. Model. Numer. Anal., 50 (2016), pp. 635–650.

[26] B. Cockburn, J. Gopalakrishnan, and R. Lazarov, *Unified hybridization of discontinuous Galerkin, mixed, and continuous Galerkin methods for second order elliptic problems*, SIAM J. Numer. Anal., 47 (2009), pp. 1319–1365.

[27] B. Cockburn and V. Quenneville-Bélair, *Uniform-in-time superconvergence of the HDG methods for the acoustic wave equation*, Math. Comp., 83 (2014), pp. 65–85.

[28] B. Cockburn and C.-W. Shu, *The local discontinuous Galerkin method for time-dependent convection-diffusion systems*, SIAM J. Numer. Anal., 35 (1998), pp. 2440–2463.

[29] L. C. Cowsat, T. F. Dupont, and M. F. Wheeler, *A priori estimates for mixed finite element methods for the wave equation*, Comput. Methods Appl. Mech. Engrg., 82 (1990), pp. 205–222.

[30] L. B. da Veiga and G. Manzini, *A virtual element method with arbitrary regularity*, IMA J. Numer. Anal., 34 (2014), pp. 759–781.

[31] W. Dai, H. Wang, P. M. Jordan, R. E. Mickens, and A. Bejan, *A mathematical model for skin burn injury induced by radiation heating*, Int. J. Heat Mass Transf., 51 (2008), pp. 5497–5510.

[32] A. Das and S. Natesan, *Higher-order convergence with fractional-step method for singularly perturbed 2D parabolic convection-diffusion problems on Shishkin mesh*, Comput. Math. Appl., 75 (2018), pp. 2387–2403.

[33] R. Dautray and J.-L. Lions, *Mathematical analysis and numerical methods for science and technology: volume 1 physical origins and classical methods*, Springer Science & Business Media, 2012.

[34] B. Deka and N. Kumar, *Error estimates in weak Galerkin finite element methods for parabolic equations under low regularity assumptions*, Appl. Numer. Math., 162 (2021), pp. 81–105.

[35] B. Deka and N. Kumar, *A systematic study on weak Galerkin finite element method for second order parabolic problems*, arXiv preprint arXiv:2103.13669, (2021).

[36] B. Deka and P. Roy, *Weak Galerkin finite element methods for parabolic interface problems with nonhomogeneous jump conditions*, Numer. Funct. Anal. Optim., 40 (2019), pp. 259–279.

[37] ——, *Weak Galerkin finite element methods for electric interface model with nonhomogeneous jump conditions*, Numer. Methods Partial Differential Equations, 36 (2020), pp. 734–755.

[38] Z. Dong and A. Ern, *Hybrid high-order and weak Galerkin methods for the biharmonic problem*, arXiv preprint arXiv:2103.16404, (2021).

[39] J. Douglas and H. H. Rachford, *On the numerical solution of heat conduction problems in two and three space variables*, Trans. Amer. Math. Soc., 82 (1956), pp. 421–439.

[40] F. Dujardin, E. Assaid, and E. Feddi, *New way for determining electron energy levels in quantum dots arrays using finite difference method*, Superlattices and Microstructures, 118 (2018), pp. 256–265.

[41] T. Dupont, *L^2-estimates for Galerkin methods for second order hyperbolic equations*, SIAM J. Numer. Anal., 10 (1973), pp. 880–889.

[42] J. Dutta and B. Deka, *Optimal a priori error estimates for the finite element approximation of dual-phase-lag bio heat model in heterogeneous medium*, J. Sci. Comput., 87 (2021), pp. 1–32.

[43] J. Dutta, N. Kumar, and B. Deka, *L^2 estimates for weak Galerkin finite element methods for second-order wave equations with polygonal meshes*, Submitted.

[44] C. M. Elliott and S. Larsson, *Error estimates with smooth and nonsmooth data for a finite element method for the cahn-hilliard equation*, Math. Comp., 58 (1992), pp. 603–630.

[45] L. C. Evans, *Partial differential equations*, vol. 19, American Mathematical Soc., 2010.

[46] G. Fichera, *Existence theorems in elasticity*, in Linear theories of elasticity and thermoelasticity, Springer, 1973, pp. 347–389.

[47] M. Fritz, V. Nikolić, and B. Wohlmuth, *Well-posedness and numerical treatment of the blackstock equation in nonlinear acoustics*, Mathematical Models and Methods in Applied Sciences, 28 (2018), pp. 2557–2597.

[48] L. Gao, D. Liang, and B. Zhang, *Error estimates for mixed finite element approximations of the viscoelasticity wave equation*, Math. Methods Appl. Sci., 27 (2004), pp. 1997–2016.

[49] E. Gekeler, *Linear multistep methods and Galerkin procedures for initial boundary value problems*, SIAM J. Numer. Anal., 13 (1976), pp. 536–548.

[50] V. Giurgiutiu, *Structural health monitoring: with piezoelectric wafer active sen-*

sors, Elsevier, 2007.

[51] G. Grimvall, *Thermophysical properties of materials*, Elsevier, 1999.

[52] M. J. Grote, A. Schneebeli, and D. Schötzau, *Discontinuous Galerkin finite element method for the wave equation*, SIAM J. Numer. Anal., 44 (2006), pp. 2408–2431.

[53] M. E. Gurtin and A. C. Pipkin, *A general theory of heat conduction with finite wave speeds*, Arch. Ration. Mech. Anal., 31 (1968), pp. 113–126.

[54] G. H. Hardy, J. E. Littlewood, G. Pólya, G. Pólya, et al., *Inequalities*, Cambridge university press, 1952.

[55] J. S. Hesthaven, *High-order accurate methods in time-domain computational electromagnetics: A review*, Advances in imaging and electron physics, 127 (2003), pp. 59–123.

[56] C. Hill and G. Ter Haar, *High intensity focused ultrasound-potential for cancer treatment*, Br. J. Radiol., 68 (1995), pp. 1296–1303.

[57] D. Hipp and B. Kovács, *Finite element error analysis of wave equations with dynamic boundary conditions: L 2 estimates*, IMA Journal of Numerical Analysis, 41 (2021), pp. 638–728.

[58] Y. Huang, J. Li, and D. Li, *Developing weak Galerkin finite element methods for the wave equation*, Numer. Methods Partial Differential Equations, 33 (2017), pp. 868–884.

[59] E. W. Jenkins, B. Rivière, and M. F. Wheeler, *A priori error estimates for mixed finite element approximations of the acoustic wave equation*, SIAM J. Numer. Anal., 40 (2002), pp. 1698–1715.

[60] Y. Kagawa, T. Tsuchiya, T. Yamabuchi, H. Kawabe, and T. Fujii, *Finite element simulation of non-linear sound wave propagation*, Journal of sound and vibration, 154 (1992), pp. 125–145.

[61] B. Kaltenbacher, V. Nikolic, and M. Thalhammer, *Efficient time integration methods based on operator splitting and application to the westervelt equation*, IMA J. Numer. Anal., 35 (2013), pp. 1092–1124.

[62] S. Karaa, *Error estimates for finite element approximations of a viscous wave equation*, Numer. Funct. Anal. Optim., 32 (2011), pp. 750–767.

[63] J. E. Kennedy, G. Ter Haar, and D. Cranston, *High intensity focused ultrasound: surgery of the future?*, Br. J. Radiol., 76 (2003), pp. 590–599.

[64] A. Khamayseh and V. de Almeida, *Adaptive hybrid mesh refinement for multiphysics applications*, in Journal of Physics: Conference Series, vol. 78, IOP Publishing, 2007, p. 012039.

[65] S. Kim and H. Lim, *High-order schemes for acoustic waveform simulation*, Appl.

Numer. Math., 57 (2007), pp. 402–414.

[66] D. D. Kosloff and E. Baysal, *Migration with the full acoustic wave equation*, Geophysics, 48 (1983), pp. 677–687.

[67] N. Kumar and B. Deka, *Developing stabilizer free weak Galerkin finite element method for second-order wave equation*, Submitted.

[68] ——, *A stabilizer free weak Galerkin finite element method for second order sobolev equation on polygonal meshe*, Submitted.

[69] ——, *A systematic study on weak galerkin finite element methods with second-order scheme in time for parabolic problems*, Submitted.

[70] ——, *Weak Galerkin finite element method for general linear socond order hyperbolic equation with variable coefficients on polygonal meshes*, Submitted.

[71] ——, *Weak Galerkin finite element method for parabolic problems with L^2 initial data*, Submitted.

[72] O. A. Ladyzhenskaia, V. A. Solonnikov, and N. N. Ural'tseva, *Linear and quasi-linear equations of parabolic type*, vol. 23, Am. Math. Soc., 1988.

[73] S. Larsson, V. Thomée, and L. B. Wahlbin, *Finite-element methods for a strongly damped wave equation*, IMA J. Numer. Anal., 11 (1991), pp. 115–142.

[74] W. Lauterborn, T. Kurz, and I. Akhatov, *Nonlinear Acoustics in Fluids*, Springer New York, 2007, pp. 257–297.

[75] P. D. Lax, *On the stability of difference approximations to solutions of hyperbolic equations with variable coefficients*, Comm. Pure Appl. Math., 14 (1961), pp. 497–520.

[76] H. Li, L. Mu, and X. Ye, *Interior energy error estimates for the weak Galerkin finite element method*, Numer. Math., 139 (2018), pp. 447–478.

[77] Q. H. Li and J. Wang, *Weak Galerkin finite element methods for parabolic equations*, Numer. Methods Partial Differential Equations, 29 (2013), pp. 2004–2024.

[78] H. Lim, S. Kim, and J. Douglas Jr, *Numerical methods for viscous and nonviscous wave equations*, Appl. Numer. Math., 57 (2007), pp. 194–212.

[79] G. Lin, J. Liu, L. Mu, and X. Ye, *Weak Galerkin finite element methods for Darcy flow: Anisotropy and heterogeneity*, J. Comput. Phys., 276 (2014), pp. 422–437.

[80] R. Lin, X. Ye, S. Zhang, and P. Zhu, *A weak Galerkin finite element method for singularly perturbed convection-diffusion–reaction problems*, SIAM J. Numer. Anal., 56 (2018), pp. 1482–1497.

[81] Y. P. Lin, *A mixed type boundary problem describing the propagation of disturbances in viscous media I, weak solution for quasi-linear equations*, J. Math. Anal.

Appl, 135 (1988), pp. 644–653.

[82] J. L. Lions and E. Magenes, *Non-homogeneous boundary value problems and applications*, vol. 2, Springer Science & Business Media, 1972.

[83] Q. H. Liu and Z. X. Zhang, *Traveling wave effect analysis on fabricated box girder bridge based on ansys*, in Applied Mechanics and Materials, vol. 587, Trans Tech Publ, 2014, pp. 1512–1517.

[84] G. Ludvigsson, K. R. Steffen, S. Sticko, S. Wang, Q. Xia, Y. Epshteyn, and G. Kreiss, *High-order numerical methods for 2d parabolic problems in single and composite domains*, J. Sci. Comput., 76 (2018), pp. 812–847.

[85] M. Luskin and R. Rannacher, *On the smoothing property of the Galerkin method for parabolic equations*, SIAM J. Numer. Anal., 19 (1982), pp. 93–113.

[86] J. Mélek, J. Nečas, M. Rokyta, and M. Růžička, *Weak and measure-valued solutions to evolutionary PDEs*, vol. 13, Chapman & Hall, London, UK, 1996.

[87] H. Motavalli, A. R. Akbarieh, and M. Parhizkar, *Analytical solution of a wave equation in cosmology*, Internat. J. Theoret. Phys., 50 (2011), pp. 2328–2333.

[88] L. Mu and Z. Chen, *A new WENO weak Galerkin finite element method for time dependent hyperbolic equations*, Appl. Numer. Math., 159 (2021), pp. 106–124.

[89] L. Mu, J. Wang, Y. Wang, and X. Ye, *A computational study of the weak Galerkin method for second-order elliptic equations*, Numer. Algorithms, 63 (2013), pp. 753–777.

[90] L. Mu, J. Wang, and X. Ye, *Weak Galerkin finite element methods on polytopal meshes*, Int. J. Numer. Anal. Model., 12 (2015), pp. 31–53.

[91] L. Mu, J. Wang, and X. Ye, *A least-squares-based weak Galerkin finite element method for second order elliptic equations*, SIAM J. Sci. Comput., 39 (2017), pp. A1531–A1557.

[92] L. Mu, J. Wang, X. Ye, and S. Zhao, *A new weak Galerkin finite element method for elliptic interface problems*, J. Comput. Phys., 325 (2016), pp. 157–173.

[93] V. Nikolić and B. Kaltenbacher, *On higher regularity for the westervelt equation with strong nonlinear damping*, Applicable Analysis, 95 (2016), pp. 2824–2840.

[94] V. Nikolić and B. Wohlmuth, *A priori error estimates for the finite element approximation of westervelt's quasi-linear acoustic wave equation*, SIAM J. Numer. Anal., 57 (2019), pp. 1897–1918.

[95] A. K. Pani, *An H^1-Galerkin mixed finite element method for parabolic partial differential equations*, SIAM Journal on Numerical Analysis, 35 (1998), pp. 712–

727.

[96] A. K. Pani and J. Y. Yuan, *Mixed finite element method for a strongly damped wave equation*, Numer. Methods Partial Differential Equations, 17 (2001), pp. 105–119.

[97] H. M. Patil and R. Maniyeri, *Finite difference method based analysis of bio-heat transfer in human breast cyst*, Thermal Science and Engineering Progress, 10 (2019), pp. 42–47.

[98] H. H. Pennes, *Analysis of tissue and arterial temperature in the resting human forearm*, J. Appl. Physiol., 1 (1948), pp. 93–122.

[99] T. Qiu and C. Tien, *Short-pulse laser heating on metals*, Int. J. Heat Mass Transf., 35 (1992), pp. 719–726.

[100] R. Rannacher, *Finite element solution of diffusion problems with irregular data*, Numer. Math., 43 (1984), pp. 309–327.

[101] M. R. M. Rao, *Ordinary differential equations, theory and applications, east*, 1980.

[102] P.-A. Raviart and J.-M. Thomas, *A mixed finite element method for 2-nd order elliptic problems*, in Mathematical aspects of finite element methods, Springer, 1977, pp. 292–315.

[103] M. L. Raynal, *On some nonlinear problems of diffusion*, in Volterra Equations, Springer, 1979, pp. 251–266.

[104] B. Rivière, *Discontinuous Galerkin methods for solving elliptic and parabolic equations: theory and implementation*, SIAM, 2008.

[105] J. C. Robinson, *Infinite-dimensional dynamical system: an introduction to dissipative parabolic PDEs and the theory of global attractors*, Cambridge Texts in Applied Mathematic, 2001.

[106] N. Saito, *Variational analysis of the discontinuous Galerkin time-stepping method for parabolic equations*, IMA J. Numer. Anal., 41 (2021), pp. 1253–1278.

[107] K. Sayevand, J. T. Machado, and V. Moradi, *A new non-standard finite difference method for analyzing the fractional navier–stokes equations*, Comput. Math. Appl., 78 (2019), pp. 1681–1694.

[108] I. Shevchenko and B. Kaltenbacher, *Absorbing boundary conditions for nonlinear acoustics: The westervelt equation*, Journal of Computational Physics, 302 (2015), pp. 200–221.

[109] D. Shi, *On the initial boundary value problem of nonlinear the equation of the moisture in soil*, Acta Math. Appl. Sin, 13 (1990), pp. 33–40.

[110] R. K. Sinha and B. Deka, *Optimal error estimates for linear parabolic problems with discontinuous coefficients*, SIAM J. Numer. Anal., 43 (2005), pp. 733–749.

[111] V. Thomée, *Galerkin finite element methods for parabolic problems*, vol. 1054, Springer, 1984.

[112] T. W. Ting, *A cooling process according to two-temperature theory of heat conduction*, J. Math. Anal. Appl., 45 (1974), pp. 23–31.

[113] D. Tzou, *A unified field theory for heat conduction from macro-to micro-scale*, ASME J. Heat Transfer, 117 (1995), pp. 8–16.

[114] D. Tzou and K. Chiu, *Temperature-dependent thermal lagging in ultrafast laser heating*, Int. J. Heat Mass Transf., 44 (2001), pp. 1725–1734.

[115] D. Y. Tzou, *A unified field approach for heat conduction from macro-to micro-scales*, (1995).

[116] ——, *Macro-to microscale heat transfer: the lagging behavior*, John Wiley & Sons, 2014.

[117] G. Vacca and L. Beirão da Veiga, *Virtual element methods for parabolic problems on polygonal meshes*, Numer. Methods Partial Differential Equations, 31 (2015), pp. 2110–2134.

[118] N. van Rensburg and B. Stapelberg, *Existence and uniqueness of solutions of a general linear second-order hyperbolic problem*, IMA J. Appl. Math., 84 (2018), pp. 1–22.

[119] N. Van Rensburg and A. Van Der Merwe, *Analysis of the solvability of linear vibration models*, Appl. Anal., 81 (2002), pp. 1143–1159.

[120] C. Wang and J. Wang, *A primal-dual weak Galerkin finite element method for second order elliptic equations in non-divergence form*, Math. Comp., 87 (2018), pp. 515–545.

[121] J. Wang, R. Wang, Q. Zhai, and R. Zhang, *A systematic study on weak Galerkin finite element methods for second order elliptic problems*, J. Sci. Comput., 74 (2018), pp. 1369–1396.

[122] J. Wang and X. Ye, *A weak Galerkin finite element method for second-order elliptic problems*, J. Comput. Appl. Math., 241 (2013), pp. 103–115.

[123] ——, *A weak Galerkin mixed finite element method for second order elliptic problems*, Math. Comp., 83 (2014), pp. 2101–2126.

[124] J. Wang, Q. Zhai, R. Zhang, and S. Zhang, *A weak Galerkin finite element scheme for the cahn-hilliard equation*, Math. Comp., 88 (2019), pp. 211–235.

[125] X. Wang, F. Gao, and Z. Sun, *Weak Galerkin finite element method for viscoelastic wave equations*, J. Comput. Appl. Math., 375 (2020), p. 112816.

[126] M. F. Wheeler, *A priori L^2 error estimates for Galerkin approximations to parabolic partial differential equations*, SIAM J. Numer. Anal., 10 (1973), pp. 723–759.

[127] T. P. Wihler and B. Rivière, *Discontinuous Galerkin methods for second-order elliptic PDE with low-regularity solutions*, J. Sci. Comput., 46 (2011), pp. 151–165.

[128] F. Xu, T. Lu, K. Seffen, and E. Ng, *Mathematical modeling of skin bioheat transfer*, Appl. Mech. Rev., 62 (2009), p. 050801.

[129] F. Xu, K. Seffen, and T. Lu, *Non-fourier analysis of skin biothermomechanics*, Int. J. Heat Mass Transf., 51 (2008), pp. 2237–2259.

[130] X. Ye and S. Zhang, *A stabilizer-free weak Galerkin finite element method on polytopal meshes*, J. Comput. Appl. Math., 371 (2020), p. 112699.

[131] Q. Zhai, R. Zhang, N. Malluwawadu, and S. Hussain, *The weak Galerkin method for linear hyperbolic equation*, Commun. Comput. Phys, 24 (2018), pp. 152–166.

[132] H. Zhang, Y. Zou, Y. Xu, Q. Zhai, and H. Yue, *Weak Galerkin finite element method for second order parabolic equations*, Int. J. Numer. Anal. Model, 13 (2016), pp. 525–544.

[133] S. Zhang, *On the nested refinement of quadrilateral and hexahedral finite elements and the affine approximation*, Numer. Math., 98 (2004), pp. 559–579.

[134] L. Zhen-dong, *The mixed finite element method for the non stationary conductionconvection problems*, Chinese J. Numer. Math. Appl., 20 (1998), pp. 29–59.

[135] S. Zhou, F. Gao, B. Li, and Z. Sun, *Weak Galerkin finite element method with second-order accuracy in time for parabolic problems*, Appl. Math. Lett., 90 (2019), pp. 118–123.

Appendix

Proof of Identity (4.3.23.) For any fixed $t_n > 0$ $(1 \le n \le M)$ and any function $\psi_h \in \mathcal{V}_h^0$, define $w_h(s) \in \mathcal{V}_h^0$ to be the continuous time weak Galerkin solution of the backward problem

$$(v_0, w_{hs}) - \mathcal{A}_w(v_h, w_h) = 0 \quad \forall v_h = \{v_0, v_b\} \in \mathcal{V}_h^0, \quad s \le t_n, \tag{7.2.2}$$

with $w_h(t_n) = \psi_h$. Assume that u_h is a solution of (4.2.5). Then, for $f = 0$ and due to (7.2.2), we obtain

$$\frac{d}{ds}(u_h(s), w_h(s)) = (u_{hs}(s), w_h(s)) + (u_h(s), w_{hs}(s)) = 0, \quad s \le t_n.$$

Next, we apply MVT to have

$$\frac{(u_h, v_h)(t_m) - (u_h, v_h)(t_{m-1})}{\tau} = \frac{d}{ds}(u_h, v_h)|_{s=\theta}, \ \theta \in (t_{m-1}, t_m),$$

and subsequently, we arrive at

$$\partial_\tau \{(u_h, w_h)\}^m = \frac{d}{ds}(u_h, w_h)|_{s=\theta} = 0. \tag{7.2.3}$$

Let $\{W_h^m\}_{m=0}^n \subset \mathcal{V}_h^0$ be the solution of discrete time backward problem

$$(v_0, \partial_\tau W_h^m) - \mathcal{A}_w(v_h, W_h^{m-1}) = 0 \quad \forall v_h = \{v_0, v_b\} \in \mathcal{V}_h^0, \ 1 \le m \le n,$$

with $W_h^n = \psi_h$. Then, it is easy to verify that

$$\partial_\tau (U_h, W_h)^m = 0. \tag{7.2.4}$$

Finally, combine (7.2.3)-(7.2.4) to have

$$\partial_\tau \{(u_h, w_h) - (U_h, W_h)\}^m = 0.$$

Estimate for $\hat{I}_{12} = \sum_{K\in\mathcal{T}_h}\Big(\nabla\mathcal{Q}_k^0 u_t - \nabla u_t, \alpha\nabla z_0\Big)$.

Statement. Let z_h be the weak Galerkin finite element approximation to (2.3.22) in the WG space $(\mathcal{P}_1(K),\ \mathcal{P}_0(\partial K),\ \big[\mathcal{P}_0(K)\big]^2)$. Then, we have

$$I_{12} \le Ch^{\lambda_2+1}\|\alpha\|_{1,\infty}\|u_t\|_{\lambda_2+1}\|\rho_t\|, \tag{7.2.5}$$

for some non-negative integer $\lambda_2 \le k$.

Proof. After adding and subtracting ∇z, we can rewrite the term $\hat{I}_{12}$ as

$$\begin{aligned}\hat{I}_{12} &= \sum_{K\in\mathcal{T}_h}\Big(\nabla\big(\mathcal{Q}_k^0 u_t - u_t\big), \alpha\big(\nabla z_0 - \nabla z\big)\Big)_K \\ &\quad + \sum_{K\in\mathcal{T}_h}\Big(\nabla\big(\mathcal{Q}_k^0 u_t - u_t\big), \alpha\nabla z\Big)_K \\ &:= I_{12}^1 + I_{12}^2. \end{aligned}\tag{7.2.6}$$

For the term I_{12}^1, we have

$$\begin{aligned}|I_{12}^1| &\le \sum_{K\in\mathcal{T}_h}\|\alpha\|_{\infty,K}\|\nabla(\mathcal{Q}_K^0 u_t - u_t)\|_K\|\nabla(z - z_0)\|_K \\ &\le C\sum_{K\in\mathcal{T}_h}\|\alpha\|_{\infty,K}h_K^{\lambda_2}\|u_t\|_{\lambda_2+1,K}h_K\|z\|_{2,K} \\ &\le Ch^{\lambda_2+1}\|\alpha\|_\infty\Big(\sum_{K\in\mathcal{T}_h}\|u_t\|_{\lambda_2+1,K}^2\Big)^{\frac{1}{2}}\Big(\sum_{K\in\mathcal{T}_h}\|z\|_{2,K}^2\Big)^{\frac{1}{2}} \\ &\le Ch^{\lambda_2+1}\|\alpha\|_{\infty,K}\|u_t\|_{\lambda_2+1}\|\rho_t\|, \end{aligned}\tag{7.2.7}$$

where $\lambda_2 \le k$. Here, we have used standard approximation property for L^2 projection and apriori estimate (2.3.24).

To estimate I_{12}^2, we first integrate by parts to obtain

$$\begin{aligned}I_{12}^2 &= \sum_{K\in\mathcal{T}_h}\Big(\nabla\big(\mathcal{Q}_k^0 u_t - u_t\big), \alpha\nabla z\Big)_K \\ &= -\sum_{K\in\mathcal{T}_h}\Big(\mathcal{Q}_k^0 u_t - u_t, \nabla\cdot(\alpha\nabla z)\Big)_K + \sum_{K\in\mathcal{T}_h}\big\langle\mathcal{Q}_k^0 u_t - u_t, \alpha\nabla z\cdot\mathbf{n}\big\rangle_{\partial K}.\end{aligned}$$

Now, use the fact that $\sum_{K\in\mathcal{T}_h}\langle v_b, \alpha\nabla z\cdot\mathbf{n}\rangle_{\partial K} = 0$ to arrive at

$$\begin{aligned}I_{12}^2 &= -\sum_{K\in\mathcal{T}_h}\Big(\mathcal{Q}_k^0 u_t - u_t, \nabla\cdot(\alpha\nabla z)\Big)_K \\ &\quad + \sum_{K\in\mathcal{T}_h}\big\langle\mathcal{Q}_k^0 u_t - u_t - \mathcal{Q}_k^b(\mathcal{Q}_k^0 u_t - u_t), \alpha\nabla z\cdot\mathbf{n}\big\rangle_{\partial K} \\ &:= L_1 + L_2. \end{aligned}\tag{7.2.8}$$

For the term L_1, we have

$$\begin{aligned} |L_1| &\leq C \sum_{K\in\mathcal{T}_h} \|\mathcal{Q}_k^0 u_t - u_t\|_K \|\nabla\cdot(\alpha\nabla z)\|_K \\ &\leq C \sum_{K\in\mathcal{T}_h} h_K^{\lambda_2+1} \|u_t\|_{\lambda_2+1,K} \|\nabla\cdot(\alpha\nabla z)\|_K \\ &\leq C\|\alpha\|_{1,\infty} h^{\lambda_2+1} \|u_t\|_{\lambda_2+1} \|\rho_t\|. \end{aligned} \tag{7.2.9}$$

Next, for the term L_2, we use the definition of L^2 projection $\mathcal{Q}_k^b$ to obtain

$$\begin{aligned} L_2 &= \sum_{K\in\mathcal{T}_h} \langle \chi - \mathcal{Q}_k^b\chi, \Big(\alpha\nabla z - \bar{\alpha}\nabla z_0\Big)\cdot\mathbf{n}\rangle_{\partial K} \\ &= \sum_{K\in\mathcal{T}_h} \langle \chi - \mathcal{Q}_k^b\chi, \Big(\alpha\nabla z - \alpha\nabla z_0\Big)\cdot\mathbf{n}\rangle_{\partial K} \\ &\quad + \sum_{K\in\mathcal{T}_h} \langle \chi - \mathcal{Q}_k^b\chi, \Big(\alpha\nabla z_0 - \bar{\alpha}\nabla z_0\Big)\cdot\mathbf{n}\rangle_{\partial K} := L_2^1 + L_2^2, \end{aligned} \tag{7.2.10}$$

where $\chi := \mathcal{Q}_k^0 u_t - u_t$.

Now, using the trace inequality (1.4.19), we observe that

$$\begin{aligned} \sum_{K\in\mathcal{T}_h} \|\chi\|_{\partial K}^2 &\leq C \sum_{K\in\mathcal{T}_h} \Big(h_K^{-1}\|\chi\|^2 + h_K\|\nabla\chi\|_K^2\Big) \\ &\leq C \sum_{K\in\mathcal{T}_h} \Big(h_K^{-1} h_K^{2\lambda_2+2} \|u_t\|_{\lambda_2+1,K}^2 + h_K h_K^{2\lambda_2} \|u_t\|_{\lambda_2+1,K}^2\Big) \\ &\leq C h^{2\lambda_2+1} \sum_{K\in\mathcal{T}_h} \|u_t\|_{\lambda_2+1,K}^2. \end{aligned} \tag{7.2.11}$$

Then, for L_2^1, we use stability of L^2 projection $\mathcal{Q}_k^b$ to obtain

$$\begin{aligned} |L_2^1| &\leq \left(\sum_{K\in\mathcal{T}_h} \|\chi\|_{\partial K}^2\right)^{1/2} \left(\sum_{K\in\mathcal{T}_h} \|\alpha\nabla(z-z_0)\|_{\partial K}^2\right)^{1/2} \\ &\leq C h^{\lambda_2+\frac{1}{2}} \|u_t\|_{\lambda_2+1} \\ &\quad \times \left(\sum_{K\in\mathcal{T}_h} \big(h_K^{-1}\|\alpha\nabla(z-z_0)\|_K^2 + h_K\|\nabla\cdot(\alpha\nabla(z-z_0))\|_K^2\big)\right)^{1/2}. \end{aligned}$$

Then, use the fact that ∇z_0 is piece-wise constants to have

$$\begin{aligned} &\sum_{K\in\mathcal{T}_h} \big(h_K^{-1}\|\alpha\nabla(z-z_0)\|_K^2 + h_K\|\nabla\cdot(\alpha\nabla(z-z_0))\|_K^2\big) \\ &\leq \sum_{K\in\mathcal{T}_h} \big(\|\alpha\|_{\infty,K} h_K^{-1} h_K^2 \|z\|_{2,K}^2 + h_K\|\nabla\cdot(\alpha\nabla z)\|_K^2 + h_K\|\nabla\cdot(\alpha\nabla z_0)\|_K^2\big) \\ &\leq C\|\alpha\|_{1,\infty} h \sum_{K\in\mathcal{T}_h} \big(\|z\|_{2,K}^2 + \|\rho_t\|_K^2 + \|\nabla z_0\|_K^2\big) \\ &\leq C\|\alpha\|_{1,\infty} h \big(\|z\|_2^2 + \|\rho_t\|^2 + \|z_h\|_{1,h}^2\big) \leq C\|\alpha\|_{1,\infty} h \|\rho_t\|^2. \end{aligned}$$

Hence, we have

$$|L_2^1| \leq C\|\alpha\|_{1,\infty} h^{\lambda_2+1} \|u_t\|_{\lambda_2+1} \|\rho_t\|. \tag{7.2.12}$$

For L_2^2 , we first observe that

$$\begin{aligned}
&\sum_{K\in\mathcal{T}_h} \|(\alpha-\bar{\alpha})\nabla z_0\|_{\partial K}^2 \\
&\leq C \sum_{K\in\mathcal{T}_h} \Big(h_K^{-1}\|\alpha-\bar{\alpha}\|_{\infty,K}^2 \|\nabla z_0\|_K^2 + h_K \|\nabla\cdot\big((\alpha-\bar{\alpha})\nabla z_0\big)\|_K^2 \Big) \\
&\leq C \sum_{K\in\mathcal{T}_h} \Big(h_K\|\alpha\|_{1,\infty,K}^2 \|\nabla z_0\|_K^2 + h_K \|\nabla\alpha\cdot\nabla z_0\|_K^2 \Big) \\
&\leq Ch\|\alpha\|_{1,\infty}^2 \sum_{K\in\mathcal{T}_h} \|\nabla z_0\|_K^2 \leq Ch\|\alpha\|_{1,\infty}^2 \|z_h\|_{1,h}^2.
\end{aligned} \tag{7.2.13}$$

Then, as an immediate consequence of estimates (7.2.11) and (7.2.13), we obtain

$$|L_2^2| \leq C\|\alpha\|_{1,\infty} h^{\lambda_2+1} \|u_t\|_{\lambda_2+1} \|\rho_t\|. \tag{7.2.14}$$

Now, use estimates (7.2.12) and (7.2.14) in (7.2.10) to have

$$|L_2| \leq C\|\alpha\|_{1,\infty} h^{\lambda_2+1} \|u_t\|_{\lambda_2+1} \|\rho_t\|. \tag{7.2.15}$$

Next, we use estimates (7.2.9) and (7.2.15) in (7.2.8) to obtain

$$|I_{12}^2| \leq C\|\alpha\|_{1,\infty} h^{\lambda_2+1} \|u_t\|_{\lambda_2+1} \|\rho_t\|. \tag{7.2.16}$$

Finally, estimates (7.2.6)-(7.2.7) and (7.2.16) leads to desire estimate.